The Rational Chemical Synthesis of a C60H12 Carbon Nanotube End-cap and Novel Geodisc Polyarenes

Author: Allison Kristen Greene

Boston College

The Graduate School of Arts and Sciences

Department of Chemistry

THE RATIONAL CHEMICAL SYNTHESIS OF A $C_{60}H_{12}$ CARBON NANOTUBE END-CAP AND NOVEL GEODESIC POLYARENES

a dissertation

by

ALLISON KRISTEN GREENE

submitted in partial fulfillment of the requirements

for the degree of

Doctor of Philosophy

May 2012

Abstract

The Rational Chemical Synthesis of a $C_{60}H_{12}$ Carbon Nanotube End-Cap and Novel Geodesic Polyarenes

Allison K. Greene

Dissertation Advisor: Dr. Lawrence T. Scott

The distinctive molecular structure of carbon nanotubes makes them desirable for electronic and chemical materials; however, current production methods are limited with respect to purity and chirality. Geodesic polyarenes serve as superb templates for the bottom up synthesis of carbon nanotube end-caps, setting the chirality and dimensions of the carbon nanotubes.

The work herein describes the synthetic efforts towards the rational synthesis of a [6,6] carbon nanotube end-cap. Chapter 1 describes the efforts towards the synthesis of a $C_{60}H_{12}$ end-cap, in which the synthesis of an advanced intermediate, *peri-bis*(dibenzo[*a,g*]corannulene) is complete; however, the insolubility of this material proved to be problematic in a subsequent cycloaddition reaction. This reaction is examined computationally in order to understand the failure of the addition of dienophile, maleic anhydride, to *peri-bis*(dibenzo[*a,g*]corannulene).

In Chapters 2 and 3, the development of solubility-enhancing methods is described. The development of a solubility-enhancing dienophile is successfully employed to induce the solubility of a formerly insoluble diene, *peri-bis*(dibenzo[*a*,*g*]corannulene), through Diels-Alder addition. Another method, employs the incorporation of *tert*-butyl groups onto *peri-bis*(dibenzo[*a*,*g*]corannulene) to successfully induce solubility. The enhanced-solubility enables the successful Diels-Alder addition of simple maleimide dienophiles, installing all necessary carbon atoms for the desired end-cap. Pyrolysis of the *bis*-anhydride derived from the aromatized *bis*-maleimide adduct afforded the $C_{60}H_{12}$ end-cap, which is the second carbon nanotube end-cap ever synthesized and the first of these dimensions.

Chapter 3 also explores a palladium catalyzed intramolecular arylation reaction to form a pivotal intermediate in the synthesis of the end-cap, dibenzo[*a*,*g*]corannulene. The mechanism for the formation of a problematic byproduct resulting from reductive dehalogenation is discussed. Utilizing a deuterium labeled solvent, it is found that deuterium is incorporated onto the hydrocarbon, indicating that the solvent (*N*,*N*-dimethylformamide-d_7) is the source of hydrogen for the reductive dehalogenation. These conditions are further exploited in Chapter 4 for the convenient perdeuteration of a variety of polycyclic aromatic hydrocarbons.

Chapter 5 describes the first synthesis of a nitrogen containing geodesic polyarene, dibenzo[*g*,*m*]azacorannulene. This synthesis is completed in seven steps from a commercially available source in a 28% overall yield.

Table of Contents

Chapter 2

Synthesis of Solubility-Enhancing Dienophiles for the Diels-Alder Addition to *Peri-bis*(dibenzo[*a,g*]corannulene)

Chapter 3

Incorporation of Solubility-Enhancing *tert*-Butyl Groups for the Complete Synthesis of a $C_{60}H_{12}$ Carbon Nanotube End-Cap

Chapter 5

A Novel Heteroatom Containing Geodesic Polyarene: Synthesis of Dibenzo[*g,m*]azacorannulene

Acknowledgements

I cannot begin to sum up all of my gratitude for the support and opportunities I have been given the past few years at Boston College. First, I need to thank Dr. Scott for giving me such a phenomenal opportunity to work on your brilliant projects. You have provided me with more than just an education, but skills I will carry on throughout my career. Your true passion for chemistry and mentoring abilities have made for an enjoyable and successful graduate career. Thank you for always being there for guidance during my years at Boston college.

To my fellow lab mates, past and present, I will always cherish our time together in the lab. From general discussions about work to discussions about life, you have all help mold me into the chemist I am today. Special thanks to Vikki, for not only getting me started in the lab, but for remaining a great friend throughout the years. Furthermore, I could not have accomplished as much without my undergraduates; Fernando, Kaitlin and Ben. It has been a wonderful experience not only seeing you all become successful chemists, but learning from you.

Without my family I could not imagine being here today. Their support over the years has allowed me to follow my dreams, and whether directly or indirectly, they have shaped me into the person I am today. For that I am grateful and so very fortunate to have a family like you.

List of Abbreviations

Å	Angstrom
aq	aqueous
br	broad (spectroscopy)
C	celcius
Calc'd	calculated
cm^{-1}	wavenumbers
δ	NMR scale
d	doublet (NMR)
DART	direct analysis in real time
DBU	1,8-diazabicyclo[5.4.0]undec-7-ene
DCTB	trans-2-[3-(4-*tert*-Butylphenyl)-2-methyl-2-propenylidene]malononitrile
dd	doublet of doublets
DDQ	2,3-dichloro-5,6-dicyano-1,4-benzoquinone
dec	decomposed
DMAc	*N*,*N*-dimethylacetamide
DMF	*N*,*N*-dimethylformamide
ε	extinction coefficient
EI	electron impact ionization
FVP	flash vacuum pyrolysis
g	gram
h	hour
HOMO	highest occupied molecular orbital
HRMS	high resolution mass spectrometry

Hz	Hertz
IR	infrared spectroscopy
kcal	kilocalorie
λ	wavelength
lit	literature
LUMO	lowest unoccupied molecular orbital
M	molarity (mol/L)
m	multiplet
m/z	mass to charge ratio
MALDI	matrix-assisted laser desorption ionization
MHz	megahertz
min	minute
mmol	millimole
mol	mole
mp	melting point
NBS	*N*-bromosuccinimide
nm	nanometer
NMR	nuclear magnetic resonance
°	degree
o	*ortho*
o-DCB	1,2-dichlorobenzene
p	*para*
PAH	polycyclic aromatic hydrocarbon
ppm	parts per million

RT	room temperature
s	singlet
sh	shoulder
t	triplet
THF	tetrahydrofuran
TMS	trimethylsilyl (group)
TMS	tetramethylsilane (NMR)
TOF	time of flight
UV	ultraviolet
Vis	visible

Chapter 1

Polycyclic Aromatic Hydrocarbons as Building Blocks for a [6,6] Carbon Nanotube

1.1 Introduction

The implementation of polycyclic aromatic hydrocarbons as organic electronic materials has garnered much interest in the recent years.[1] Bowl-shaped polycyclic aromatic hydrocarbons have been extensively studied by numerous laboratories.[2] These geodesic polyarenes, consisting of five- and six- membered rings, map directly onto fullerenes and are considered fullerene fragements. More importantly, they demonstrate reactivity on the interior carbons similar to that of fullerenes.[3] An extension of these classes of curved polycyclic aromatic hydrocarbons and fullerenes are carbon nanotubes. Carbon nanotubes can be visitualized as a tube of sp^2-hybridized carbon atoms, sometimes incorporating curved polycyclic aromatic hydrocarbons as end-caps on the tube.

The discovery of carbon nanotubes in 1991[4] has inspired significant research on these super materials in recent years. These materials are proposed to advance electronic materials by allowing for devices to be produced on the nanometer scale, which is impossible with conventional lithography on silicon chips.[5] In order to utilize carbon nanotubes in electronic devices, a fully conductive tube must be prepared. Unfortunately, not all carbon nanotubes are created equally with respect to their physical and electronic properties. Carbon nanotubes may arise as a single walled tube, or they can be multiwalled, with tubes within a tube. Among the single walled carbon nanotubes, there are three varieties, commonly referred to as arm-chair, zig-zag and chiral (Figure 1-1). Among these varieties, only arm-chair carbon nanotubes are always conductive, whereas

only one third of zig-zag carbon nanotubes are conductive and only select chiral tubes are conductive.

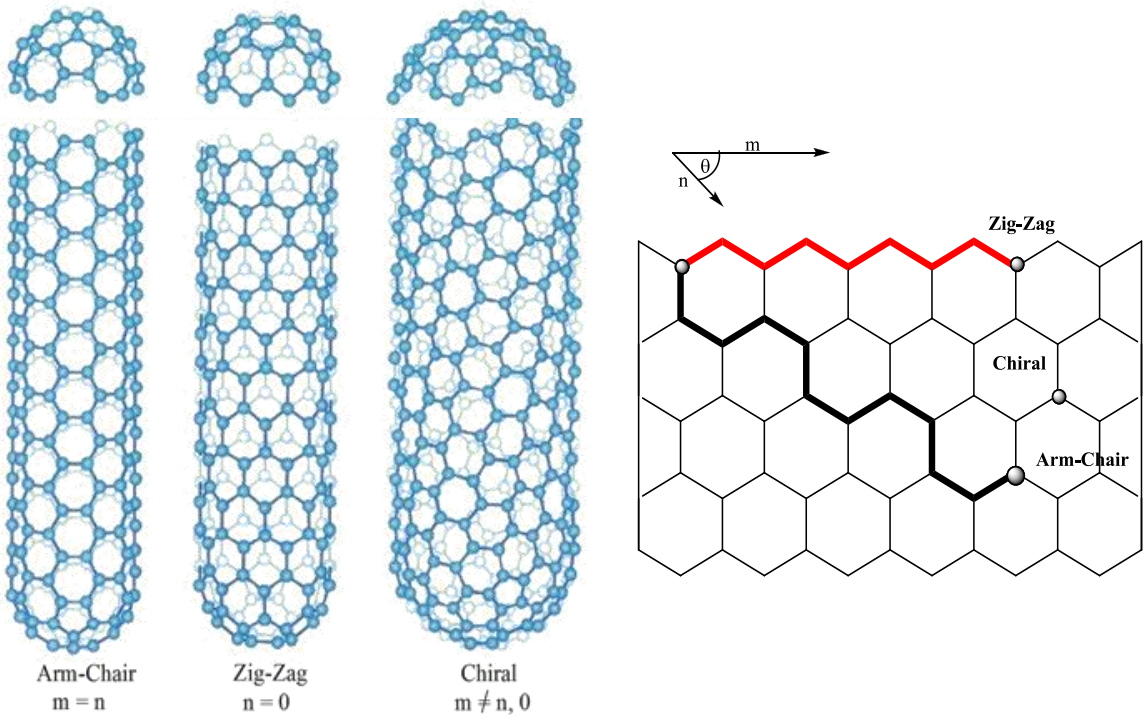

Figure 1-1. Single Walled Carbon Nanotubes

To date, efforts to synthesize pure single walled carbon nanotubes of just one structure have not been fruitful. Although signficiant advances have been made in the production of bulk carbon nanotubes, control of the diameter and type of carbon nanotube has remained a challenege. Without the ability to control the specific morphology of the tube, carbon nanotubes with differing physical properties have been produced in bulk mixtures, which has made applications, particularly in electronics, limited.[6] To overcome these limitations, a bottom-up synthesis of these desirable materials is necessary. By

strategically establishing the dimensions of the carbon nanotube through a polycyclic aromatic hydrocarbon template, synthesis of a carbon nanotube can be envisioned.

A route towards synthesizing a short arm-chair carbon nanotube, or end-cap, has recently been accomplished by Scott *et al.*[7] It was proposed that a short [5,5] arm-chair carbon nanotube, **1-1**, could be prepared by rational chemical synthesis, as shown in Figure 1-2. From this short carbon nanotube, a [5,5] arm-chair carbon nanotube, which would be fully conductive, could be prepared and applied to electronic devices.

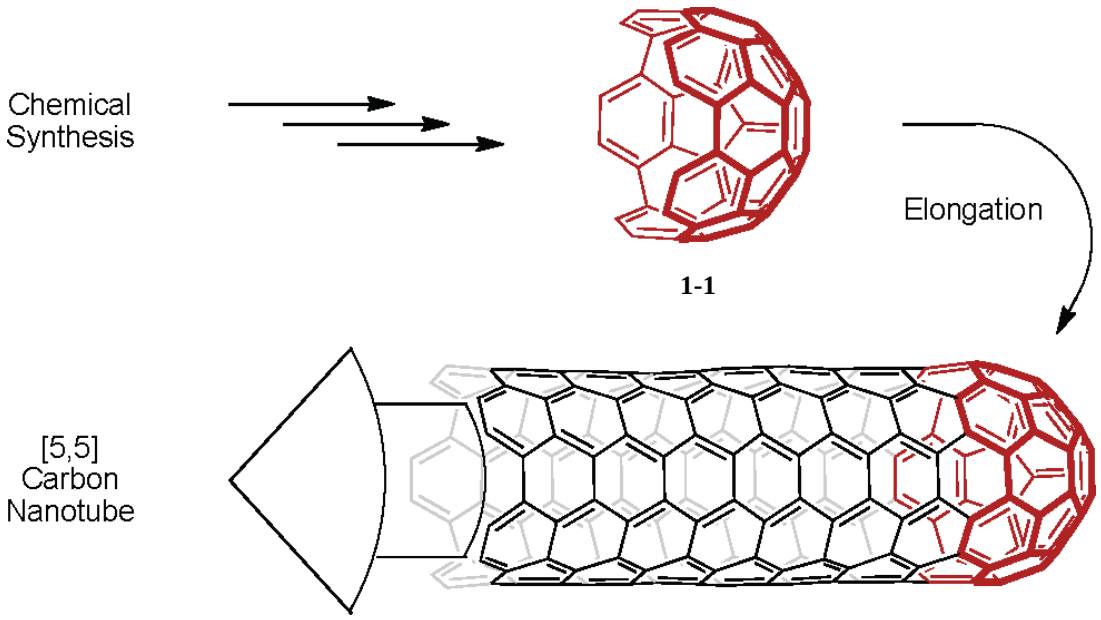

Figure 1-2. Proposed Synthesis of a [5,5] Arm-Chair Carbon Nanotube

The synthesis of **1-1** was achieved in three steps beginning from corannulene, **1-2**, a synthetically accessable hydrocarbon recently synthesized by Siegel *et al.* in kilogram quantities.[8] From **1-2**, pentachlorination with iodine monochloride afforded **1-3**, which installed the required functionality to expand the hydrocarbon framework. Compound **1-3**

was poised for a five-fold Negishi coupling with 2,6-dichlorophenylzinc chloride, forming **1-4**, which contained the final 30 carbon atoms necessary for the short [5,5] carbon nanotube **1-1**. Flash vacuum pyrolysis (FVP) was employed to stitch **1-4** up to the desired [5,5] carbon nanotube, **1-1**, at 1100 ˚C and 0.25 torr in 2-3% yield.

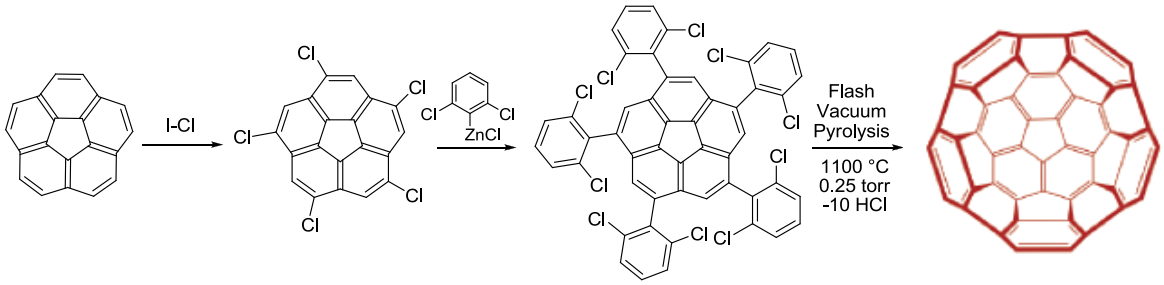

1-2 **1-3** **1-4** **1-1**

Scheme 1-1. Synthesis of a Short [5,5] Carbon Nanotube

With the successful synthesis of **1-1**, extension of this short carbon nanotube was desired. As shown in Figure 1-3, a mechanism for growing the carbon nanotube was proposed, utilizing acetylene as the dienophile for the Diels-Alder addition to the bay region of **1-1**, installing a new benzene ring. With successive addition of acetylene around the rim of **1-1**, a new layer of benzene rings would be formed, installing a new layer of bay regions. The newly formed bay regions would be poised to add another layer of benzene rings through Diels-Alder addition, and this process could be envisioned to add, theoretically, an infinite number of new layers of benzene rings, extending the length of the carbon nanotube.

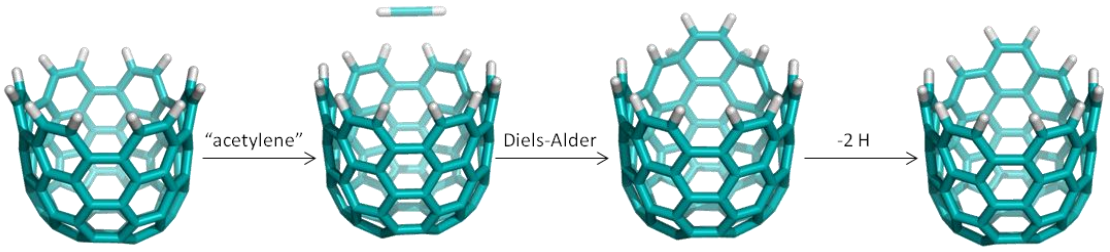

Figure 1-3. Proposed Growth of an Arm-Chair Carbon Nanotube

Although acetylene would be the simplest dienophile from which to grow a carbon nanotube from a template by Diels-Alder addition, acetylene is not a very reactive dienophile.[9] Investigations into masked acetylenes had shown that nitroethylene, generated in situ from nitroethanol and phthalic anhydride, showed promise as a highly reactive dienophile to install new benzene rings. As shown in Scheme 1-2, the addition of nitroethylene to dimesitylbisanthene **1-5** successfully formed two new benzene rings at the bay regions, providing **1-6** in 84% yield. It is expected that this chemistry may be employed to successfully grow arm-chair carbon nanotubes from templates, such as **1-1**.

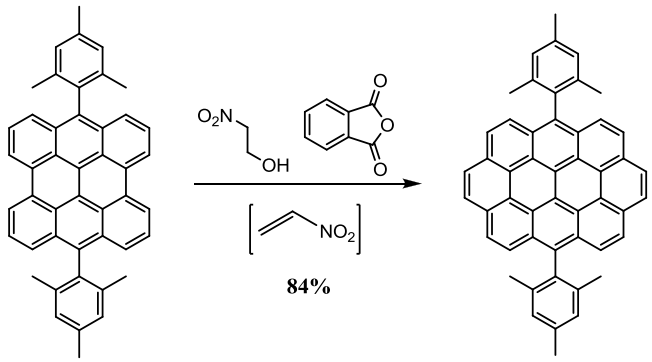

1-5 **1-6**

Scheme 1-2. Diels-Alder Addition of Nitroethylene

1.2 Proposed Synthesis of a [6,6] Carbon Nanotube

With the successful synthesis of **1-1** complete, investigations into arm-chair carbon nanotubes of different diameters have been explored.[10] The synthesis of a [6,6] carbon nanotube (**1-7**) was proposed as shown in Scheme 1-3. As envisioned with the synthesis of the [5,5] end-cap (**1-1**), it was proposed that a short [6,6] arm-chair carbon nanotube, **1-8**, could be synthesized from the curved geodesic polyarene dibenzo[*a*,*g*]corannulene (**1-9**). Utilizing **1-9** as an initial building block to establish the dimensions and type of a carbon nanotube end-cap (**1-8**), a [6,6] carbon nanotube (**1-7**) can be foreseen. It is apparent that the molecular framework must be built up significantly from **1-9** to **1-8**, as well as incorporation of considerable curvature. Utilizing the central 5-membered ring of **1-9** to install the initial curvature of the carbon framework, an expanded retrosynthetic analysis was explored (Scheme 1-4).

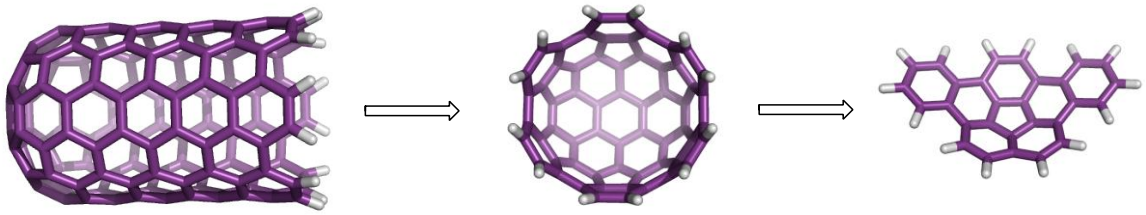

1-7 **1-8** **1-9**

Scheme 1-3. Retrosynthetic Analysis of a [6,6] Carbon Nanotube

From **1-8**, six carbon-carbon bonds may be broken to form intermediate **1-10**, which contains all 60 carbon atoms necessary to form **1-8**, as well as some radical generating functionality. From **1-10**, it was anticipated that through the formation of a 1,2-diradical

or *ortho*-benzyne, cyclization of four 5-membered rings, followed by a cyclodehydrogenation to form two 6-membered rings, would install significant curvature and the desired end-cap **1-8**. Precedent exists for *ortho*-benzyne generation via flash vacuum pyrolysis of anhydrides and maleimides to form 5- or 6-membered rings.[10a] As shown in Equation 1, FVP of 1,4-diphenylnaphthalene-2,3-dicarboxylic acid anhydride or the imide analogue promotes formation of an *ortho*-benzyne, which behaves as a 1,2-diradical. Translocation of the radical onto the phenyl ring allows for cyclization of the 5-membered ring. This process can be repeated a second time to form indeno[1,2,3-*cd*]fluoranthene.

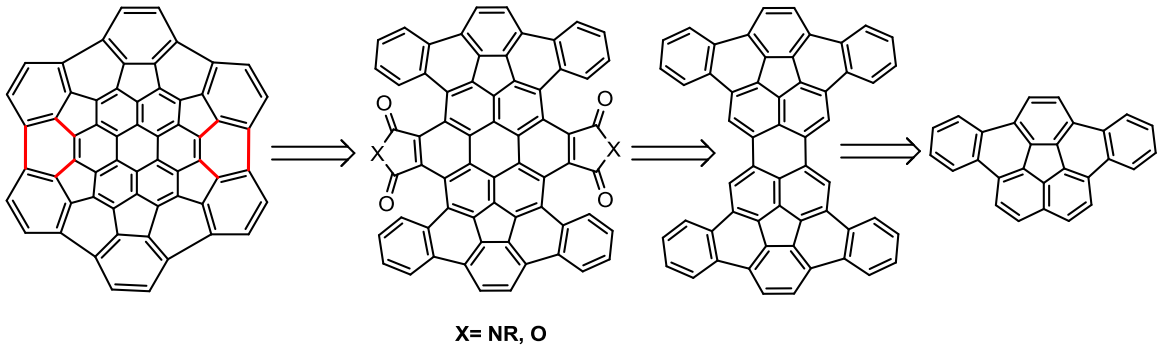

Scheme 1-4. Expanded Retrosynthetic Analysis of a [6,6] Carbon Nanotube End-Cap

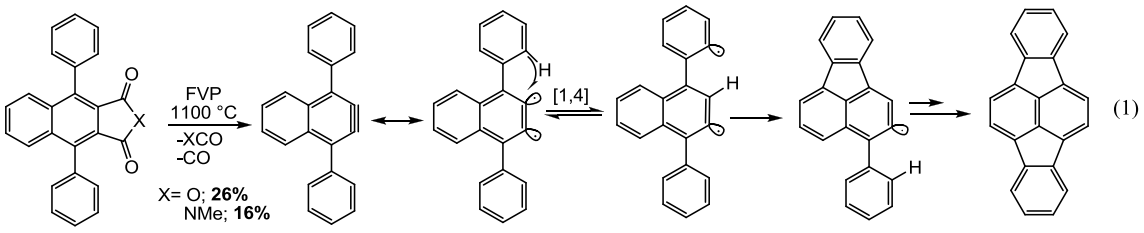

In order to install the required radical or benzyne generating functionality, a C_{56} building block (**1-11**) was envisioned. Compound **1-11** can be seen as the direct dimer of **1-9**, and is all but four carbon atoms short of the desired end-cap, **1-8**. Fortunately, **1-11** is poised for Diels-Alder addition at the perylene core, which provides an opportunity to install the necessary carbon atoms as well as some 1,2-radical generating functionality. Addition of either a maleic anhydride or a maleimide as a dienophile to **1-11**, would form **1-10**, installing the desired 1,2-diradical generating functionality.[11]

1.3 Dibenzo[*a*,*g*]corannulene as a Building Block for a [6,6] Carbon Nanotube

The synthesis of derivatized corannulenes has been well documented by the Scott lab and others.[10,12] The first synthesis of corannulene and dibenzo[*a*,*g*]corannulene utilized flash vacuum pyrolysis (FVP), which is pictured in Figure 1-4. FVP utilizes high temperatures and low pressure to attain reactivity that is otherwise not possible on the bench top. In the case of **1-9**, a compound with radical generating functionality, 7,10-bis(2-bromophenyl)fluoranthene (**1-12**), was pyrolyzed to form two new 6-membered rings and the corannulene core of **1-9** in 36% yield.[13]

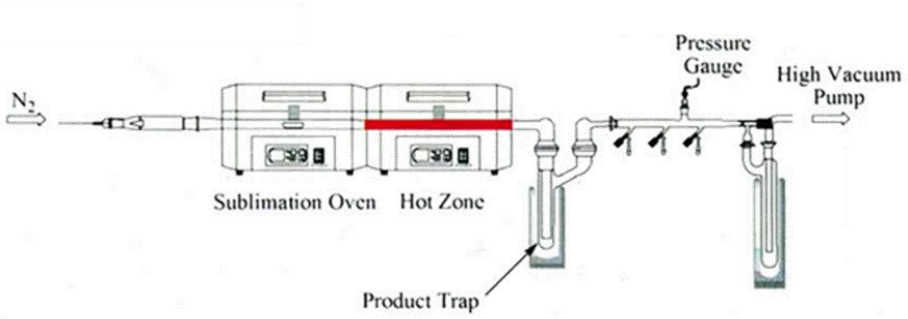

Figure 1-4. Flash Vacuum Pyrolysis Apparatus

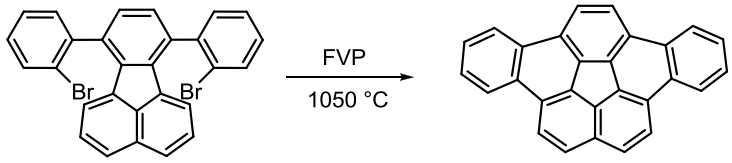

1-12 **1-9**

Scheme 1-5. Synthesis of Dibenzo[*a,g*]corannulene by Flash Vacuum Pyrolysis

In 2000, Scott *et al*. developed the first solution phase synthesis of **1-9**, employing a palladium catalyzed intramolecular arylation (Scheme 1-6).[14] Utilizing the same precursor, **1-12**, as shown in the FVP reaction in Scheme 1-5, the intramolecular arylation reaction proceeded with $Pd(PCy_3)_2Cl_2$, DMAc and DBU at 150 ˚C, to afford **1-9** in 50% yield. One complication to this reaction was the formation of the unwanted byproduct **1-14**, which was a result of a reductive dehalogenation. The mechanism of this reaction will be explored in depth in Chapter 3. Further exploration into this reaction had shown that the use of a chlorinated precursor, **1-13**, instead of the brominated precursor, **1-12**, was much more efficient and provided **1-9** in 80% yield.[10a] Most notably, this reaction does not require the elaborate FVP apparatus and may be run on the bench top.

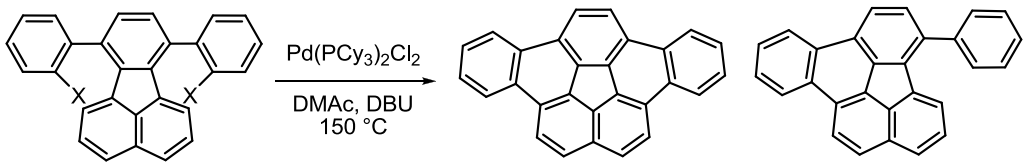

1-12; X=Br
1-13; X=Cl

1-9 **1-14**

Scheme 1-6. Intramolecular Arylation Conditions

With the aim of building up molecular complexity quickly and the recent developments in the intramolecular arylation, **1-9** was synthesized according to literature precedent in

four steps starting from a simple commercially available *o*-substituted benzene (Scheme 1-7).[10a,14] Synthesis of the symmetrical *o*-substituted biaryl ketone, **1-18** or **1-19,** was accomplished utilizing a coupling reaction with diiron nonacarbonyl with **1-15, 1-16** or **1-17** in 73%, 57% or 72% yield, respectively.[15] The ketone (**1-18** or **1-19**) was poised for a double aldol condensation with **1-20** to afford the cyclopentadienone, **1-21** or **1-22,** in >98% yield. In order to build up the fluoranthene core, a Diels-Alder/retro Diels-Alder reaction was employed with norbornadiene as the dienophile to afford **1-12** in 71% yield and **1-13** in 65% yield. Both the brominated and chlorinated precursors were subjected to the optimized intramolecular arylation conditions affording **1-9** in 80% yield from **1-13** and 45% yield from **1-12**.

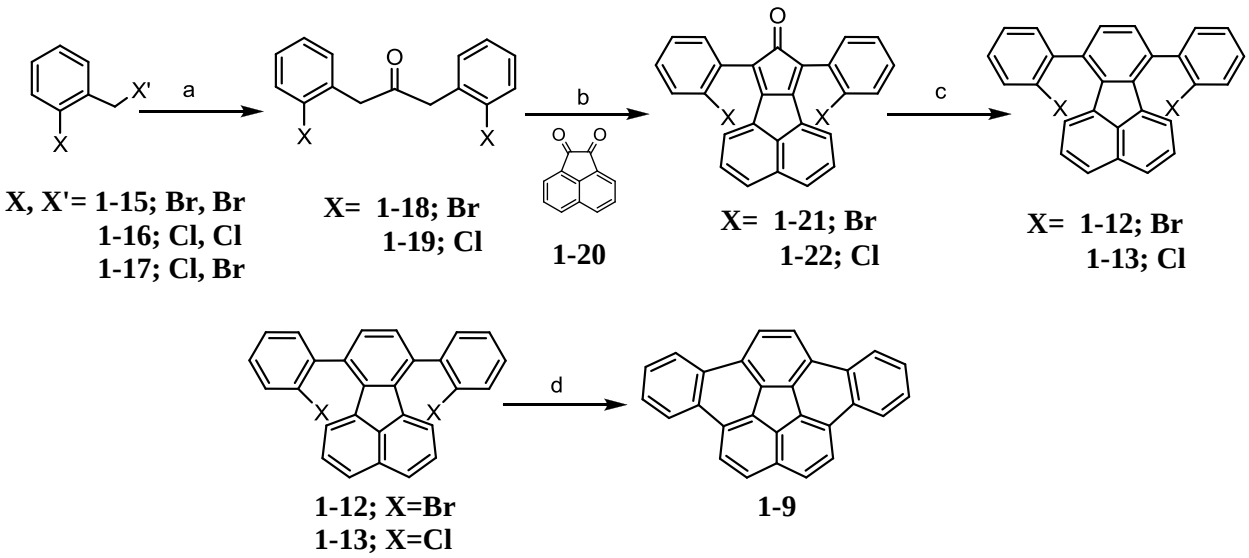

a) $Fe_2(CO)_9$, benzene, 80 ˚C; **73% (X, X'=Br), 57% (X, X'=Cl), 72% (X=Cl, X'=Br),** b) KOH, MeOH, r.t.; >**98% (X=Br),** >**98% (X=Cl)** c) norbornadiene, 90 ˚C; **71% (X=Br), 65% (X=Cl)** d) $Pd(PCy_3)_2Cl_2$, DMAc, DBU, 150 ˚C; **80% (X=Cl); 45% (X=Br)**.

Scheme 1-7. Synthesis of Dibenzo[*a,g*]corannulene

1.4 Cyclodehydrogenation: The Synthesis of *Peri-bis*(dibenzo[*a,g*]corannulene)

In order to build up complexity, cyclodehydrogenation conditions were explored to form **1-11** directly from **1-9**. This strategy provided the most direct route towards the formation of new carbon-carbon bonds without adding excess functionality to the hydrocarbon. Precedent exists for intramolecular transformations under Scholl conditions, specifically utilizing aluminum chloride as the Lewis acid and copper(II) triflate as the oxidant, as shown in Scheme 1-8.[16] In this work, Müllen *et al.* subjected hexaphenylbenzene, **1-23**, to Scholl conditions, forming hexa-*peri*-hexabenzocoronene, **1-24**, in a 6-fold cyclodehydrogenation. These conditions have been further elaborated in a variety of

systems, and numerous Lewis acid and oxidant combinations have been successfully employed.[17]

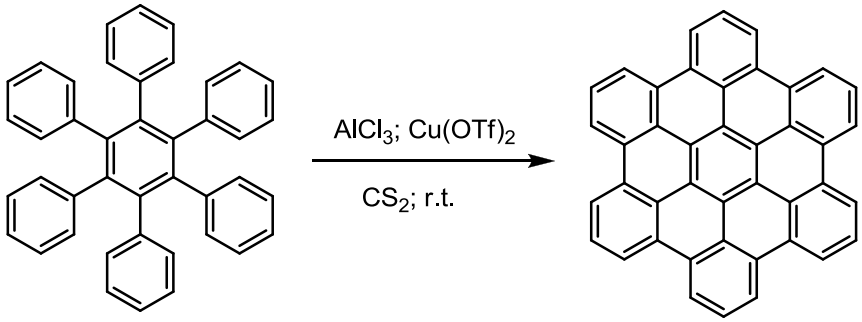

1-23 **1-24**

Scheme 1-8. Cyclodehydrogenation of Hexaphenylbenzene

To date, there are a multitude of intramolecular cyclodehydrogenation as well as a handful of intermolecular cyclodehydrogenation reported in the literature.[18] Notably, there are no examples in the literature of an intermolecular cyclodehydrogenation on a curved aromatic system. The reactivity of **1-9** had been explored previously, and it was predicted and proven that the most reactive site is at the base of the dibenzo[*a*,*g*]corannulene core (Eq. 2).[9a]

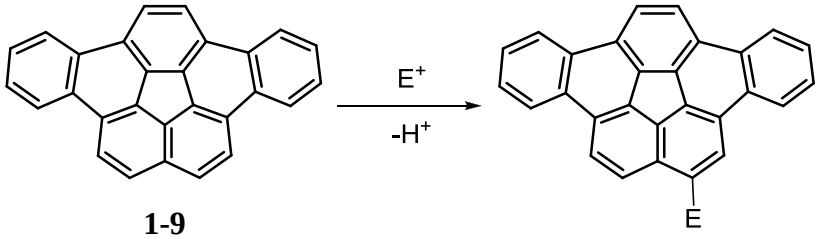

1-9 (2)

With the reactivity of **1-9** understood, investigations were turned to the direct coupling of **1-9** to form **1-11**, a $C_{56}H_{24}$ advanced intermediate. Compound **1-9** was subjected directly to Scholl conditions, utilizing aluminum chloride and copper(II) triflate in carbon

disulfide at 60 ˚C, to afford **1-11** in 91% yield (Scheme 1-9). This advanced intermediate is all but four carbon atoms short of the desired $C_{60}H_{12}$ carbon nanotube end-cap; however, **1-11** is completely insoluble due to its propensity to form aggregates. The chemical reactivity of this molecule was explored extensively.

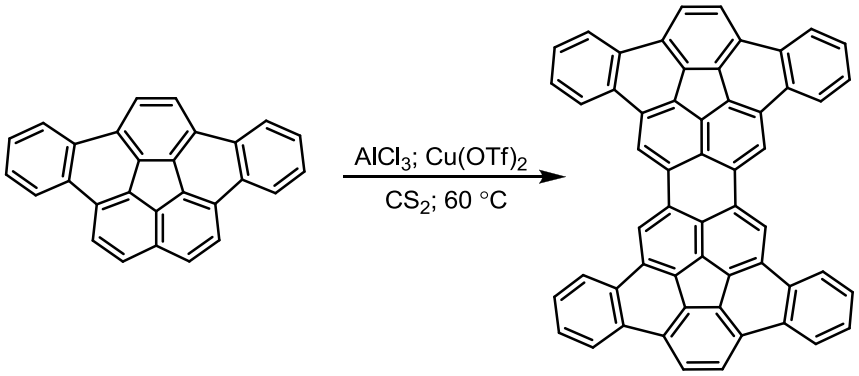

1-9 **1-11**

Scheme 1-9. Dimerization of Dibenzo[*a,g*]corannulene

1.5 Diels-Alder Addition

In order to install the final four carbon atoms necessary to form the desired end-cap **1-8**, Diels-Alder addition to **1-11** was explored. Diels-Alder addition of a variety of dienophiles to a common PAH, perylene (**1-25**), is well documented. In 1957, Clar *et al.* provided the first example of a Diels-Alder addition of maleic anhydride to **1-25**.[19] The reaction was achieved in molten maleic anhydride (202 ˚C), and only mono addition occurred, **1-27**, with all rings fully aromatized. The loss of four equivalents of hydrogen from **1-26** to form the fully aromatic product, **1-27**, was due to the presence of *p*-chloranil acting as an oxidant (Scheme 1-10). The harsh conditions are indicative of how difficult it is to disrupt the aromaticity of **1-25**, in which, after addition, the aromatic

system is similar to that of phenanthrene (**1-26**). To date, there are no reported Diels-Alder additions to phenanthrene.

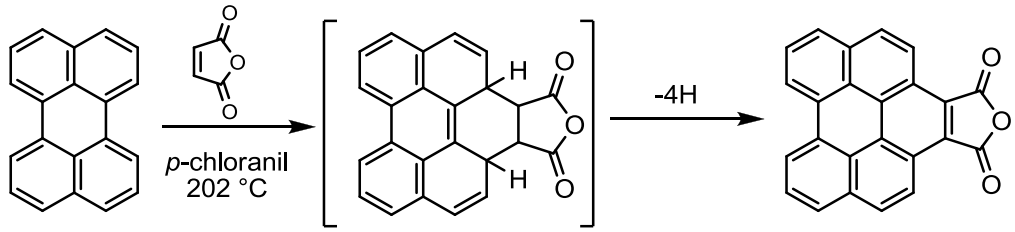

1-25 **1-26** **1-27**

Scheme 1-10. Diels-Alder Addition to Perylene

It was clear that disrupting the small aromatic system of **1-25** was costly, so Diels-Alder additions to larger aromatic systems were explored. Clar then explored the addition of maleic anhydride to tetrabenzoperylene **1-28**, and the double addition of maleic anhydride was observed, again with complete aromatization to form **1-29** (Scheme 1-11).[20] This result suggests that the larger and more delocalized aromatic system should favor the Diels-Alder addition, because the initial loss in aromaticity is less energetically costly.

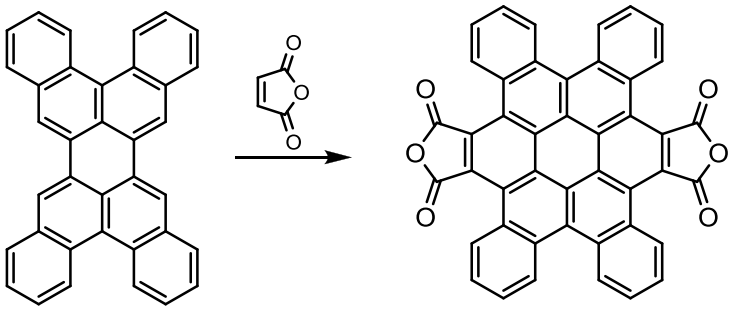

1-28 **1-29**

Scheme 1-11. Diels-Alder Addition to Tetrabenzoperylene

The site-specificity of the [4+2] cycloaddition to **1-11** had been previously explored, and it was determined that the most likely place for cycloaddition to occur would be at the

bay region of the perylene core of **1-11** (Figure 1-5).[9a] Calculations had shown that the bay region at the perylene core had the shortest distances between the termini of the "diene" (3.152 Å), compared to other bay regions (3.224 Å and 3.259 Å) on the fullerene fragment **1-11**. Also, the bay region at the perylene core is planar, unlike the other reactive sites, which are distorted from planarity. A molecular orbital map for the highest occupied molecular orbital (HOMO) was also calculated for **1-11** (Figure 1-6). The HOMO orbital map shows that the largest coefficient lies at the perylene core, which is favorable for Diels-Alder addition at that position.

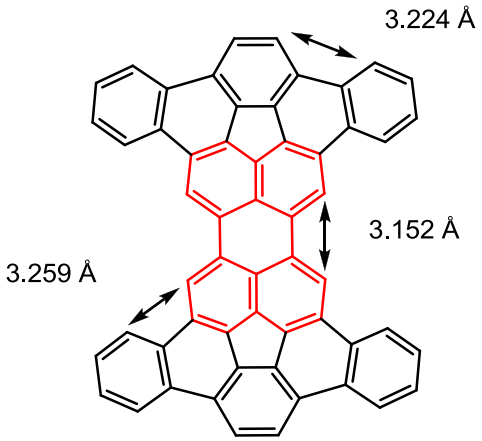

1-11

Figure 1-5. Bond Distances of Potential Reactive Dienes (B3LYP/6-31G*)

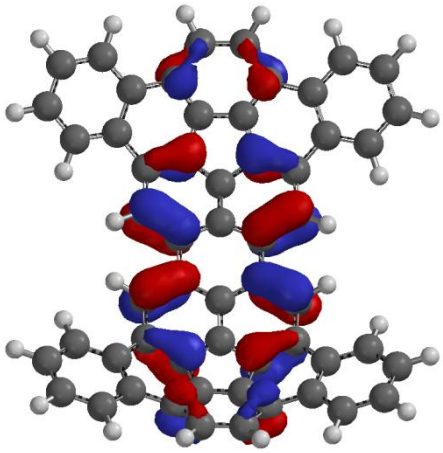

1-11

Figure 1-6. HOMO Map of *Peri-bis*(dibenzo[*a,g*]corannulene) (B3LYP/6-31G*)

Initial investigations into the Diels-Alder addition of maleic anhydride to **1-11** proved to be unsuccessful under a variety of reaction conditions (Scheme 1-12). Reactions with high boiling solvents, *o*-dichlorobenzene and nitrobenzene, in sealed vessels at elevated temperatures, with and without an external oxidant, were completely unsuccessful and only starting material was recovered. Utilizing molten maleic anhydride and chloranil, which Clar had found success with, was also unsuccessful in this case.

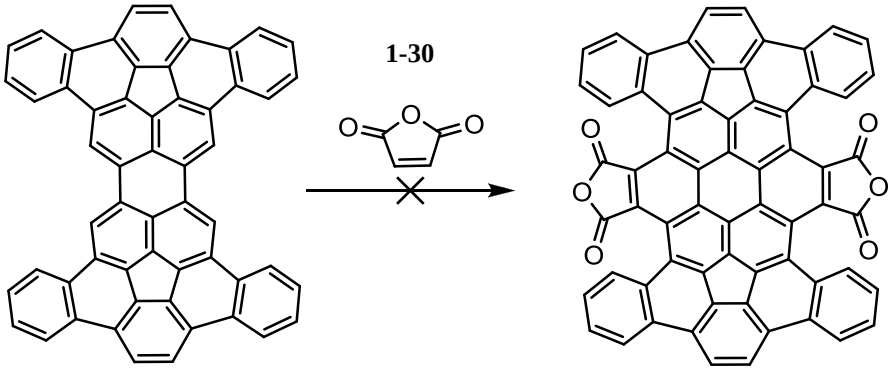

1-11 **1-31**

Scheme 1-12. Diels-Alder Addition of Maleic Anhydride

These results were very disappointing and perplexing due to the fact that addition to perylene and tetrabenzoperylene had been successful; however, the insolubility of **1-11** was suspected to be an issue. Focus was turned towards a new set of dienophiles, maleimides, which are known to have reactivities similar to that of maleic anhydride in Diels-Alder additions.[21] Specifically, *N*-methyl (**1-32**) and *N*-phenyl (**1-33**) maleimide were investigated as dienophiles (Scheme 1-13).

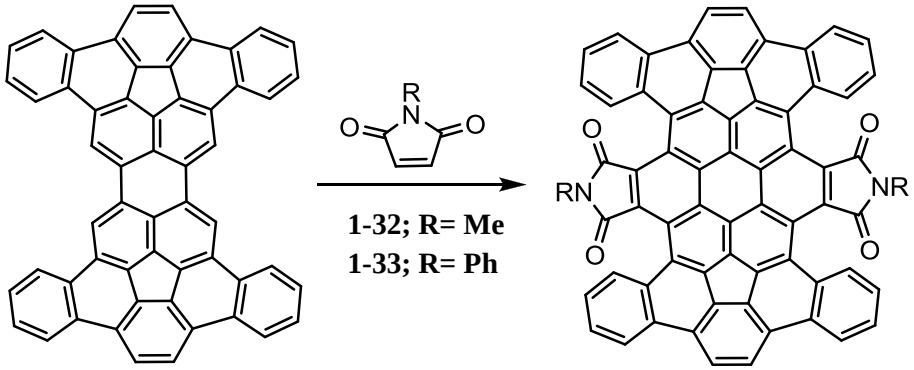

1-11

R= Me; 1-34
R= Ph; 1-35

Scheme 1-13. Diels-Alder Addition of *N*-Phenyl and *N*-Methyl Maleimide

Initial investigations with **1-33** proved to be successful, which was confirmed by high resolution MALDI-TOF mass spectrometry. Double Diels-Alder addition, to form **1-35**, had occurred when **1-11** was subjected to heating in a pressure vessel with *o*-dichlorobenzene and 20 equivalents of **1-33** for 5 days; however, both the starting material and product were insoluble, making purification very problematic. A simple wash of the crude mixture with ethanol and hexanes removed any excess maleimide present, but separation of the fully aromatic product, **1-35**, from any remaining starting material was impossible. It should be noted that the Diels-Alder addition provided the

product with full aromatization of the rings, **1-35**, even in the absence of an external oxidant. As shown in Equation 3, it was likely that the maleimides themselves act as the oxidant in this reaction. Experiments were conducted with *p*-chloranil; however, some chlorination was seen, and no significant improvement in the conversion of the fully aromatic product was seen. Curiously, the mono-addition product (**1-36**) observed had rearomatized the perylene core, but still retained the two hydrogens of the dienophile.

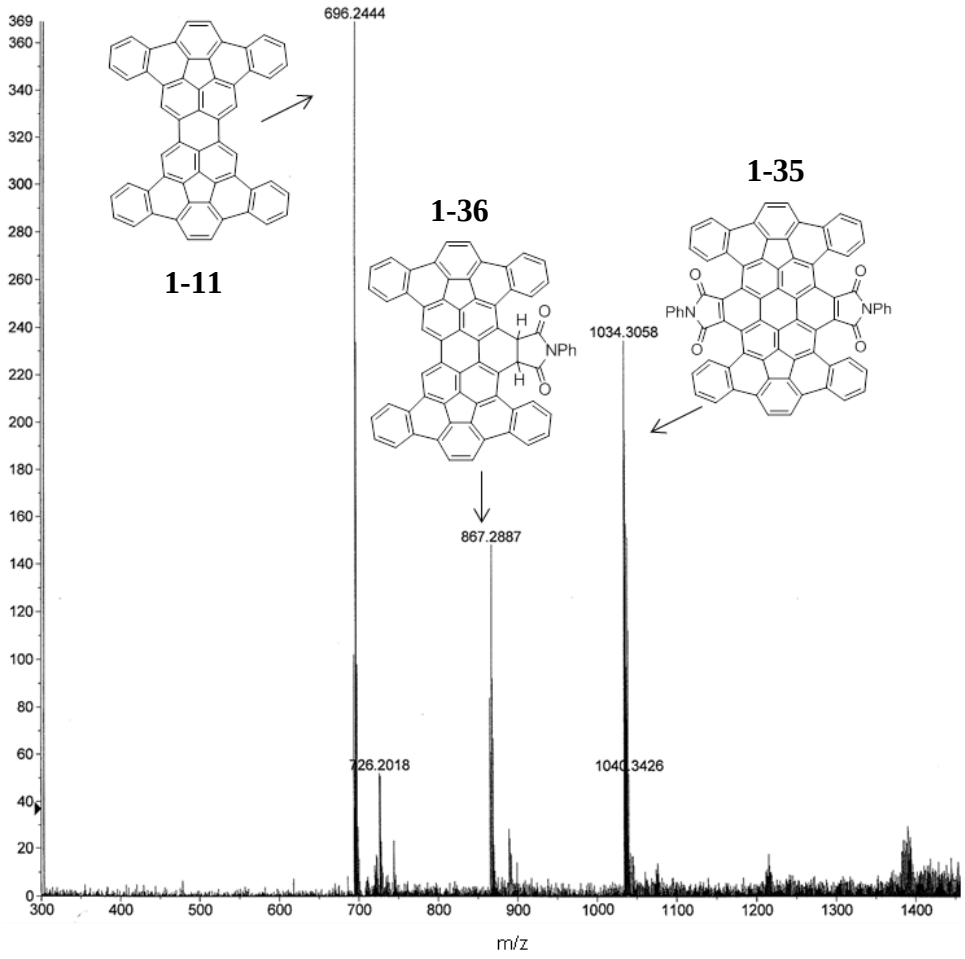

Figure 1-7. MALDI-TOF Mass Spectrum of the Diels-Alder Adduct

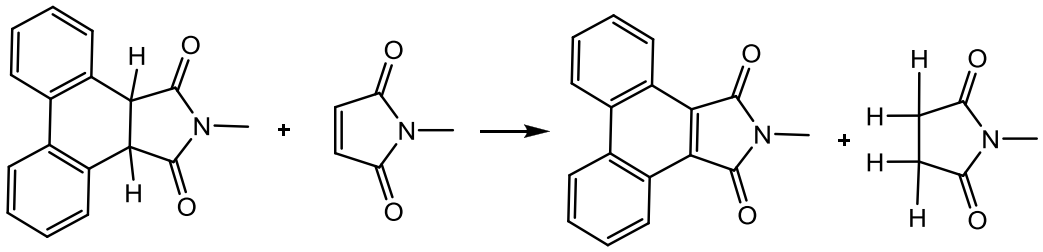

(3)

Focus was turned towards pushing the reaction to completion; unfortunately, even after heating for 14 days at 180 ˚C, starting material (**1-11**) was always present in the reaction mixture (Figure 1-7). A higher boiling solvent, nitrobenzene, which has a boiling point of 210 ˚C, was also investigated. The reaction was run at elevated temperatures, up to 230 ˚C, in a sealed tube over the course of 7 days. Unfortunately, minimal improvement in the conversion of the reaction was seen, and conversion could not be quantitated. Concern over the stability of the maleimides was investigated, and **1-33** proved to be very robust under the given reaction conditions, with a significant quantity of unreacted maleimide recovered from the crude reaction mixture.

Despite the limited success in the isolation of significant quantities of **1-35**, another maleimide, *N*-methylmaleimide (**1-32**), which is less bulky than **1-35**, was also investigated. Fortunately, **1-32** also successfully added twice to **1-11**, providing the product **1-34**, in which all rings were fully aromatic. As previously observed, there was always a significant quantity of **1-11** detected via mass spectrometry in the crude reaction mixture. The overall insolubility of both **1-11** and **1-34** was clearly a limiting factor in the success of the Diels-Alder addition.

1.6 Computational Investigation of the Diels-Alder Addition

The Diels-Alder addition of two dienophiles of interest, **1-30** and **1-32**, were examined computationally in order to understand the overall process and to gain perspective as to why **1-30** failed as a dienophile in the parent system. A simple model system was initially analyzed, in which the overall energetics of the Diels-Alder addition of dienophiles, **1-30** and **1-32**, to cyclopentadiene, **1-37**, were studied using DFT calculations (Schemes 1-14 and 1-15). The energetics for both dienophiles were very similar, with the endo transition state of the maleic anhydride adduct, **1-38**, slightly lower in energy than of the transition state **1-40**. The resulting adducts were again similar in energy, with **1-41** slightly lower in energy than the maleic anhydride adduct **1-39**. In order to gain a better perspective, the Diels-Alder addition to **1-11** needed to be examined in depth.

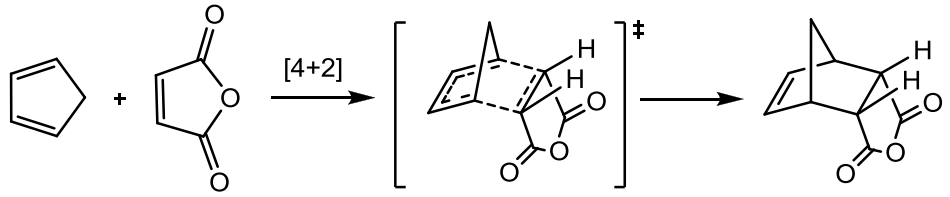

1-37 **1-30** **1-38** **1-39**

0.0 kcal/mol 12.0 kcal/mol -21.6 kcal/mol

Scheme 1-14. Endo Diels-Alder Addition of Maleic Anhydride to Cyclopenadiene (B3LYP/6-31G*)

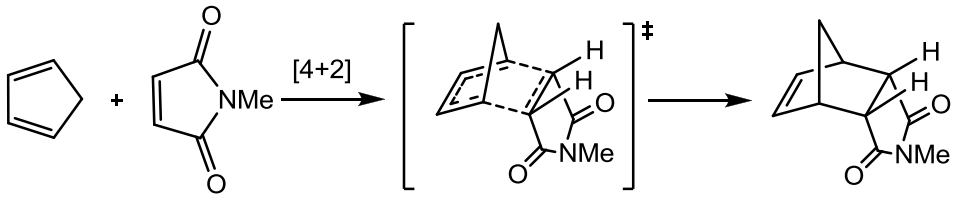

1-37 **1-32** **1-40** **1-41**

0.0 kcal/mol 13.0 kcal/mol -24.3 kcal/mol

Scheme 1-15. Endo Diels-Alder Addition of *N*-Methylmaleimide to Cyclopenadiene (B3LYP/6-31G*)

The Diels-Alder addition of **1-30** and **1-32** to **1-11** was examined using DFT calculations.[22] It was first necessary to determine the lowest energy Diels-Alder adduct, which had the possibility of adding endo or exo and to the concave face of the molecule or to the convex face of the molecule. As shown in Figure 1-8, the lowest energy adduct was endo addition from the convex face of the molecule, with all hydrogen atoms *cis*. The most energetically costly addition is the exo addition to the concave face.

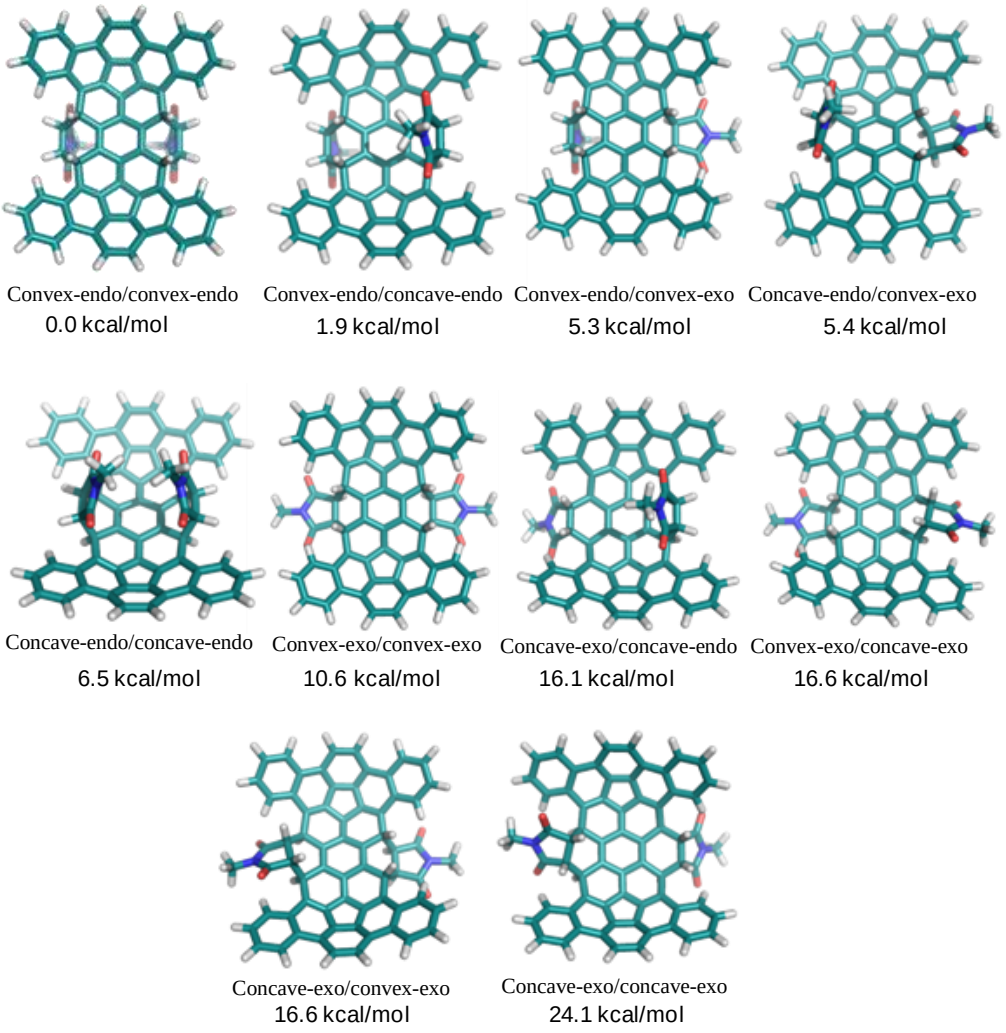

Figure 1-8. Energetics of the Various Stereoisomeric Diels-Alder Addition Products (B3LYP/6-31G*//AM1)

The single Diels-Alder addition to **1-11** was investigated, as shown in Scheme 1-16. The addition of **1-32** to **1-11** had a transition state energy of 24.5 kcal/mol (**1-42**), and the overall addition was endothermic by 4.4 kcal/mol (**1-43**), as shown in Figure 1-9.

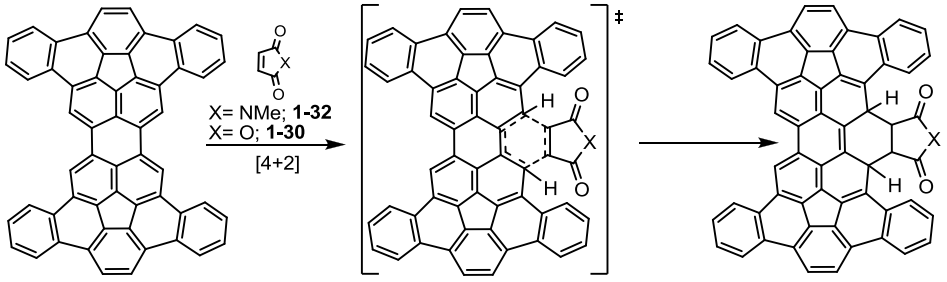

1-11 **X= NMe; 1-42** **1-43**
X= O; 1-44 **1-45**

Scheme 1-16. First Diels-Alder Addition to *Peri-bis*(dibenzo[*a,g*]corannulene)

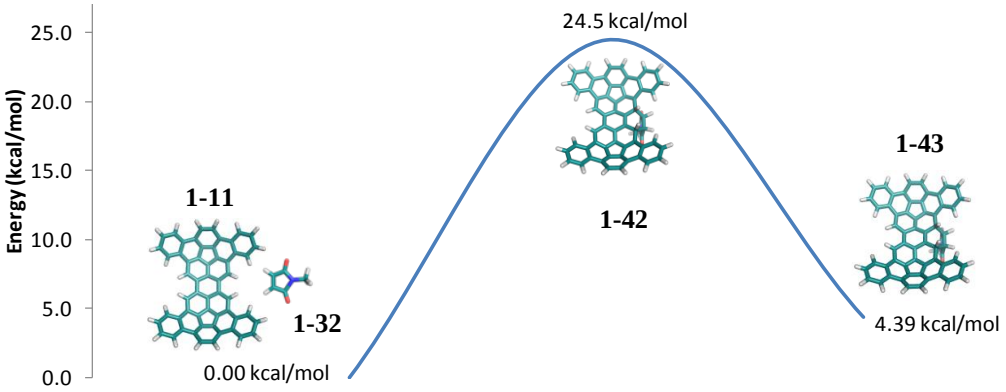

Figure 1-9. Diels-Alder Addition of *N*-Methylmaliemide (B3LYP/6-31G*//AM1)

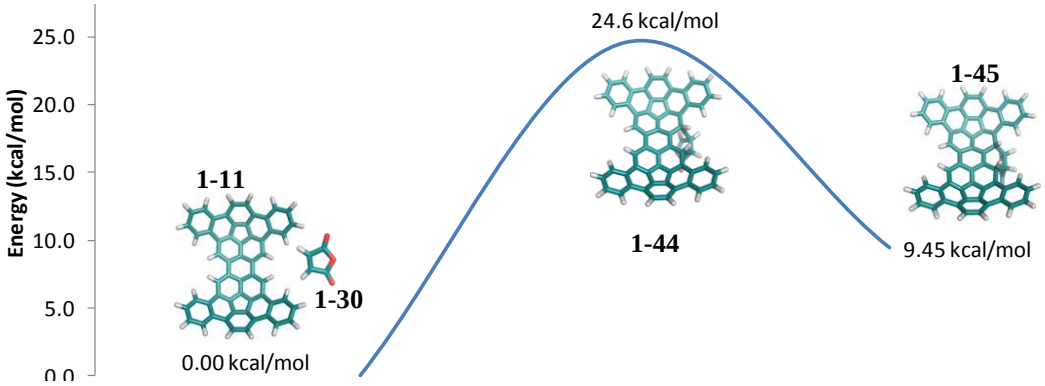

Figure 1-10. Diels-Alder Addition of Maleic Anhydride (B3LYP/6-31G*//AM1)

Addition of **1-30** to **1-11** was also examined. The activation energy was found to be 24.6 kcal/mol (**1-44**), and the overall addition was endothermic by 9.5 kcal/mol (**1-45**), as shown in Figure 1-10. From these calculations it can be seen that the activation energies are very comparable; however, the addition of **1-32** is overall less energetically costly, and **1-43** sits lower in energy than the adduct **1-45**.

Next, it was proposed that thermal rearomatization of the central aromatic core would occur, by a retro [4+2] addition of H_2, prior to the addition of another dienophile, as shown in Scheme 1-17. The loss of H_2 was examined, and the transition state energies were found to be 35.1 kcal/mol (Figure 1-11, **1-46**) and 33.7 kcal/mol (Figure 1-12, **1-48**). The rearomatization processes were endothermic by 10.2 kcal/mol (**1-47**) and 9.74 kcal/mol (**1-49**). Again, the energies were very similar in magnitude for the rearomatization and loss of H_2; however, this barrier was greater than that of the Diels-Alder addition.

The second Diels-Alder addition was examined, beginning with the rearomatized adducts **1-47** and **1-49**, as shown in Scheme 1-18. Again the transition state energies were very similar, 11.9 kcal/mol (Figure 1-13, **1-50**) and 11.1 kcal/mol (Figure 1-14, **1-52**). The overall addition is exothermic by 21.8 kcal/mol (**1-51**) and 22.5 kcal/mol (**1-53**).

Finally, the second loss of H_2 was examined, as shown in Scheme 1-19. The overall energy barriers for this process were the largest, again with relatively similar barrier heights for both dienophiles; 49.8 kcal/mol (**1-54**) and 49.5 kcal/mol (**1-56**) as shown in Figures 1-15 and 1-16. Overall, the product was lower in energy for the *N*-

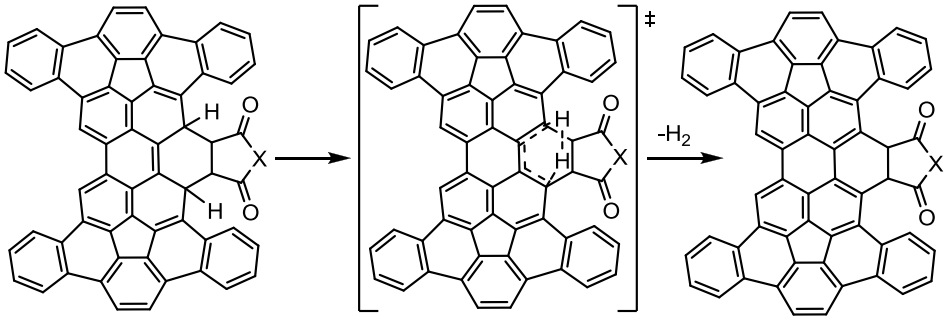

X= NMe; 1-43 **1-46** **1-47**
X= O; 1-45 **1-48** **1-49**

Scheme 1-17. Rearomatization of Mono Diels-Alder Adduct

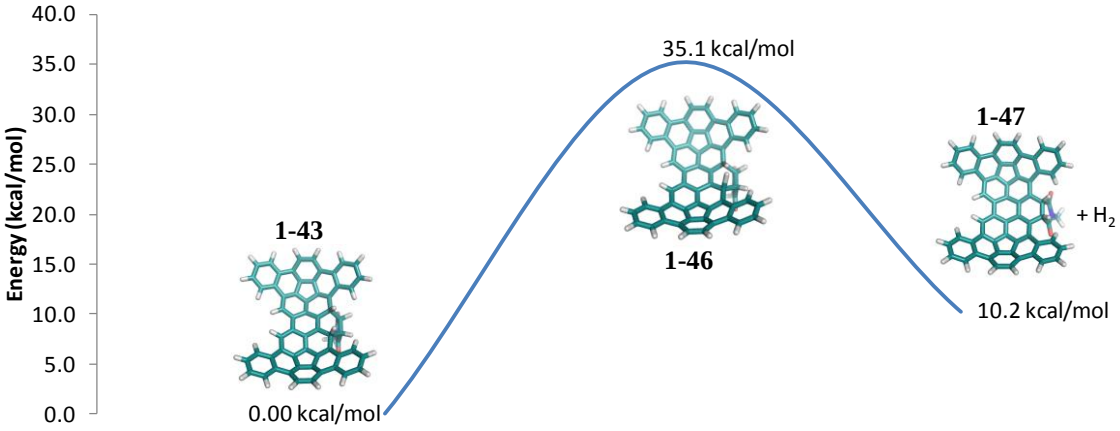

Figure 1-11. Rearomatization of Mono Diels-Alder Adduct (*N*-Methylmaleimide) (B3LYP/6-31G*//AM1)

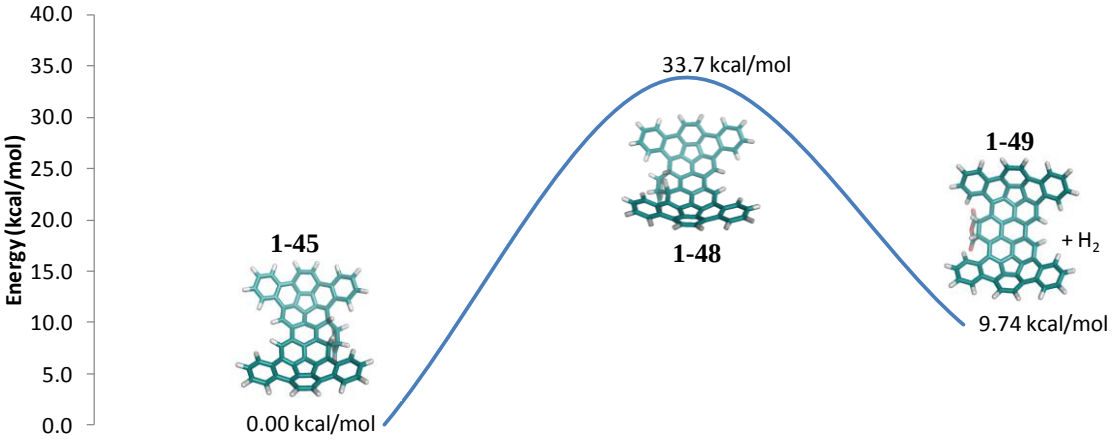

Figure 1-12. Rearomatization of Mono Diels-Alder Adduct (Maleic Anhydride) (B3LYP/6-31G*//AM1)

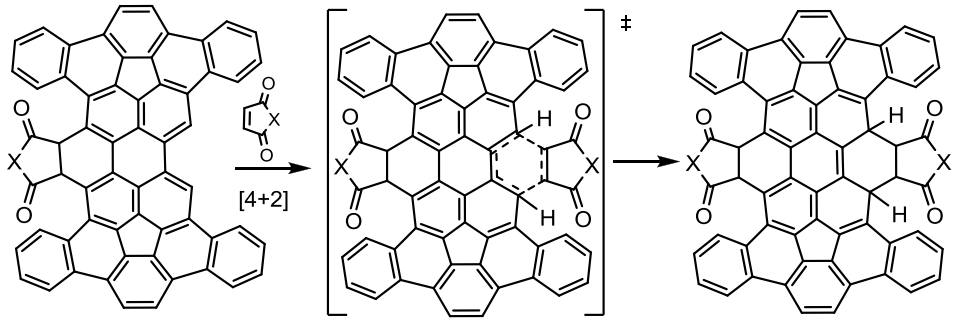

X= NMe; 1-47 **1-50** **1-51**
X= O; 1-49 **1-52** **1-53**

Scheme 1-18. Second Diels-Alder Addition after Rearomatization

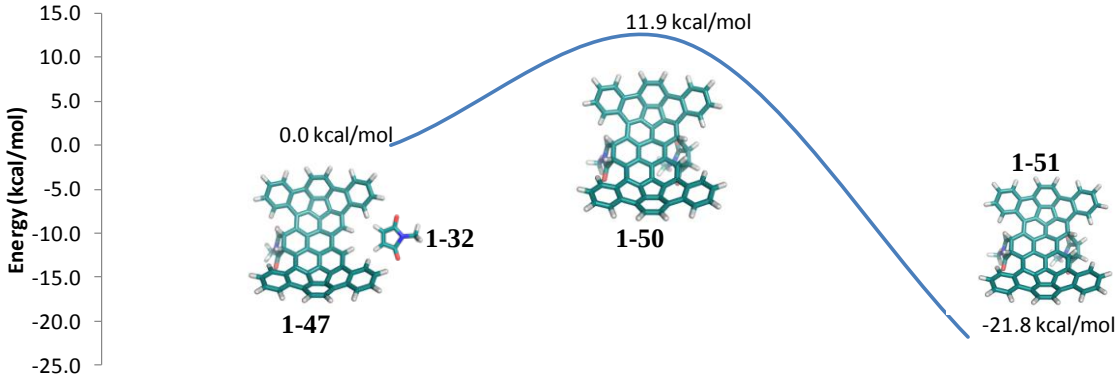

Figure 1-13. Second Diels-Alder Addition of *N*-Methylmaleimide after Rearomatization (B3LYP/6-31G*//AM1)

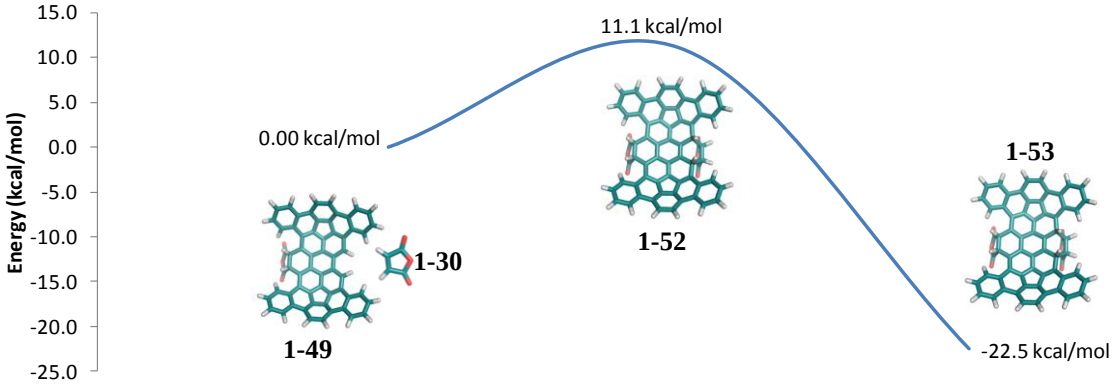

Figure 1-14. Second Diels-Alder Addition of Maleic Anhydride after Rearomatization (B3LYP/6-31G*//AM1)

methylmaleimide adduct at 26.5 kcal/mol (**1-55**) than for the maleic anhydride adduct at 29.1 kcal/mol (**1-57**).

With activation energies being lower for the Diels-Alder additions than for the subsequent barriers of H_2 loss, it was concluded that the overall barriers to rearomatization dictated whether or not the Diels-Alder additions were viable. The activation energies for loss of the second H_2 was the highest in this entire process, for both **1-30** and **1-32**, which indicates that the Diels-Alder addition must be reversible, and the loss of hydrogen is the rate determining step.

The similarities of the energy barriers for each individual process are misleading. The lower endothermicity of the first Diels-Alder step is key. The difference in energy between diene + dienophile (products **1-32** versus **1-30**) and the transition state for the rate determining step is lower for the *N*-methylmaleimide Diels-Alder addition.

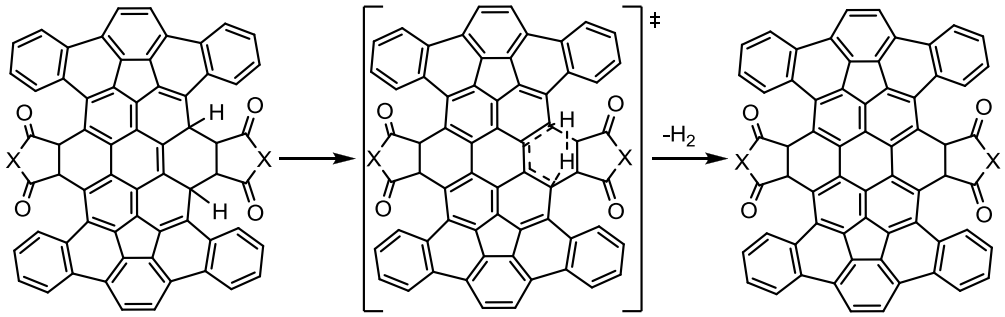

Scheme 19. Second Rearomatization of the Double Diels-Alder Adduct

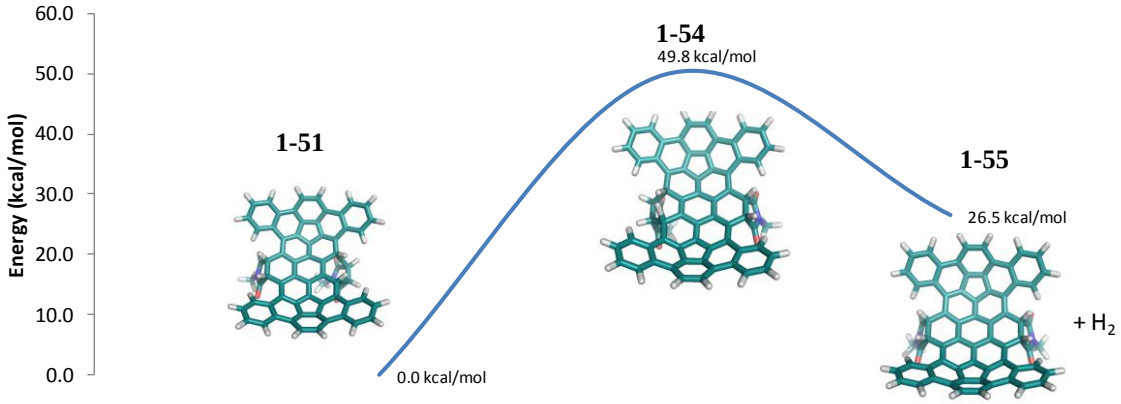

Figure 1-15. Second Rearomatization (*N*-Methylmaleimide) (B3LYP/6-31G*//AM1)

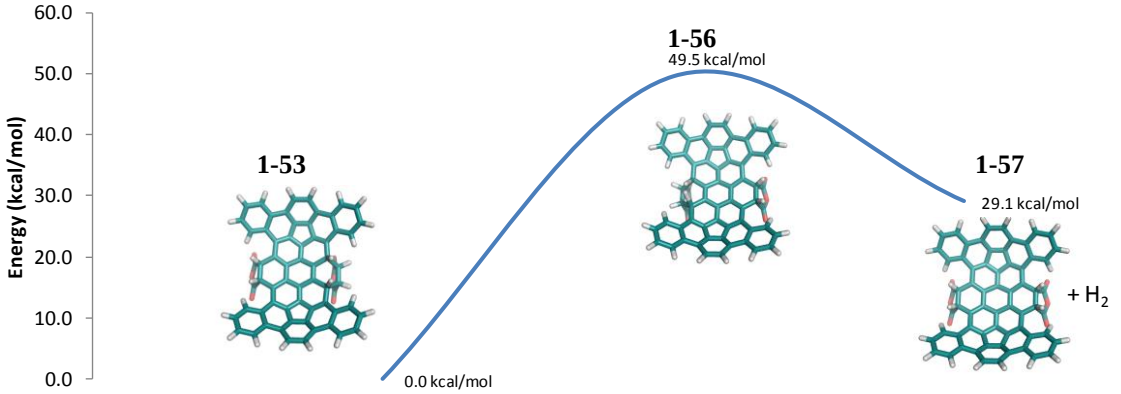

Figure 1-16. Second Rearomatization (Maleic Anhydride) (B3LYP/6-31G*//AM1)

With the Diels-Alder addition being reversible and the rearomatization being the rate-determining step, the overall process was examined in order to quantitatively compare the Diels-Alder addition of the two dienophiles, as shown in Figure 1-17. The overall process for the addition of two equivalents of *N*-methylmaleimide (**1-32**), and loss of two equivalents of H_2, is endothermic by 19.3 kcal/mol. The overall process is also endothermic for two additions of maleic anhydride (**1-30**), and the loss of two equivalents of H_2, by 25.8 kcal/mol. Most notably, the activation energy of the first rearomatization is lower in energy by 3.7 kcal/mol for the *N*-methylmaleimide adduct (**1-46**) than the maleic anhydride adduct (**1-48**), and this difference in energy may have been the determining factor in the success of the overall Diels-Alder addition of the maleimides and the failure of maleic anhydride. The second Diels-Alder addition has a lower activation energy for the *N*-methylmaleimide adduct (**1-51**), and is overall exothermic by 7.2 kcal/mol versus 3.3 kcal/mol for the maleic anhydride adduct (**1-53**). The final rearomatization has the highest barrier for both adducts (**1-54** and **1-56**); however, the barrier is overall lower in energy for the *N*-methylmaleimide adduct (**1-55**).

It is likely that the barrier for the retro [4+2] H_2 addition is just too high for the successful rearomatization of **1-45**, making maleic anhydride an unsuitable dienophile in this particular system. Once H_2 is lost, the compound cannot go back to starting materials.

The rationale behind this energy difference may be due to electronic effects. The maleimide is expected to have a significant positive charge on the nitrogen atom due to

resonance effects, whereas the positive charge on the oxygen atom of the anhydride (**1-30**) from resonance effects does not contribute as significantly (Equation 4).[23] This positive charge build up on the nitrogen atom may be stabilized by the aromatic system of **1-11** after Diels-Alder addition of *N*-methylmaleimide (**1-32**), forming the more stable *N*-methylmaleimide adduct **1-43**. The lower energy *N*-methymaleimide product trends throughout the Diels-Alder additions as well as the rearomatization steps.

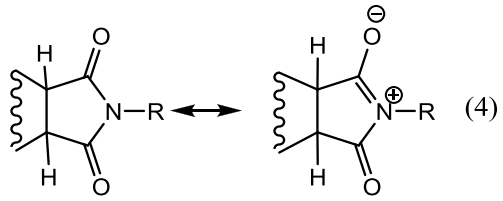

(4)

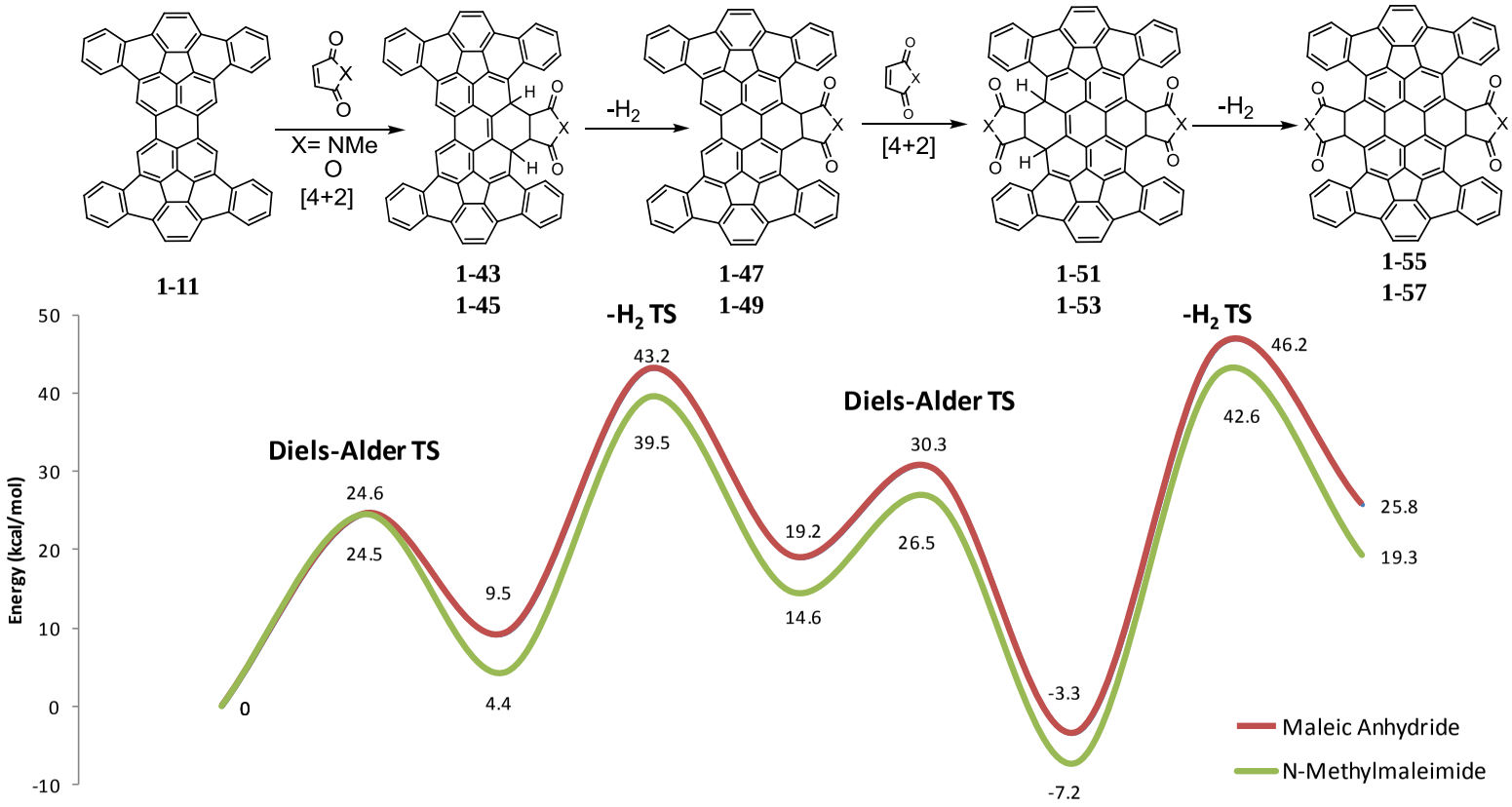

Figure 1-17. Overall Energetics of the Double Diels-Alder Addition (B3LYP/6-31G*//AM1)

1.7 Conclusion

With the successful synthesis of **1-9**, a pivotal intermediate towards the synthesis of a [6,6] carbon nanotube end-cap (**1-8**), molecular complexity was quickly built up. Cyclodehydrogenation was successfully explored and applied to the first direct coupling of a curved polycyclic aromatic hydrocarbon, **1-9**, to form **1-11**. The bay regions of intermediate **1-11**, which contains 56 of the necessary 60 carbon atoms to complete the end-cap **1-8**, was utilized in the successful double Diels-Alder addition of maleimides, installing necessary radical generating functionality. Unfortunately, the insolubility of both starting material and product resulted in a crude reaction mixture that had neither reached full conversion nor could it be purified, complicating progress towards the final target **1-8**. A computational study of the Diels-Alder addition of **1-30** and **1-32** determined that the rearomatization of the central aromatic core is likely the limiting factor in the success of the addition of the dienophiles, and that until rearomatization occurs, the addition is reversible. This barrier is likely too great for the addition of maleic anhydride to be successful.

1.8 Experimentals

1.8.1 General Procedure

All chemicals were purchased from commercial sources and used without further purification unless otherwise noted. The following dry solvents, *o*-dichlorobenzene, *N*,*N*-dimethylacetamide, tetrahydrofuran, dichloromethane, toluene and carbon disulfide, were obtained from a Glass Contour solvent purification system. NMR analysis was performed on 500 MHz and 600 MHz Varian spectrometers unless otherwise noted. NMR shifts were reported in ppm downfield of TMS with chloroform-d_1 (δ_H = 7.26 and δ_C = 77.23) as the standard reference unless otherwise noted. Chromatography was performed with Sorbent Technologies silica gel (porosity = 60 Å, particle size = 32-63 μm) or standard grade neutral alumina (150 mesh). Preparative layer chromatography was performed on 20 cm × 20 cm Analtech silica GF uniplates, alumina GF or reverse phase C18 silica gel plates. Mass spectrometry was carried out at the Boston College mass spectrometry laboratory with MALDI-TOF, DART-TOF, APPI and ESI spectrometers. Infrared spectrometry (IR) was run on a Nicolet Avatar 360 FT-IR spectrophotometer. UV-Vis spectra were recorded on a Hewlett Packard diode array spectrophotometer with a 1 cm cell.

1.8.2. 1,3-*Bis*(2-chlorophenyl)propan-2-one

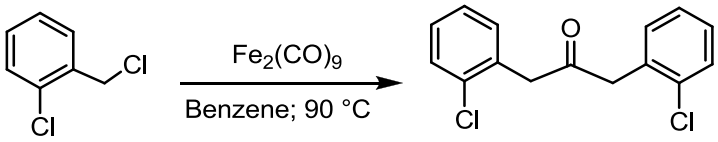

A flame-dried round bottom flask, equipped with a reflux condenser, was purged with nitrogen and charged with 45.3 g (0.124 mol) of $Fe_2(CO)_9$. Anhydrous benzene (325 mL) was added via cannula immediately, and the reaction mixture was stirred.[*] 2-chlorobenzyl chloride (20.0 g, 0.124 mol) was added, and the solution was allowed to stir at reflux for 24 h. A color change was observed from orange to yellow to green over 24 h. The reaction mixture was cooled to room temperature and flushed through a short pad of silica gel with dichloromethane as the eluent. Solvent was removed under reduced pressure. Recrystallization with hexanes afforded 9.86 g (57%) of the desired product as white crystals. **^{1}H NMR** (500 MHz, $CDCl_3$) δ(ppm): 7.46-7.38 (m, 2H), 7.24-7.22 (m, 6H), 3.97 (s, 4H). (Lit.[10a])

[*] $Fe_2(CO)_9$ is pyrophoric and must be handled with care. After addition under nitrogen, the solvent must be added quickly. Once submerged in solvent, the reagent is stable.

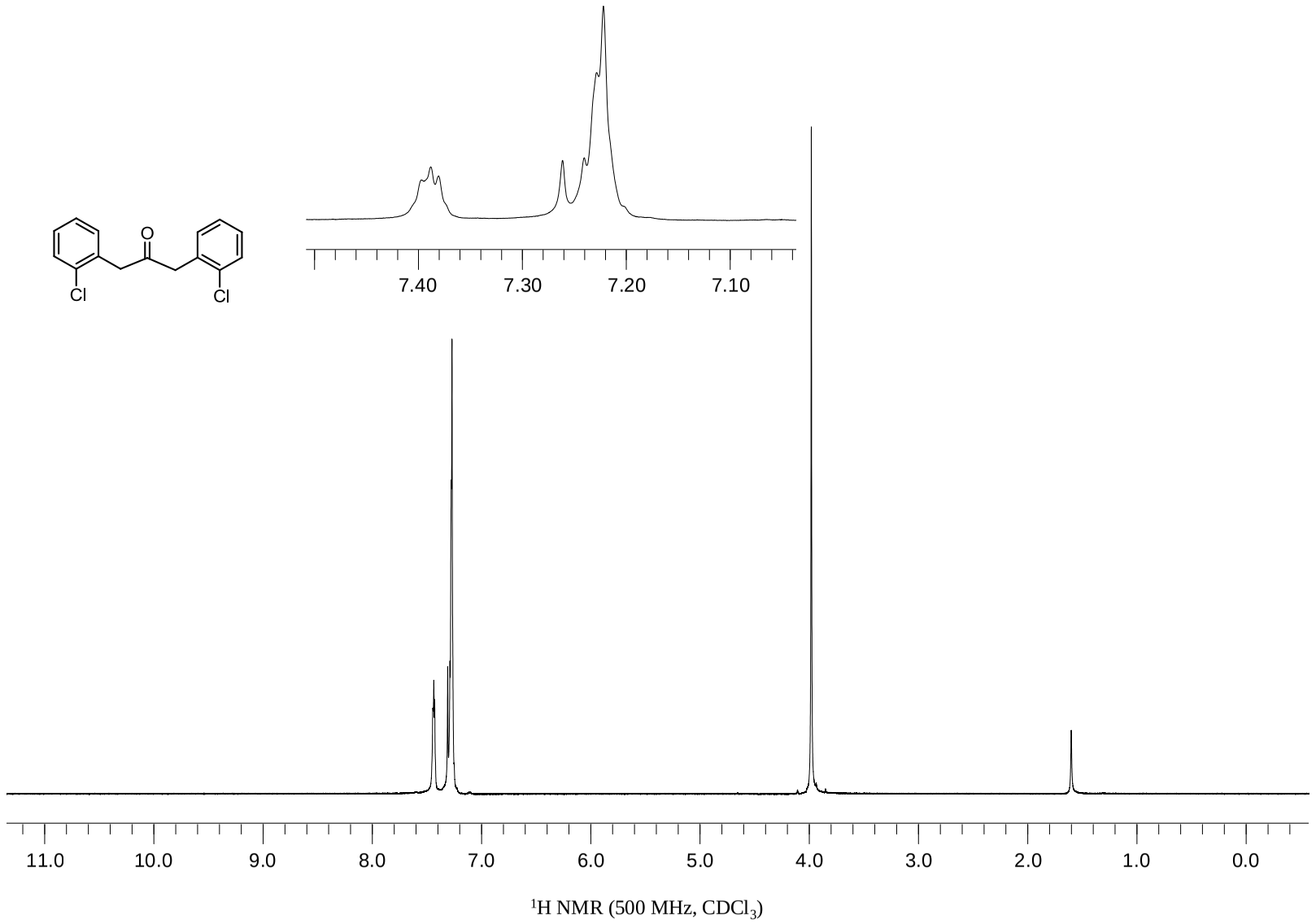

^{1}H NMR (500 MHz, $CDCl_3$)

1.8.3. 1,3-*Bis*(2-bromophenyl)propan-2-one

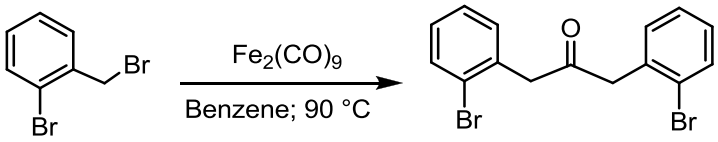

A flame-dried round bottom flask, equipped with a reflux condenser, was purged with nitrogen and charged with 18.9 g (0.052 mol) of $Fe_2(CO)_9$. Anhydrous benzene (175 mL) was added via cannula immediately, and the reaction mixture was stirred.* 2-bromobenzyl bromide (10.0 g, 0.0400 mol) was added, and the solution was allowed to stir at reflux for 24 h. A color change was observed from orange to yellow to green over 24 h. The reaction mixture was cooled to room temperature and flushed through a short pad of silica gel with dichloromethane as the eluent. Solvent was removed under reduced pressure. Recrystallization with hexanes afforded 5.64 g (76%) of 1,3-*bis*(2-bromophenyl)propan-2-one as white crystals. **^{1}H NMR** (500 MHz, $CDCl_3$) δ(ppm): 7.57 (d, *J* = 7.5 Hz, 2H), 7.28 (t, *J* = 7.5 Hz, 2H), 7.23 (d, *J* = 7.5 Hz, 2H), 7.13 (t, *J* = 7.5 Hz, 2H), 3.96 (s, 4H). (Lit.[10a])

* $Fe_2(CO)_9$ is pyrophoric and must be handled with care. After addition under nitrogen, the solvent must be added quickly. Once submerged in solvent, the reagent is stable.

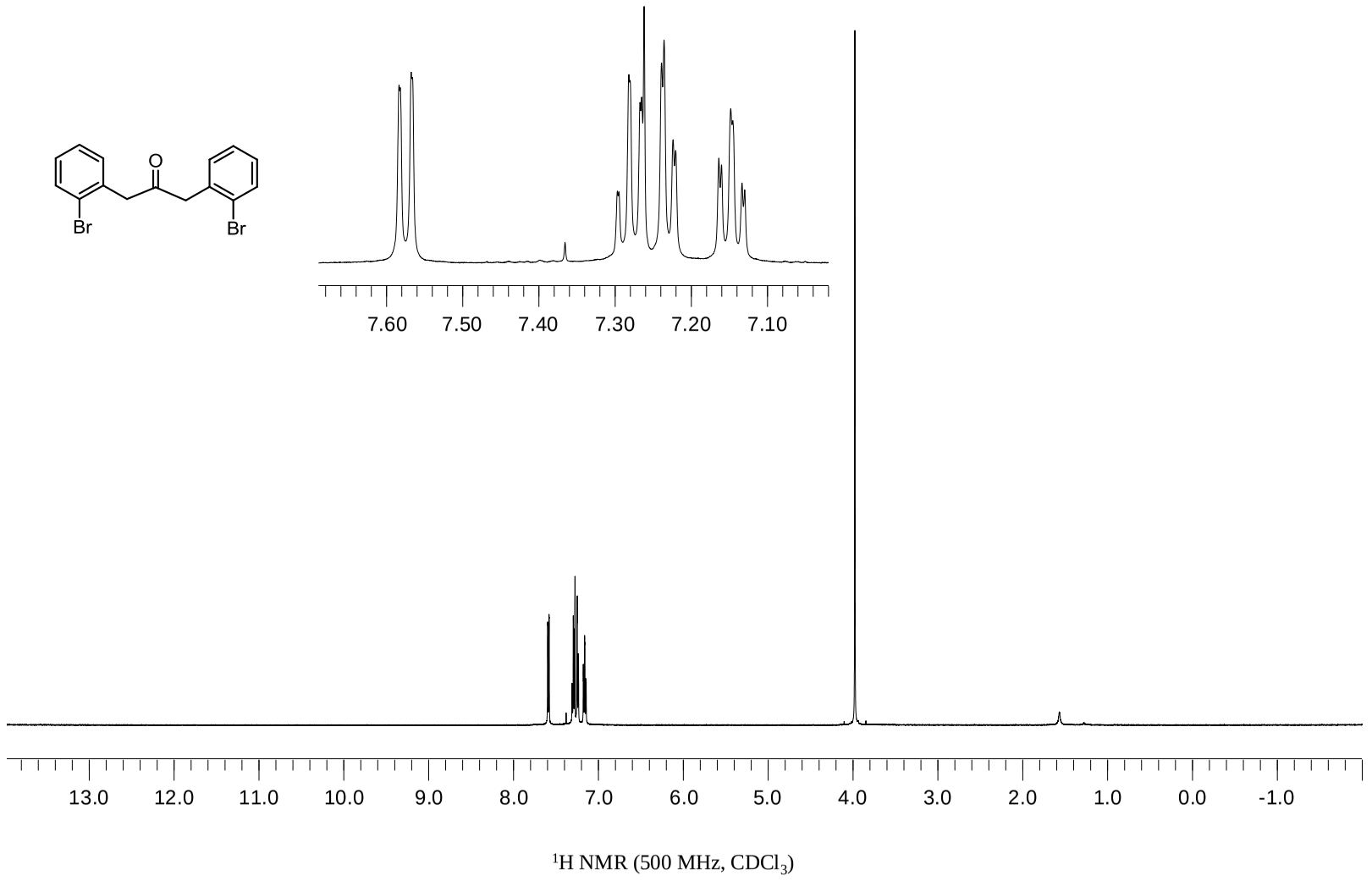

^{1}H NMR (500 MHz, $CDCl_3$)

1.8.4. 7,9-*Bis*(2-chlorophenyl)-8H-cyclopenta[*a*]acenaphthylen-8-one

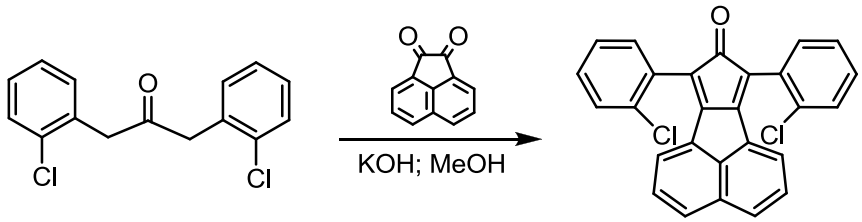

To a 500 mL Erlenmeyer flask, 7.00 g (0.0251 mol) of 1,3-*bis*(2-chlorophenyl)propan-2-one and 4.57 g (0.0251 mol) of acenaphthenequinone were added. KOH (1.83 g, 0.0326 mol) was dissolved in methanol (200 mL), and the basic solution was added to the reaction mixture. The mixture was stirred at room temperature for 2 h. A color change from yellow to purple was observed instantly upon addition of the basic solution. The resulting suspension was allowed to sit overnight without stirring. The purple precipitate was removed by vacuum filtration and washed with methanol to give 10.1 g (95%) of the desired product. **^{1}H NMR** (500 MHz, $CDCl_3$, for a mixture of diastereomers) δ(ppm): 7.86 (d, *J* = 8.0 Hz, 2H), 7.59-7.51 (m, 8H), 7.39-7.35 (m, 4H). (Lit.[10a])

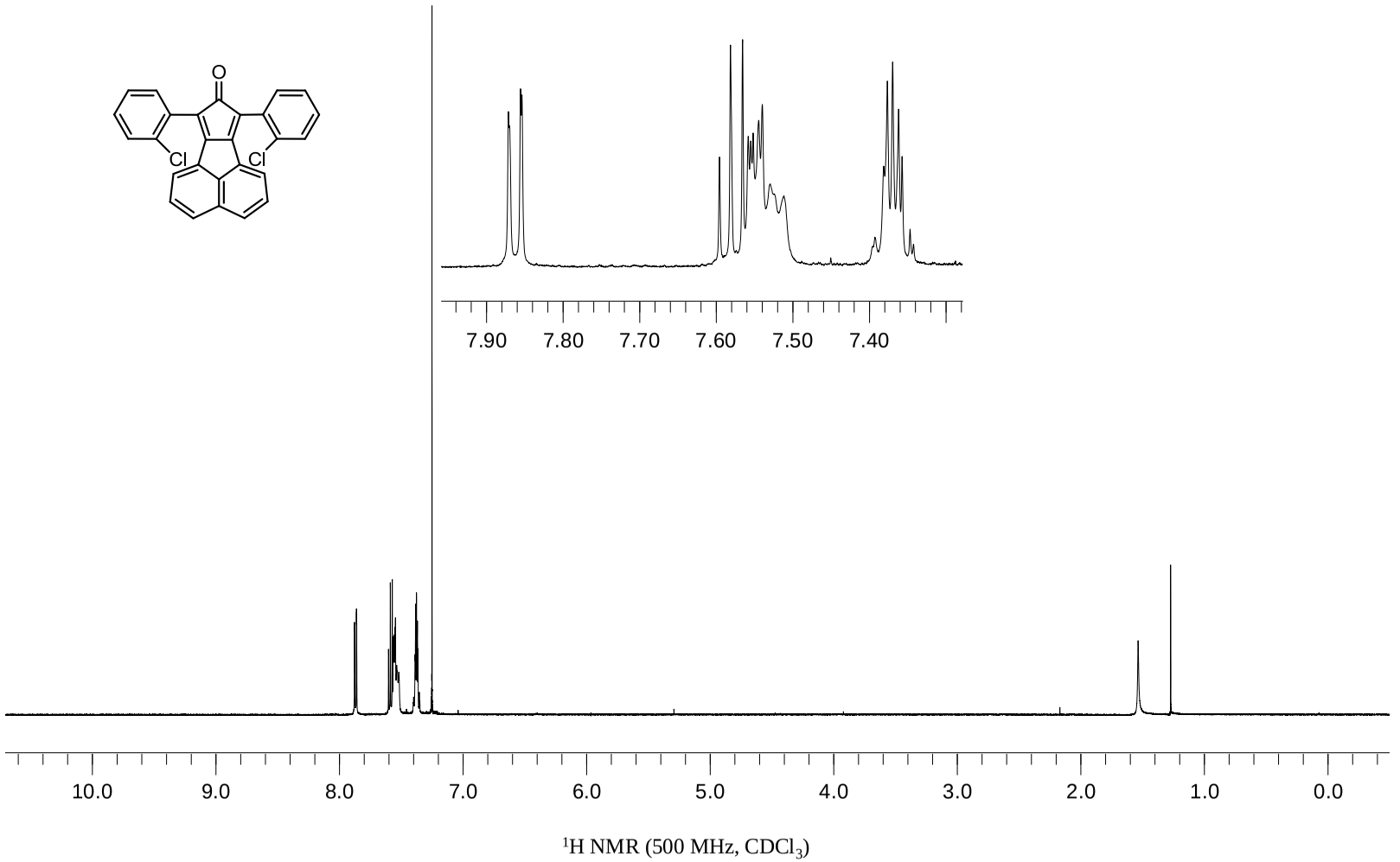

^{1}H NMR (500 MHz, $CDCl_3$)

1.8.5. 7,9-*Bis*(2-bromophenyl)-8H-cyclopenta[*a*]acenaphthylen-8-one

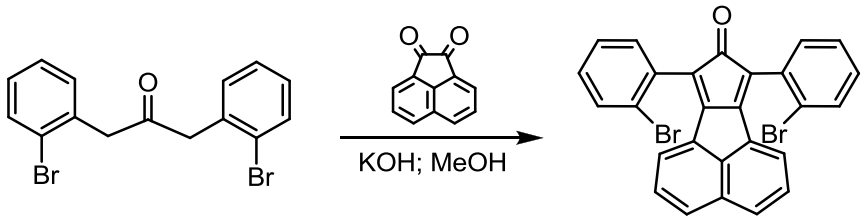

To a 500 mL Erlenmeyer flask, 7.00 g (0.0190 mol) of 1,3-*bis*(2-bromophenyl)propan-2-one and 3.46 g (0.0190 mol) of acenaphthenequinone were added. KOH (0.82 g, 0.0146 mol) was dissolved in methanol (200 mL), and the basic solution was added to the reaction mixture. The mixture was stirred at room temperature for 2 h. A color change from yellow to purple was observed instantly upon addition of the basic solution. The resulting suspension was allowed to sit over night without stirring. The purple precipitate was removed by vacuum filtration and washed with methanol to give 8.84 g (90%) of the desired product. **^{1}H NMR** (500 MHz, $CDCl_3$, for a mixture of diastereomers) δ(ppm): 7.91 (d, *J* = 8.0 Hz, 2H), 7.77 (d, *J* = 8.0 Hz, 2H), 7.62-7.56 (m, 4H), 7.54-7.52 (m, 2H), 7.48-7.45 (m, 2H), 7.35-7.30 (m, 2H). (Lit.[10a])

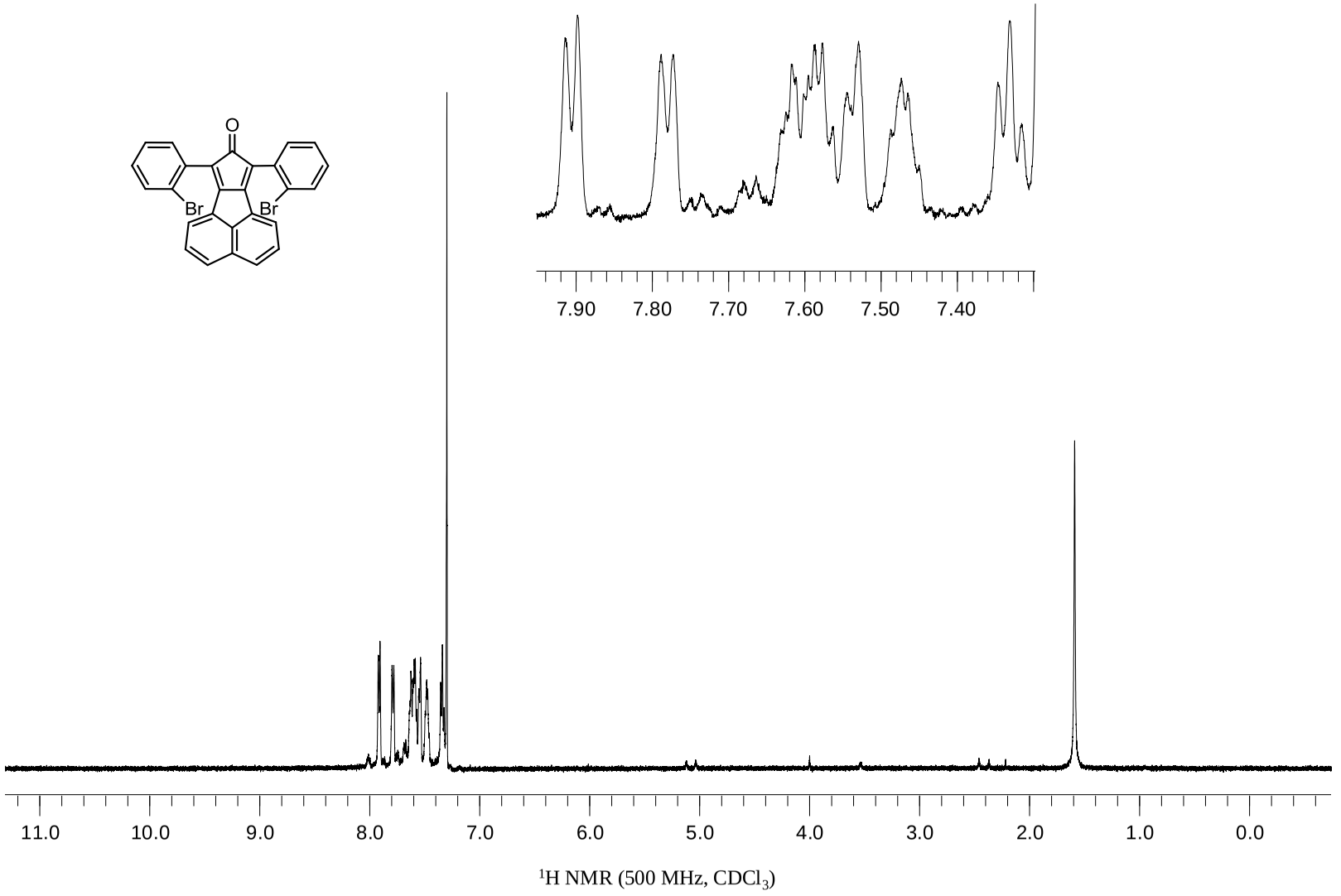

^{1}H NMR (500 MHz, $CDCl_3$)

1.8.6. 7,10-*Bis*(2-chlorophenyl)fluoranthene

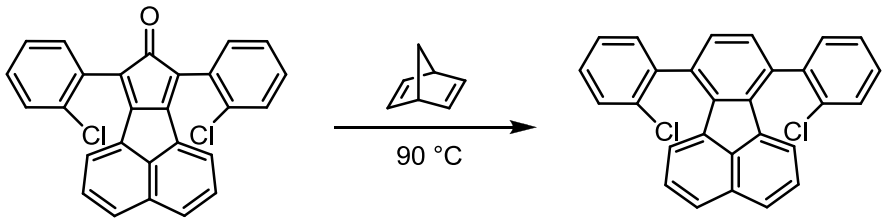

To a round bottom flask, 10.0 g (0.0236 mol) of 7,9-*bis*(2-chlorophenyl)-8H-cyclopenta[*a*]acenaphthylen-8-one and 50.0 mL norbornadiene were added. The reaction mixture was stirred at reflux for 5 d. The mixture was cooled to room temperature, and the solvent was removed under reduced pressure. The resulting oily residue was purified by silica gel chromatography with 3:1 hexanes : dichloromethane as the eluent to afford 6.30 g (64 %) of the desired product as a yellow solid. **^{1}H NMR** (500 MHz, $CDCl_3$) δ(ppm): 7.75 (d, *J* = 8.0 Hz, 2H), 7.64-7.62 (m, 2H), 7.60 (dd, *J* = 8.0 Hz, *J* = 2.0 Hz, 2H of major diastereomer), 7.54 (dd, *J* = 8.0 Hz, *J* = 2.0 Hz, 2H of minor diastereomer), 7.50-7.45 (m, 4H), 7.36 (dd, *J* = 8.0 Hz, *J* = 2.0 Hz, 2H), 7.287 (s, 2H of major diastereomer), 7.284 (s, 2H of minor diastereomer), 6.88 (d, *J* = 8.0 Hz, 2H of minor diastereomer), 6.87 (d, *J* = 8.0 Hz, 2H of major diastereomer). (Lit.[10a])

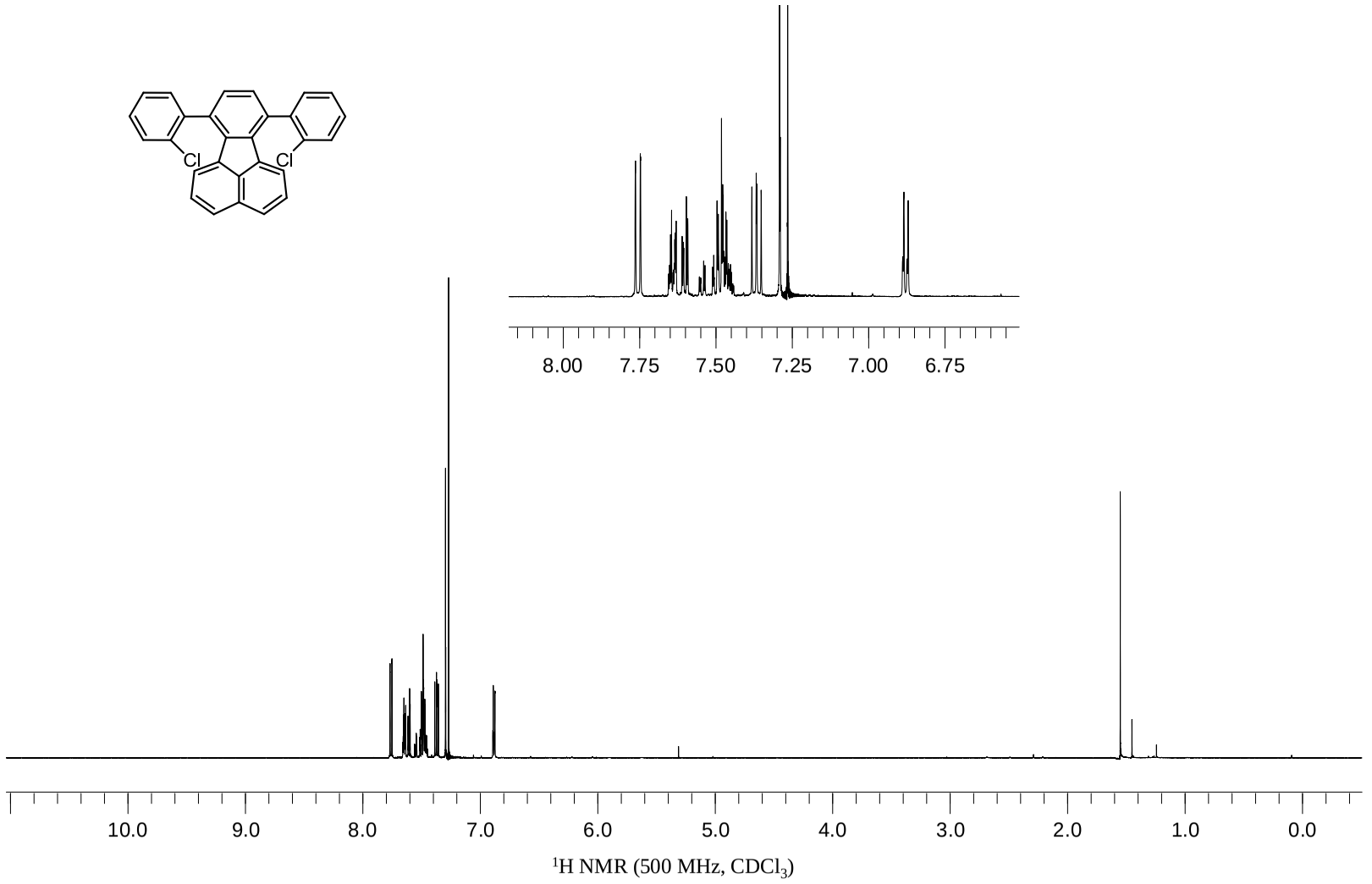
Cl
Cl
8.00
7.75
7.50
7.25
7.00
6.75
10.0
9.0
8.0
7.0
6.0
5.0
4.0
3.0
2.0
1.0
0.0
^{1}H NMR (500 MHz, $CDCl_3$)

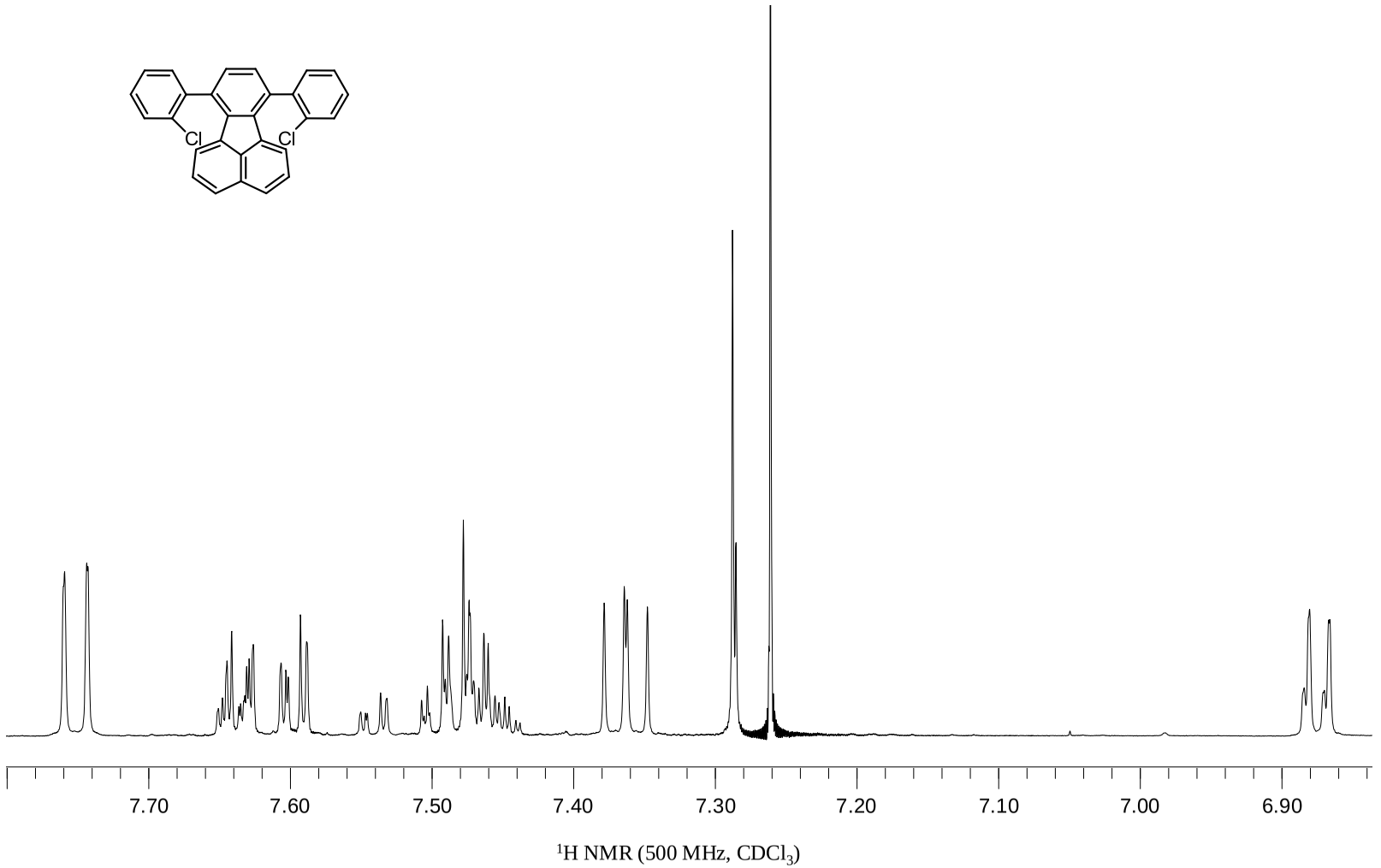

^{1}H NMR (500 MHz, $CDCl_3$)

1.8.7. 7,10-*Bis*(2-bromophenyl)fluoranthene

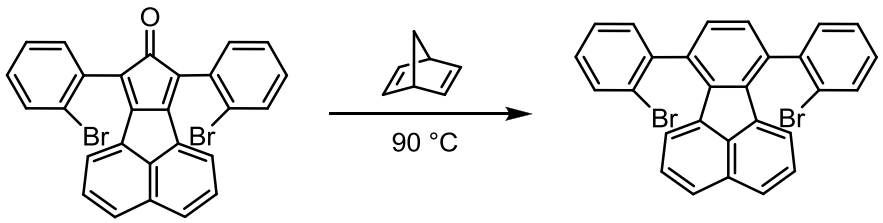

To a round bottom flask, 20.1 g (0.0390 mol) of 7,9-*bis*(2-bromophenyl)-8H-cyclopenta[*a*]acenaphthylen-8-one and 150 mL norbornadiene were added. The reaction mixture was stirred at reflux for 5 d. The mixture was cooled to room temperature and the solvent was removed under reduced pressure. The resulting oily residue was purified by silica gel chromatography with 3:1 hexanes : dichloromethane as the eluent to afford 14.2 g (71 %) of the desired product as a yellow solid. **^{1}H NMR** (500 MHz, $CDCl_3$) δ(ppm): 7.84 (d, *J* = 8.0 Hz, 2H of major diastereomer), 7.83 (d, *J* = 8.0 Hz, 2H of minor diastereomer), 7.76 (d, *J* = 7.5 Hz, 2H), 7.61 (d, *J* = 8.0 Hz, 2H of major diastereomer), 7.60 (d, *J* = 8.0 Hz, 2H of minor diastereomer), 7.53 (t, *J* = 7.5 Hz, 2H of major diastereomer), 7.52 (t, *J* = 7.5 Hz, 2H of minor diastereomer), 7.42 (t, *J* = 7.5 Hz, 2H of major diastereomer) 7.41 (t, *J* = 7.5 Hz, 2H of minor diastereomer), 7.36 (dd, *J* = 7.5 Hz, *J* = 1.0 Hz, 2H), 7.269 (s, 2H of major diastereomer), 7.265 (s, 2H of minor diastereomer), 6.83 (d, *J* = 8.0 Hz, 2H). (Lit.[10a])

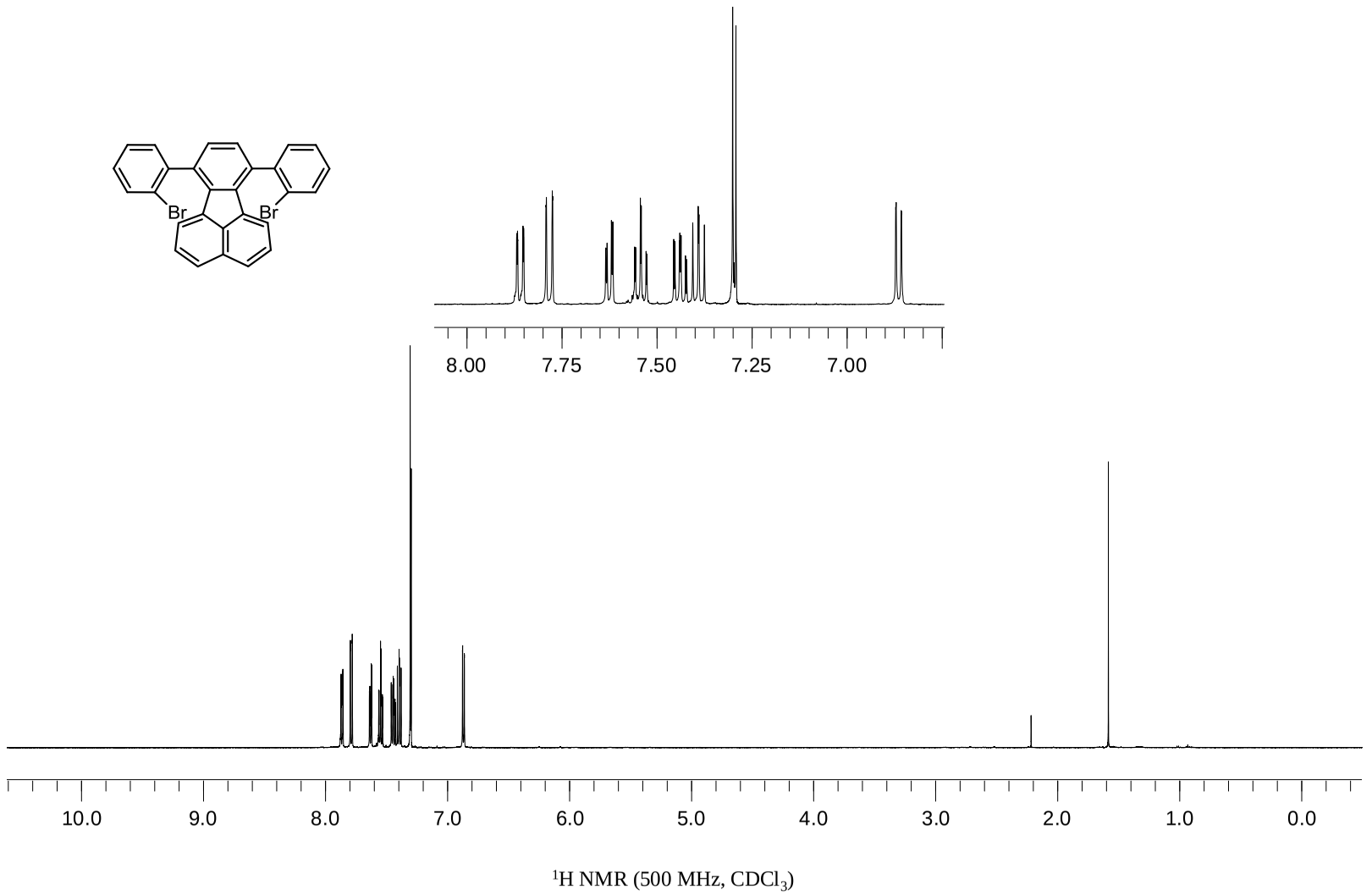

^{1}H NMR (500 MHz, $CDCl_3$)

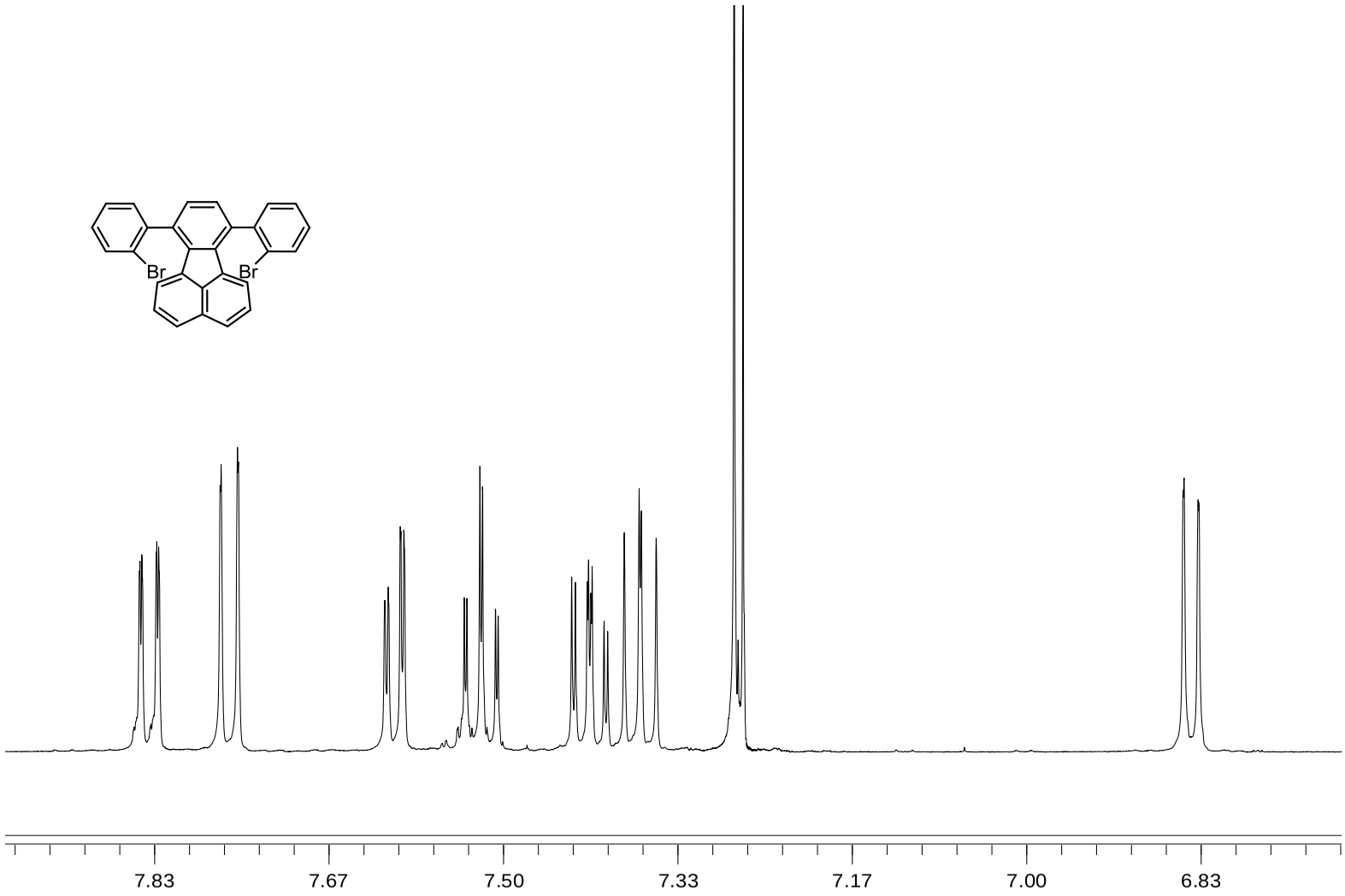

^{1}H NMR (500 MHz, $CDCl_3$)

1.8.8. Dibenzo[*a,g*]corannulene

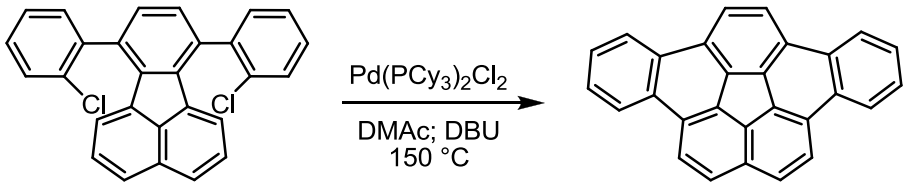

To a flame-dried, nitrogen purged pressure vessel equipped with a stir bar, 2.00 g (4.73 mmol) of 7,10-*bis*(2-chlorophenyl)fluoranthene and 270 mg (0.473 mmol) of $Pd(PCy_3)_2Cl_2$ were added under a nitrogen atmosphere. Anhydrous DMAc (17.0 mL) and DBU (14.3 mL) were added via syringe, and the reaction mixture was stirred. The vessel was sealed and heated in a pre-heated oil bath at 150 ˚C for 3 d. The mixture was cooled to room temperature and flushed through a short pad of neutral alumina with dichloromethane as the eluent. The filtrate was washed with 10 % HCl (2x) and once with water. The organic layer was dried over magnesium sulfate and concentrated to dryness under vacuum. The product was recrystallized in hexanes to provide 1.32 g (80%) of the desired product as a tan solid. **^{1}H NMR** (500 MHz, $CDCl_3$) δ(ppm): 8.73-8.71 (m, 2H), 8.68-8.67 (m, 2H), 8.38 (s, 2H), 8.28 (d, *J* = 8.5 Hz, 2H), 8.00 (d, *J* = 8.5 Hz, 2H), 7.78-7.76 (m, 4H). (Lit.[10a])

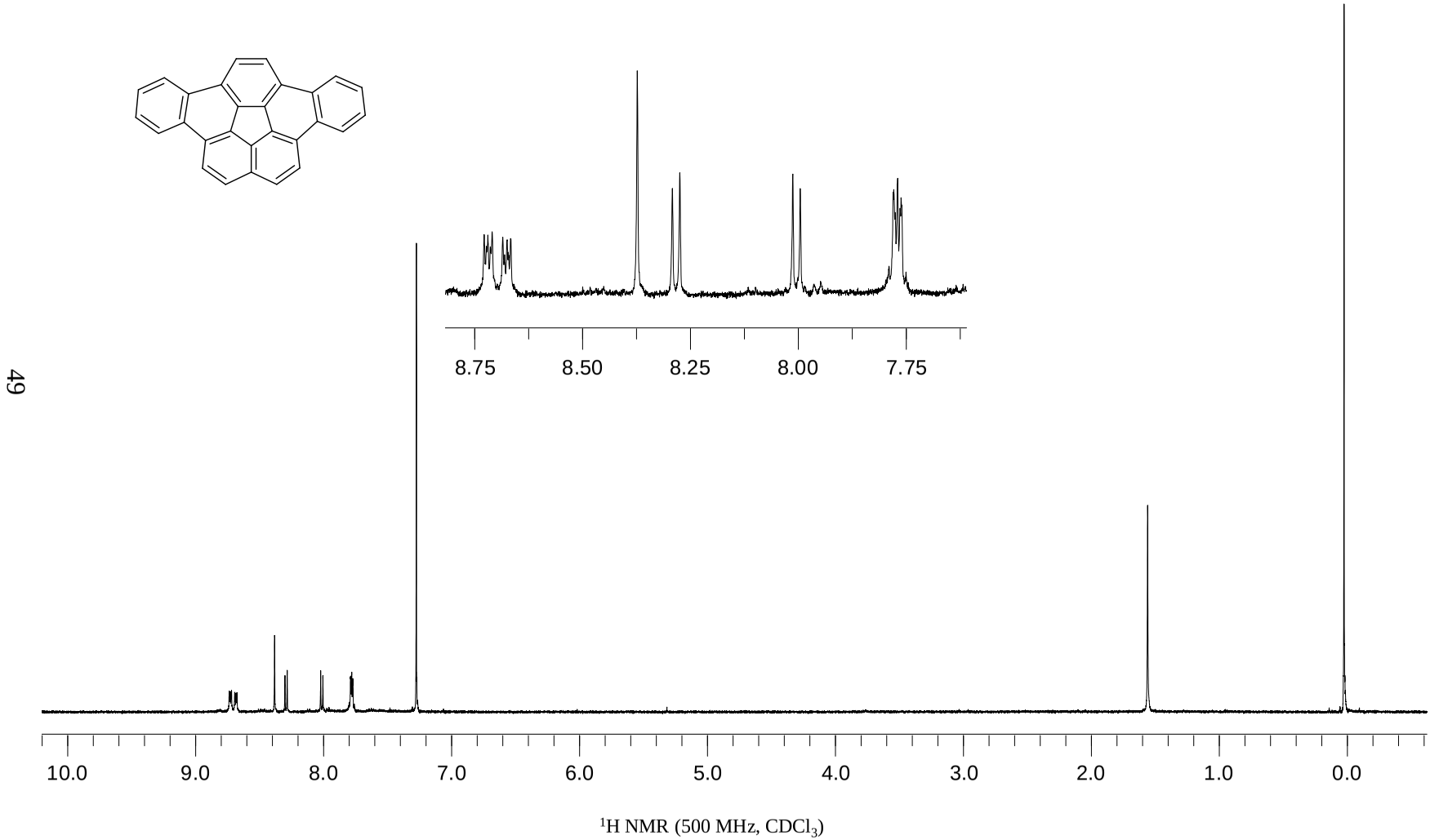

^{1}H NMR (500 MHz, $CDCl_3$)

1.8.9. *Peri-bis*(dibenzo[*a,g*]corannulene)

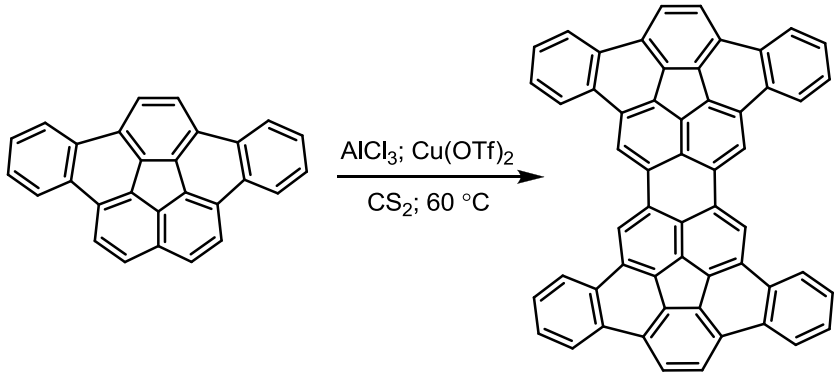

To a flame-dried, nitrogen purged pressure vessel, equipped with a stir bar, was added 1.60 g (12.0 mmol) of $AlCl_3$ and 1.99 g (5.50 mmol) of $Cu(OTf)_2$. To this mixture, 50.0 mL of anhydrous CS_2 and 0.700 g (2.00 mmol) dibenzo[*a,g*]corannulene were added and stirred. The vessel was sealed and placed in a 60 ˚C pre-heated oil bath overnight. The mixture was cooled to room temperature poured into cold 10% HCl. The resulting precipitate was removed by vacuum filtration and washed vigorously with dichloromethane, methanol and water to provide 0.633 g (91%) of a redish-brown solid. **HRMS** (MALDI-TOF): Calc'd for $C_{56}H_{24}$ (M^+) 696.1878, found 696.1879. (Lit.[10a])

EI MS of *Peri-bis*(dibenzo[*a*,*g*]corannulene)

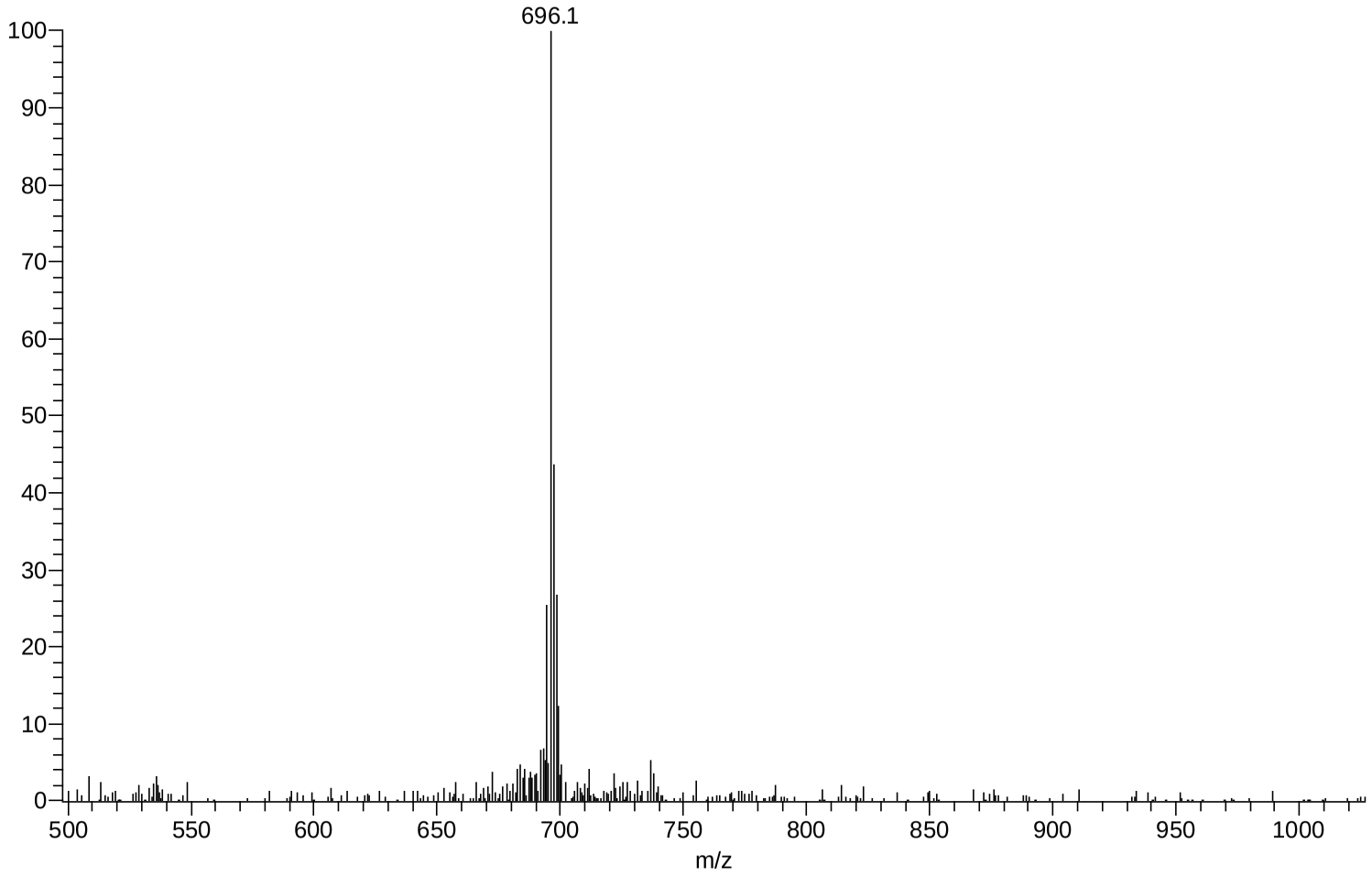

1.8.10. Tetrabenzo[*a,g,o,u*]circum[5.6.5]quinarene-7,8,15,16-tetracarboxylic acid 7,8:15,16-*bis*(*N*-phenylimide)

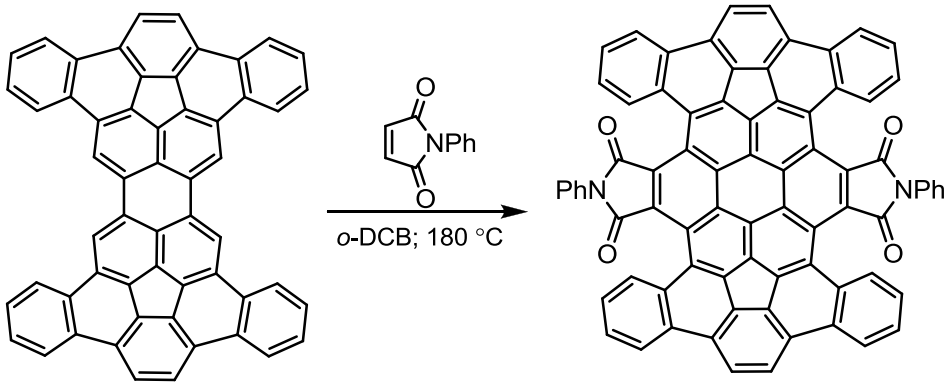

To a flame-dried, nitrogen purged pressure vessel, equipped with a stir bar, was added 50.0 mg (0.0718 mmol) of *peri*-*bis*(dibenzo[*a*,*g*]corannulene) and 374 mg (2.16 mmol) of *N*-phenylmaleimide. Anhydrous *o*-dichlorobenzene (1.00 mL) was added, and the reaction mixture was stirred under nitrogen. The vessel was sealed and placed in a pre-heated oil bath (180 ˚C) for 5 d. The reaction mixture was cooled to room temperature and stirred in ethanol for 1 h. The dark red precipitate was filtered and washed with hexanes and ethanol to provide 46.0 mg of a dark red solid. **HRMS** (MALDI-TOF): Calc'd for $C_{76}H_{30}N_2O_4$ (M^+) 1034.2201, found 1034.2292.

MALDI-TOF MS (DCTB Matrix) of Tetrabenzo[*a,g,o,u*]circum[5.6.5]quinarene-7,8,15,16-tetracarboxylic acid 7,8:15,16-*bis*(*N*-phenylimide)

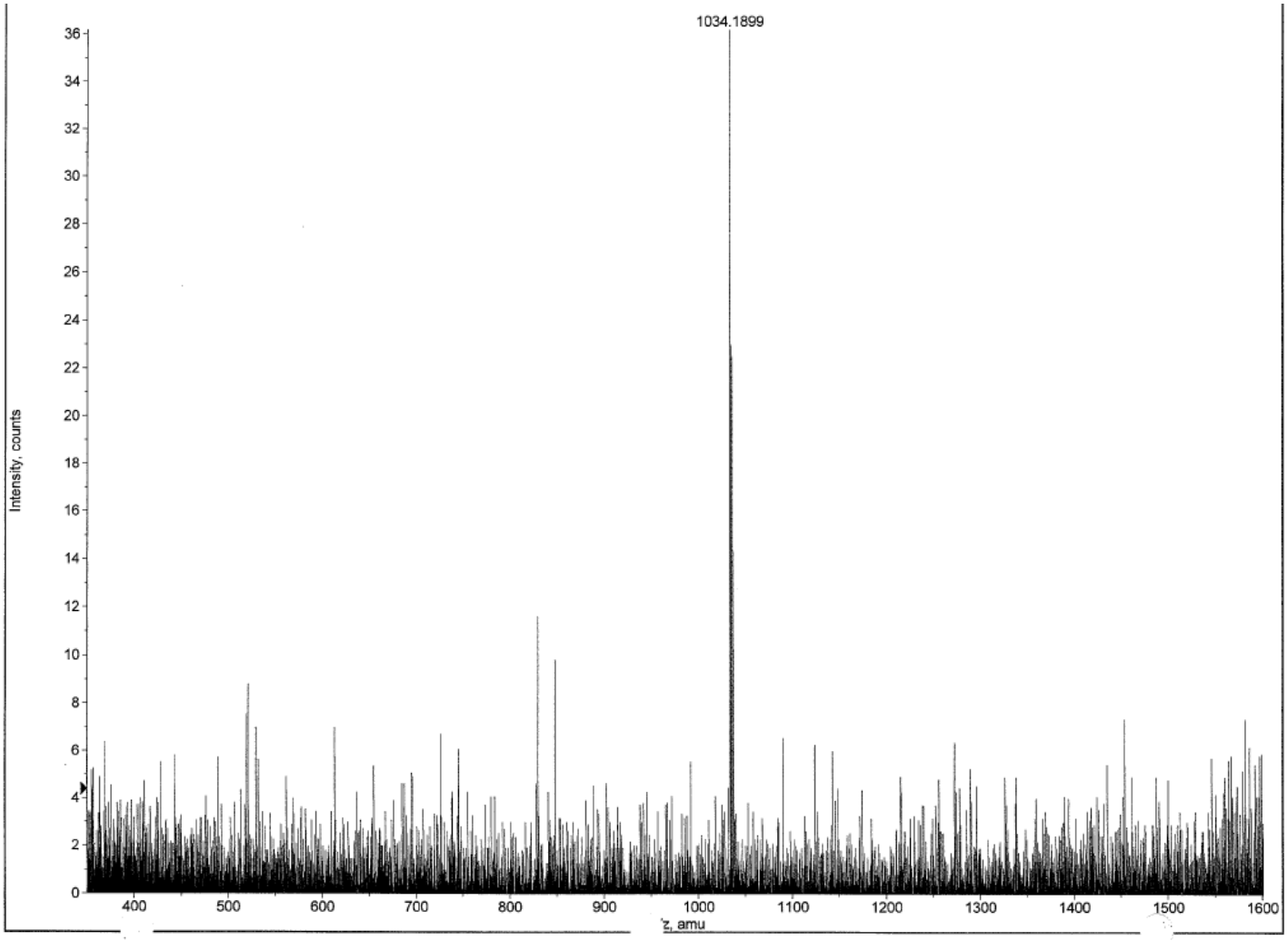

1.8.11. Tetrabenzo[*a,g,o,u*]circum[5.6.5]quinarene-7,8,15,16-tetracarboxylic acid 7,8:15,16-*bis*(*N*-methylimide)

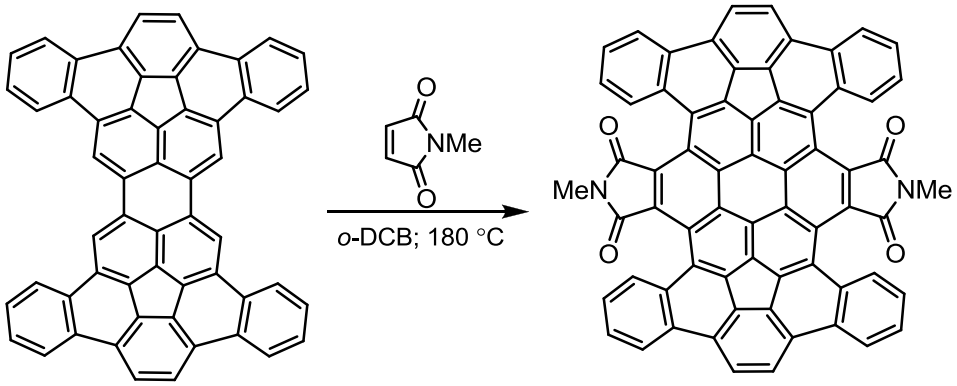

To a flame-dried, nitrogen purged pressure vessel, equipped with a stir bar, was added 25.0 mg (0.0359 mmol) of *peri-bis*(dibenzo[*a,g*]corannulene and 79.8 mg (0.718 mmol) of *N*-methylmaleimide. Anhydrous *o*-dichlorobenzene (0.50 mL) was added, and the reaction mixture was stirred under nitrogen. The vessel was sealed and placed in a pre-heated oil bath (180 ˚C) for 5 d. The reaction mixture was cooled to room temperature and stirred in ethanol for 1 h. The dark red precipitate was filtered and washed with hexanes and ethanol to provide 21.0 mg of a dark red solid. **HRMS** (MALDI-TOF): Calc'd for $C_{66}H_{26}N_2O_4$ (M^+) 910.1893, found 910.1889.

MALDI-TOF MS (DCTB Matrix) of Tetrabenzo[*a,g,o,u*]circum[5.6.5]quinarene-7,8,15,16-tetracarboxylic acid 7,8:15,16-*bis*(*N*-methylimide)

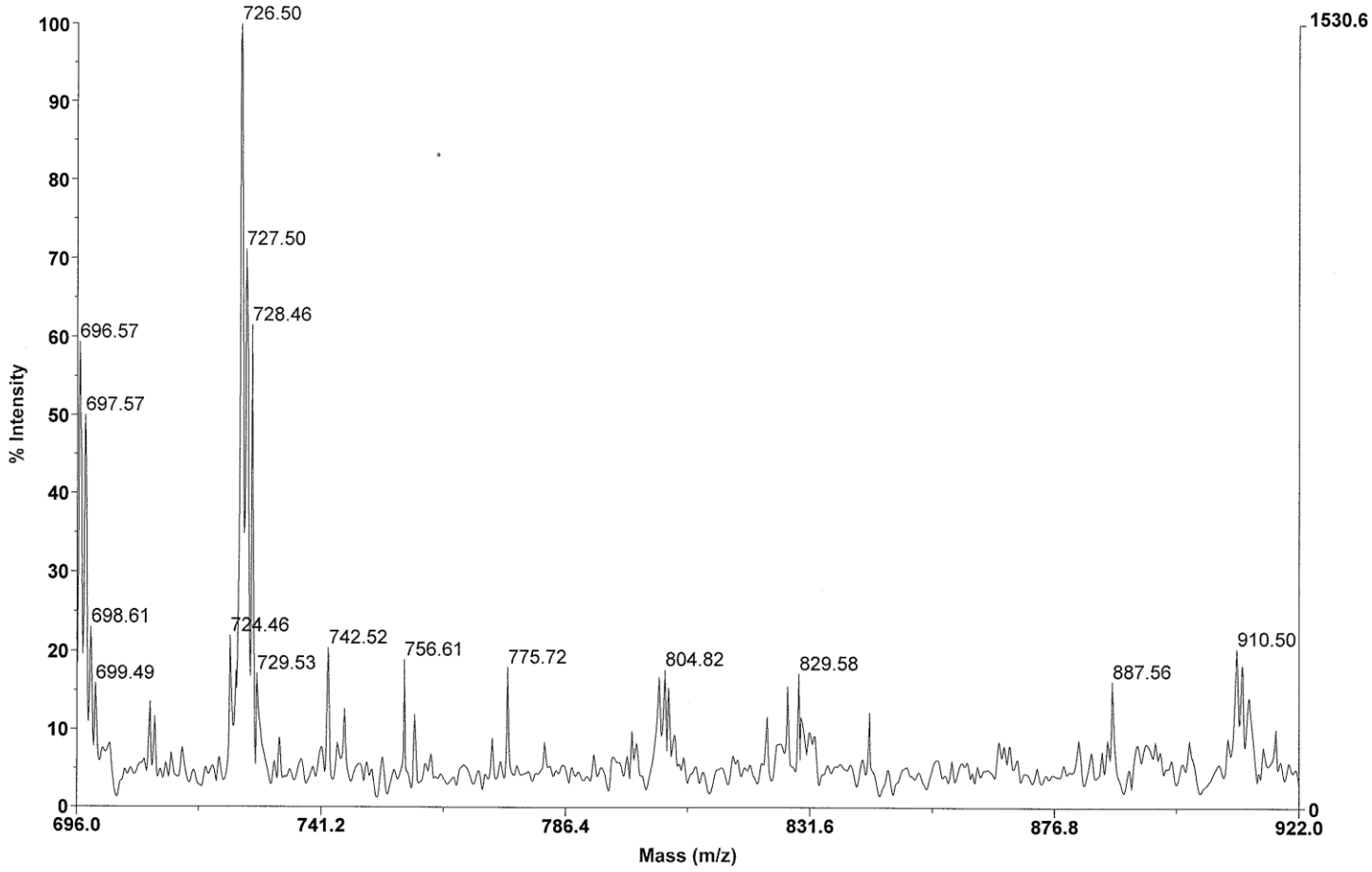

1.8.12. Spartan Calculations:

All calculations were performed using density functional theory at the B3LYP/6-31G* level employing the program Spartan ’06 or ‘10. Initial geometry optimizations or transition state searches were completed at the Semi-empirical AM1 level of theory and then single point energy calculations or transition state searches were performed using density functional theory at B3LYP/6-31G*. Complete vibration analyses were performed to confirm that all starting materials have no imaginary frequencies and that all transition states (TS) have one imaginary frequency.

Table 1-1. Calculated energies of molecules in Figures 1-17, 1-18. XYZ Coordinates of Calculations for the Structures in Figure 1-17 and 1-18 can be found in Appendix A.

Molecule	Energy (hartree)
1-11	-2148.52585
1-30	-379.289461
1-32	-398.744208
1-42	-2547.23111
1-44	-2525.77617
1-43	-2547.26306
1-45	-2527.800246
H_2	-1.17548426
1-46	-2547.207059
1-48	-2527.746464
1-47	-2547.246744
1-50	-2944.79645
1-52	-2905.88100
1-51	-2944.85013
1-53	-2905.92976
1-54	-2944.77034
1-55	-2905.85427
1-56	-2943.63235
1-57	-2904.70797

1.9 References

[1] Shirota, Y. *J. Mater. Chem.* **2000**, *10*, 1-25.

[2] Tsefrikas, V. M.; Scott, L. T. *Chem. Rev*. **2006**, *106*, 4868−4884.

[3] (a) Scott, L. T. *Pure Appl. Chem.* **1996**, *68*, 291-300 (b) Scott, L. T.; Bronstein, H. E.; Preda, D. V.; Ansems, R. B. M.; Bratcher, M. S.; Hagen, S. *Atual. Fis.-Quim. Org.* **1999**, *11*, 138-150. (c) Scott, L. T.; Bronstein, H. E.; Preda, D. V.; Ansems, R. B. M.; Bratcher, M. S.; Hagen, S. *Pure Appl. Chem.* **1999**, *71*, 209-219. (d) Bronstein, H. E.; Scott, L. T. *J. Org. Chem.* **2008**, *73*, 88-93.

[4] Iijima, S. *Nature* **1991**, *354*, 56-58.

[5] Collins, P. G.; Avouris, P. *Sci. Am.* **2000**, *283*, 62−69.

[6] Guldi, D. M.; Martin, N. *Carbon Nanotubes and Related Structures: Synthesis, Characterization, Functionalization, and Applications;* Wiley-VCH: Weinheim, 2010.

[7] Scott, L. T.; Jackson, E. A.; Zhang, Q.; Steinberg, B. D.; Bancu, M.; Li, B. *J. Am. Chem.Soc*. **2012**, *134*, 107−110.

[8] Butterfield, A. M.; Gilomen, B.; Siegel, J. S. *Org. Process Res. Dev.* **2012**, (doi.org/10.1021/op200387s).

[9] Fort, E. H. Ph.D. Dissertation, Boston College, Chestnut Hill, MA, 2010.

[10] (a) Tsefrikas, V. M. Ph.D. Dissertation, Boston College, Chestnut Hill, MA, 2007. (b) Jackson, E. A. Ph.D. Dissertation, Boston College, Chestnut Hill, MA, 2008. (c) Quimby, J. M. Ph.D. Dissertation, Boston College, Chestnut Hill, MA, 2011. (d) Hill, T. Ph.D. Dissertation, Boston College, Chestnut Hill, MA, 2007.

[11] Brown, R. F. C. *Aust. J. Chem.* **2010**, *63*, 1002–1006.

[12] (a) Seiders, T. J.; Baldridge, K. K., Siegel, J. S. *J. Am. Chem. Soc.* **1996**, *118*, 2754-2755. (b) Wu, Y. T.; Siegel, J. S. *Chem. Rev.* **2006**, *106*, 4843-4867.

[13] Bratcher, M. S. Ph. D. Dissertation, Boston College, Chestnut Hill, MA, 1996.

[14] Reisch, H. A.; Bratcher, M. S.; Scott, L. T. *Org. Lett.* **2000**, *2*, 1427-1430.

[15] (a) Bhandari, S; Ray, S. *Synth. Commun.* **1998**, *28*, 765-771. (b) Sauriat-Dorizon, H.; Maris, T.; Wuest, J. D. *J. Org. Chem.* **2003**, *68*, 240-246.

[16] Stable, A.; Hervig, P.; Müllen, K.; Rabe, J. P. *Angew. Chem. Int. Ed. Engl.* **1995**, *34*, 1609-1611.

[17] (a) Rempala, P.; Kroulik, J.; King, B. T. *J. Am. Chem. Soc.* **2004**, *126*, 15002-15003. (b) Rempala, P.; Kroulik, J.; King, B. T. *J. Org. Chem.* **2006**, *71*, 5067-5081. (c) King, B. T.; Kroulik, J.; Robertson, C. R.; Rempala, P.; Hilton, P. L.; Korinek, J. D.; Gortari, J. M. *J. Org. Chem.* **2007**, *72*, 2279-2288. (d) Wehmeier, M.; Wagner, M.; Müllen, K. *Chem. Eur. J.* **2001**, *7*, 2197-2205.

[18] (a) Kovacic, P.; Lange, R. M. *J. Org. Chem.* **1963**, *28*, 968-972. (b) Kovacic, P.; Jones, M. B. *Chem. Rev.* **1987**, *87*, 357-379. (c) Takada, T.; Arisawa, M.; Gyoten, M.; Hamada, R.; Tohma, H.; Kita, Y. *J. Org. Chem.* **1998**, *63*, 7698-7706. (d) Churruca, R.; SanMartin, R.; Carril, M.; Urtiaga, M. K.; Solans, X.; Tellitu, I.; Dominguez, E. *J. Org. Chem.* **2005**, *70*, 3178-3187.

[19] Clar, E.; Zander, M. *J. Chem. Soc.* **1957**, 4616-4619.

[20] Clar, E.; McAndrew, B. *Tetrahedron* **1972**, *28*, 1137.

[21] Sauer, J.; Wiest, H.; Mielert, A. *Chem. Ber.* **1964**, *97*, 3183.

[22] The geometry of all compounds were optimized using Spartan ’06 and Spartan ‘10. The Semi-Empirical geometries were optimized at the AM1 level of theory and single point DFT energies were calculated at the B3LYP/6-31G* level of theory.

[23] Kemnitz, C. R.; Loewen, M. J. *J. Am. Chem. Soc.* **2007**, *129*, 2521-2528.

Chapter 2

Synthesis of Solubility-Enhancing Dienophiles for the Diels-Alder Addition to *Peri-bis*(dibenzo[*a*,*g*]corannulene)

2.1 Introduction

The limited solubility of *peri-bis*(dibenzo[*a,g*]corannulene) (**1.11**) had presented significant complications in the double Diels-Alder addition of *N*-methyl and *N*-phenyl maleimides to **1-11**, as presented in chapter 1. More importantly, if the efficiency of the Diels-Alder addition was not improved, this synthetic route towards the desired [6,6] carbon nanotube end-cap would not be viable. It had been shown that addition of maleimides as dienophiles was possible, installing the final four carbon atoms necessary for the desired end-cap and incorporating the 1,2-diradical generating functionality required to stitch up the Diels-Alder adduct to the end-cap.[1] However, the insolubility of **1-11** hampered the reaction from ever reaching completion, even under harsh and forcing conditions. Furthermore, the insolubility of the resulting Diels-Alder adducts impeded purification.

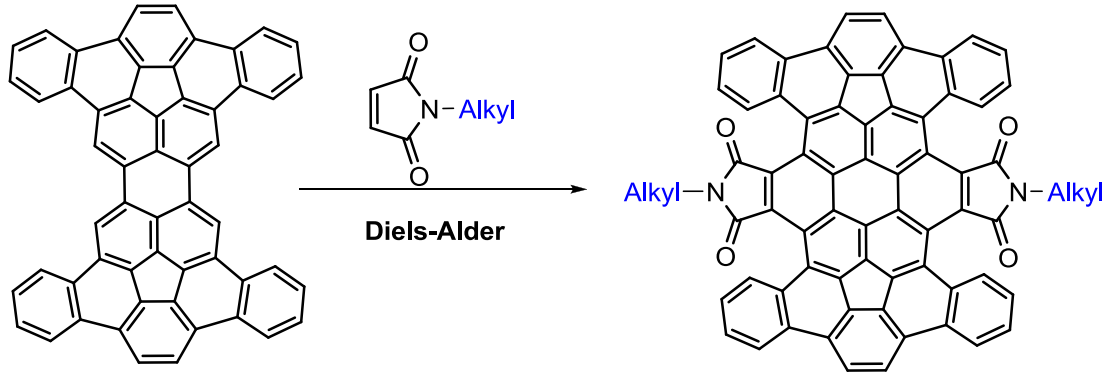

1-11 **2-1**

Scheme 2-1. Proposed Diels-Alder Addition of Alkyl Maleimides

Due to these factors, the introduction of solubility-enhancing groups through Diels-Alder addition were explored (Scheme 2-1). The introduction of bulky alkyl groups, through the

Diels-Alder addition of bulky alkyl maleimides, should break up the problematic aggregation, forming a soluble Diels-Alder adduct, **2-1**, allowing for separation and purification of the desired product from the insoluble starting material.

2.2 Synthesis of Alkyl Maleimides

Aiming to introduce solubility through the addition of a solubilizing group on the dienophile via the Diels-Alder addition to **1-11**, the synthesis of an alkyl maleimide was explored. Since introduction of a large alkyl group onto the molecule would add significant mass, which was of concern in later stages of the synthesis, it was desirable to make the alkyl group removable. It was expected that a tertiary alkyl group should be acid labile, which would allow for elimination of the alkyl group but leave the maleimide intact, providing a simplified 1,2-diradical generating intermediate for the formation of the end-cap (Scheme 2-2).

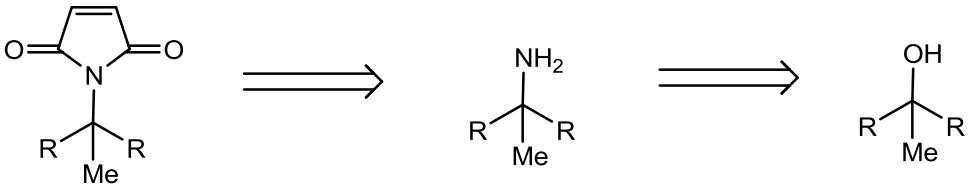

R= Me; **2-2** R= Pr; **2-3** | **2-4** **2-5** | **2-6** **2-7**

Scheme 2-2. Retrosynthetic Analysis

The simplest alkyl maleimide considered was *N-tert*-butylmalimide (**2-2**); however, it was decided that the *tert*-butyl group would likely not provide enough bulk to break up the aggregation of the molecules. Focus was turned towards synthesizing an alkyl maleimide containing larger alkyl chains, specifically where R= propyl (**2-3**), while still

maintaining the tertiary methyl group necessary for future removal. Access to maleimide **2-3** can be envisioned from the tertiary amine **2-5**, which may be accessed from a tertiary alcohol **2-7**.

Beginning with the symmetrical ketone, **2-8**, Grignard addition with methyl magnesium bromide provided **2-7** in an 85% yield (Scheme 2-3). The alcohol, **2-7**, was subjected to Ritter conditions[2] with acetonitrile to form the desired acetamide, **2-9**, in a 93% yield**.** From the amide **2-9,** it was proposed that hydrolysis of the amide would provide access to the tertiary amine, **2-5**; however, this hydrolysis was plagued with inconsistencies.

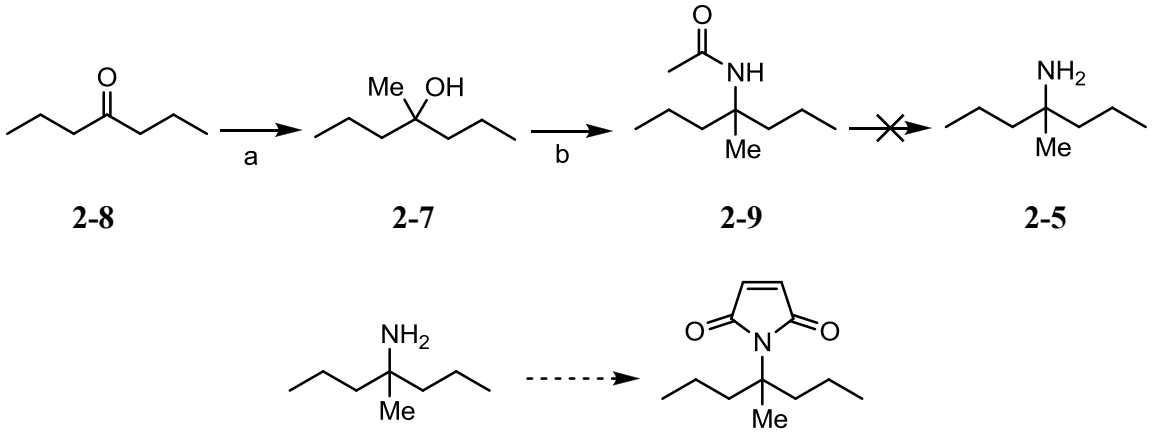

a) 1. MeMgBr, Et_2O, 0 ˚C 2. 10% HCl; **85%** b) H_2SO_4, ACN, AcOH, RT; **93%**

Scheme 2-3. Attempted Synthesis of an Alkyl Maleimide

Initial hydrolysis investigations using strongly acidic conditions were explored but failed to provide any trace of the desired amine (Table 2-1, entries 1, 2 and 3). Strongly basic hydrolysis conditions were also explored with potassium hydroxide in both water and ethylene glycol but failed to provide any isolable amine, and significant decomposition

was observed (Table 2-1, entries 4, 5 and 6).[3] It was apparent from literature precedent that the hydrolysis of tertiary amides was a challenging process, and, unfortunately, the isolation of **2-5** was unsuccessful.[4] Due to these pitfalls, this route was abandoned, and a new, more efficient route was explored.

Table 2-1. Amide Hydrolysis Conditions

Entry	Acid or Base	Solvent	T (° C)	Time (h)	Result
1	HCl (conc.)	-	110	24	Decomposition
2	HCl (6M)	-	110	6	Decomposition
3	HCl (1M)	-	110	16	No reaction
4	KOH (6M)	H_2O	110	16	No reaction
5	KOH (10M)	Ethylene Glycol	150	24	Decomposition*
6	KOH (10M)	Ethylene Glycol	150	48	Decomposition

* Product was detected by HRMS but pure product was never isolated; A small amount of starting material was recovered.

Due to the difficulties in forming a tertiary amine, a commercially available *tert*-octylamine (**2-10**) was employed to synthesize *tert*-octylmaleimide (**2-11**) as shown in Scheme 2-4.[5] The tertiary octyl group still maintained the desired bulky functionality necessary to disrupt aggregation and should also be acid labile. **2-10** was reacted with maleic anhydride in toluene to provide intermediate **2-11** in a 98% yield.[6] The amide was successfully cyclized to the desired maleimide (**2-12)** utilizing acetic anhydride and triethylamine in a 35% yield. The cyclization was proven to be a slow process. Further optimizations were not successful; however, the inexpensive starting materials allowed for this reaction to be run on multi-gram scale, and significant quantities of **2-12** were produced.

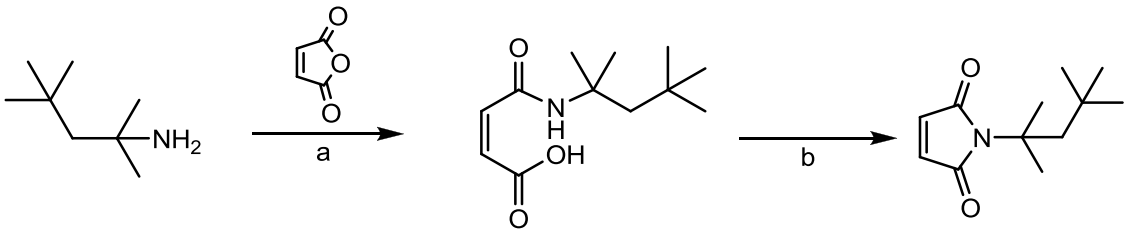

2-10 **2-11** **2-12**

a) Toluene, 50 ˚C; **98%** b) Ac_2O, NEt_3, 70 ˚C; **35%**

Scheme 2-4. Synthesis of *N-tert*-octylmaleimide

2.3 Diels-Alder Addition of *N-tert*-octylmaleimide

With the successful synthesis of **2-12**, the use of this bulky alkyl maleimide in a Diels-Alder reaction with **1-11** was yet to be proven. As explored in chapter 1, the insolubility of **1-11** significantly hampered the efficiency of the Diels-Alder addition. Given the opportunity to enhance the solubility of the Diels-Alder adduct (**2-13**), it was proposed that separation of the desired product from the insoluble starting material would be facile and provide a quantitative look into the efficiency of the Diels-Alder addition (Scheme 2-5).

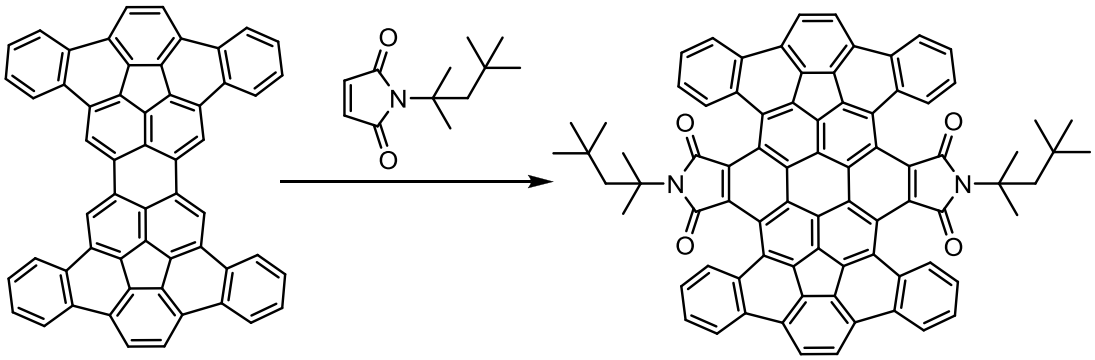

1-11 **2-13**

Scheme 2-5. Diels-Alder Addition of *N-tert*-octylmaleimide

The optimal Diels-Alder conditions were investigated in depth (Table 2-2). Initial screening with *o*-dichlorobenzene (*o*-DCB) as the solvent provided minimal success (entry 1). Increasing the reaction temperature, utilizing nitrobenzene as the solvent, showed an increase in mono Diels-Alder addition (entry 2). An increase in reaction time significantly improved the reaction (entry 3); however, an increase in the reaction temperature in *o*-DCB did not improve the reaction (entry 4). As seen in Figure 2-1, entries 3 and 4 both showed mono and di Diels-Alder addition; however, aromatization only occurred to reform the perylene core for both mono (*m/z* 903) and di addition (*m/z* 1110) products. Addition of an oxidizing agent, *p*-chloranil, provided double Diels-Alder addition, with all rings fully aromatized to form the coronene core of **2-13** (*m/z* 1106), in a 5% isolated yield (entry 5). Most importantly, the Diels-Alder adducts were soluble and isolable. It was found that the oxidizing agent was not necessary, and the reaction could be run at reflux, instead of in a pressure vessel, providing a 6% isolated yield of the double Diels-Alder adduct (entry 6).

Table 2-2. Conditions for the Diels-Alder Addition of *N-tert*-octylmaleimide

Entry	Solvent	MI (eq.)	Additive	T (° C)	t (days)	Result (yield)
1	*o*-DCB	5	-	180[a]	1	Mono addition[c]
2	nitrobenzene	8	-	210[a]	1	Mono addition[c]
3	*o*-DCB	5	-	180[a]	3	Mono and Di addition[c]
4	*o*-DCB	5	-	200[a]	3	Mono and Di addition[c]
5	*o*-DCB	10	*p*-chloranil	180[b]	3	Di addition (5%)[d]
6	*o*-DCB	10	-	180[b]	4	Di addition (6%)[d]
7	1,2,4-trichlorobenzene	10	*p*-chloranil	215[b]	6	Di addition (11%)[d]
8	1,2,4-trichlorobenzene	10	-	215[a]	6	Di addition (11%)[d]

[a] Reaction was run in a pressure vessel. [b] Reaction was run open to air at reflux. [c] Starting material was recovered, and aromatization of the perylene core occurred. [d] Product was completely aromatized, losing a total of 8 H, and forming the coronene core of **2-13**. MI = *N-tert*-octylmaleimide, *o*-DCB = *o*-dichlorobenzene

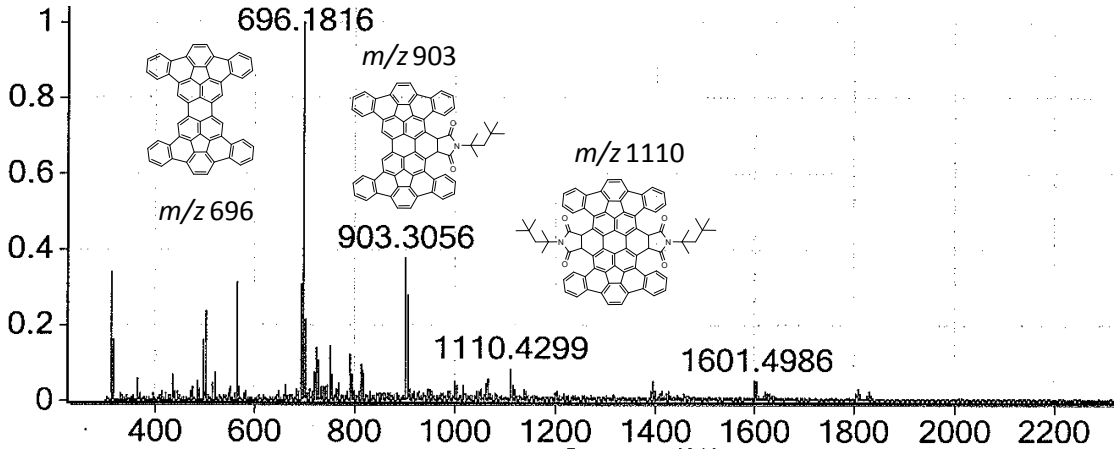

Figure 2-1. MALDI-TOF Mass Spectrum of Entry 3 (Table 2-2)

A higher boiling solvent, 1,2,4-trichlorobenzene, with a boiling point of 215 ˚C, afforded successful double addition of **2-13** in an 11% isolated yield (entries 7 and 8). The double Diels-Alder addition was confirmed by MALDI-TOF mass spectrometry, affording the fully rearomatized product **2-13** (m/z 1106, Figure 2-2).

The desired product proved to be highly soluble in a variety of common organic solvents, namely benzene, dichloromethane and carbon disulfide, allowing for simple separation of the product from the insoluble starting material. Preparative layer reverse phase C_{18} chromatography was used to purify **2-13**, resulting in an 11% yield of a red solid. ^{1}H NMR of the purified **2-13** shows a distinctive pattern in the aromatic region; however, the quality of the spectrum, even at elevated temperatures, was hampered due to aggregation of the molecules (Figure 2-3). The recovered starting material (**1-11**) was resubjected to the reaction conditions to afford more product; however, the low yield and long reaction times were limiting. Unfortunately, the yield was not increased with longer reaction

times, and although the product was separable from the starting material, the inefficiency of the Diels-Alder addition made this process impractical.

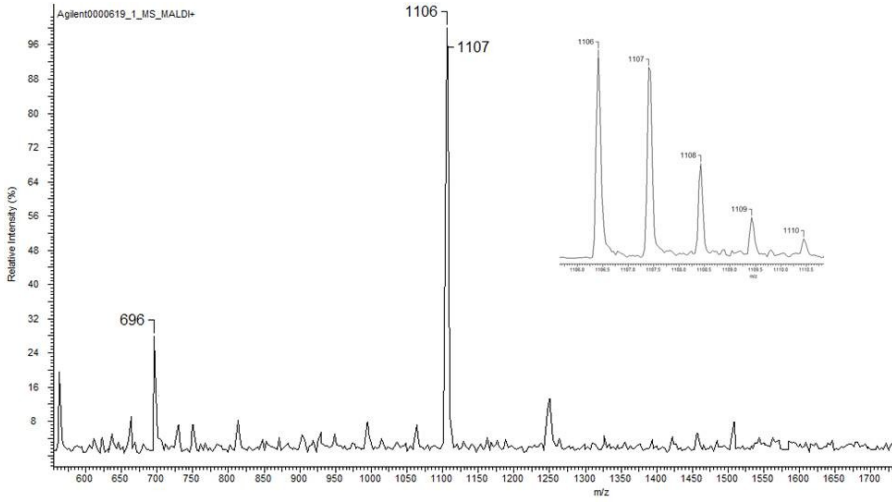

Figure 2-2. MALDI-TOF Mass Spectrum of 2-13

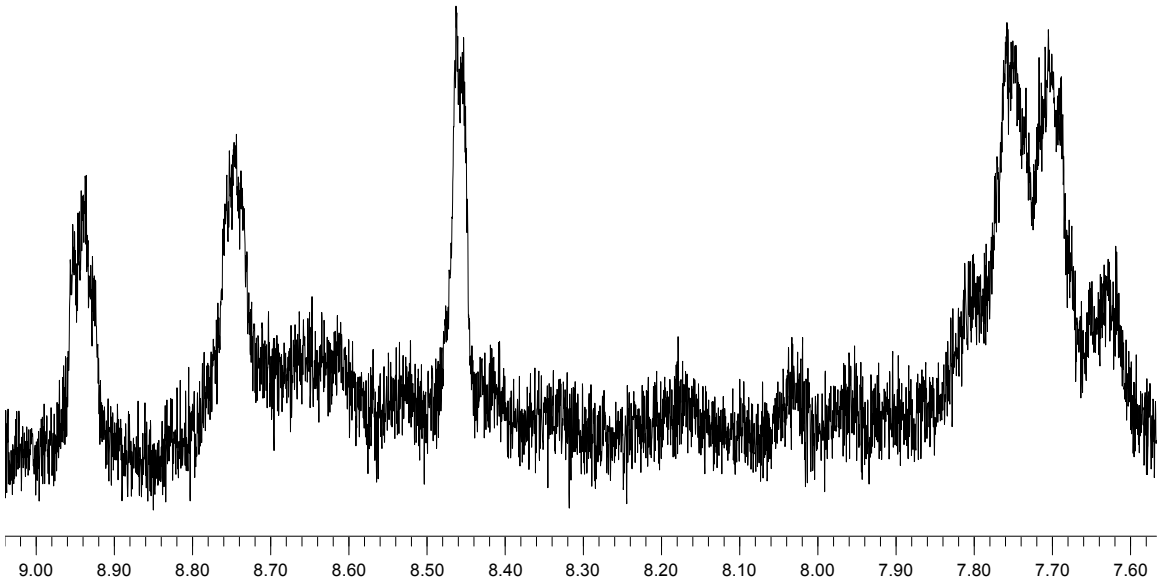

Figure 2-3. ^{1}H NMR (500 MHz, $C_2D_2Cl_4$, 80 ˚C) of 2-13

2.4 Conclusion

The successful synthesis of a bulky alkyl maleimide, **2-12**, provided a suitable dienophile for the Diels-Alder addition to **1-11**. More importantly, **2-12** enhanced the solubility of the Diels-Alder adduct **2-13**, allowing for purification and separation of the desired material. Unfortunately, this process was low yielding, with long reaction times limiting the overall throughput of material.

2.5 Experimental Section

2.5.1. 4-Methylheptan-4-ol

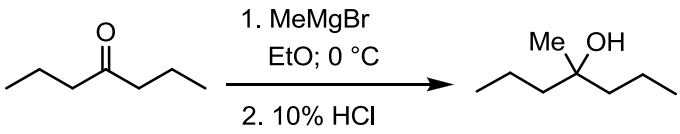

To a flame-dried round bottom flask, purged with nitrogen, was added 1.00 g (8.76 mmol) of 4-heptanone and 10.0 mL of anhydrous tetrahydrofuran. A second round bottom flask, equipped with a magnetic stir bar, was flame-dried, purged with nitrogen and cooled in an ice bath. The flask was charged with 6.10 mL of 2.88 M methylmagnesium bromide (in diethyl ether), and the solution was stirred at 0 ˚C. The tetrahydrofuran solution was added dropwise, under nitrogen, to the Grignard solution over the course of 30 min. The reaction mixture was slowly warmed to room temperature over 2 h and then quenched with 10% HCl. The mixture was extracted with diethyl ether, and the organic extracts were dried over $MgSO_4$. Evaporation of the solvent provided the desired product as a clear, colorless oil in 0.968 g (85%). **^{1}H NMR** (500 MHz, $CDCl_3$) δ (ppm): 1.44-1.38 (m, 4H), 1.35-1.30 (m, 4H), 1.13 (s, 3H), 0.91 (t, J = 7.5 Hz, 6H). **^{13}C NMR** (125 MHz, $CDCl_3$) δ (ppm): 72.3, 43.8, 26.4, 16.7, 14.2. **HRMS** (DART-TOF) calc'd for $C_8H_{22}NO$ $(M+NH_4)^+$ 148.1701, found 148.1699. **IR** (cm^{-1}, NaCl) 3375 (O-H).

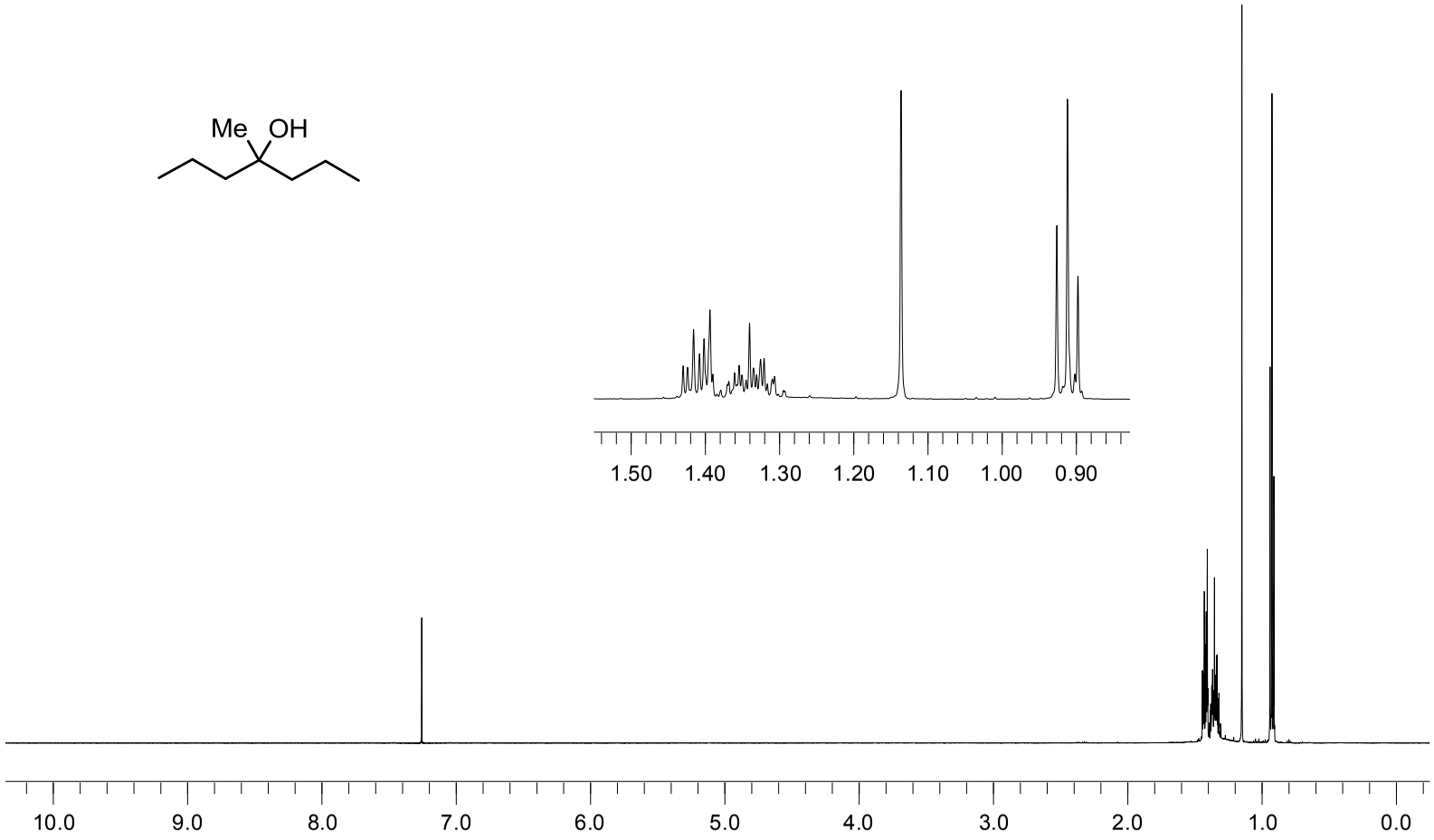

^{1}H NMR (500 MHz, $CDCl_3$)

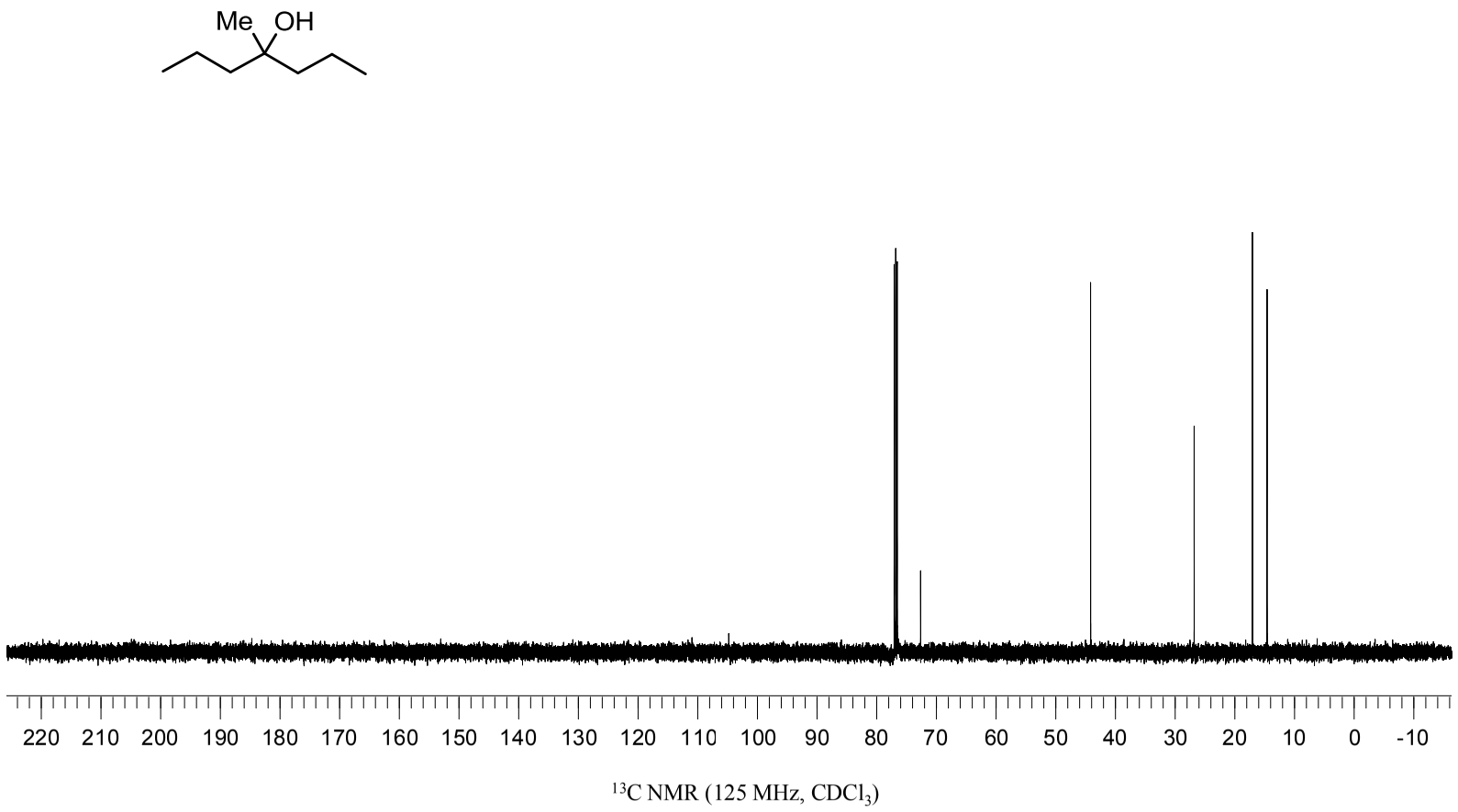

^{13}C NMR (125 MHz, $CDCl_3$)

2.5.2. *N*-(1-methyl-1-propylbutyl)acetamide

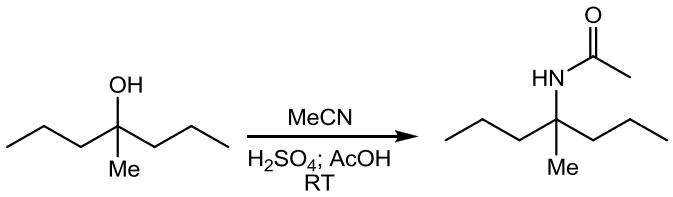

To a mixture of 4-methyl-4-heptanol (10.0 g, 0.0768 mol) and 3.97 mL (0.0768 mol) acetonitrile in acetic acid (10 mL), was added a solution of sulfuric acid (7.34 mL, 0.138 mol) in acetic acid (10 mL) dropwise. The reaction mixture was stirred at room temperature for 2 h and then quenched with 2M sodium acetate, washed with water and extracted with dichloromethane. The organic extracts were combined, and solvent was evaporated to yield a white crystalline solid, 12.23 g (93%): **mp** 62-64 ˚C; **^{1}H NMR** (400 MHz, $CDCl_3$) δ (ppm): 5.12 (s, 1H), 1.91 (s, 3H), 1.69 (ddd, *J* = 16.8, 10.8, 6.0 Hz, 2H), 1.57 (ddd, *J* = 16.8, 11.2, 5.6 Hz, 2H), 1.21-1.29 (m, 4H), 1.26 (s, 3H), 0.91 (t, *J* = 7.6 Hz, 6H); **^{13}C NMR** (100 MHz, $CDCl_3$) δ (ppm): 169.36, 56.57, 40.97, 24.64, 24.61, 17.12, 14.67; **IR** (KBr, cm^{-1}): 3298 (N-H), 1654 (C=O), 1560 (C-N-H); **HRMS** (DART) calc'd for $C_{10}H_{22}NO$ $(M+1)^+$ 172.17006, found 172.17014.

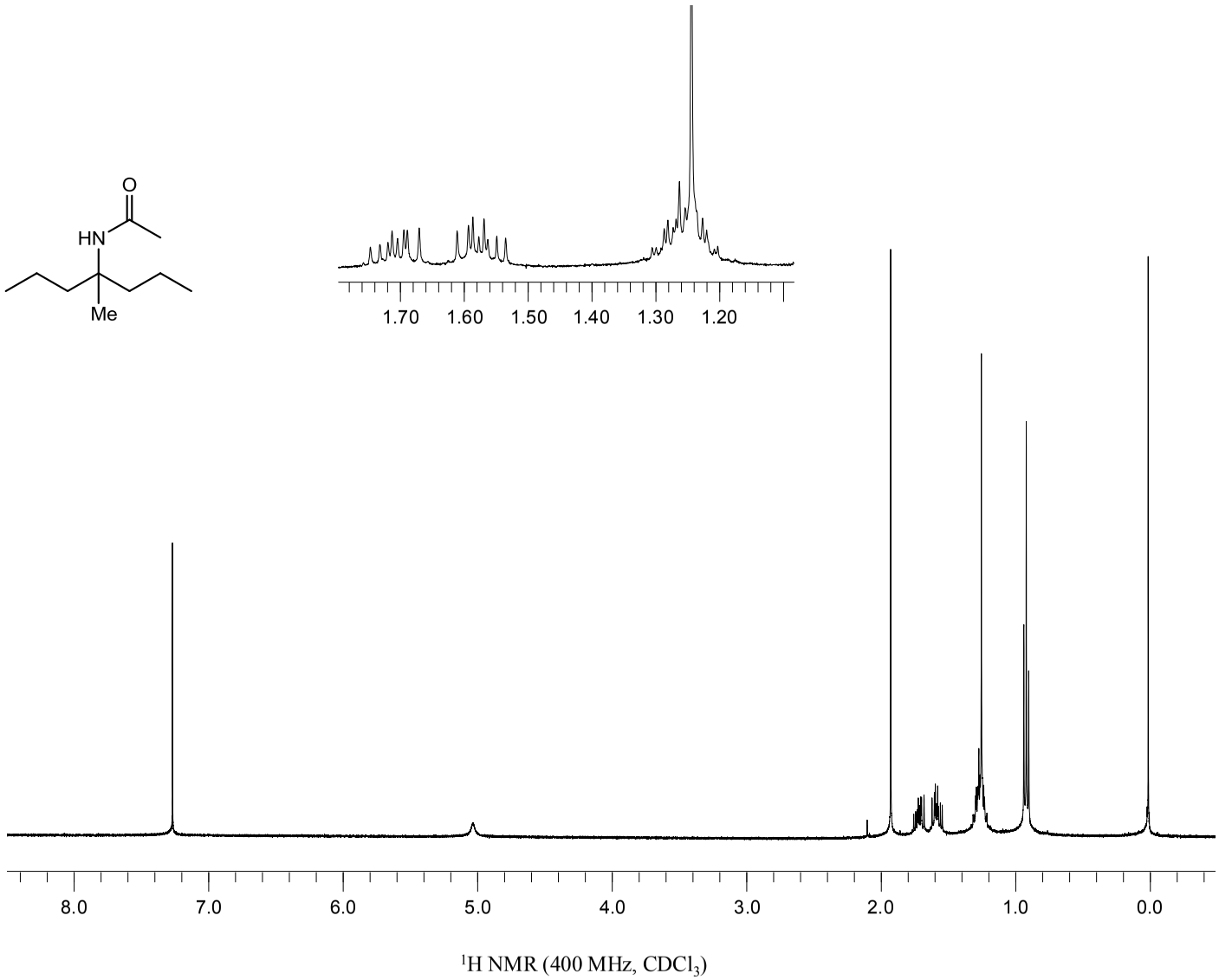

^{1}H NMR (400 MHz, $CDCl_3$)

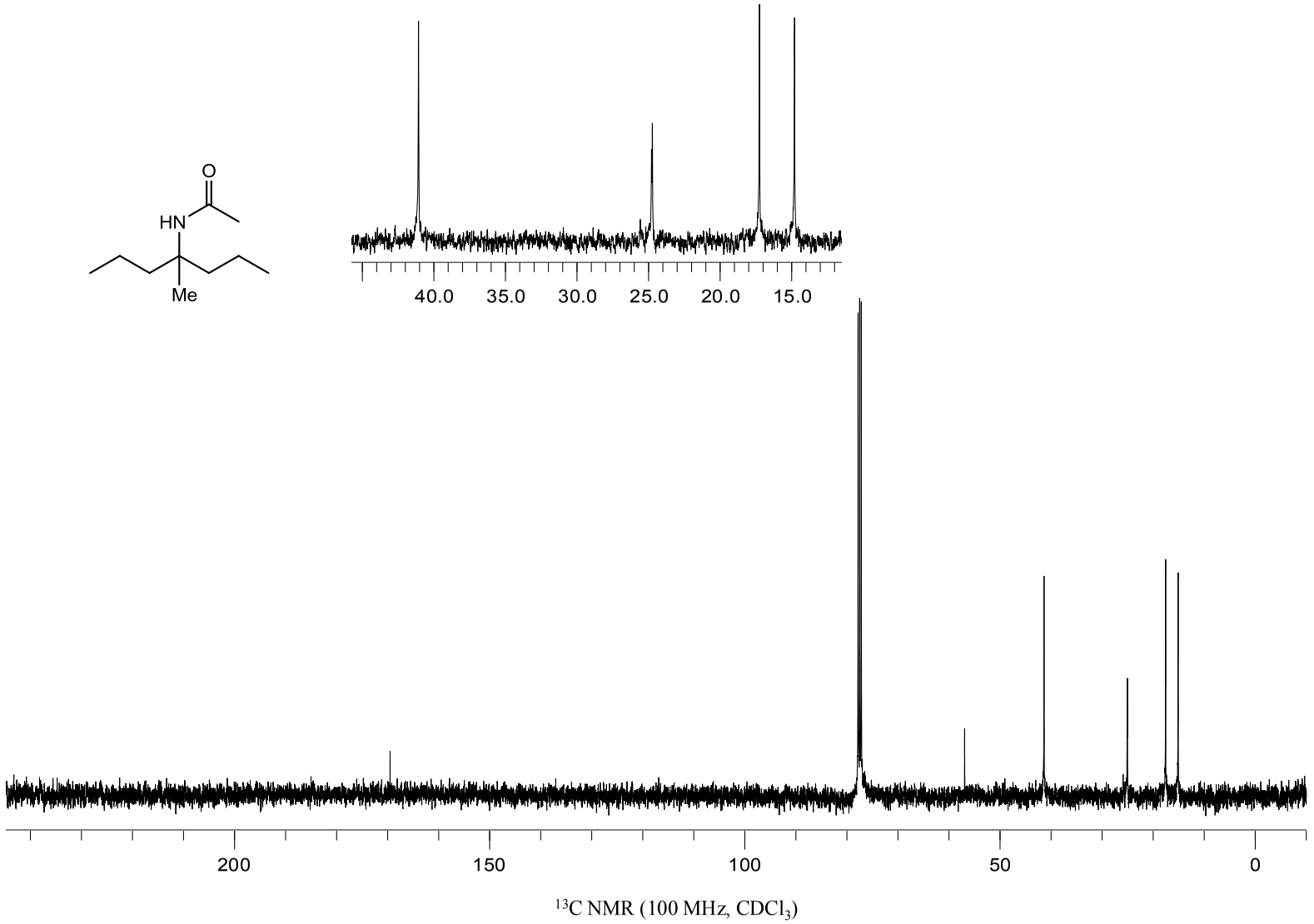

^{13}C NMR (100 MHz, $CDCl_3$)

2.5.3. 4-Oxo-4-(*tert*-octylamino)but-2-enoic acid

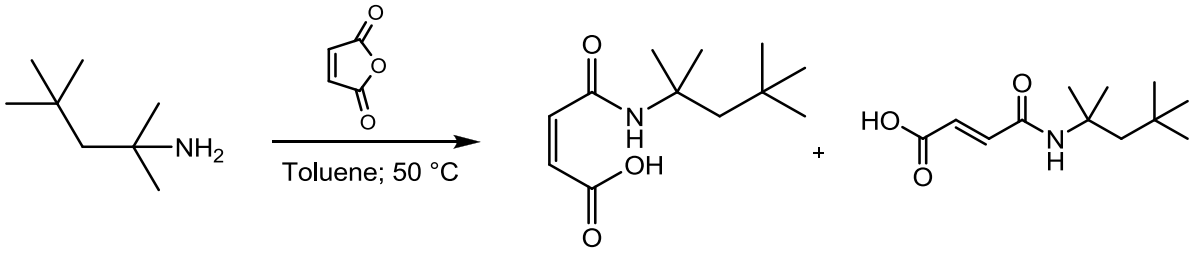

To a flame-dried round bottom flask purged with nitrogen, was added 16.7 g (0.170 mol) maleic anhydride and 100 mL anhydrous toluene. The mixture was stirred, and *tert*-octylamine (20.0 g, 0.170 mol) was added dropwise. The mixture was heated to 50 ˚C for 2 h. After cooling to room temperature, a fluffy white precipitate was filtered and dried under vacuum to provide 34.9 g (98%) of the desired product as a mixture of isomers. **MP:** 106-110 ˚C. **^{1}H NMR** (500 MHz, $CDCl_3$, for a mixture of isomers) δ(ppm): 7.78 (bs, 2H), 6.32 (d, J = 12.5 Hz, 1H of E isomer), 6.24 (s, 2H of Z isomer), 6.14 (d, J = 12.5 Hz, 1H of E isomer), 1.81 (s, 2H of Z isomer), 1.73 (s, 2H of E isomer), 1.50 (s, 6H of E isomer), 1.48 (s, 6H of Z isomer), 1.05 (s, 9H of E isomer), 1.02 (s, 9H of Z isomer). **^{13}C NMR** (125 MHz, $CDCl_3$, for a mixture of isomers) δ(ppm): 169.7, 165.7, 136.0, 135.9, 133.0, 57.3, 56.7, 52.7, 50.8, 31.34, 31.29, 28.8, 27.4. **HRMS** (DART-TOF): Calc'd for $C_{12}H_{22}NO_3$ $(M+1)^+$ 228.1600, found 228.1609.

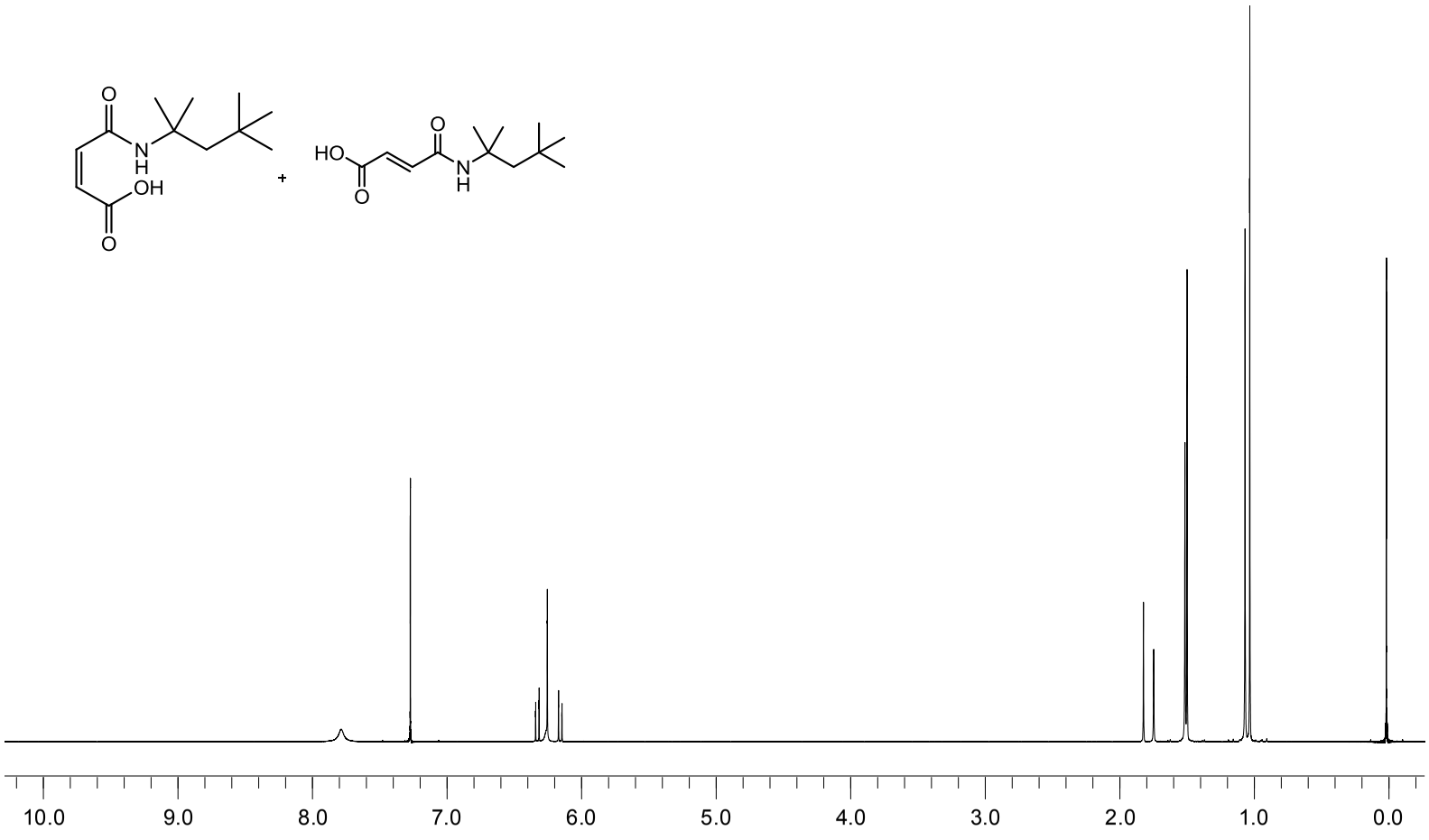

^{1}H NMR (500 MHz, $CDCl_3$)

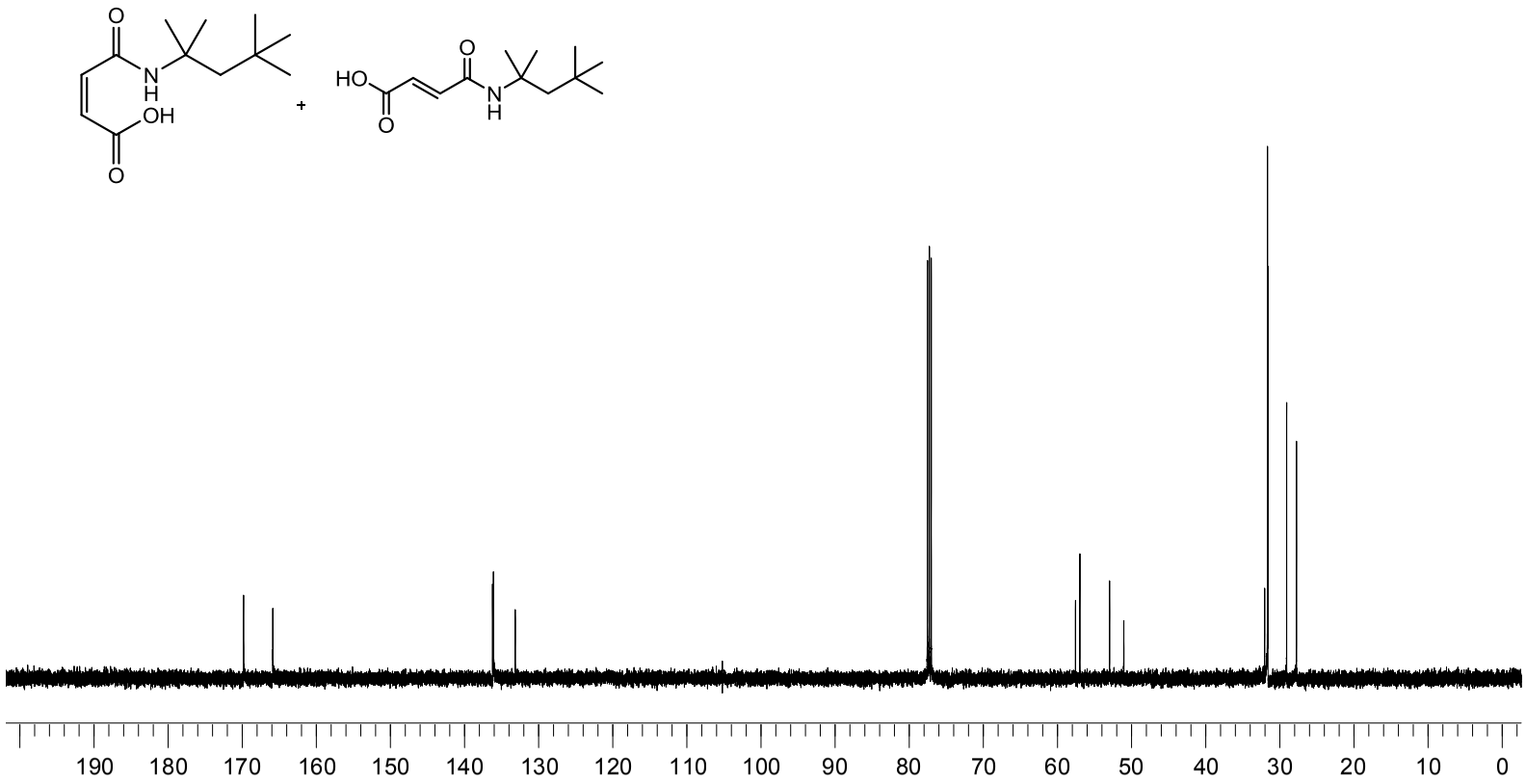

^{13}C NMR (125 MHz, $CDCl_3$)

2.5.4. 1-(*Tert*-octyl)-1*H*-pyrrole-2,5-dione

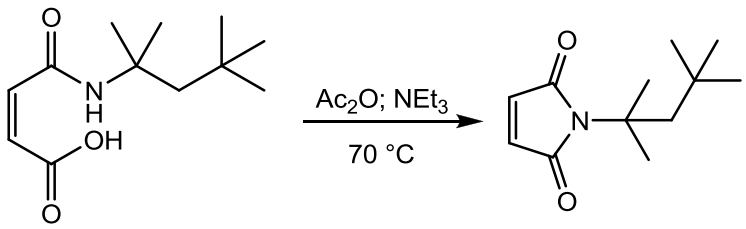

To a 250 mL round bottom flask equipped with a reflux condenser and magnetic stir bar, was added 10.0 g (0.0441 mol) of 4-oxo-4-(*tert*-octylamino)but-2-enoic acid and 100 mL acetic anhydride. Triethylamine (30.3 g, 0.299 mol) was added dropwise to the stirred reaction mixture. A color change was observed from a clear, colorless solution to a brown solution over 15 min. The mixture was heated to reflux for 15 h. The reaction mixture was cooled to room temperature and stirred in cold water for 30 min. The mixture was extracted with hexanes and ethanol three times. The organic extracts were dried with magnesium sulfate and concentrated to dryness under reduced pressure. The crude product was recrystallized in hexanes to provide 3.43 g (37 %) of an orange solid. **Mp**: 55-58 ˚C. **^{1}H NMR** (500 MHz, $CDCl_3$) δ(ppm): 6.52 (s, 2H), 1.89 (s, 2H), 1.66 (s, 6H), 0.92 (s, 9H). **^{13}C NMR** (125 MHz, $CDCl_3$) δ(ppm): 172.6, 134.0, 60.8, 50.8, 31.5, 31.0, 29.9. **IR** (KBr, cm^{-1}) 1702 (C=O). **HRMS** (DART-TOF): Calc'd for $C_{12}H_{20}NO_2$ $(M+1)^+$ 210.1494, found 210.1495.

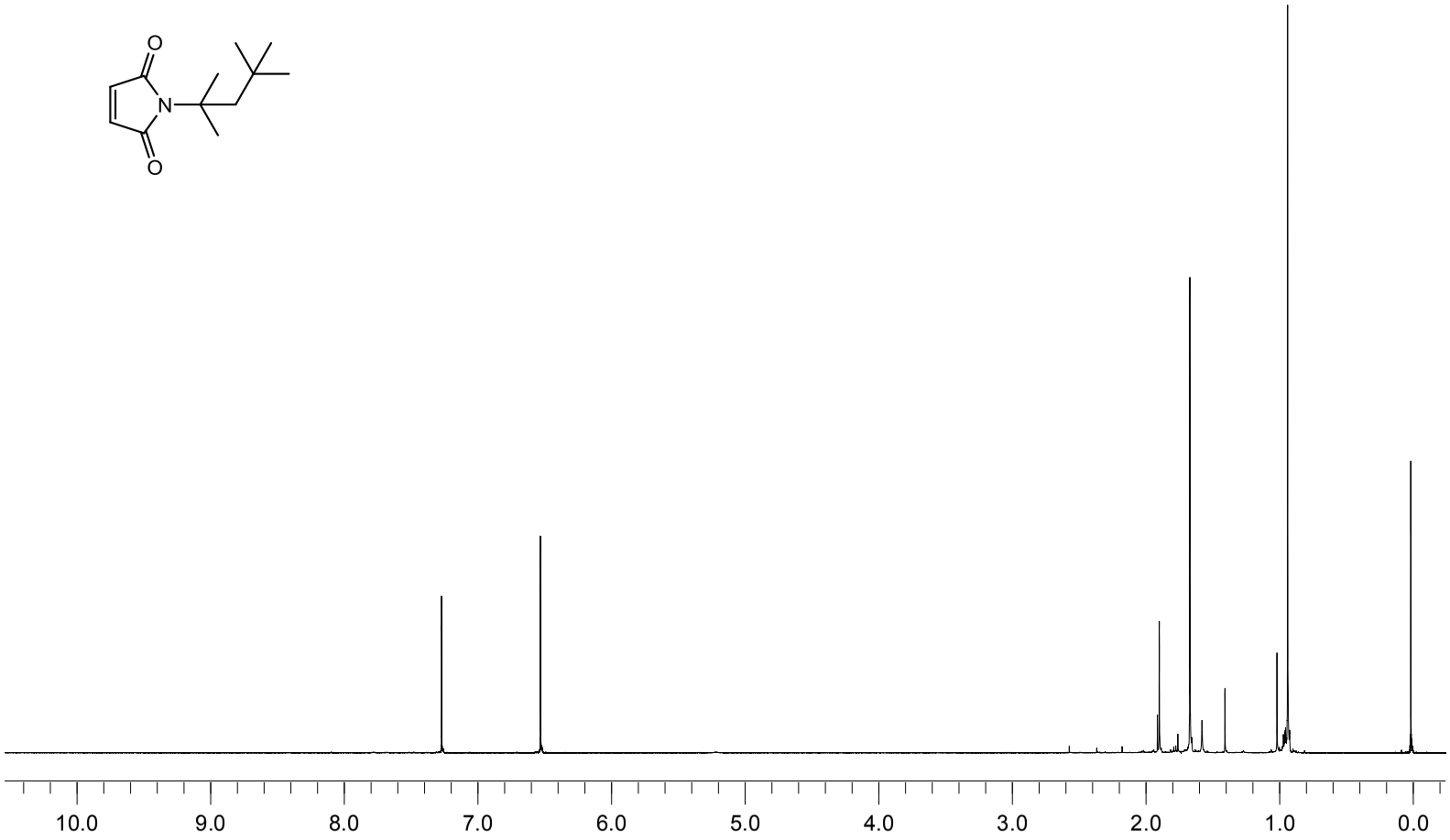

^{1}H NMR (500 MHz, $CDCl_3$)

^{13}C NMR (125 MHz, $CDCl_3$)

2.5.5. Tetrabenzo[*a,g,o,u*]-7,8,15,16-tetrahydrocircum[5.6.5]quinarene-7,8,15,16-tetracarboxylic acid 7,8:15,16-*bis*(*N*-*tert*-octylimide)

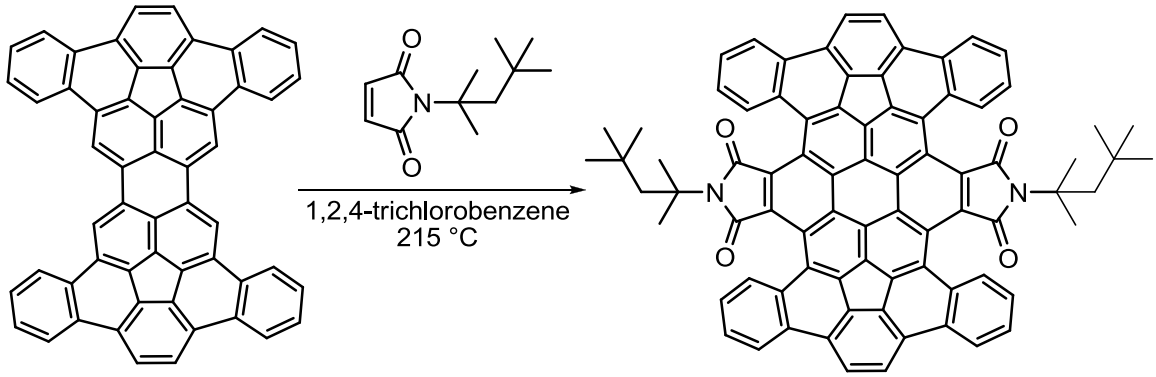

To a flame-dried, nitrogen purged pressure vessel equipped with a magnetic stir bar, was added 26.4 mg (0.0379 mmol) *peri*-*bis*(dibenzo[*a,g*]corannulene) and 90.0 mg (0.379 mmol) 1-(*tert*-octyl)-1*H*-pyrrole-2,5-dione. 1,2,4-trichlorobenzene (1.00 mL) was added via syringe, and the reaction mixture was stirred. The vessel was sealed and placed in a pre-heated sand bath (215 ˚C) for 6 d. The reaction mixture was cooled to room temperature, and solvent was removed under reduced pressure. The crude red solid was washed with hexanes and dried under reduced pressure. Reverse phase C18 silica preparative layer chromatography with 1:1 hexanes: dichloromethane as the eluent afforded 4.60 mg (11 %) of the desired product as a bright red solid. **MP**: >310 ˚C (dec). **UV-Vis** (CH_2Cl_2) λ_{max} (ε, $cm^{-1}M^{-1}$): 282 (25839), 394 (sh, 5708). **HRMS** (MALDI-TOF): Calc'd for $C_{80}H_{54}N_2O_4$ (M^+) 1106.4083, found 1106.4078. ^{1}H NMR spectra show signals in the aromatic region; however, the spectra are not clear, likely due to aggregation in solution (Figure 2-2).

MALDI-TOF MS (DCTB Matrix)

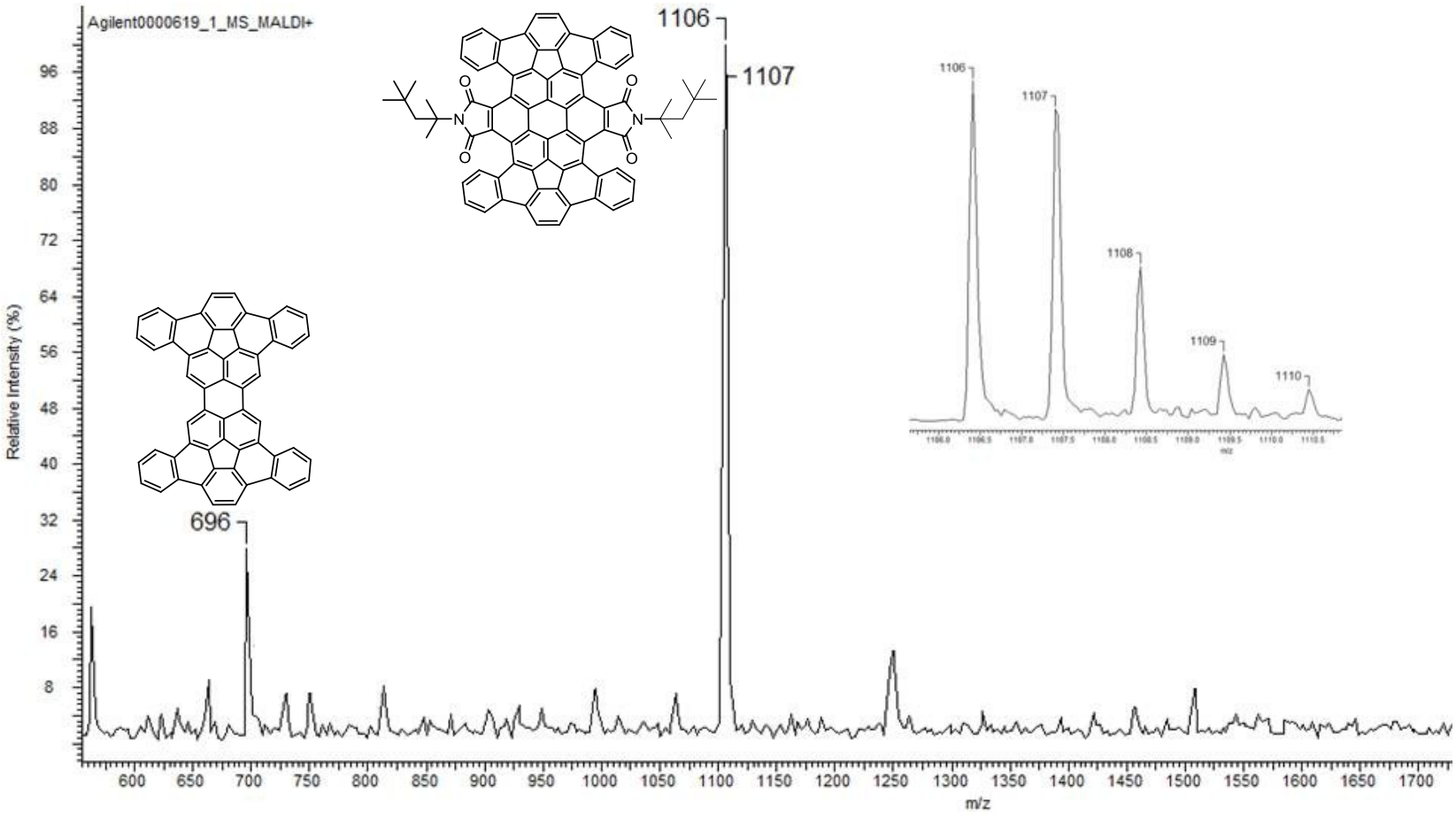

Tetrabenzo[*a,g,o,u*]-7,8,15,16-tetrahydrocircum[5.6.5]quinarene-7,8,15,16-tetracarboxylic acid 7,8:15,16-*bis* (*N*-*tert*-octylimide)

UV Spectrum of Tetrabenzo[*a,g,o,u*]-7,8,15,16-tetrahydrocircum[5.6.5]quinarene-7,8,15,16-tetracarboxylic acid 7,8:15,16-*bis*(*N-tert*-octylimide)

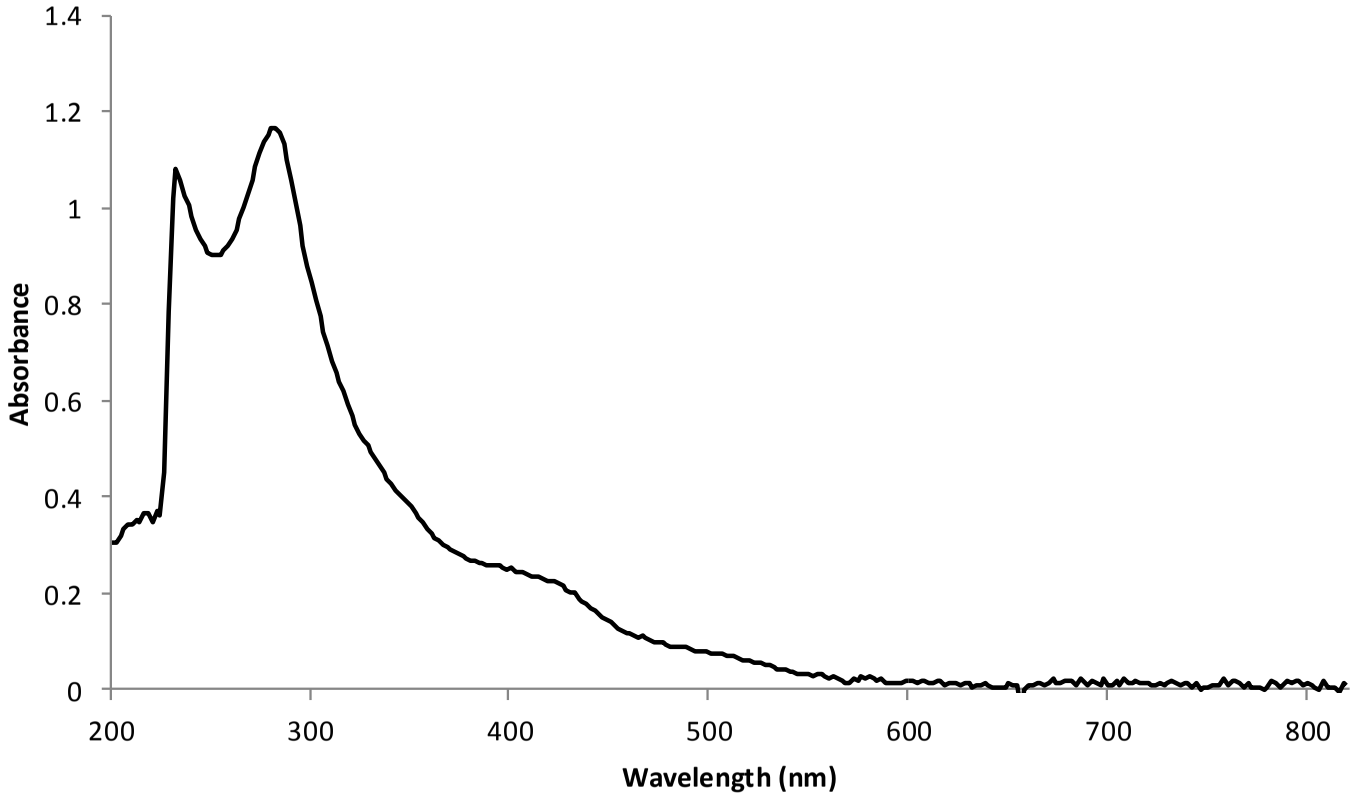

2.6 References

[1] Tsefrikas, V. M. Ph.D. Dissertation., Boston College, Chestnut Hill, MA, 2007.

[2] (a) Ritter, J.; Kalish, J. *J. Am. Chem. Soc.* **1948**, *70*, 4048–4050. (b) Baum, J. C.; Milne, J. E.; Murry, J. A.; Thiel, O. R. *J. Org. Chem.* **2009**, *74*, 2207-2209.

[3] (a) Glynn, D. L.; Zelle, R. E.; Grieco, P. A. *J. Org. Chem.* **1983**, *48*, 2424-2426. (b) Evans, D. A.; Carter, P. H.; Dinsmore, C. J.; Barrow, J. C.; Katz, J. L.; Kung, D. W. *Tetrahedron Lett.* **1997**, *38*, 4535-4538. (c) Gassman, P. G.; Hodgson, P. K. G.; Balchunis, R. J. *J. Am. Chem. Soc.* **1976**, *98*, 1275-1276.

[4] Gassman, P. G.; Schenk, W. N. *J. Org. Chem.* **1977***, 42*, 918–920.

[5] Hooley, R. J.; Rebek, J. *Org. Biomol. Chem.* **2007**, *5*, 3631-3636.

[6] Pal, B.; Pradhan, P. K.; Jaisankar, P.; Giri, V. S. *Synthesis* **2003**, *10,* 1549-1552.

Chapter 3

Incorporation of Solubility-Enhancing *tert*-Butyl Groups for the Complete Synthesis of a $C_{60}H_{12}$ Carbon Nanotube End-Cap

3.1 Introduction

In order to enhance the solubility of the problematic and insoluble *peri*-*bis*(dibenzo[*a,g*]corannulene) (**1-11**), a synthetic route incorporating bulky *tert*-butyl groups on the hydrocarbon (**3-2**) was explored (Scheme 3-1). It has been well documented that *tert*-butyl groups aid the solubility of large and/or linear polyacenes.[1] It was envisioned that installing alkyl groups in the appropriate positions would help disrupt the problematic aggregation and enhance the solubility of the desired molecule. The installation of these bulky groups was proposed from the beginning of the synthesis or at a later stage; both of these methods will be discussed in depth.

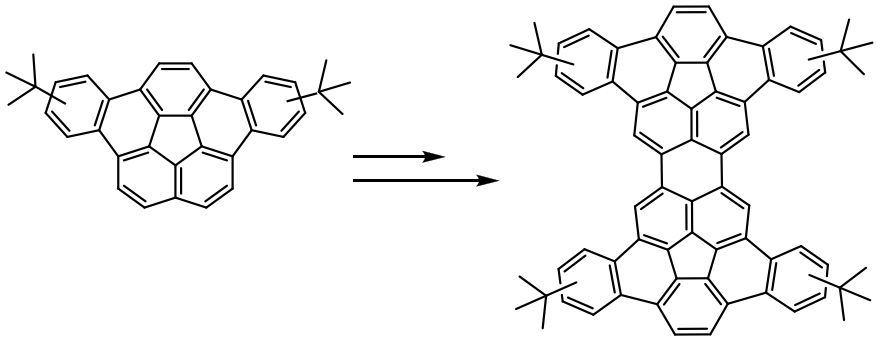

3-1 **3-2**

Scheme 3-1. Proposed Synthetic Targets

3.2 Synthesis of 4,11-Di-*tert*-butyldibenzo[*a,g*]corannulene

With the implementation of solubility-enhancing groups by the introduction of a bulky alkyl group, it had been shown that aggregation was suppressed and a soluble material was achieved, as shown in Chapter 2. To further explore solubility-enhancement, installation of strategically placed *tert*-butyl groups onto the hydrocarbon framework was explored (Scheme 3-2). Synthesis of tetra-*tert*-butyl-*peri*-*bis*(dibenzo[*a,g*]corannulene)

(**3-3**) was envisioned from 4,11-di-*tert*-butyldibenzo[*a*,*g*]corannulene (**3-4**). The synthesis of **3-4** can be achieved from the simple toluene derivative **3-5**, which will incorporate the *tert*-butyl group from the initial step of the synthesis in a set position.

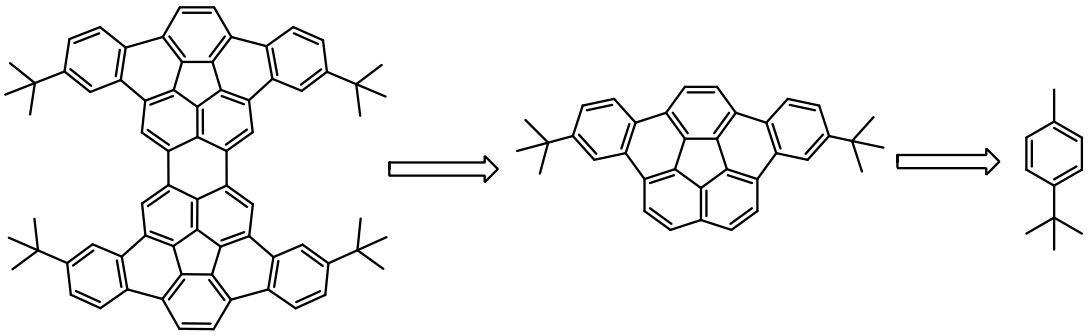

3-3 **3-4** **3-5**

Scheme 3-2. Retrosynthetic Analysis of *Peri-bis*(4,11-di-*tert*-butyldibenzo[*a*,*g*]corannulene)

Beginning with commercially available *para*-*tert*-butyltoluene (**3-5**), bromination to install an aryl bromine was accomplished to afford **3-6** in 67% (Scheme 3-3). From **3-6**, a benzylic bromination with *N*-bromosuccinimide provided **3-7** in 74% yield. It should be noted that this reaction had a tendency to over brominate at the benzylic position, so the reaction must be monitored very closely. A benzylic coupling of **3-7**, with diiron nonacarbonyl afforded the symmetrical ketone **3-8** in 81% yield.

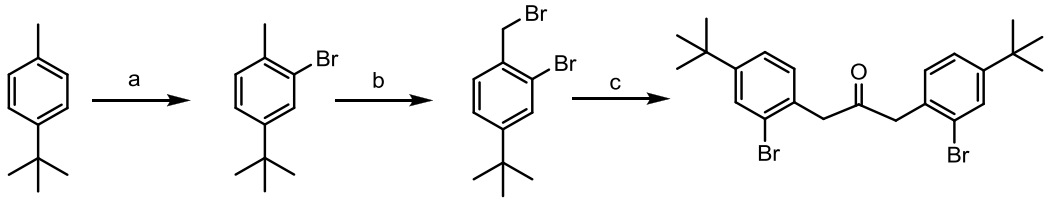

3-5 **3-6** **3-7** **3-8**

a) Br_2, AcOH, 50 ˚C; **67%** b) NBS, CCl_4, 77 ˚C; **74%** c) $Fe_2(CO)_9$, benzene, 80 ˚C; **81%**

Scheme 3-3. Synthesis of 1,3-*Bis*(2-bromo-4-*tert*-butylphenyl)propan-2-one

Utilizing a synthesis analogous to the synthesis of dibenzo[*a*,*g*]corannulene, shown in Chapter 1, the ketone **3-8** was subjected to an aldol condensation with acenaphthenequinone, **3-9**, to afford **3-10** in 74% yield (Scheme 3-4). In order to install the fluoranthene core, **3-10** was subjected to Diels-Alder/ retro Diels-Alder conditions with norbornadiene to afford **3-11** in 81% yield.

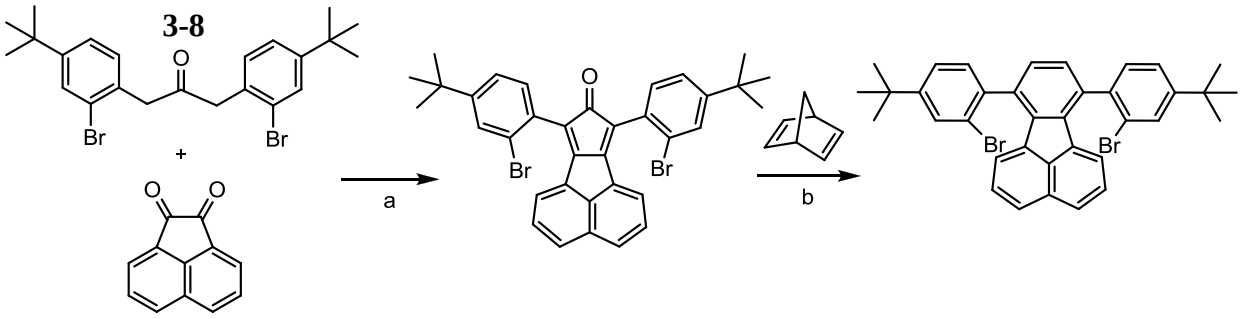

a) KOH, methanol, RT; **74%** b) Norbornadiene, 90 ˚C; **81%**

Scheme 3-4. Synthesis of 7,10-*Bis*(2-bromo-4-*tert*-butylphenyl)fluoranthene

3.3 Intramolecular Arylation Studies

A previous synthesis of dibenzo[*a*,*g*]corannulene, **3-16**, from **3-12**, had been optimized, as shown in Chapter 1. However, the brominated precursor, **3-12**, typically resulted in a decreased yield due to reductive dehalogenation.[2] The problematic reductive dehalogenation was not seen with the chlorinated precursors and was presumably due to a weaker carbon-Pd-bromine complex, **3-13**, formed after oxidative addition, as shown in Scheme 3-5. In order to achieve cyclization, a C-H activation must occur (**3-14**), forming the proposed palladacycle **3-15**. From this intermediate, it was not clear whether the

formation of complex **3-15** was reversible. It was believed that if this step were reversible, it may promote reductive dehalogenation.

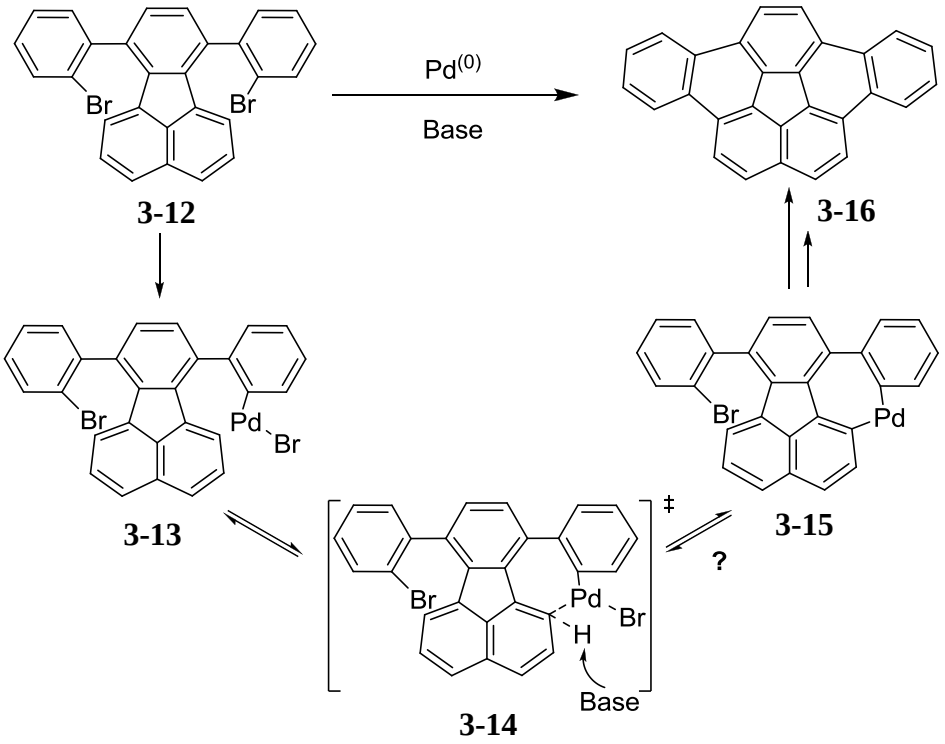

Scheme 3-5. Proposed Palladium Catalyzed Reaction Pathway

If the aryl palladium complex, **3-13**, did not undergo the desired intermolecular C-H activation, it might react with a solvent molecule, in this specific case DMAc, by way of the proposed transition state **3-18**. A complexed solvent molecule would be poised for δ-hydride elimination, forming intermediate **3-19**, which could be followed by reductive elimination to form the reductive dehalogenation product, **3-20** (Scheme 3-6).

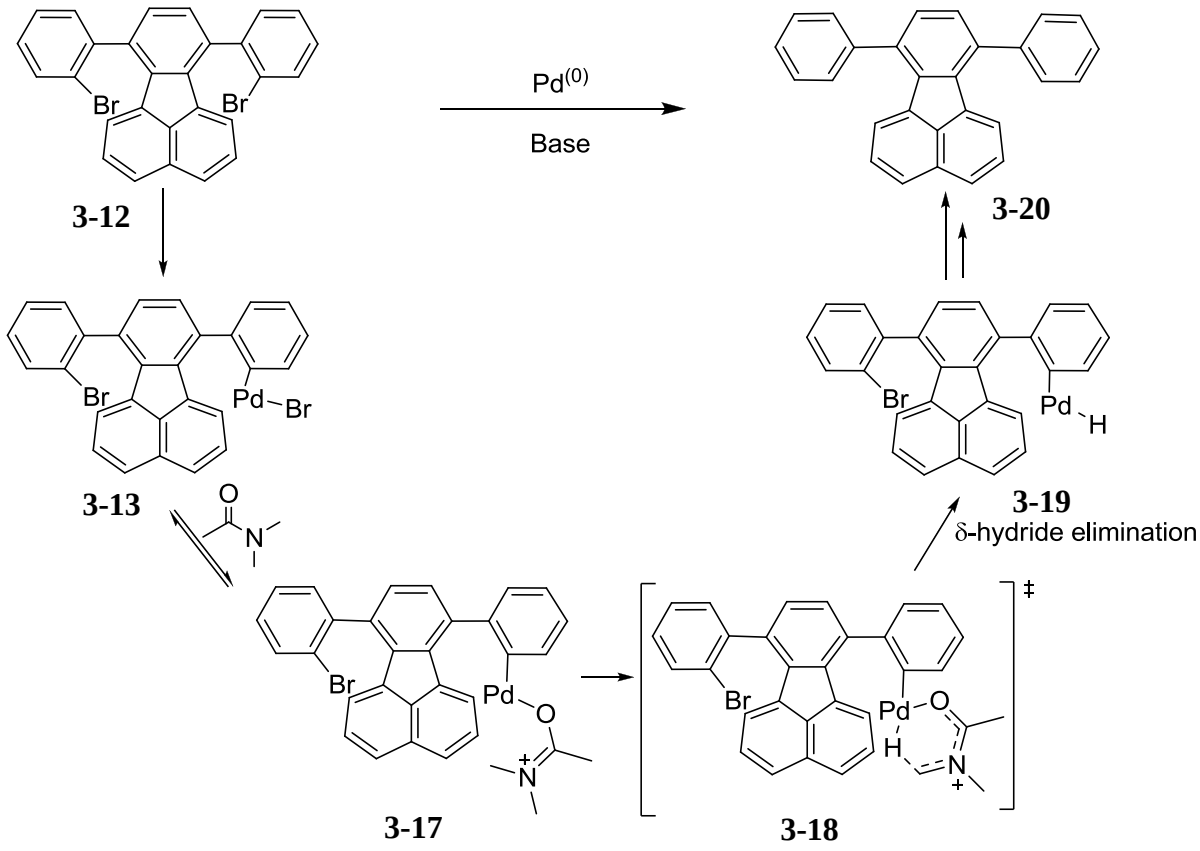

Scheme 3-6. Proposed Palladium Catalyzed Reductive Dehalogenation Pathway

It was suspected that the results seen with **3-12** would also hold true for the present molecule under study, **3-11**. As shown in Table 3-1, entry 1, standard conditions, $Pd(PCy_3)_2Cl_2$, DBU and DMAc, resulted in 68% of the desired compound **3-4** and 32% of the undesired mono-reductive dehalogenation product, **3-21**. These percents were determined by ^1H NMR integration, and it should be noted that the isolated yield of the desired product was limited to 20% of **3-4**. Isolation of the desired product **3-4** was significantly hampered due to the presence of **3-21**, which co-crystallize with **3-4,** and the two compounds were not separable with chromatographic techniques.

Recent advances in intra- and intermolecular arylation methods have shown that the use of carbonate bases effectively strengthened the palladium complex **3-13** by coordination of the carbonate to the metal center.[3] A recent report by Buchwald *et al.* utilized palladium (II) acetate, XPhos and potassium carbonate, and these conditions were applied to **3-11**; yet, only starting material was recovered, entry 2.[4] A change in base to potassium *tert*-butoxide, was investigated; however, this promoted complete reductive dehalogenation, **3-22**, with no cyclized products detected, entry 4. The original conditions were revisited, and pivalic acid was added, which is suspected to strengthen the palladium complex **3-13** in the same way the carbonate bases were proposed to; however, these conditions actually promoted reductive dehalogenation, increasing the amount of **3-21** formed, entry 5.[5]

Table 3-1. Intramolecular Arylation Optimization

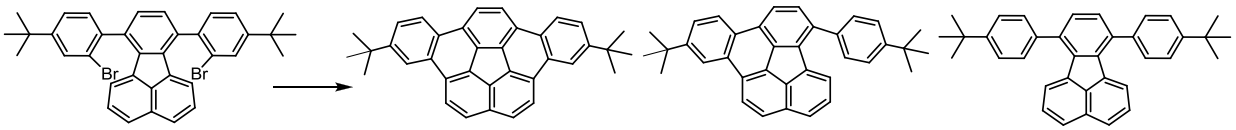

3-11 **3-4** **3-21** **3-22**

Entry	Catalyst (mol%)	Base (eq)	Additive	Solvent	T (˚C)	t	Result[a] 3-11	3-4	3-21	3-22	Isolated Yield of 3-4
1	$Pd(PCy_3)_2Cl_2$ (10)	DBU (40)		DMAc	150	22 h	-	**68**	32	-	20%
2	$Pd(OAc)_2$ (10)	Cs_2CO_3 (1.2)	XPhos 15 mol%	DMAc	150	15 h	100	-	-	-	
3	RuPhos Precatalyst (2)	DBU (40)		toluene	125	24 h	-	-	-	100	
4	$Pd(PCy_3)_2Cl_2$ (10)	*t*-BuOK (40)		DMAc	150	15 h	-	-	-	100	
5	$Pd(PCy_3)_2Cl_2$ (10)	DBU (40)	PivOH 1 eq	DMAc	150	15.5 h	-	**30**	70	-	
6	$Pd(PCy_3)_2Cl_2$ (10)	DBU (40)	LiCl 2 eq	DMAc	150	15 h	-	**75**	25	-	40%
7	$Pd(PCy_3)_2Cl_2$ (10)	DBU (40)	LiCl 20 eq	DMAc	150	15 h	-	**75**	25	-	40%
8	$Pd(PCy_3)_2Cl_2$ (10)	DBU (40)	LiCl 10 eq	1,4-di-*t*-butylbenzene	150	15 h	-	**81**	19	-	50%

[a]Relative yields were determined by ^{1}H NMR integration.

Since it was known that the chlorinated precursor lead to a higher yield of cyclization products, it was believed that halogen exchange, replacing bromine with chlorine would increase the yield of the desired product **3-4**. Adding lithium chloride to the standard conditions increased the ratio of **3-4** to **3-21** (from 2:1 to 3:1), and it was found that as little as two equivalents of lithium chloride was effective, entries 6 and 7. Furthermore, as discussed and shown in Scheme 3-6, it was suspected that solvent may be a source of the hydrogen for reductive dehalogenation. If the reaction was run with a solvent that lacked highly activated hydrogen atoms, then the reductive dehalogenation was expected to be diminished. An exotic solvent that contains no sterically accessible activated C-H bonds, 1,4-di-*t*-butylbenzene, was employed in place of DMAc, and did indeed improve the ratio of **3-4** to **3-21** (4:1, respectively), increasing the isolated yield to 50%, entry 8. Removal of the solvent, 1,4-di-*tert*-butylbenzene (b.p. 236 ˚C), was accomplished via sublimation; however, it should be noted that on large scale, complete removal of the solvent was challenging. With the isolate yield significantly improved, this recipe provided a viable route towards the desired product.

To further probe the hydrogen source for the reductive dehalogenation products, **3-21** and **3-22**, the reaction was run under standard conditions but with *N*,*N*-dimethylformamide-d_7 (DMF-d_7) instead of DMAc, which was expected to incorporate deuterium onto **3-21** and **3-22**. It should be noted that DMF has been shown to give comparable results to DMAc in this specific reaction.[2] As shown in Scheme 3-7, **3-11** was subjected to intramolecular arylation conditions with $Pd(PCy_3)_2Cl_2$, DMF-d_7, and DBU at 150 ˚C for 16 h, and the reaction mixture was analyzed by DART-TOF and ^{1}H NMR, which confirmed at least

one deuterium atom was incorporated. Quantification of the deuterium incorporation was hampered due to the formation of a significant quantity of **3-4**, as shown in Figure 3-1.

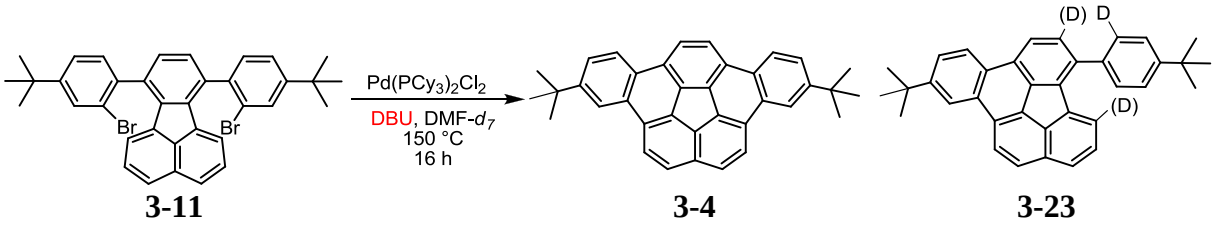

3-11 **3-4** **3-23**

Scheme 3-7. Intramolecular Arylation in DMF-d_7

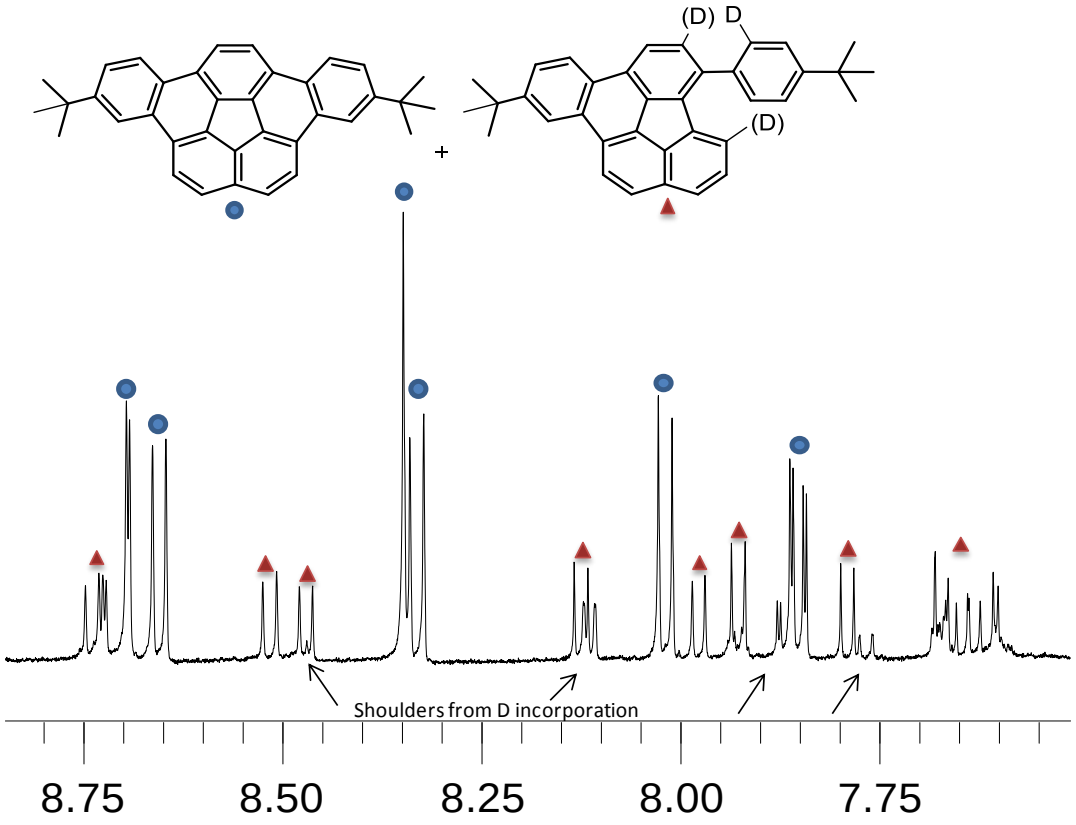

Figure 3-1. ^{1}H NMR (500 MHz, $CDCl_3$) of Intramolecular Arylation in DMF-d_7

Utilizing potassium *tert*-butoxide as a base, which is known to promote reductive dehalogenation (Table 3-1, entry 4), would allow for a better quantification of the deuterium incorporated product. As shown in Scheme 3-8**,** the reaction was run with

$Pd(PCy_3)_2Cl_2$, potassium *tert*-butoxide and DMF-d_7, which resulted in complete reductive dehalogenation and incorporation of at least eight deuterium atoms, which was confirmed by high resolution mass spectrometry, ^{1}H NMR and ^{13}C NMR. As shown in Figure 3-2, the NMR spectra of **3-24** shows significant changes when compared to the spectra of **3-22**. From the ^{1}H NMR, it is clear that the spectrum is simplified due to significant deuterium incorporation at multiple sites. The specific sites of deuteration were assigned, and deuterium was incorporated at more sites than was initially expected. If the solvent was involved in the reductive dehalogenation, then deuterium incorporation at the position of the halogen was expected, In fact, deuteration was seen at the position of the halogen, incorporating a single deuterium on the phenyl ring. Unexpectedly, a total of eight sites incorporated deuterium, including the top of the fluoranthene core and in two unique positions on the naphthalene moiety.

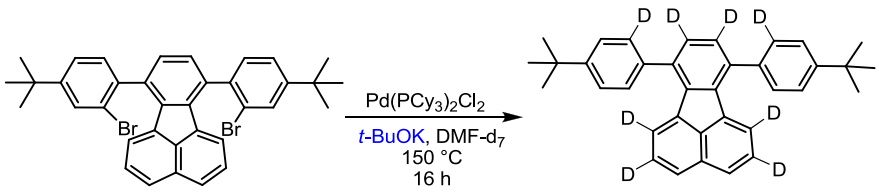

3-11 **3-24**

Scheme 3-8. Intramolecular Arylation with Potassium *Tert*-butoxide and DMF-d_7

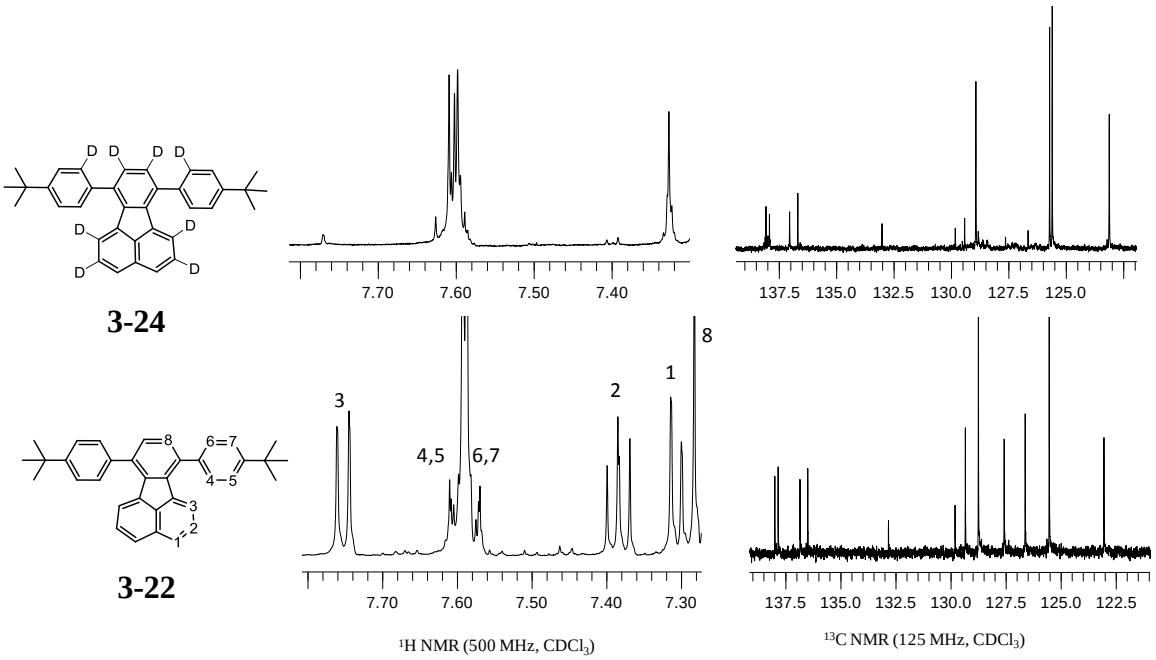

Figure 3-2. ^{1}H and ^{13}C NMR Comparison of Deuterium Incorporation

The surprising incorporation of eight deuterium atoms necessitated further investigation. It was postulated that the metal catalyst could possibly walk around the hydrocarbon, which has only limited precedent in the literature.[6] Another possibility was direct C-H activation, which could incorporate deuterium through H/D exchange catalyzed by palladium. To test these possibilities, the reaction was run with the standard conditions omitting either catalyst or base, as shown in Scheme 3-9. Not surprisingly, the reaction, when run without base did not incorporate any deuterium; however, when the reaction was run without palladium, the mixture of potassium *t*-butoxide and DMF-d_7 incorporated six deuterium atoms, **3-25**, with the site specificity being more ambiguous than was seen with both base and catalyst present. This result indicates that the base is facilitating H/D exchange, likely through the decomposition of DMF-d_7 at high temperatures. This H/D exchange will be discussed in further detail in Chapter 4. Based

on the aforementioned results, the solvent was likely a source of hydrogen, facilitating the reductive dehalogenation; however, the model system was more complex than initially expected and resulted in an unprecedented H/D exchange of polycyclic aromatic hydrocarbons.

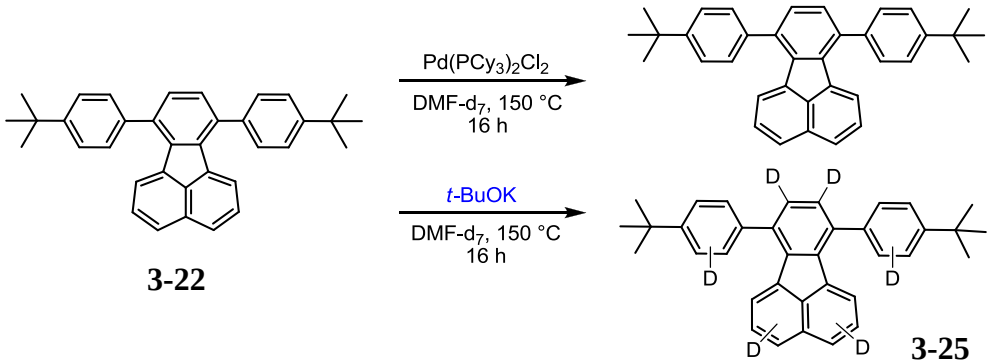

3-22 **3-25**

Scheme 3-9. Probing the Deuterium Incorporation

3.4 Synthesis of 1,1′-Bi(4,11-di-*tert*-butyldibenzo[*a,g*]corannulenyl)

With the optimized conditions and successful preparation of **3-4** in modest yields, synthesis of the desired target **3-3** was explored. As discussed in Chapter 1, dibenzo[*a,g,*]corannulene was directly dimerized to form **1-11**. In the case of **3-4**, direct dimerization to form **3-3** was unsuccessful under standard Scholl conditions due to the acid lability of the *tert*-butyl groups, resulting in direct elimination of the necessary solubility-enhancing functionality. An expanded synthetic route was explored, as shown in Scheme 3-10. Beginning with **3-4**, mono-bromination was achieved with iodine monobromide, incorporating bromine at the base of the fluoranthene core, **3-26**. Unfortunately, this reaction typically resulted in a common byproduct, over-bromination, which was difficult to control. Utilizing the halogen as a handle for direct homocoupling, $Ni(COD)_2$ was successfully employed to form **3-27** in 63% yield. Although this route

provided an advanced intermediate, **3-27**, the overall route was limited due to the low yield and laborious workup of **3-4**.

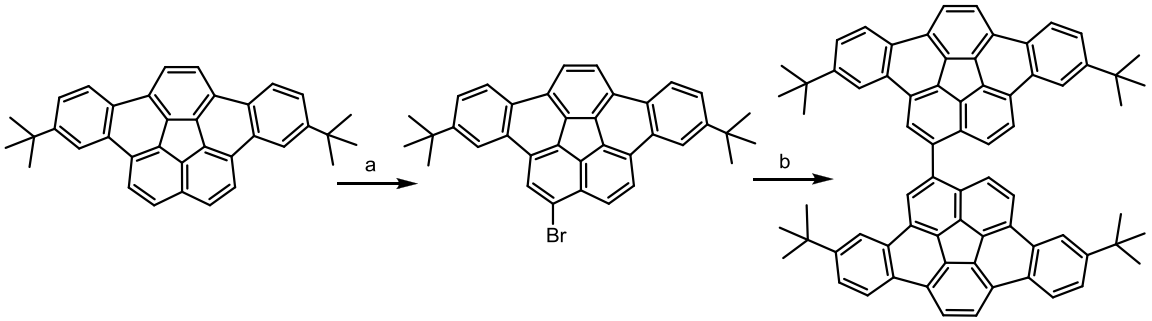

3-4 **3-26** **3-27**

a) IBr, DCM, RT; **57%** b) $Ni(COD)_2$, COD, 2,2'-bipyridyl, DMF, 60 ˚C; **63%**

Scheme 3-10. Synthesis of 1,1′-Bi(4,11-di-*tert*-butyldibenzo[*a,g*]corannulenyl)

3.5 Synthesis of 1,1′-Bi(5,10-di-*tert*-butyldibenzo[*a,g*]corannulenyl)

It was determined that the low yielding synthesis of **3-4** was problematic, and the issue of the brominated precursor, **3-11** (Table 3-1), would be solved by synthesizing the chlorinated precursor. A new synthetic route was designed, as shown in Scheme 3-11. A different tetra-*tert*-butyl-*peri*-*bis*(dibenzo[*a,g*]corannulene) (**3-28**) was targeted. This isomer can be synthesized in the same manner proposed previously, by preparation of **3-29**. These advanced precursors can be envisioned from the commercially available *p*-*tert*-butylchlorobenzene (**3-30**), which will incorporate the desired chlorine atom on the phenyl ring from the beginning of the synthesis.

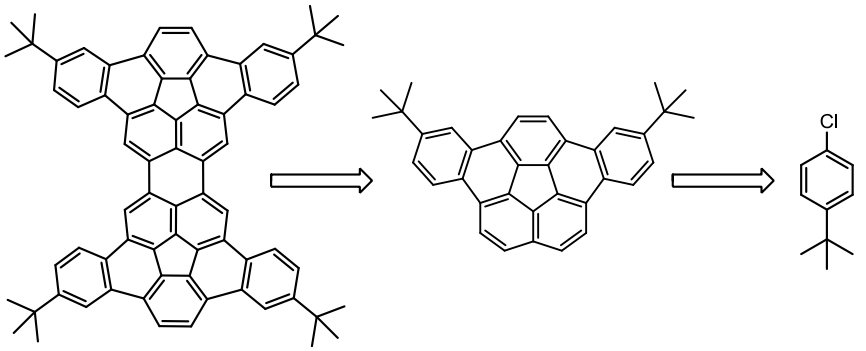

3-28 **3-29** **3-30**

Scheme 3-11. Retrosynthetic Analysis of *Peri-bis*(5,10-di-*tert*-butyldibenzo[*a,g*]corannulene)

Beginning from **3-30**, *ortho*-bromination with bromine afforded **3-31** in 98% yield (Scheme 3-12). A Suzuki coupling installed the desired methyl group, forming **3-32** in good yields. Benzylic bromination was accomplished with NBS to afford **3-33** in 92% yield. As previously seen, the benzylic bromination typically afforded a small amount of over-bromination at the benzylic position.

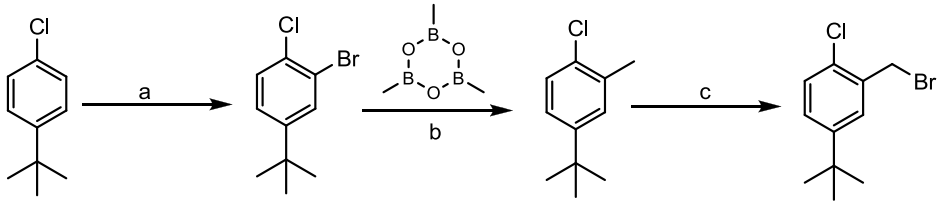

3-30 **3-31** **3-32** **3-33**

a) Br_2, AcOH, 50 ˚C; **98%**. b) $Pd(PPh_3)_4$, Cs_2CO_3, THF/H_2O, 95 ˚C; **90%**. c) NBS, CCl_4, 80 ˚C; **92%**

Scheme 3-12. Synthesis of 2-(Bromomethyl)-4-*tert*-butyl-1-chlorobenzene

With the desired benzylic halide installed, **3-33** was subjected to reaction conditions with diiron nonacarbonyl, affording the desired symmetrical ketone, **3-34**, Scheme 3-13. The biaryl ketone underwent a double aldol condensation with potassium hydroxide in methanol to afford the cyclopentadienone, **3-35**. As previously described, the cyclopentadienone was poised for a Diels-Alder/ retro Diels-Alder with a dienophile. In

this particular synthesis, nitroethylene was utilized as a dienophile, generated in situ from nitroethanol with phthalic anhydride to form **3-36** in 85% yield. There were some benefits of utilizing nitroethylene as a dienophile, versus the previously used norbornadiene, where the reaction time was significantly decreased from 3-5 days to just 24 hours.

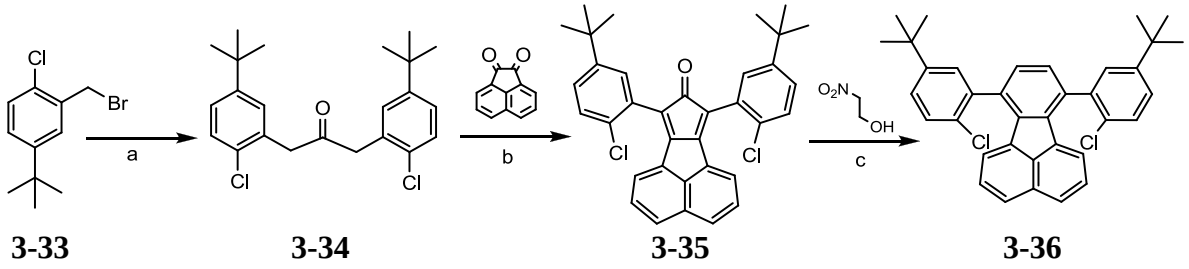

3-33 **3-34** **3-35** **3-36**

a) $Fe_2(CO)_9$, benzene, 80 ˚C; **64%** b) KOH, MeOH, RT; **55%** c) Phthalic Anhydride, toluene, 140 ˚C; **85%**

Scheme 3-13. Synthesis of 7,10-*Bis*(5-*tert*-butyl-2-chlorophenyl)fluoranthene

With the chlorinated material in hand, **3-36** was subjected to standard intramolecular arylation conditions, to form the desired dibenzo[*a*,*g*]corannulene, **3-29**, in 84% yield, Scheme 3-14. The previously problematic reductive dehalogenation product was not observed in this intramolecular arylation, and a significant increase from 50% with the brominated precursor, **3-11**, to 84% from the chlorinated precursor, **3-36**. With the ability to synthesize significant quantities of the specifically *tert*-butyl material, compound **3-29** was subjected to bromination conditions with iodine monobromide to afford **3-36** in good yields. As previously seen, over bromination of **3-29** was problematic, always forming a small amount of dibrominated material. Again, compound **3-36** was subjected to homocoupling conditions with Ni (0) to afford the homodimer of **3-29**, compound **3-37**, which is all but one carbon-carbon bond short of the desired target, **3-28**.

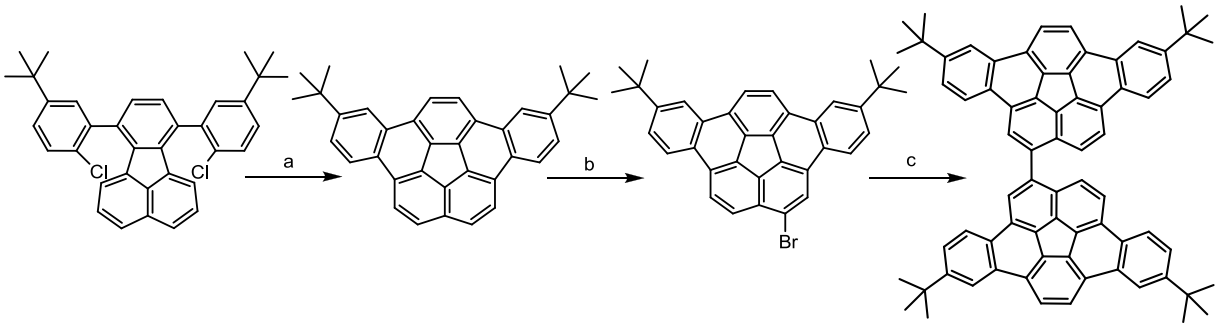

3-36 **3-29** **3-36** **3-37**

a) $Pd(PCy_3)_2Cl_2$, DBU, DMAc, 150 ˚C; **84%** b) IBr, DCM, RT; **64%** c) $Ni(COD)_2$, COD, 2,2'-bipyridyl, DMF, 60 ˚C; **74%**.

Scheme 3-14. Synthesis of 1,1′-Bi(5,10-di-*tert*-butyldibenzo[*a,g*]corannulenyl)

3.6 Intramolecular Cyclodehydrogenation

The two isomers of the tetra-*tert*-butyl homodimers completed, **3-27** and **3-37**, were poised for cyclization to form the perylene core and desired materials **3-3** and **3-28**. Initial studies with **3-27** aimed to utilize Scholl conditions to promote the cyclization. It was shown in Chapter 1 that a Lewis acid and oxidant provided the direct dimer of dibenzo[*a,g*]corannulene very efficiently. These conditions were a concern for the present system, due to the acid labile *tert*-butyl groups; however, initial screenings with Scholl conditions provided some promising results, as shown in Table 3-2.

The optimal conditions, a mixture of aluminum chloride and copper (II) triflate, afforded cyclization in as little as 4 minutes in dichloroethane. Further investigation found that the cyclodehydrogenation was concentration and temperature dependent; the cyclization reaction was in competition with dealkylation, which was also promoted by the Lewis acid. It was found that increasing the temperature diminished the dealkylation and

increased the rate of the cyclodehydrogenation. Milder reaction conditions were also explored, with BF_3Et_2O and PIFA; however, no cyclodehydrogenation was observed. The acid labile nature of the *tert*-butyl groups was increasingly an issue, and although they remained intact, it appeared by ^1H NMR that the alkyl groups were scrambling, affording mixtures of isomers and still impeding both the analysis of the ^1H NMR and isolation of the desired product, **3-3**. It should be noted that a few other common Lewis acids ($MoCl_5$ and $FeCl_3$) were examined but lead to no reaction with this particular substrate.

Table 3-2. Cyclodehydrogenation

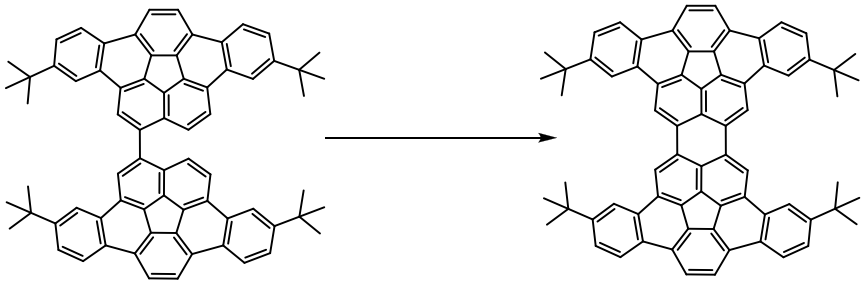

3-27 **3-3**

Lewis Acid	Oxidant	Solvent [M]	T (˚C)	t (min)	Result
10 eq $AlCl_3$	2 eq $Cu(OTf)_2$	DCM [0.0072]	r.t.	30	Cyclization with some *t*-butyl loss
10 eq $AlCl_3$	2 eq $Cu(OTf)_2$	DCM [0.0072]	0	30	t-butyl loss
10 eq $AlCl_3$	**2 eq $Cu(OTf)_2$**	**DCE [0.0054]**	**80**	**4**	**Cyclization with minor t-butyl loss**
10 eq $AlCl_3$	2 eq $Cu(OTf)_2$	DCE [0.0054]	r.t.	60	No Reaction
3.2 eq $BF_3{\cdot}Et_2O$	2 eq PIFA	DCM [0.011]	-40	4 h	No Reaction
10 eq $MoCl_5$	2 eq $Cu(OTf)_2$	DCM [0.0054]	r.t.	2 h	No Reaction
10 eq $FeCl_3$	2 eq $Cu(OTf)_2$	DCM [0.0054]	r.t.	5 h	No Reaction

Recently, multiple publications have utilized DDQ and either methane sulfonic acid or trifluoromethane sulfonic acid to form new carbon-carbon bonds in polycyclic aromatic hydrocarbons.[7] These conditions were applied to compound **3-37**, but initial findings were not promising (Scheme 3-15). Excess acid was found to lead to dealkylation;

however, when employing a slight excess of trifluoromethane sulfonic acid (2 equivalents) and DDQ (1 equivalent) in dichloromethane at room temperature, it was discovered that cyclization occurred in 5 minutes. After purification on reverse phase silica gel preparative layer chromatography, ^{1}H NMR analysis again provided an indecipherable spectrum, in which the aromatic region was significantly overlapping and splitting was not well defined, Figure 3-3. Addition of the acid, dropwise up to 1.1 equivalent, to a mixture of DDQ (5 equivalents) and **3-37** in dichloromethane, provided what appeared to be an intermolecular reaction, forming undesirable polymers, and the desired intramolecular cyclodehydrogenation was not occurring efficiently.

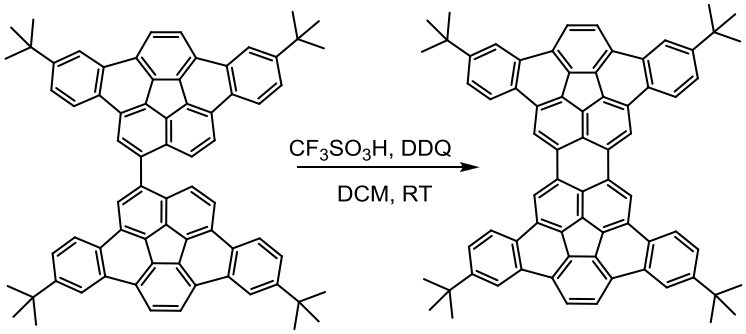

3-37 **3-28**

Scheme 3-15. Synthesis of *Peri-bis*(5,10-di-*tert*-butyldibenzo[*a,g*]corannulene)

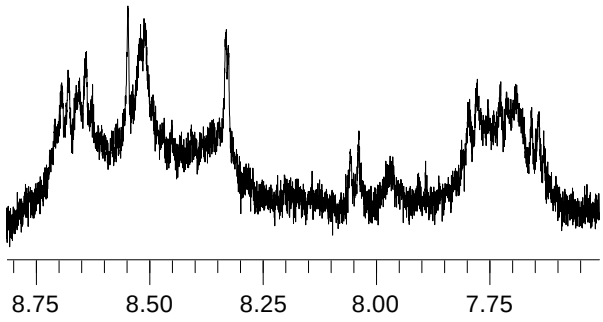

Figure 3-3. Crude ^{1}H NMR of *Peri-bis*(5,10-di-*tert*-butyldibenzo[*a,g*]corannulene)

3.7 Friedel-Crafts Alkylation of *Peri-bis*(dibenzo[*a,g*]corannulene)

Without the ability to isolate pure, specifically *tert*-butyl material (either **3-3** or **3-28**), another route was explored to incorporate *tert*-butyl groups. The terta-alkylation of **1-11** had previously been explored.[8] It was known that the Friedel-Crafts tetra alkylation with *tert*-butylchloride would afford **3-2**, a tetra-*tert*-butyl PAH; however, this method formed many isomers due to the lack of site specificity. It was expected that the alkylation would only take place at the β position of the benzo rings, since these are the most sterically accessible positions on the molecule. As shown in Scheme 3-16, the tetra alkylation was achieved with *tert*-butylchloride and aluminum chloride in 45% yield to give a bright red, soluble material, **3-2**. The solubility of **3-2** was a marked improvement, and it was clear that the *tert*-butyl groups were very effective towards breaking up the problematic aggregation of **1-11**. The improved solubility in common organic solvents, e.g., dichloromethane, benzene, and carbon disulfide, allowed for effective purification of this material on neutral alumina; it was found that material recovery was diminished when silica gel was used, which may be due to the acid sensitivity of the *tert*-butyl groups. Unfortunately, ^{1}H NMR analysis was not fruitful due to the multiple isomers formed, making the aromatic region uninterpretable; however, analysis by high resolution MALDI-TOF mass spectrometry confirmed the product **3-2**. With soluble material in hand, further functionalization of the hydrocarbon **3-2** was explored.

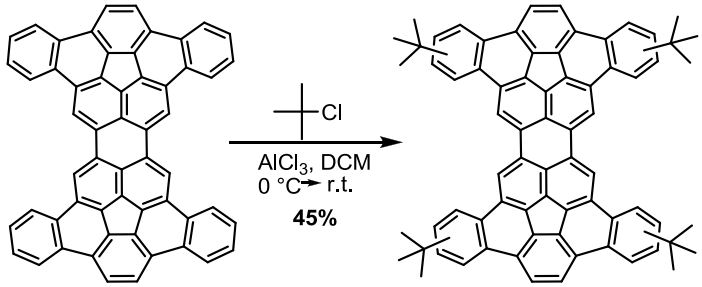

1-11 **3-2**

Scheme 3-16. Synthesis of Tetra-*tert*-butyl-*peri*-*bis*(dibenzo[*a,g*]corannulene)

3.8 Diels-Alder Addition

The effect of solubility had yet to be explored with regards to the Diels-Alder addition of dienophiles to **3-2**. As discussed in Chapter 1, the insolubility of **1-11** complicated the purification, isolation and overall efficiency of the Diels-Alder addition of *N*-methyl- and *N*-phenylmaleimide. As shown in Chapter 2, the solubility of the Diels-Alder adduct aided in isolation of pure product, but the insolubility of **1-11** significantly affected the conversion of the reaction.

Subjecting **3-2** to Diels-Alder conditions with *N*-methylmaleimide in *o*-dichlorobenzene at 180 ˚C, for 5 days afforded a soluble double Diels-Alder adduct, **3-38**, in very good yield, 85%, as shown in Scheme 3-17. It was clear from this reaction that the conversion was significantly improved due to the solubility of the starting material. Most importantly, the resulting product, **3-38**, was very soluble in common organic solvents, allowing for purification by chromatography. As was seen with **3-2**, ^{1}H NMR analysis was complicated due to the various alkylation isomers. The formation of **3-38** was confirmed by high resolution MALDI-TOF mass spectrometry. It should be noted that

the isolated product had lost the original bay region hydrogens to re-form the aromatic perylene core. As discussed in Chapter 1, the Diels-Alder reactions are assumed to give *cis*-ring fusions, but the relative stereochemistry of the two imides (*syn vs anti*) could not be determined by NMR analysis due to the resulting complex spectrum. The two stereoisomers of **3-38** provided **3-39** by a final aromatization of the newly formed 6-membered rings, installing the desired coronene core, which was achieved with DDQ in benzene at elevated temperatures, to afford **3-39** in 90% yield.

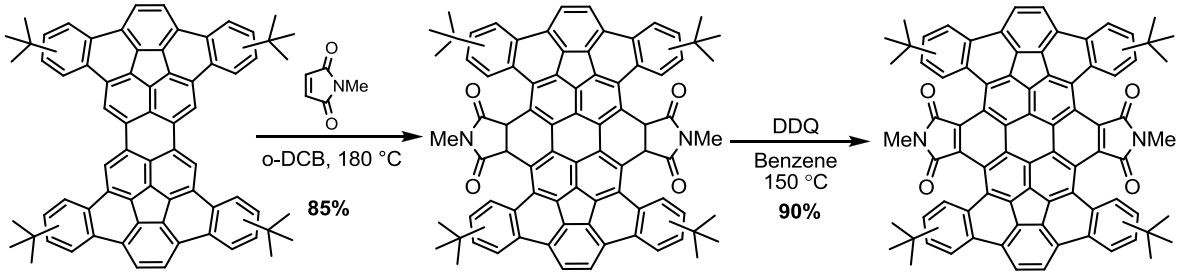

3-2 **3-38** **3-39**

Scheme 3-17. Diels-Alder Addition of *N*-Methylmaleimide

With this successful Diels-Alder addition, a very advanced precursor, **3-39**, encompassed all necessary carbon atoms for the desired [6,6] carbon nanotube end-cap, or $C_{60}H_{12}$ bowl. The addition of the maleimides provided a benzyne generating functionality. Maleimides have been shown to produce benzynes under pyrolysis conditions, as discussed in Chapter 1; however, anhydrides have been more commonly used as benzyne generating functionality and represent the simplest precursor possible. Unfortunately, even beginning with the soluble starting material, no Diels-Alder addition of maleic anhydride was observed, as shown in Table 3-3. With this failure, methods were sought to convert the imides into anhydrides through hydrolysis.

Table 3-3. Attempted Diels-Alder Addition of Maleic Anhydride

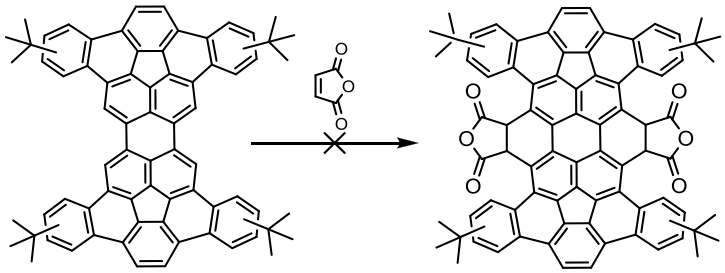

Entry	Maleic Anhydride	Solvent	Temp (˚C)	Time	Result
1	20 eq	*o*-DCB	180	5 d	No Reaction
2	20 eq	*o*-DCB	220	5 d	No Reaction[a]
3	20 eq	*o*-DCB	230	14 d	No Reaction

[a] 5 equiv. of *p*-chloranil was used.

3.9 Hydrolysis of Maleimides

Initial investigations for the hydrolysis of the *N*-methylmaleimide adduct, **3-39**, provided limited results. It was found that typical acid or base hydrolysis conditions were ineffective with this particular substrate (**3-39**). The strain encountered in the formation of a tetrahedral intermediate (**3-41**) in the hydrolysis of was a matter of concern, since the imide moiety is in a congested region of the molecule. Computational analysis of the hydrolysis was examined, utilizing an isodesmic reaction to identify the strain built up from the formation of a tetrahedral intermediate. *N*-Methylphthalimide was used to represent a 'strain-free' tetrahedral intermediate, **3-40**, and compared to the tetrahedral intermediate of **3-41**. It was found that there was only a small energy increase for the formation of the tetrahedral intermediate **3-41**, only 1.2 kcal/mol, which indicates that the strain of the hydrolysis intermediate should not be an issue in this reaction.

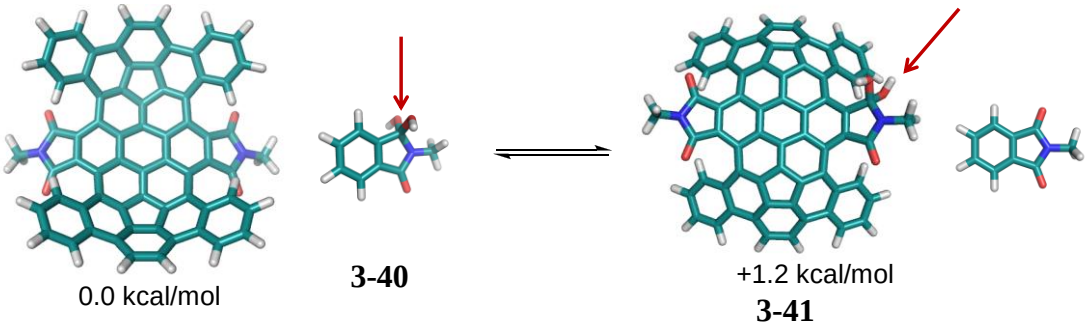

Figure 3-3. Isodesmic Reaction Study of the Tetrahedral Intermediate (B3LYP/6-31G*)

As discussed in Chapter 2, the Diels-Alder addition of *tert*-octylmaleimide to **1-11** provided soluble material, and a route to convert this bulky imide to an anhydride was pursued. A test system was developed by synthesizing *tert*-octylphthalimide (**3-43**) from phthalic anhydride (**3-42**), Scheme 3-18. A variety of hydrolysis conditions were tested, including phase transfer catalysts, specifically $(n\text{Bu})_4\text{NBr}$ with potassium hydroxide in xylene and water; however, only 10% conversion to the anhydride was observed. It was not until the solvent and base combination of *tert*-butanol and potassium hydroxide with 10% water were applied, that 98% yield of the desired anhydride (**3-42**) was observed.[9]

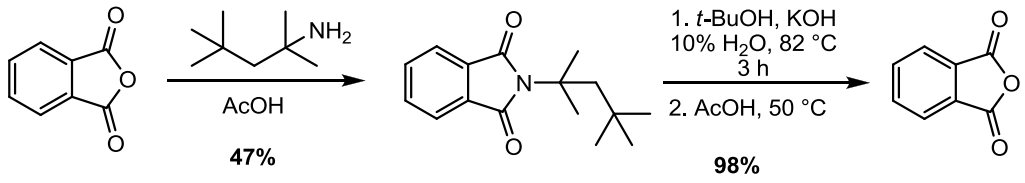

3-42 **3-43** **3-42**

Scheme 3-18. Hydrolysis Test System

It should be noted that a variety of other solvents, with potassium hydroxide, were attempted, including *n*-butanol, methanol, and ethylene glycol, but all failed to provide formation of the anhydride.

The hydrolysis conditions in Scheme 3-18 were applied to the parent system as shown in Scheme 3-19. Hydrolysis of the *N*-methylmaleimide moiety was successfully accomplished with *tert*-butanol and potassium hydroxide after 3 days to afford the dianhydride, **3-44**, in 98% yield. The increase in reaction time with the parent system is likely due to the limited solubility of **3-39** in *tert*-butanol. With the successful synthesis of **3-44**, the simplified precursor to the end-cap was poised for flash vacuum pyrolysis experiments.

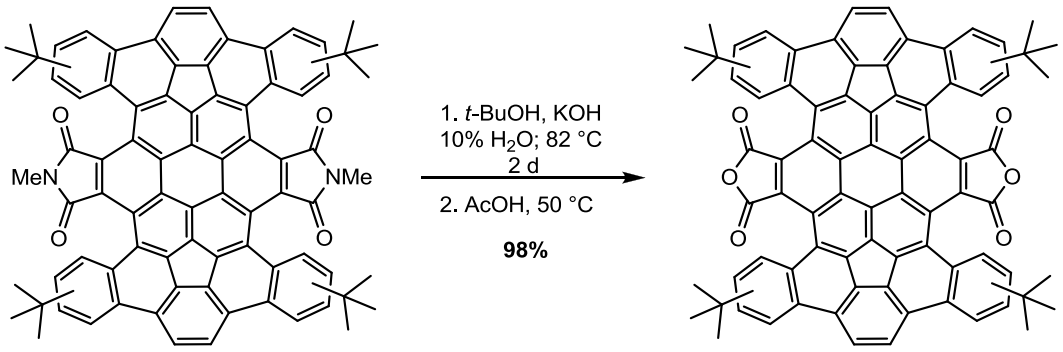

3-39 **3-44**

Scheme 3-19. Hydrolysis of *N*-methylmaleimide

3.10 Flash Vacuum Pyrolysis to Form a [6,6] Carbon Nanotube End-Cap

With the hydrocarbon framework in place, **3-44** was poised to be subjected to flash vacuum pyrolysis (FVP) conditions aiming to form the desired $C_{60}H_{12}$ end-cap.[10] Previous syntheses have successfully employed FVP to generate radicals from the

homolytic cleavage of weak bonds, leading to the formation of highly curved hydrocarbons.[11] It was clear that significant curvature would need to be imposed in order to form the desired end-cap. As shown in Figure 3-4, the *bis*-anhydride, **3-45**, is relatively planar, but once the benzyne centers are generated, formation of four new 5-membered rings would produce the highly curved intermediate, **3-46**. Precedent for the formation of *ortho*-benzyne centers has been previously reported and discussed in Chapter 1.[12] From this intermediate, cyclodehydrogenation to form two additional 6-membered rings would complete the desired end-cap, **1-8**.

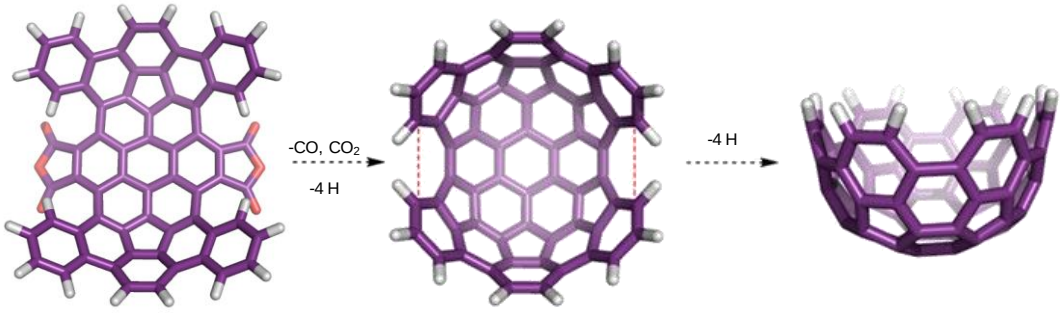

3-45 **3-46** **1-8**

Figure 3-4. Proposed Cyclization to the Desired End-Cap

One question remained regarding the *tert*-butyl groups; it was not clear what the fate of these alkyl groups would be during pyrolysis. Initial attempts to remove the *tert*-butyl groups proved unsuccessful, as shown in Scheme 3-20. The material was subjected to acidic conditions to eliminate the alkyl functionality, and an insoluble material was recovered; however, analysis of this material did not provide any evidence of the desired parent compound, **3-45**.

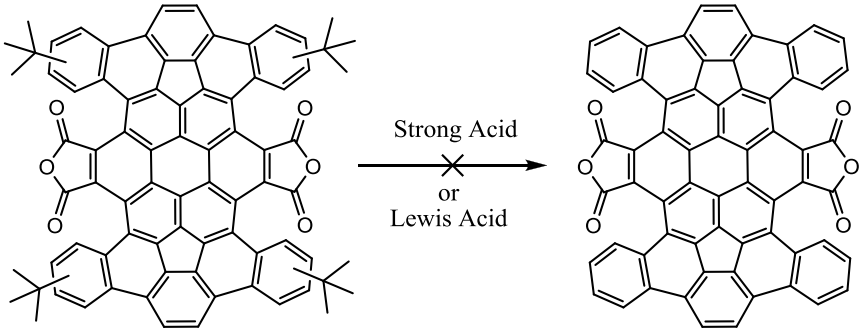

3-44 **3-45**

Scheme 3-20. Attempted Dealkylation

In the face of this setback, it was decided that pyrolysis of a test system that contained *tert*-butyl groups should be investigated prior to exerting extensive efforts to remove the *tert*-butyl groups. Pyrolysis of 7,10-*bis*(2-bromo-4-*tert*-butylphenyl)fluoranthene as the test system is expected to form dibenzo[*a*,*g*]corannulene, provided the *tert*-butyl groups eliminate cleanly. As shown in Scheme 3-21, pyrolysis of **3-11** indeed provided dibenzo[*a*,*g*]corannulene in 30% yield. This yield was only slightly diminished from the yield of the pyrolysis of 7,10-*bis*(2-bromophenyl)fluoranthene, which afforded dibenzo[*a*,*g*]corannulene in 36% yield. No remnants of the *tert*-butyl groups were detected, and the pyrolysis proceeded cleanly. This result confirmed that removal of the *tert*-butyl groups from the parent system prior to pyrolysis should not be necessary.

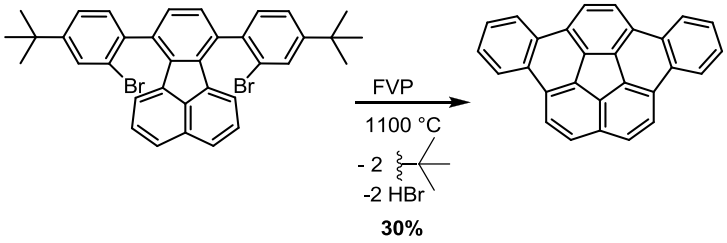

3-11 **3-16**

Scheme 3-21. Pyrolysis of 7,10-*Bis*(2-bromo-4-*tert*-butylphenyl)fluoranthene

Initial pyrolysis experiments with **3-44** to form the desired end-cap, **1-8**, were very promising (Scheme 3-22). Subjecting **3-44** to pyrolysis conditions, 1100 ˚C and 0.50 torr, with a steady stream of nitrogen gas, afforded a small amount of orange material. Upon completion of the experiment, the glass surfaces were extracted with dichloromethane, removing any soluble material from the tube and traps. The glass surfaces remained slightly colored, which could not be removed by a large variety of organic solvents, even at elevated temperatures. Only extensive soaking with a potassium hydroxide/isopropanol solution removed the color. Initial experiments were run on a 300 mg scale and afforded almost no degraded starting materials in the boat, or carbon soot in the hot zone; however, only 5 mg of crude material was extracted from the apparatus after pyrolysis. The slow introduction of material into the hot zone by temperature gradient sublimation provided less carbon soot, but the crude material isolated from the reaction was very minimal. The low mass recovery was improved by directly inserting the starting material (**3-44**), absorbed onto quartz sand, into the hot zone all at once, improving the isolated crude material, on a 150 mg scale, to 13 mg; however, more carbon soot was produced.

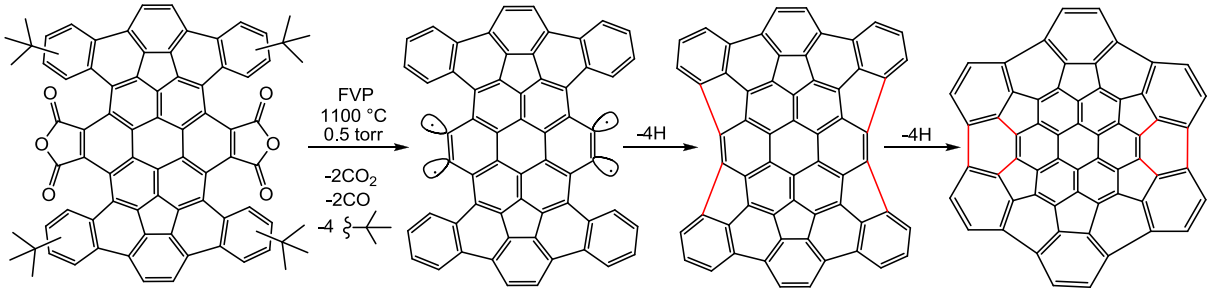

3-44 **3-47** **3-46** **1-8**

Scheme 3-22. Pyrolysis of the *Bis*-anhydride Diels-Alder Adduct to form $C_{60}H_{12}$

The crude pyrolysates were initially analyzed with MALDI-TOF mass spectrometry, from which a high resolution spectrum confirmed the formation of the $C_{60}H_{12}$ end-cap (*m/z* 732), **1-8** (Figure 3-5). This indicated that the anhydrides successfully eliminated CO and CO_2 to form the reactive benzyne centers, facilitating the formation of four new 5-membered rings and two new 6-membered rings. As seen in the spectrum, two other peaks are also prominent, *m/z* 760, and *m/z* 788. These peaks do not correspond to any fragments of the target end-cap but are actually heavier by 28 and 56 mass units, respectively. We speculate that these byproducts might correspond to materials that have retained one or two carbonyl groups, respectively. Attempts to obtain molecular formulas by high resolution mass spectrometry, however, were not fruitful in this case, and the identity of these peaks cannot currently be assigned with certainty. Also, a peak at *m/z* 696 was observed, which corresponds to a common contaminant, *peri-bis*(dibenzo[*a*,*g*]corannulene).

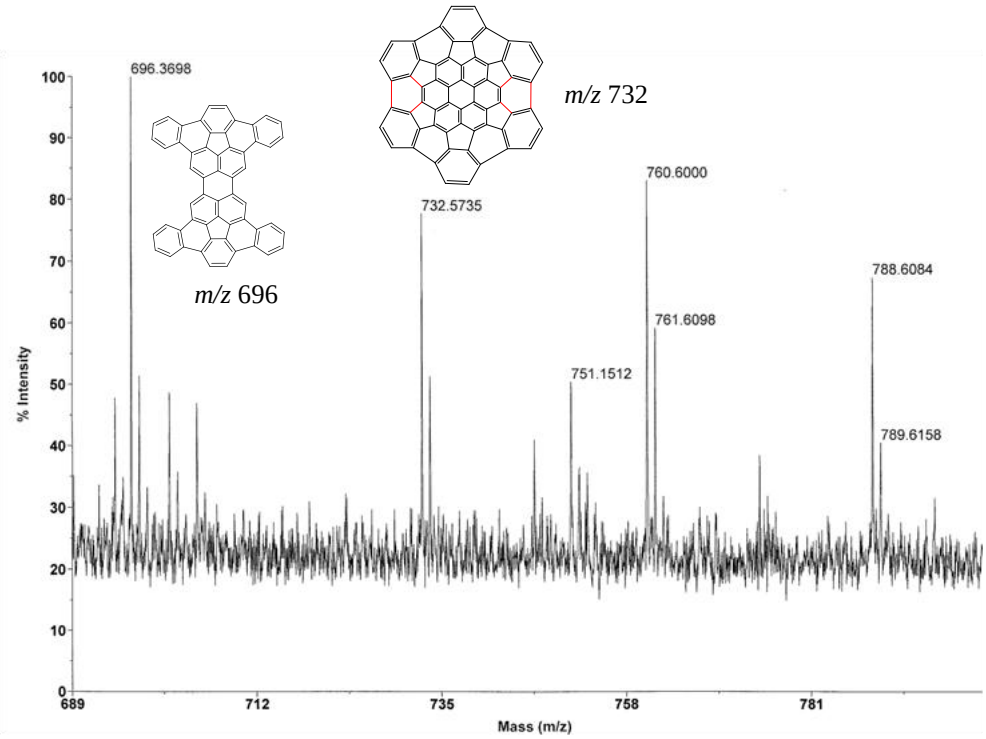

Figure 3-5. MALDI-TOF Mass Spectrum of the Crude Pyrolysate

As discussed in Chapter 1, regarding the synthesis of the [5,5] end-cap, ^{1}H NMR spectroscopy shows a singlet at 7.63 ppm for the $C_{50}H_{10}$ end-cap.[11b] DFT NMR calculations were performed for both end-caps, as shown in Table 3-4. The predicted NMR spectrum for the $C_{50}H_{10}$ end-cap corresponds nicely with the experimental spectrum, predicting a singlet at 7.64 ppm versus the experimental observed singlet at 7.63 ppm. From these calculations, it is predicted that the ^{1}H NMR chemical shift for the $C_{60}H_{12}$ end-cap should fall close to 7.40 ppm.

Table 3-4. ^{1}H NMR Calculations

Compound	B3LYP/6-31G*//AM1	B3LYP/6-31G*// B3LYP/6-31G*	Experimental
$C_{50}H_{10}$	7.81	7.64	7.63 (CD_2Cl_2)
$C_{60}H_{12}$	7.60	7.40	-

As shown in Figure 3-6, the ^{1}H NMR spectrum of the crude pyrolysate exhibited very distinctive signals from 7.62-7.28 ppm, which were confirmed to correspond to a byproduct formed in the pyrolysis, *p*-terphenyl. With this major contaminant in the crude mixture, it was difficult to determine whether or not a singlet for the 12 identical protons of the end-cap was present. The presence of *p*-terphenyl was further confirmed by GC/MS, which also indicated a small amount of biphenyl in the mixture. It is likely that the biphenyl signals overlap with those of the *p*-terphenyl in the ^{1}H NMR spectrum. As shown in Equation 1, terphenyl might be formed in the pyrolysis of **3-44** by an "unzipping" mechanism, involving successive β-scissions and intermittent hydrogen abstractions. Biphenyl could break off as a side product. Due to the abundance of these impurities, purification of the crude pyrolysate was investigated.

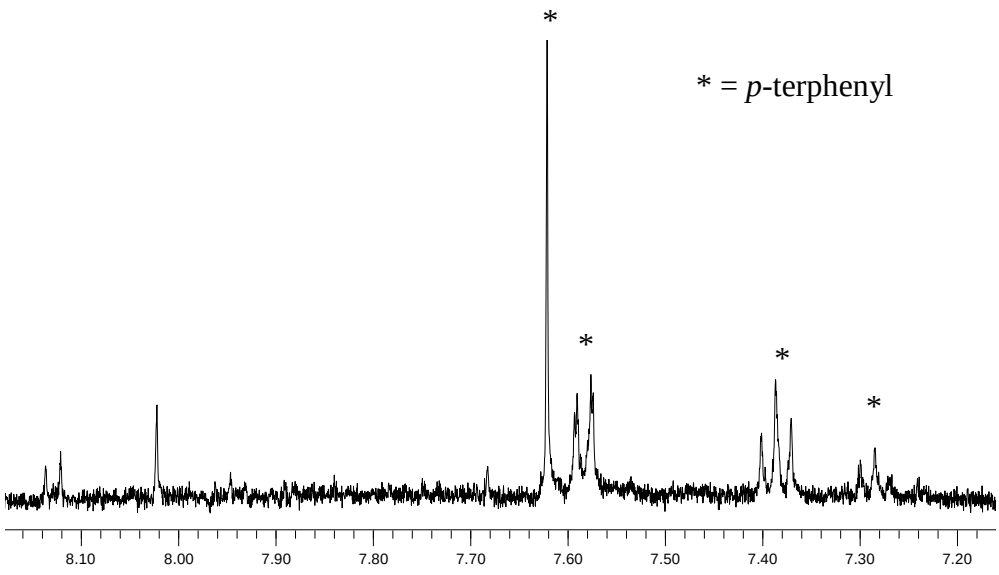

Figure 3-6. ^{1}H NMR of the Crude Pyrolysate (CD_2Cl_2, 500 MHz)

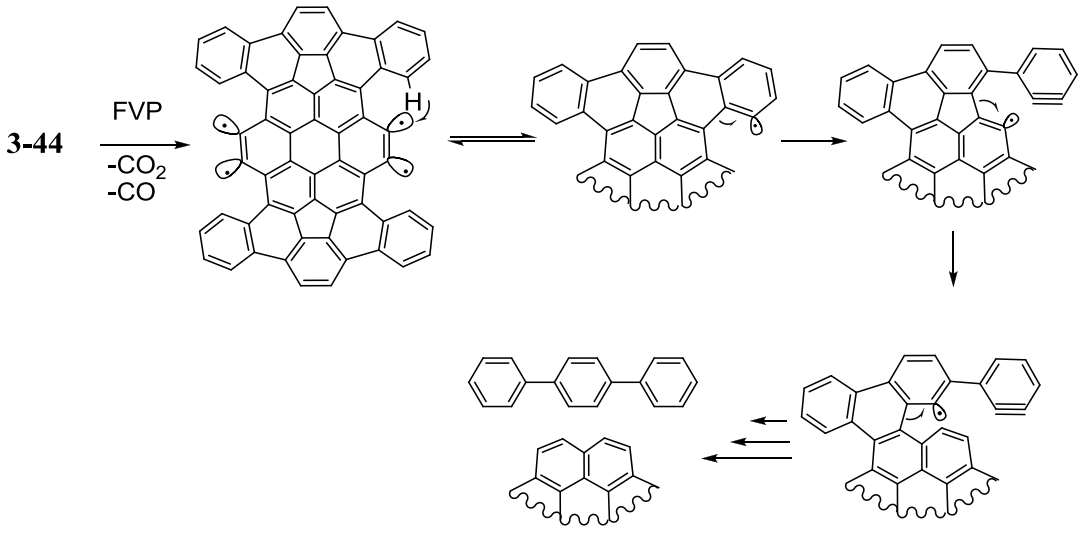

(1)

The $C_{50}H_{10}$ [5,5] nanotube end-cap is highly soluble in a variety of organic solvents, specifically dichloromethane, and was successfully purified by silica gel chromatography. It was therefore expected that the $C_{60}H_{12}$ [6,6] nanotube end-cap (**1-8**) would also be soluble, and, in fact, the crude material was soluble in dichloromethane. Purification of the crude mixture was initially attempted by reverse phase silica gel chromatography, with dichloromethane/hexanes as the eluent, but no material of *m/z* 732 was recovered, indicating that the material likely adhered to the solid support. The only material recovered from chromatography was a small amount of biphenyl, which was confirmed by GC/MS.

Focus was turned towards recrystallization of the crude material. The crude material was washed with hexanes; however, it appeared that the material was too soluble in hexanes, and it was not possible to remove the impurities by this method. Recrystallization in

methanol precipitated a small amount of orange solid, 0.6 mg, which was collected and analyzed. The ^{1}H NMR, as shown in Figure 3-7, was the characteristic spectrum of *p*-terphenyl. Further analysis of the methanol filtrate, Figure 3-8, recovered 8 mg of predominantly *p*-terphenyl; however, there were significant signals further downfield. These signals are likely too far downfield to be the desired end-cap, but they may correspond to the *m/z* 760 and 788 peaks seen in the MALDI-TOF spectrum (Figure 3-5).

Although the molecular formulas for the masses *m/z* 760 and *m/z* 788 were not confirmed by high resolution mass spectrometry, the masses corresponded closely to the molecular formulas $C_{61}H_{12}O$ or $C_{62}H_{16}$ for *m/z* 760 and $C_{62}H_{12}O_2$ or $C_{64}H_{20}$ for *m/z* 788. It is likely that these structures, although not confirmed, would be less symmetric than the end-cap, and would also have hydrogens in bay- or cove-regions, causing the downfield shift seen in the proton NMR. These proposed molecular formulas are likely representative of the signals seen in Figures 3-8, with chemical shifts between 8.10 and 7.66 ppm. It was not inconceivable that these masses may correspond to incomplete reaction of the starting material, in which all of the desired C-C bonds may not have formed, potentially trapping CO.

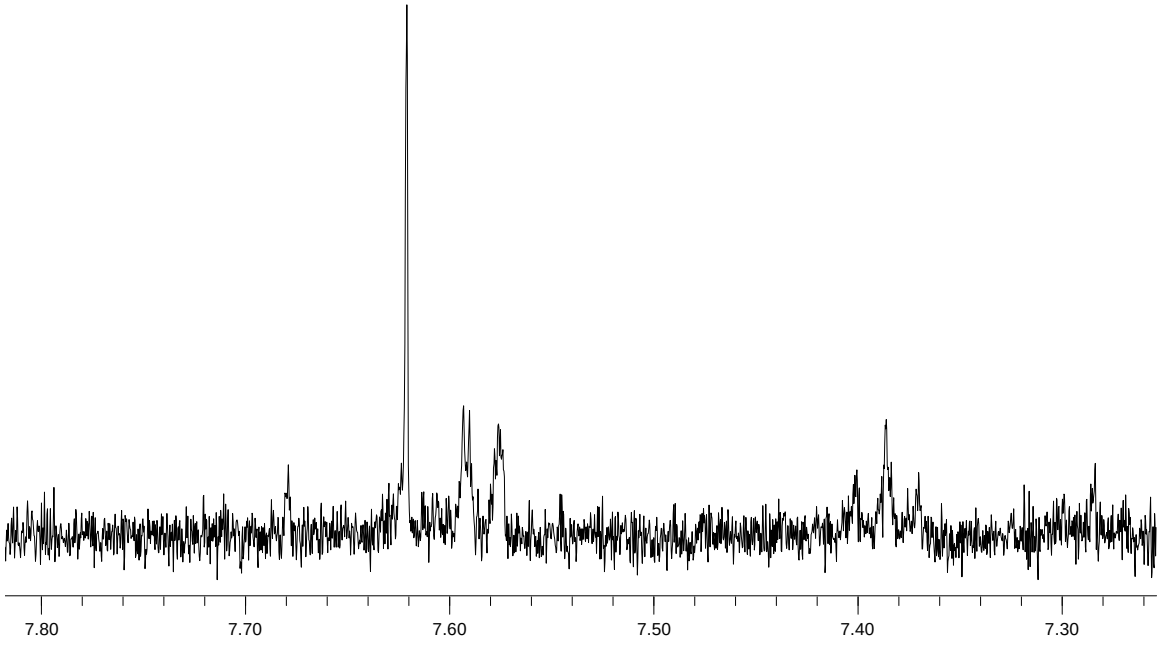

Figure 3-7. ^{1}H NMR of Methanol Precipitate (CD_2Cl_2, 500 MHz)

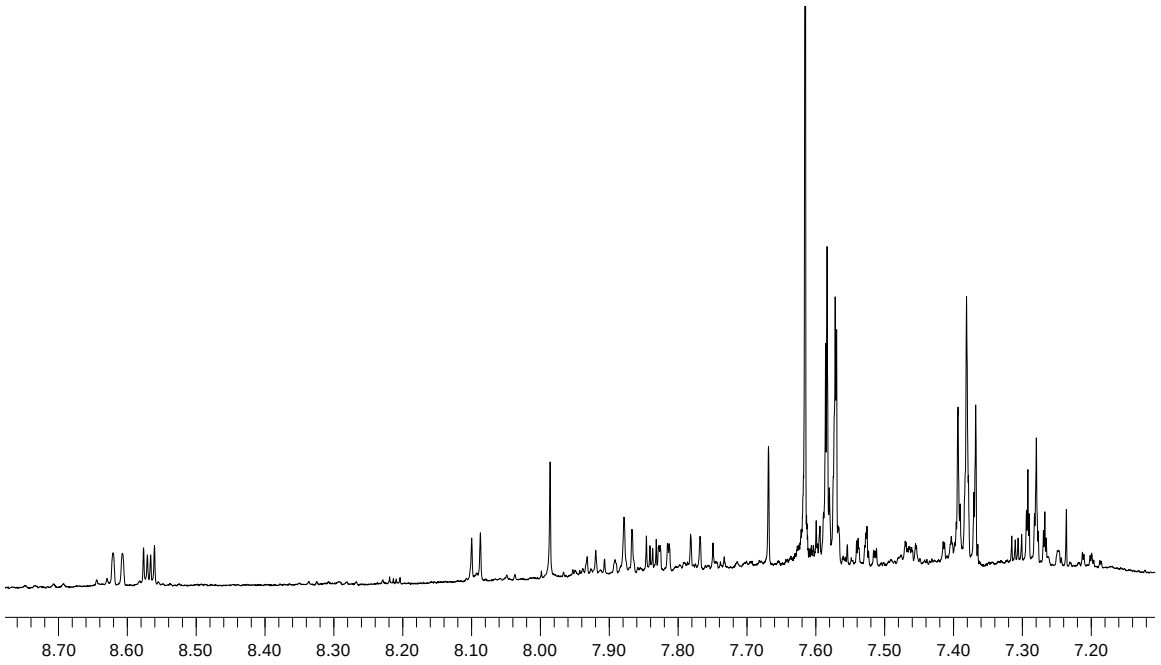

Figure 3-8. ^{1}H NMR of Methanol Filtrate (CD_2Cl_2, 600 MHz)

Two possible byproducts of the pyrolysis were proposed (**3-48** and **3-46**), and NMR calculations were performed to aid in their characterization (shown in Table 3-5). The first byproduct, a diketone (**3-48**), fits the observed mass, *m/z* 788, in the MALDI-TOF spectrum. It was predicted to have three unique hydrogens in the proton NMR, with chemical shifts (ppm) at 7.71 (d), 7.66 (d), and 7.58 (s). It was believe that this byproduct could arise from incomplete fragmentation of **3-44**, with retention of two equivalents of CO. The second byproduct examined, **3-46**, could arise from incomplete cyclization, where the final two 6-membered rings were not cyclized. The proton NMR spectrum for this highly symmetric molecule was predicted to have four unique hydrogens, with chemical shifts (ppm) at 7.69 (d), 7.67 (d), 7.64 (s), and 7.19 (t). Although **3-46** was not detected by mass spectrometry, it is predicted to be a pivotal intermediate for the formation of the desired end-cap.

Comparing the experimental proton NMR spectrum of the filtrate (Figure 3-8) to the predicted spectra for both **3-48** and **3-46**, clearly reveals some differences, specifically the signals further downfield of 7.80 ppm in the experimental spectrum. More importantly, there is a large cluster of signals from 7.90-7.70 ppm and one singlet at 7.67 ppm that may correspond to the diketone, **3-48**. Unfortunately, on such a small scale, it was not possible to separate out these proposed byproducts from the crude mixture.

Table 3-5. NMR Calculations of Possible Pyrolysis Byproducts

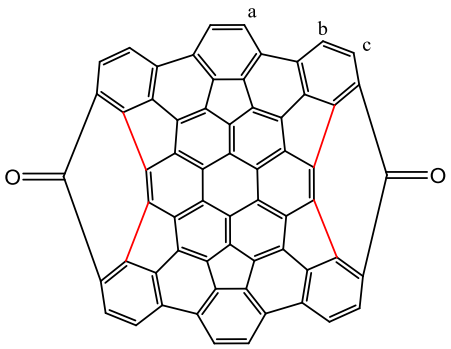

$C_{62}H_{12}O_2$

3-48

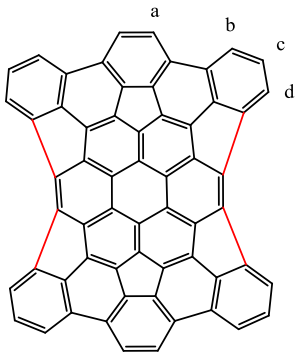

$C_{60}H_{16}$

3-46

		B3LYP/6-31G*//AM1	B3LYP/6-31G*// B3LYP/6-31G*
$C_{62}H_{12}O_2$	**a**	7.70	7.58
	b	7.83	7.71
	c	7.51	7.66
$C_{60}H_{16}$	**a**	7.82	7.64
	b	7.85	7.69
	c	7.29	7.19
	d	7.80	7.67

Analysis of the crude mixture by UV-Vis showed absorbance from 234 nm to 520 nm (Figure 3-9). The presence of *p*-terphenyl was confirmed with an authentic UV-Vis spectrum (Figure 3-10), in which a λ_{max} at 280 nm was observed. The reference cell was spiked with *p*-terphenyl, effectively subtracting the *p*-terphenyl absorption from the crude spectrum, as shown in Figure 3-11, which indicates that there is a larger aromatic system present with absorptions beyond 500 nm.

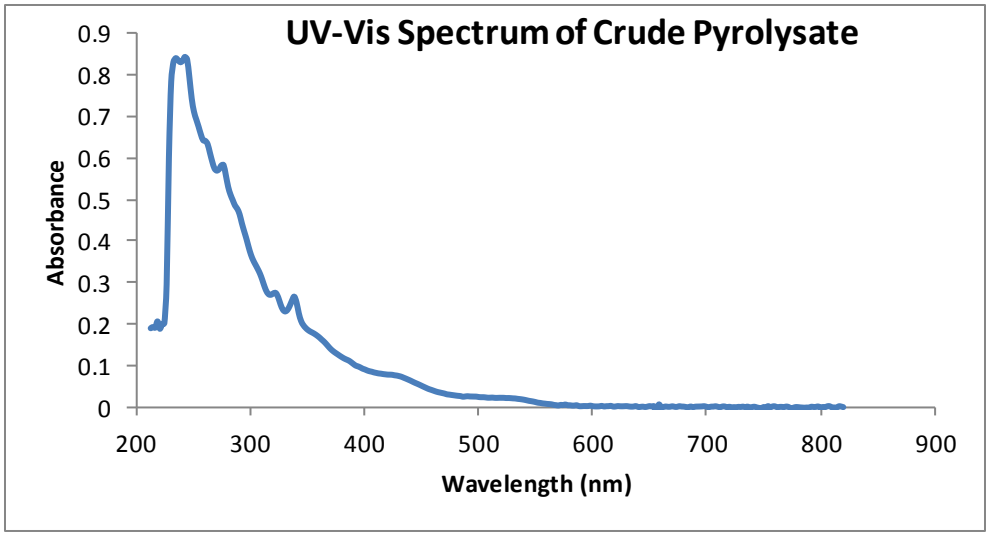

Figure 3-9. UV-Vis Spectrum of Crude Pyrolysate

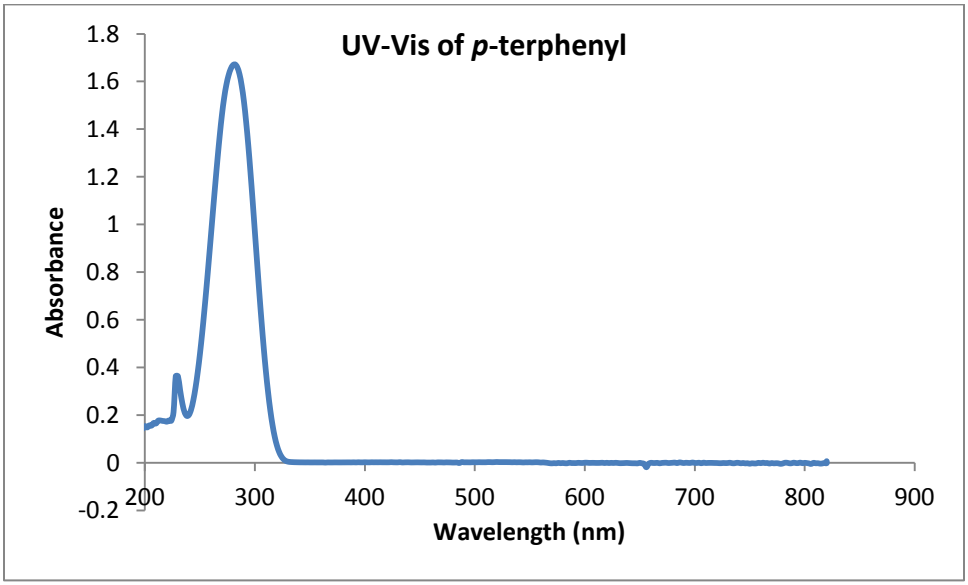

Figure 3-10. UV-Vis of *p*-Terphenyl

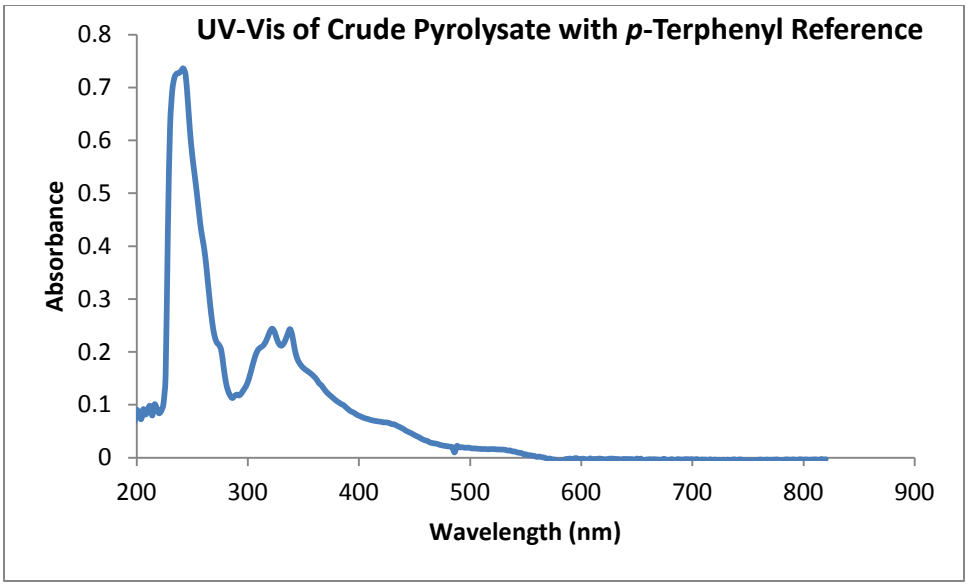

Figure 3-11. Crude Pyrolysate with *p*-Terphenyl in the Reference Beam

Unfortunately, further attempts to remove *p*-terphenyl were unsuccessful. It was found that the crude material containing the end-cap, which is orange in color, is still very soluble in methanol, and precipitation of more material was not possible. It was likely that the concentration of the desired end-cap was just too small, and purification away from *p*-terphenyl on this scale was not possible. Successful purification of the desired end-cap would be facilitated by increasing the material balance from the pyrolysis. With more of the desired material in the crude mixture, purification of the material should be more facile than was seen with the small scale discussed.

3.11 Conclusion

The incorporation of solubility-enhancing *tert*-butyl groups provided highly soluble material. Although incorporation of the *tert*-butyl groups in specific positions was not a viable route towards the desired $C_{60}H_{12}$ end-cap (**1-8**), direct alkylation of *peri*-

bis(dibenzo[*a,g*]corannulene) provided a very soluble tetra-alkyl intermediate **3-2**. Successful Diels-Alder addition of *N*-methylmaleimide, followed by hydrolysis to form the *bis*-anhydride (**3-44**) provided an optimal pyrolysis precursor. Subjection of the *bis*-anhydride (**3-44**) to FVP conditions at 1100 ˚C and 0.5 torr, afforded 13 mg of an orange solid that contained the desired end-cap (**1-8**). Unfortunately, purification of the end-cap was hampered due to the significant formation of a byproduct, *p*-terphenyl, and its high solubility in organic solvents as well as its propensity to adhere to reverse phase silica gel; these difficulties prevented complete isolation of the desired end-cap. With this unique material in hand, future studies on the properties and applications in material science are just around the corner.

3.12 General Experimental

3.12.1. Flash Vacuum Pyrolysis

Flash vacuum pyrolysis is a thermal method used to shock gas-phase molecules at high temperatures, short reaction times and low pressure. The figure below represents a schematic of the apparatus used for each pyrolysis experiment.

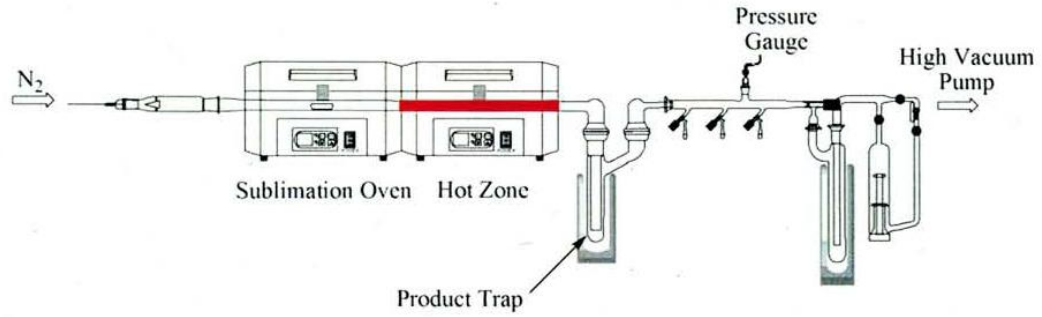

As shown, a quartz tube (2.5 cm I.D./ 107 cm length) was placed in two side-by-side ovens (Lindberg Blue; heating coil length 36 cm each). The space between the ovens was wrapped with quartz wool to maintain the temperature across the two ovens. At one terminus of the quartz tube is a nitrogen inlet, controlled with a fine micrometer. At the other terminus was a vertical trap, cooled with liquid nitrogen, followed by a second liquid nitrogen trap and a high vacuum pump. The pressure of the system was monitored with a mercury manometer or a digital manometer, reading from 0.10 to 1 torr.

A typical experiment consisted of the starting material being absorbed onto quartz sand, dried overnight and placed in one or multiple quartz boats, depending on the scale of the experiment. The quartz boats, loaded with the sample, were placed near the terminus of

the tube and accompanied by a magnet, used to move the boats forward towards the hot zone. Depending on the experiment, the hot zone was heated to a desired temperature (up to 1100 ˚C) and once at a set temperature, the sublimation oven was used to sublime the starting material into the gas phase (if possible), where the molecules were carried by ultra high purity nitrogen gas through the hot zone. If the material could not be sublimed, it was pushed, using the magnet, directly into the hot zone. The material was collected in the trap and upon completion, the apparatus was cooled. Once cooled, the tube and trap were washed with the appropriate solvent, typically dichloromethane, to remove the organic product, which was then purified as specified for each reaction.

3.12.2. 2-Bromo-4-*tert*-butyltoluene

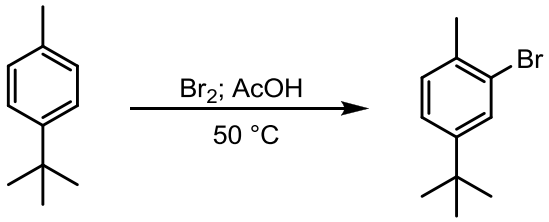

At room temperature, elemental bromine (63.0 g, 0.406 mol) was added dropwise to a stirred solution of 4-*tert*-butyltoluene (50.0 g, 0.338 mol) and 150 mL glacial acetic acid. The reaction mixture was stirred and heated to 50 ˚C for 24 h. The mixture was cooled to room temperature and quenched with 10% sodium bisulfate and extracted with hexanes. The organic extracts were washed with water, dried over magnesium sulfate and evaporated to dryness. The crude oil was purified on silica gel chromatography with hexanes as the eluent to give 50.1 g (67%) of the desired product as a clear oil. **^{1}H NMR** (500 MHz, $CDCl_3$) δ(ppm): 7.53 (d, *J* = 2.0 Hz, 1H), 7.22 (dd, *J* = 8.0 Hz, 2.0 Hz, 1H), 7.15 (d, *J* = 8.0 Hz, 1H), 2.36 (s, 3H), 1.30 (s, 9H). (Lit.[8])

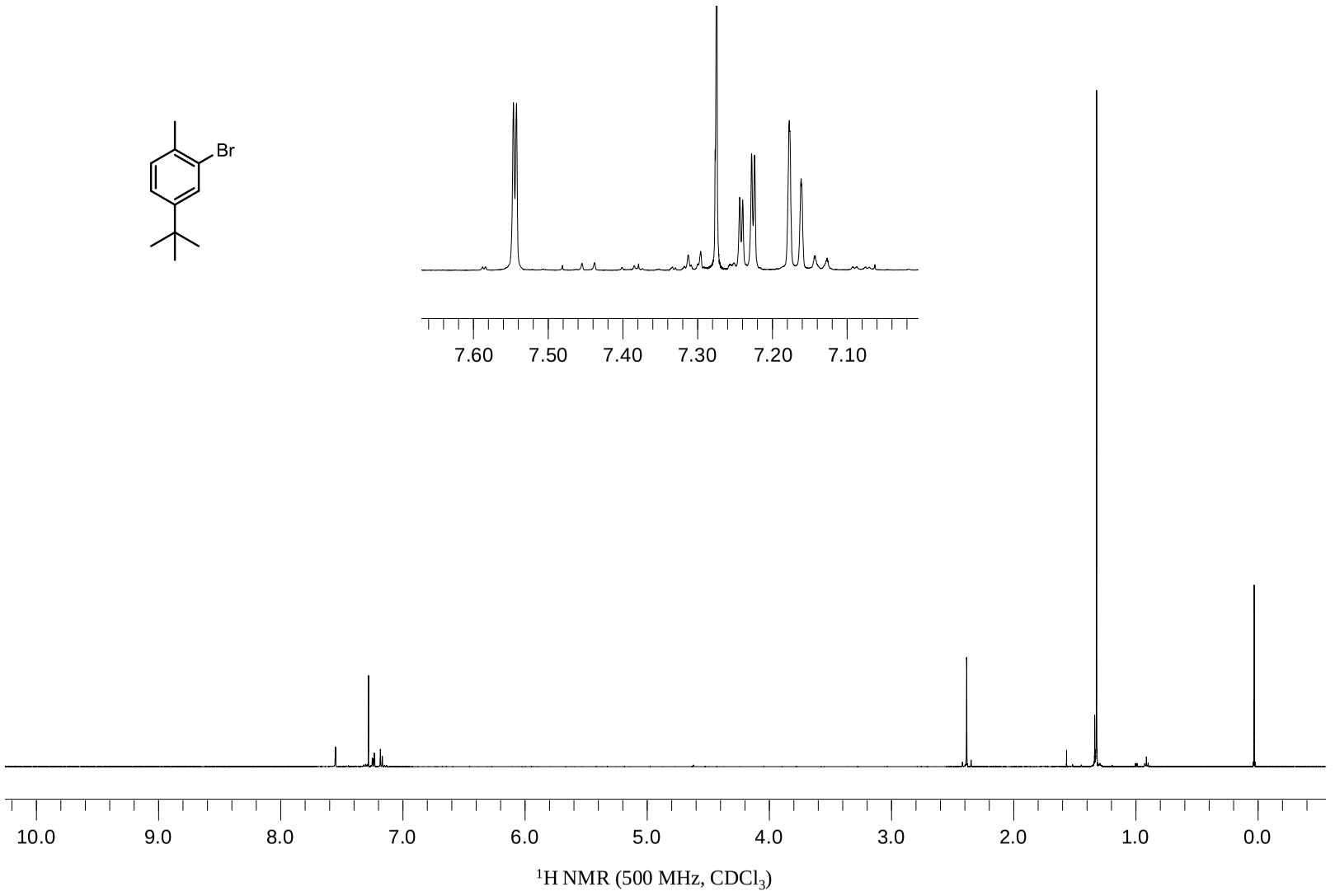

^{1}H NMR (500 MHz, $CDCl_3$)

3.12.3. 2-Bromo-1-(bromomethyl)-4-*tert*-butylbenzene

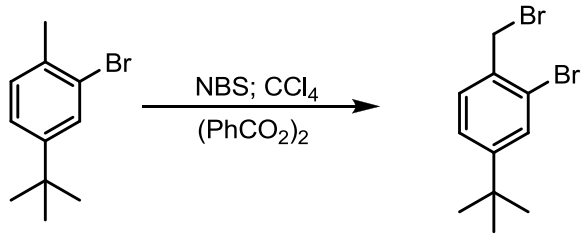

To a solution of 2-bromo-4-*tert*-butyltoluene (33.2 g, 0.147 mol) in 250 mL carbon tetrachloride was added *N*-bromosuccinimide (28.5 g, 0.162 mol) and ~10 mg benzoyl peroxide. The reaction mixture was stirred and heated to reflux for 4 h. The mixture was cooled to room temperature, and the succinimide was removed by filtration. The filtrate was washed with 10% KOH(aq), and the organic layer was dried over magnesium sulfate to afford 33.3 g (74%) of the desired product as a clear oil.[*] **^{1}H NMR** (500 MHz, $CDCl_3$) δ(ppm): 7.57 (d, *J* = 2.0 Hz, 1H), 7.38 (d, *J* = 8.0 Hz, 1H), 7.31 (dd, *J* = 8.0 Hz, 2.0 Hz, 1H), 4.60 (s, 2H), 1.30 (s, 9H). (Lit.[8])

[*] Over bromination of the benzylic position occurred rapidly if the reaction was not monitored closely by GCMS. Traces of over bromination were present in every reaction mixture.

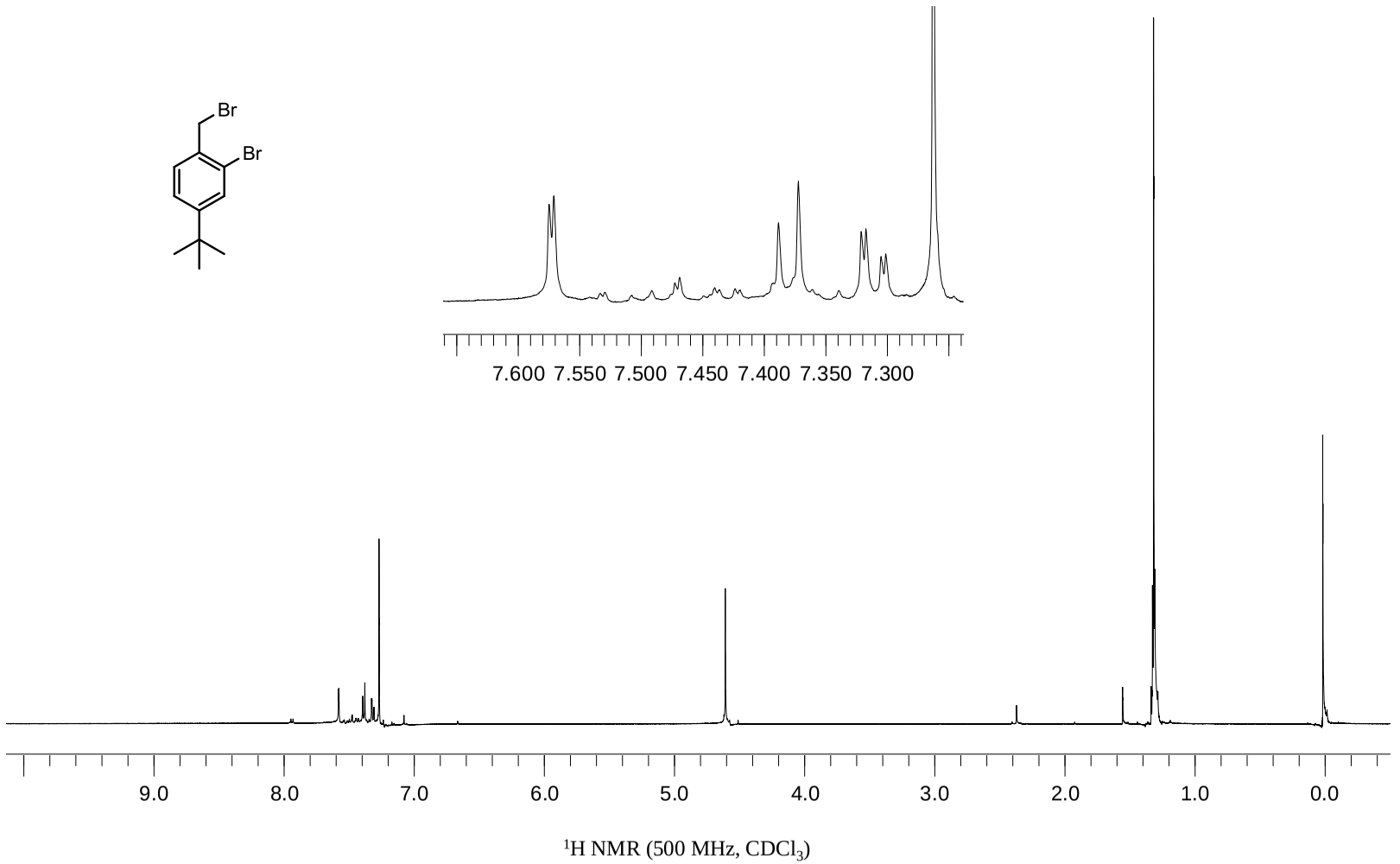

^{1}H NMR (500 MHz, $CDCl_3$)

3.12.4. 1,3-*Bis*(2-bromo-4-*tert*-butylphenyl)propan-2-one

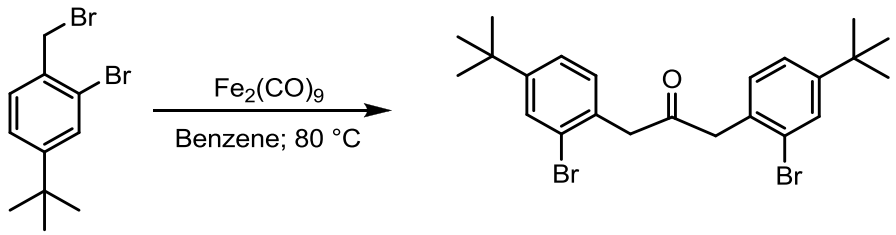

A flame dried, nitrogen purged round bottom flask, equipped with a reflux condenser, was charged with 25.0 g (0.0687 mol) of $Fe_2(CO)_9$, and 21.0 g (0.0687 mol) of 2-bromo-1-(bromomethyl)-4-*tert*-butylbenzene was added. Anhydrous benzene (250 mL) was added via cannula, and the solution was allowed to stir at reflux for 24 h.[†] A color change was observed from orange to yellow to green over 24 h. The reaction mixture was cooled to room temperature and flushed through a short pad of silica gel with dichloromethane as the eluent. Solvent was removed under reduced pressure which afforded 13.5 g (81%) of the desired product as a yellow oil. **^{1}H NMR** (500 MHz, $CDCl_3$ for a mixture of diastereomers) δ(ppm): 7.56 (d, *J* = 2.0 Hz, 2H), 7.28 (m, 2H of minor diastereomer), 7.23 (m, 2H of major diastereomer), 7.05 (d, *J* = 8.0 Hz, 2H), 4.10 (s, 4H), 1.30 (s, 18H). (Lit.[8])

[†] $Fe_2(CO)_9$ is pyrophoric and must be handled with care. After addition under nitrogen, the solvent must be added quickly. Once submerged in solvent, the reagent is stable.

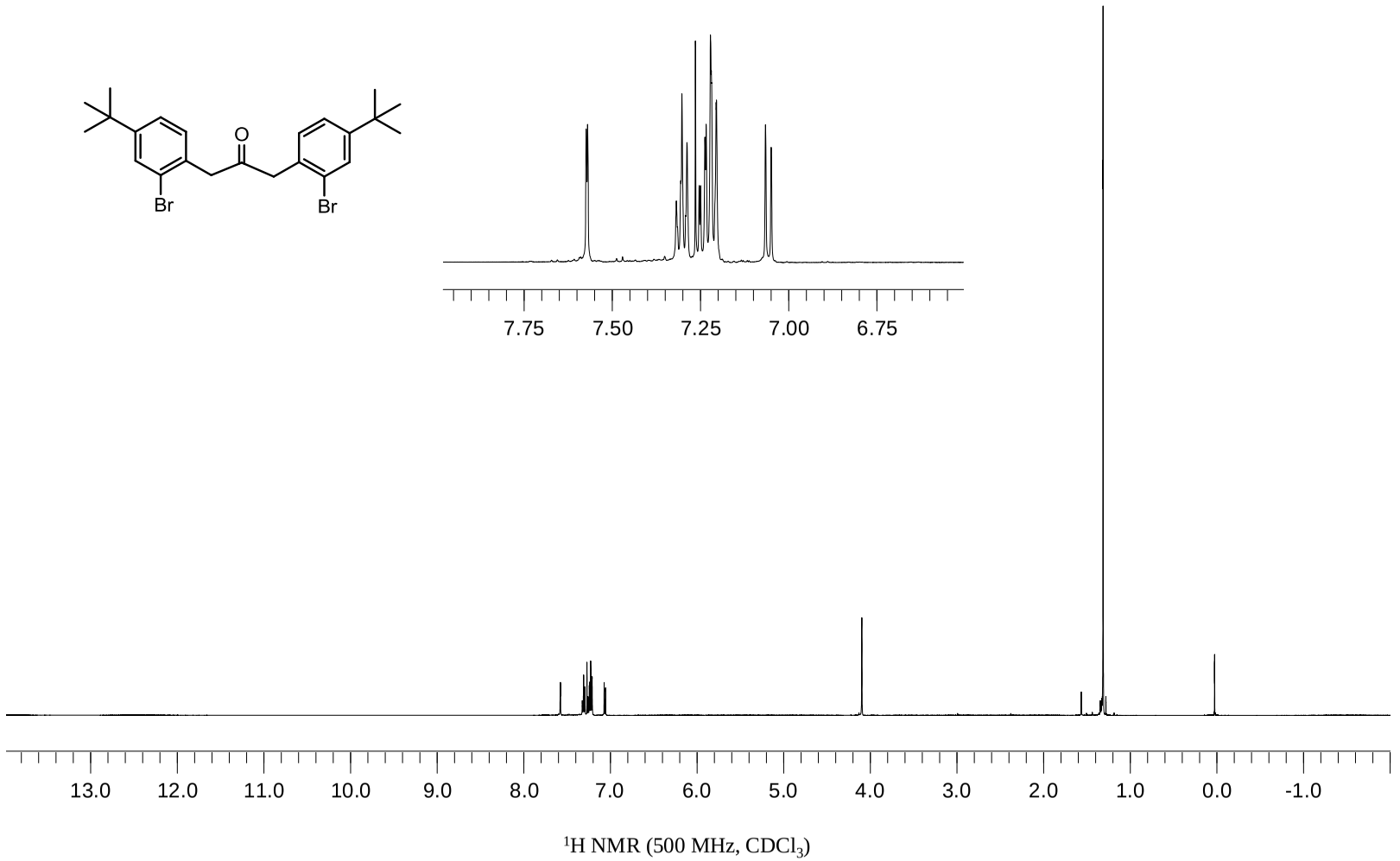

^{1}H NMR (500 MHz, $CDCl_3$)

3.12.5. 7,9-*Bis*(2-bromo-4-*tert*-butylphenyl)-8H-cyclopenta[*a*]acenaphthylen-8-one

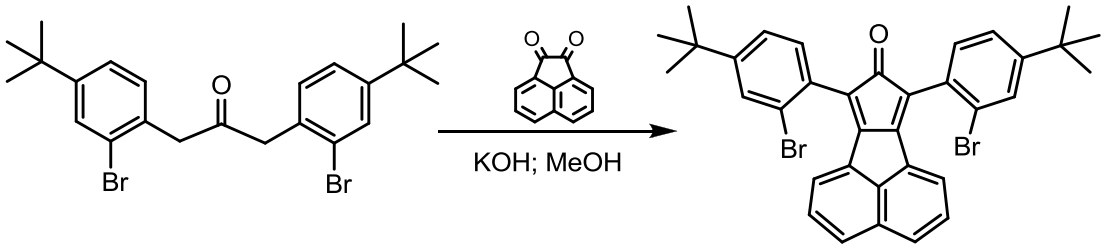

To a 500 mL Erlenmeyer flask, 8.74 g (0.0182 mol) of 1,3-*bis*(2-bromophenyl)propan-2-one and 3.31 g (0.0182 mol) of acenaphthenequinone were added. KOH (1.33 g, 0.0237 mol) was dissolved in methanol (250 mL), and the basic solution was added to the reaction mixture. The mixture was stirred at room temperature for 2 h. A color change from yellow to purple was observed instantly upon addition of the basic solution. The resulting suspension was allowed to sit overnight without stirring. The purple precipitate was removed by vacuum filtration and washed with methanol to give 8.42 g (74%) of the desired product. **^{1}H NMR** (500 MHz, $CDCl_3$) δ(ppm): 7.83 (m, 2H), 7.71-7.70 (m, 2H), 7.56-7.55 (m, 4H), 7.44-7.43 (m, 4H), 1.35 (s, 18H). (Lit.[8])

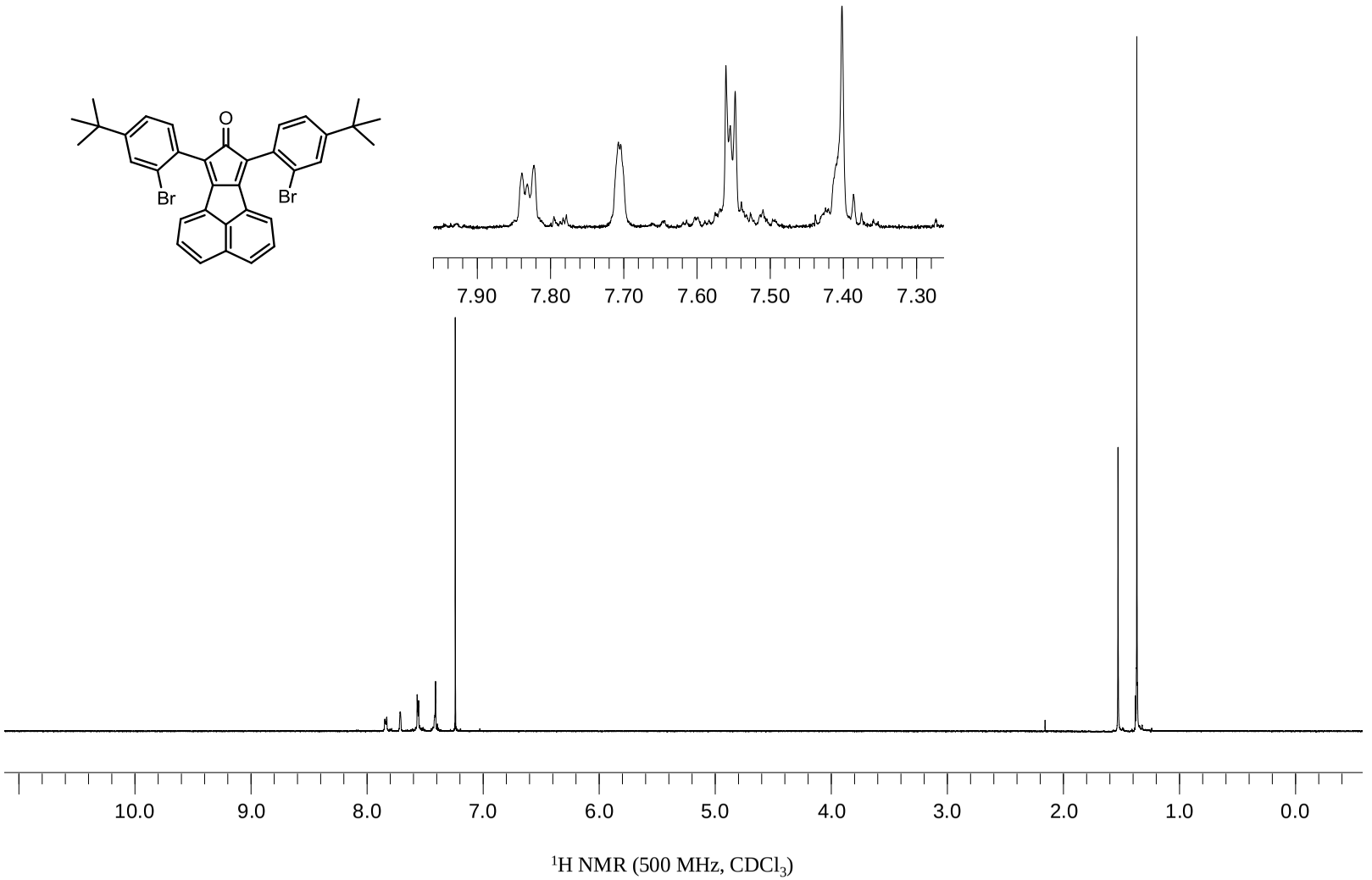

^{1}H NMR (500 MHz, $CDCl_3$)

3.12.6. 7,10-*Bis*(2-bromo-4-*tert*-butylphenyl)fluoranthene

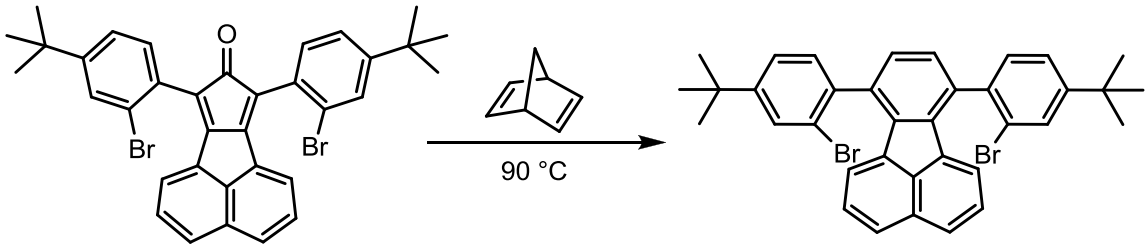

To a round bottom flask, 6.00 g (9.58 mmol) of 7,9-*bis*(2-bromo-4-*tert*-butylphenyl)-8H-cyclopenta[*a*]acenaphthylen-8-one, and 75.0 mL norbornadiene were added. The reaction mixture was stirred at reflux for 5 d. The mixture was cooled to room temperature and the solvent was removed under reduced pressure. The resulting oily residue was purified by silica gel chromatography with 3:1 hexanes : dichloromethane as the eluent to afford 4.82 g (81%) of the desired product as a yellow solid. **^{1}H NMR** (500 MHz, $CDCl_3$, for a mixture of diasteromers) δ(ppm): 7.82-7.81 (m, 2H), 7.74 (d, *J* = 8.0 Hz, 2H), 7.505 (s, 2H of major diastereomer), 7.502 (s, 2H of minor diastereomer), 7.36 (dd, *J* = 8.0 Hz, 7.5 Hz, 2H), 7.26 (s, 2H of major diastereomer), 7.25 (s, 2H of minor diastereomer), 6.85 (d, *J* = 7.0 Hz, 2H), 1.45 (s, 18H). (Lit.[8])

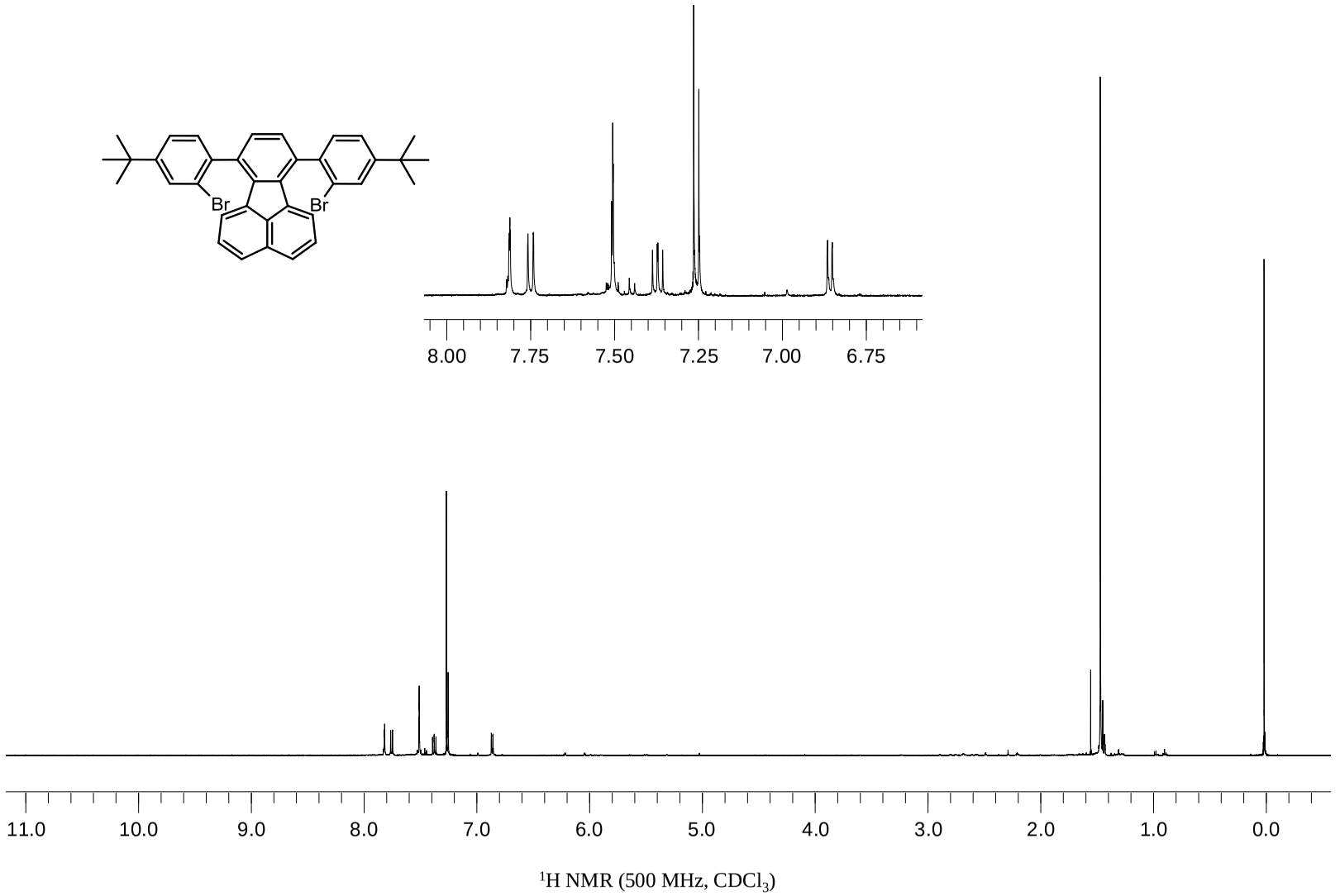

^{1}H NMR (500 MHz, $CDCl_3$)

3.12.7. 4-11-Di-*tert*-butyldibenzo[*a,g*]corannulene (3-4) and 10-*Tert*-butyl-3-(4-*tert*-butylphenyl)indeno[1,2,3,4-*defg*]chrysene (3-21)

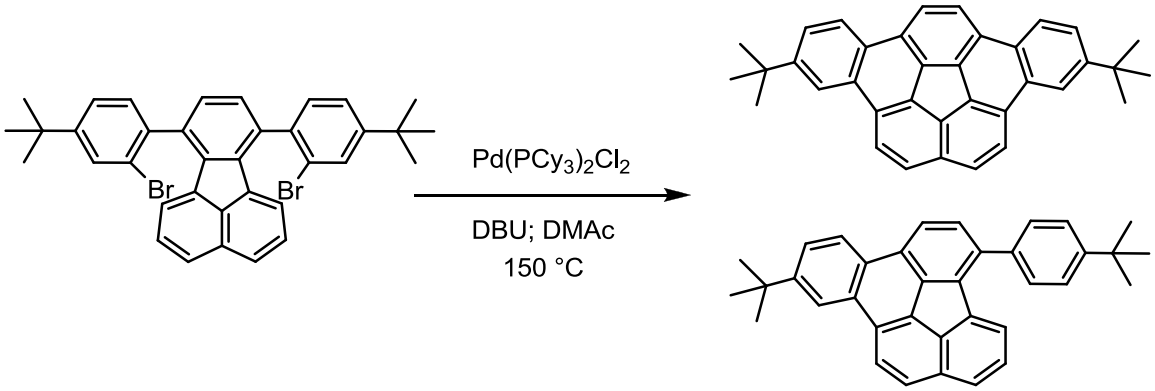

To a flame-dried, nitrogen purged pressure vessel, equipped with a stir bar, 1.00 g (1.60 mmol) of 7,10-*bis*(2-bromo-4-*tert*-butylphenyl)fluoranthene and 120 mg (0.160 mmol) of $Pd(PCy_3)_2Cl_2$ were added under a nitrogen atmosphere. DMAc (14.3 mL) and DBU (9.52 mL) were added via syringe, and the reaction mixture was stirred. The vessel was sealed and heated in a pre-heated oil bath at 150 ˚C for 16 h. The mixture was cooled to room temperature and flushed through a short pad of neutral alumina with dichloromethane as the eluent. The filtrate was washed with 10 % HCl(aq) twice and once with water. The organic layer was dried over magnesium sulfate and concentrated to dryness under vacuum to provide a 1:1 mixture of **3-4** to **3-21**. The crude product was repeatedly washed with hexanes to provide 148 mg (20%) of **3-4** as a yellow solid.[‡] **^{1}H NMR** (500 MHz, $CDCl_3$) δ(ppm): 8.67 (d, *J* = 2.0 Hz, 2H), 8.63 (d, *J* = 8.5 Hz, 2H), 8.32 (s, 2H), 8.31 (d, *J* = 8.5 Hz, 2H), 7.97 (d, *J* = 8.5 Hz, 2H), 7.84 (dd, *J* = 8.0 Hz, 2.0 Hz, 2H), 1.52 (s, 18H). (Lit.[8])

[‡] After successive hexanes washes, the filtrate contained significant amounts of the desired product **3-4**. Column chromatography was unsuccessful in effectively separating **3-4** from **3-21**. The undesired **3-21** was not isolated.

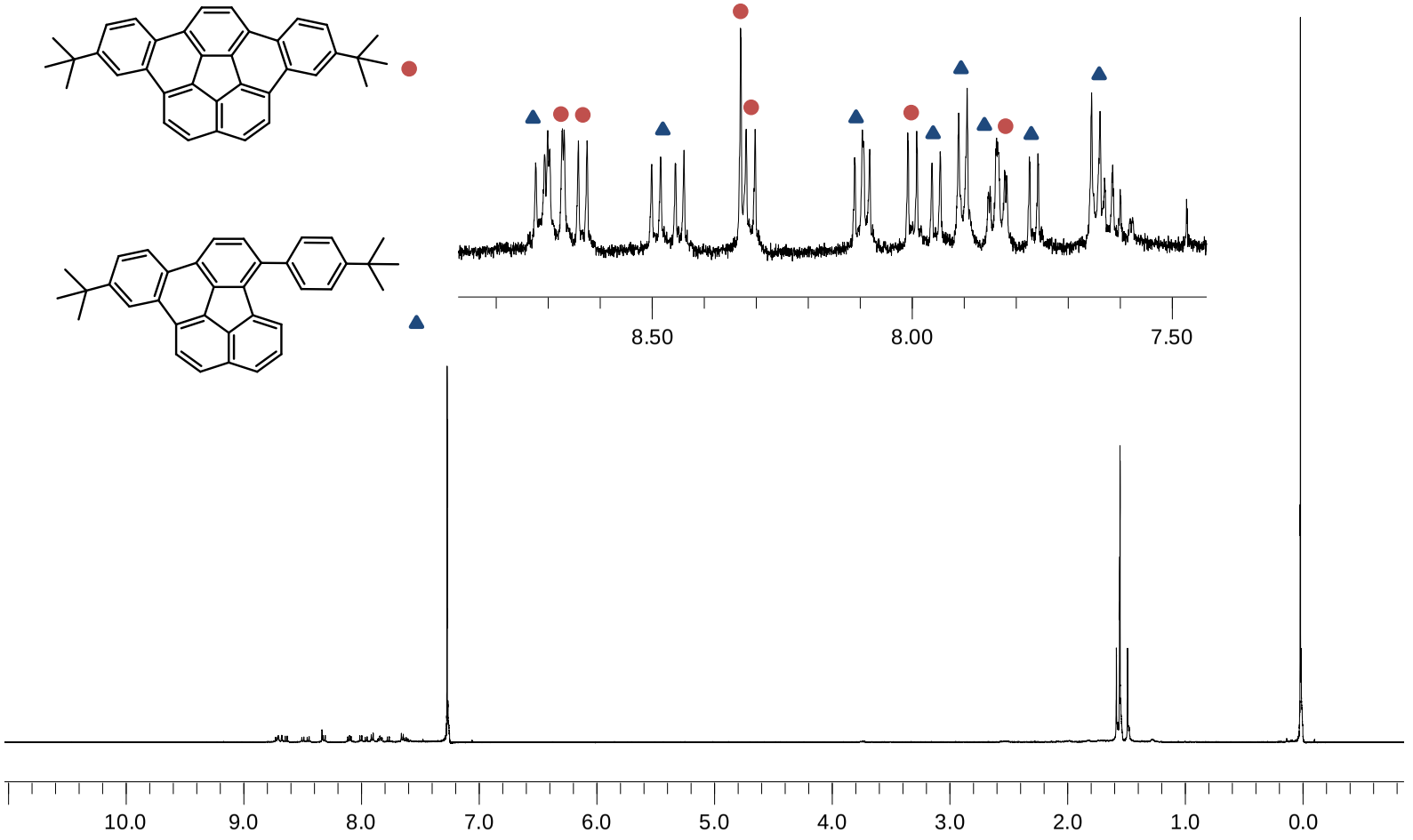

^{1}H NMR (500 MHz, $CDCl_3$)

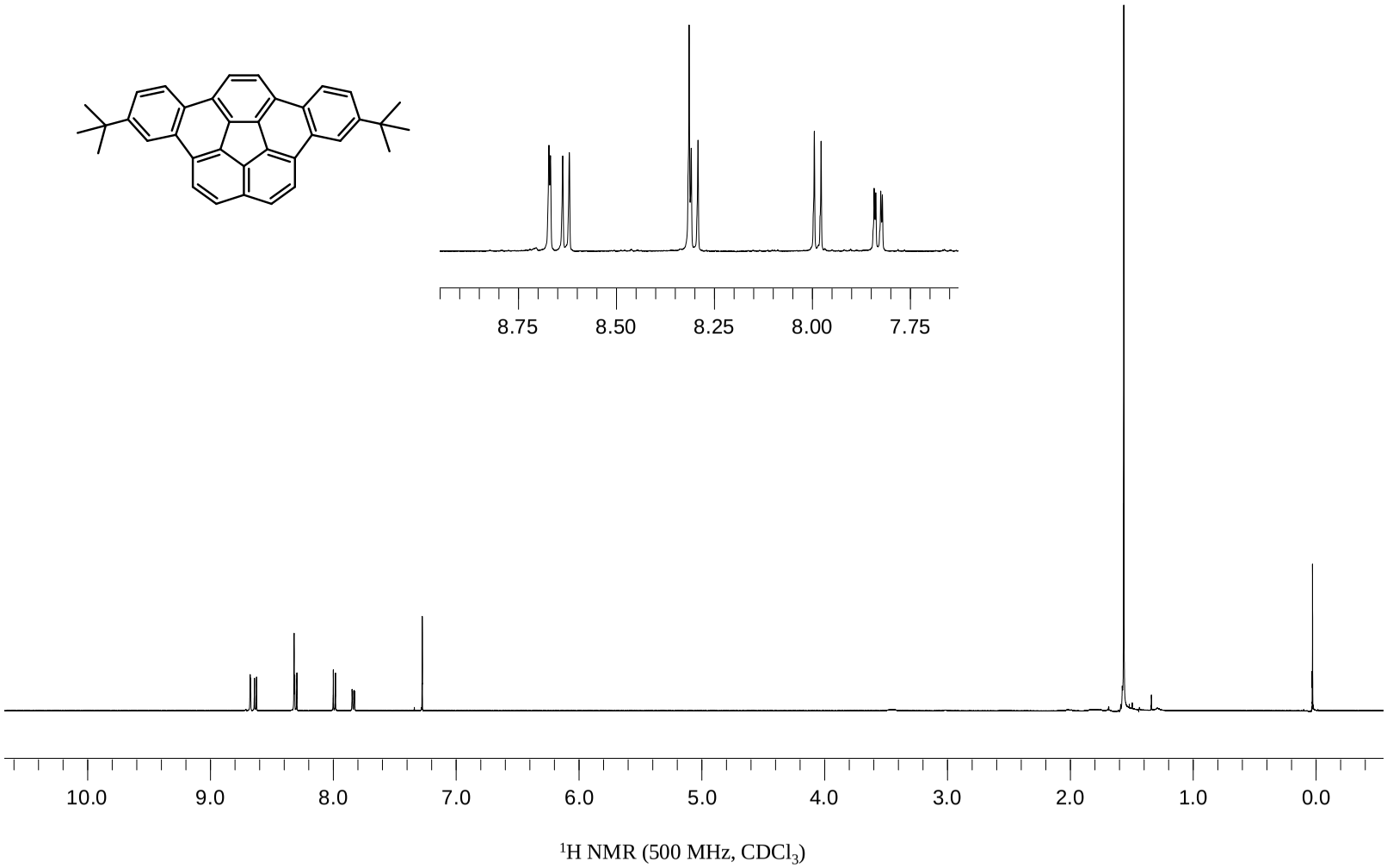

^{1}H NMR (500 MHz, $CDCl_3$)

4-11-Di-*tert*-butyldibenzo[*a,g*]corannulene (3-4) and

10-*Tert*-butyl-3-(4-*tert*-butylphenyl)indeno[1,2,3,4-*defg*]chrysene (3-21)

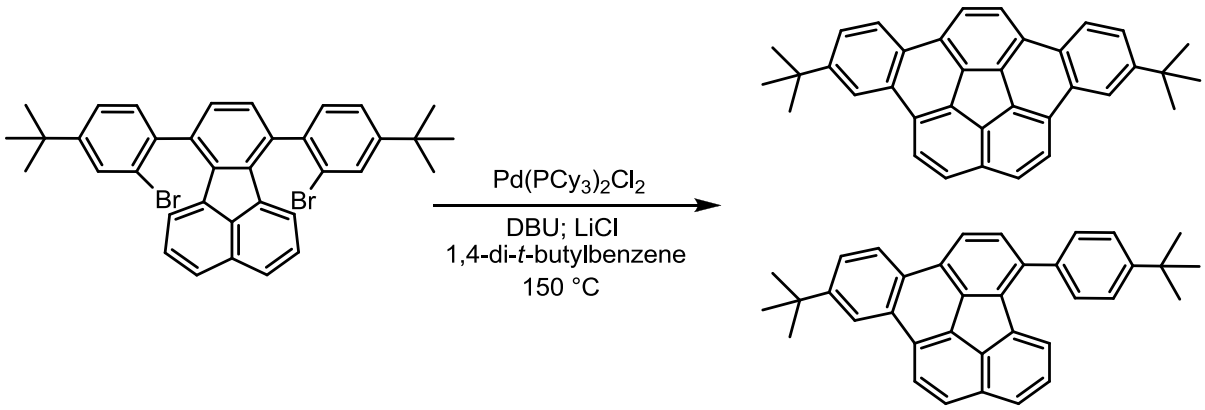

To a flame-dried, nitrogen purged pressure vessel, equipped with a stir bar, 200 mg (0.323 mmol) of 7,10-*bis*(2-bromo-4-*tert*-butylphenyl)fluoranthene and 24.0 mg (0.0323 mmol) of $Pd(PCy_3)_2Cl_2$ were added under a nitrogen atmosphere. 1,4-Di-*tert*-butylbenzene (3.00 g) and DBU (5.00 mL) were added via syringe, and the reaction mixture was stirred. The vessel was sealed and heated in a pre-heated oil bath at 150 ˚C for 16 h. The mixture was cooled to room temperature and flushed through a short pad of neutral alumina with dichloromethane as the eluent. The filtrate was washed with 10 % HCl(aq) twice and once with water. The organic layer was dried over magnesium sulfate and concentrated to dryness under vacuum. Sublimation of 1,4-di-*tert*-butylbenzene provided a 4:1 mixture of **3-4** to **3-21**. The desired product was recrystallized in hexanes to provide 74.6 mg (50%) of the desired product as a tan solid. (Lit.[8])

3.12.8. 1-Bromo-4,11-di-*tert*-butyldibenzo[*a*,*g*]corannulene

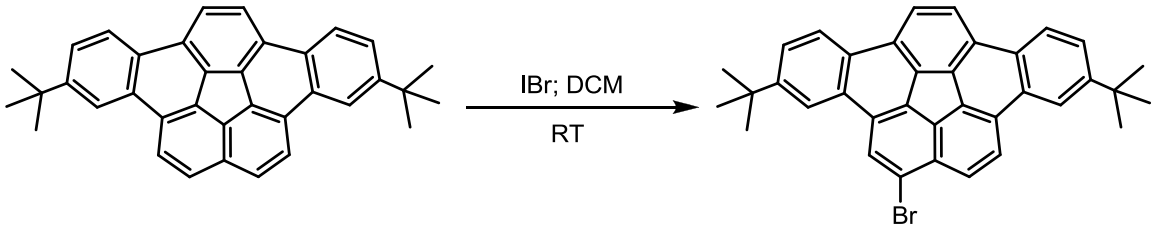

To a flame-dried, nitrogen purged, round bottom flask equipped with a magnetic stir bar was added 170 mg (0.354 mmol) of 4,11-di-*tert*-butyldibenzo[*a*,*g*]corannulene and 159 mg (0.772 mmol) of iodine monobromide. Anhydrous dichloromethane (9.62 mL) was added, and the reaction mixture was stirred at room temperature for 4 h. The reaction was quenched with sodium bisulfate and extracted with dichloromethane and water. The organic layer was dried with magnesium sulfate and concentrated to dryness under vacuum. The crude product was washed with hot hexanes to provide 109 mg (57%) of the desired product as a tan solid. **^{1}H NMR** (500 MHz, $CDCl_3$) δ(ppm): 8.67 (d, *J* = 2.0 Hz, 1H), 8.63 (d, *J* = 8.5 Hz, 1H), 8.61 (d, *J* = 8.5 Hz, 1H), 8.57 (d, *J* = 2.0 Hz, 1H), 8.48 (s, 1H), 8.33 (d, *J* = 9.0 Hz, 1H), 8.31 (d, *J* = 8.5 Hz, 1H), 8.29 (d, *J* = 8.5 Hz, 1H), 8.13 (d, *J* = 8.5 Hz, 1H), 7.84-7.82 (m, 2H), 1.53 (s, 9H), 1.52 (s, 9H). (Lit.[8])

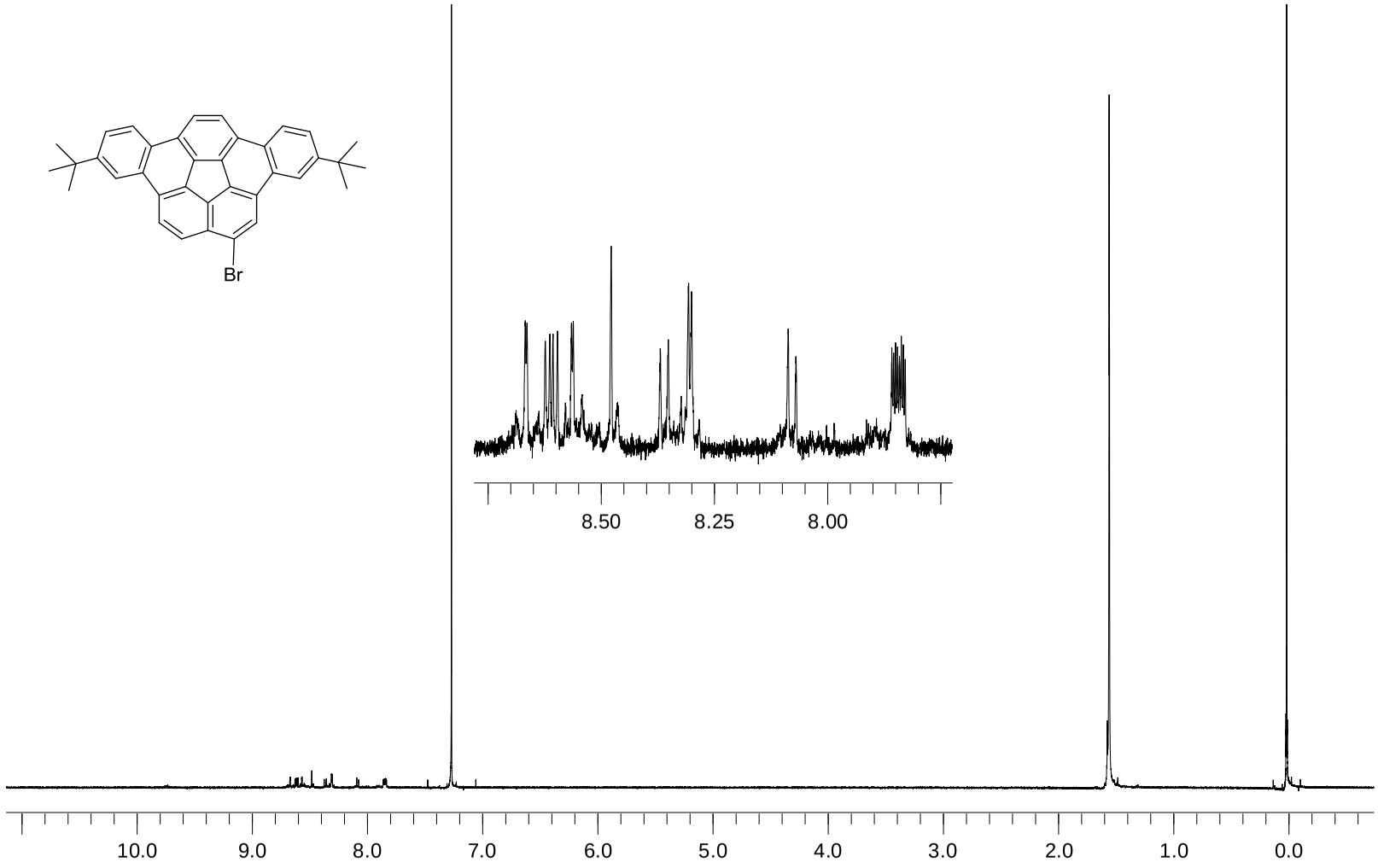

^{1}H NMR (500 MHz, $CDCl_3$)

3.12.9. 1,1′-Bi(4,11-di-*tert*-butyldibenzo[*a,g*]corannulenyl)

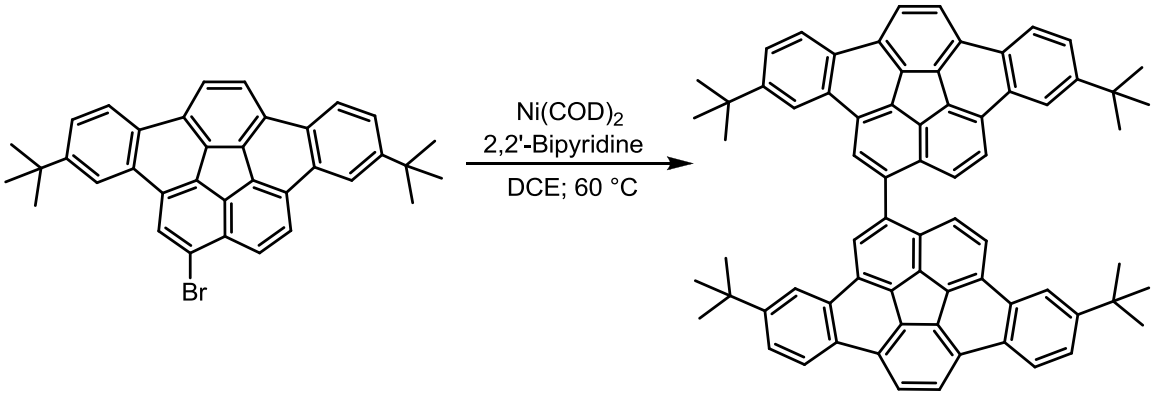

To a flame-dried, nitrogen purged Schlenk flask, equipped with a magnetic stir bar, was added 89.1 mg (0.165 mmol) of 1-bromo-4,11-di-*tert*-butyldibenzo[*a,g*]corannulene, 60.0 mg (0.198 mmol) of $Ni(COD)_2$, 35.4 mg (0.198 mmol) of 2,2'-bipyridine and 22.7 µL of 1,5-cyclooctadiene. Anhydrous dimethyl formamide (0.75 mL) was added, and the reaction was placed in a pre-heated oil bath (60 ˚C) with stirring for 5 h. The reaction was cooled to room temperature and diluted with dichloromethane. The mixture was flushed through a short pad of silica gel with dichloromethane as the eluent and washed with water, 10% NaOH(aq) and dichloromethane. The organic extract was dried with magnesium sulfate and concentrated to dryness. The crude product was washed with hot hexanes to provide 48.5 mg (63%) of the desired product as a yellow solid. **^{1}H NMR** (500 MHz, $CDCl_3$) δ(ppm): 8.73 (d, *J* = 2.0 Hz, 2H), 8.72 (d, *J* = 2.0 Hz, 2H), 8.70 (d, *J* = 9.0 Hz, 2H), 8.66 (d, *J* = 9.0 Hz, 2H), 8.61 (s, 2H), 8.43 (d, *J* = 8.5 Hz, 2H), 8.40 (d, *J* = 8.5 Hz, 2H), 8.18 (d, *J* = 9.0 Hz, 2H), 7.88-7.82 (m, 3H), 1.51 (s, 36H). (Lit.[8])

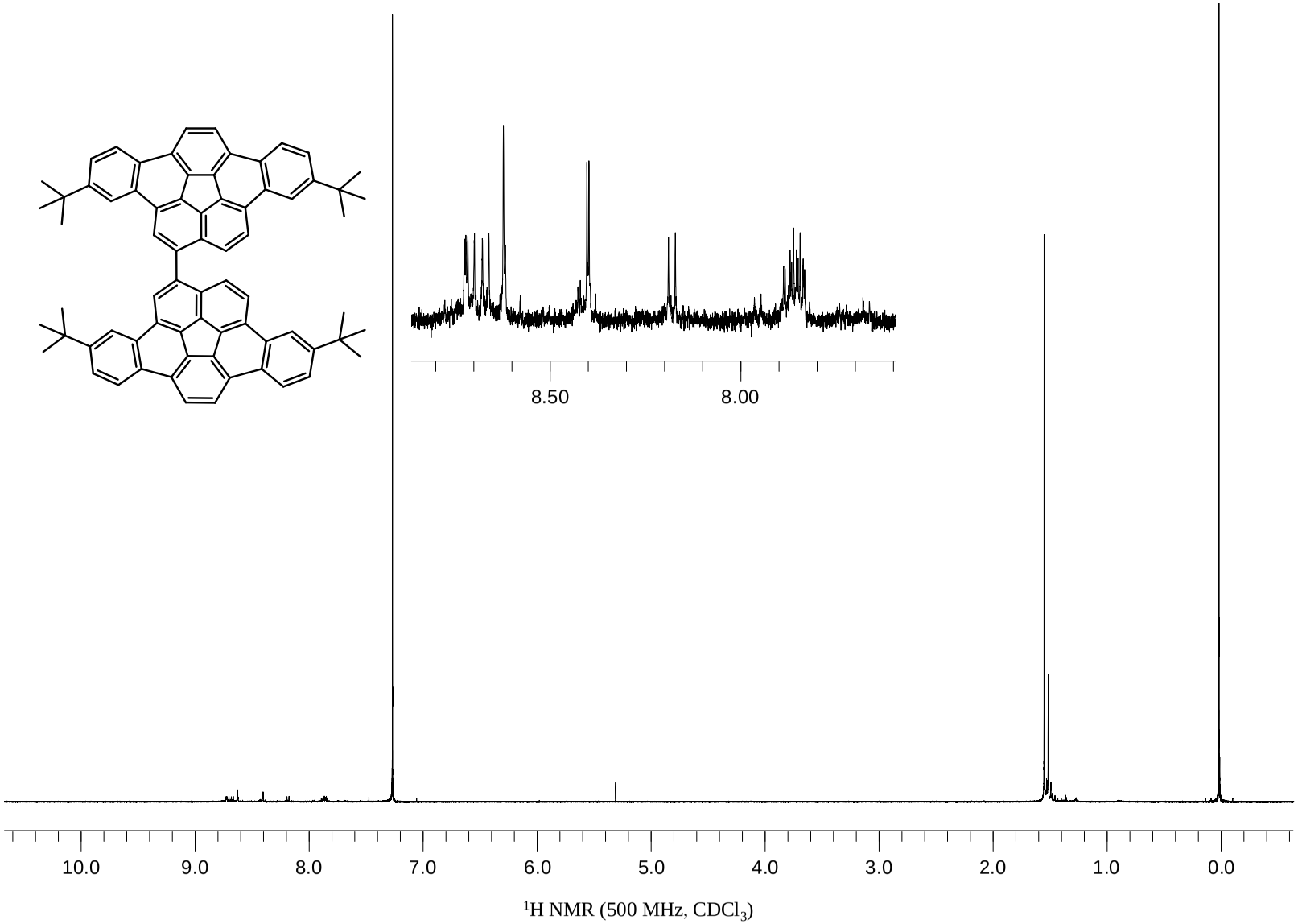

^{1}H NMR (500 MHz, $CDCl_3$)

3.12.10. 4,11-Di-*tert*-butyldibenzo[*a,g*]corannulene and 10-*Tert*-butyl-3-(4-*tert*-butylphenyl-2-d_1)indeno[1,2,3,4-*defg*]chrysene

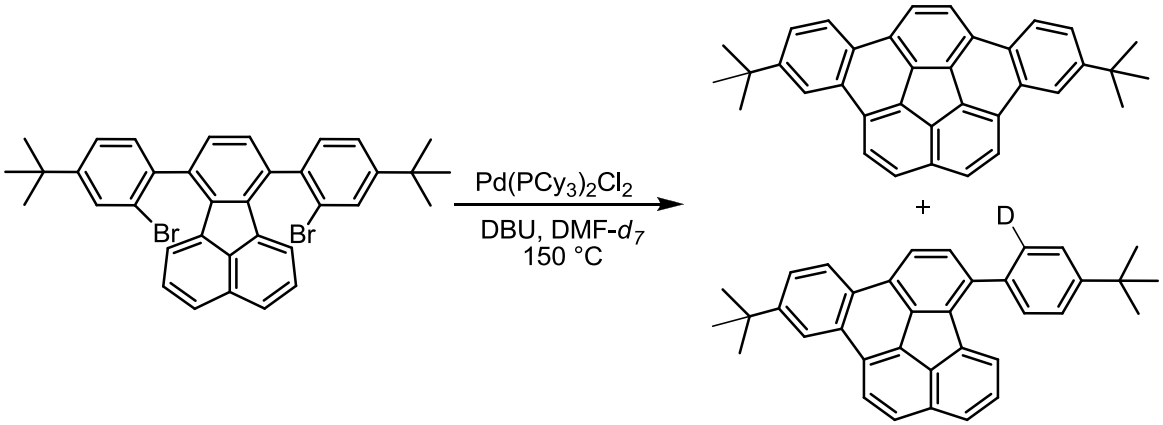

To a flame-dried, nitrogen purged pressure vessel, equipped with a magnetic stir bar, was added 20.0 mg (0.0321 mmol) of 7,10-*bis*(2-bromo-4-*tert*-butylphenyl)fluoranthene and 3.20 mg (0.00321 mmol) $Pd(PCy_3)_2Cl_2$. Dimethylformamide-d_7 (0.30 mL) was added via syringe, and the mixture was stirred. DBU (0.25 mL) was added, and the vessel was sealed. The mixture was placed in a pre-heated oil bath (150 ˚C) for 16 h. The reaction mixture was then cooled to room temperature and flushed through a short pad of alumina with dichloromethane as the eluent. The crude mixture was analyzed by HRMS and ^{1}H NMR to identify the incorporation of deuterium. The mixture was not purified any further. **HRMS** (DART-TOF): Calc'd for $C_{36}H_{32}D$ $(M+1)^+$ 466.2645, found 466.2624. **EI-MS** *m/z* (rel. abundance, %): 466 (20), 465 (40), 464 (30), 463 (30), 462 (100).

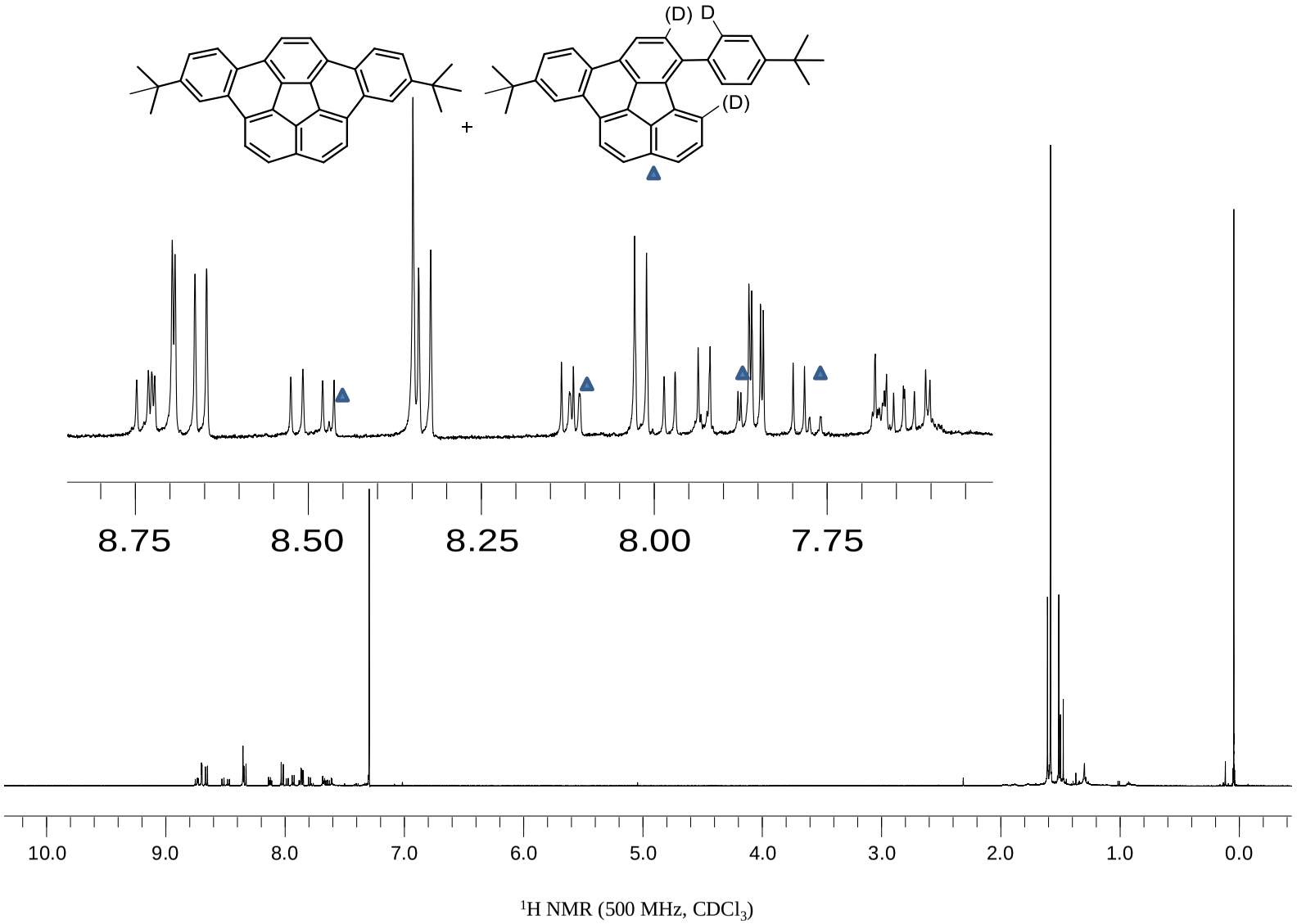

^{1}H NMR (500 MHz, $CDCl_3$)

3.12.11. 7,10-*Bis*(4-*tert*-butylphenyl-2-d_1)fluoranthene-1,2,5,6,8,9-d_6

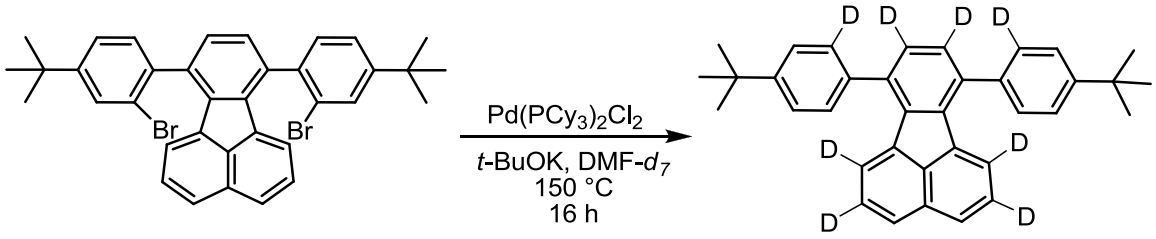

To a flame-dried, nitrogen purged pressure vessel, equipped with a magnetic stir bar, was added 20.0 mg (0.0321 mmol) 7,10-*bis*(2-bromo-4-*tert*-butylphenyl)fluoranthene and 3.20 mg (0.00321 mmol) $Pd(PCy_3)_2Cl_2$. Dimethylformamide-d_7 (0.30 mL) was added via syringe, and the mixture was stirred. Potassium *tert*-butoxide (144 mg, 1.28 mmol) was added, and the vessel was sealed. The mixture was placed in a pre-heated oil bath (150 ˚C) for 16 h. The reaction mixture was then cooled to room temperature and flushed through a short pad of alumina with dichloromethane as the eluent. The organic solvent was removed under reduced pressure to provide 8.4 mg (74%) of a tan solid. **^{1}H NMR** (500 MHz, $CDCl_3$) δ(ppm): 7.63-7.59 (m, 6H), 7.33 (s, 2H), 1.47 (s, 18H). **^{1}H NMR** (500 MHz, Acetone-d_6) δ(ppm): 7.68-7.66 (m, 4H), 7.61-7.58 (m, 2H), 7.30 (s, 2H), 1.48 (s, 18H). **^{13}C NMR** (125 MHz, $CDCl_3$) δ(ppm): 150.7, 138.2, 138.0, 137.1, 136.7, 133.0, 129.9, 129.4, 128.95, 128.91, 127.1, 126.6, 125.7, 125.6, 123.1, 34.8, 31.5. **HRMS** (DART-TOF): Calc'd for $C_{36}H_{27}D_8$ $(M+1)^+$ 475.3241, found 475.3246. **EI-MS** *m/z* (rel. abundance, %): 476 (35), 475 (55), 474 (100), 473 (70), 472 (30).

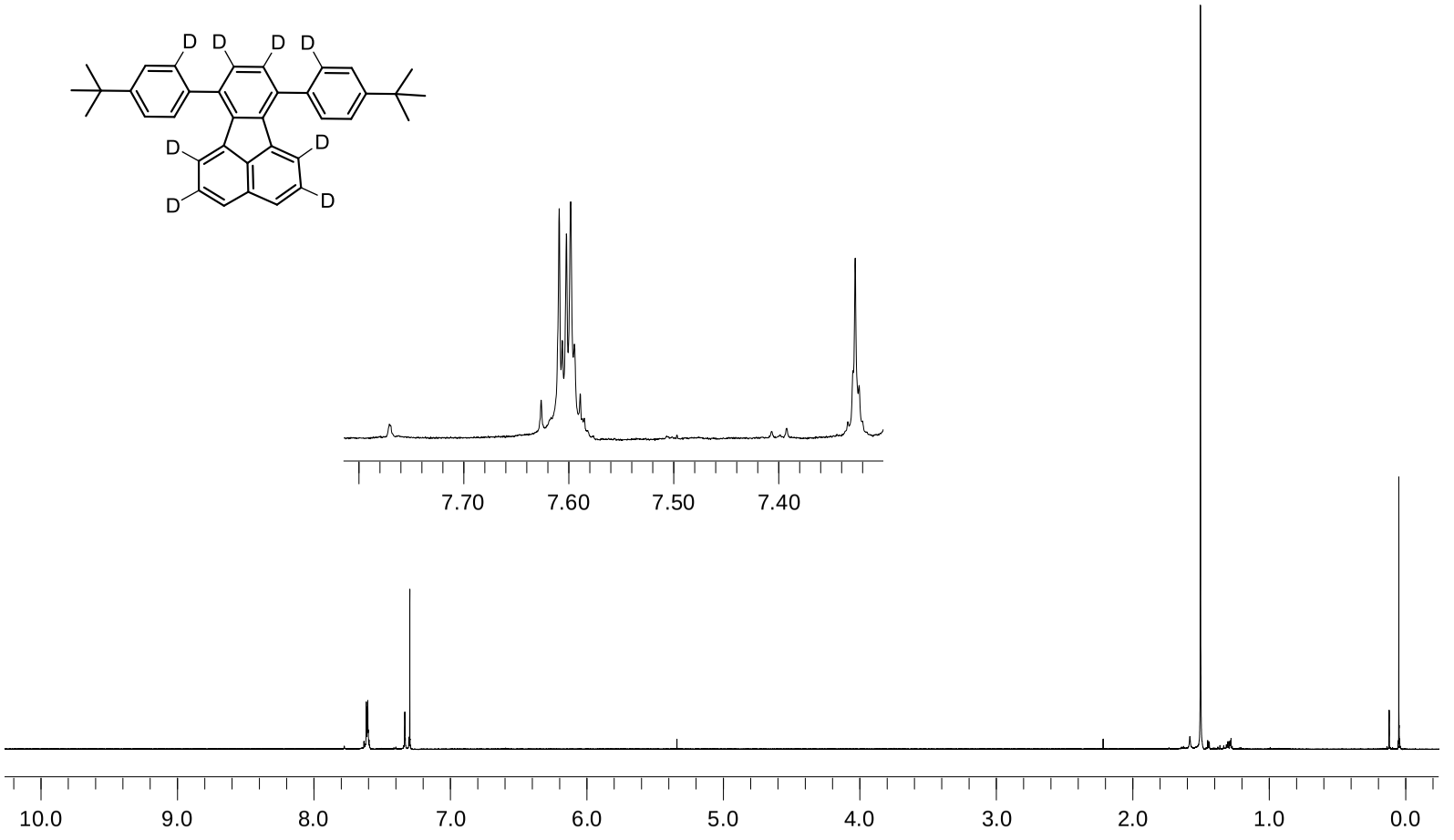

^{1}H NMR (500 MHz, $CDCl_3$)

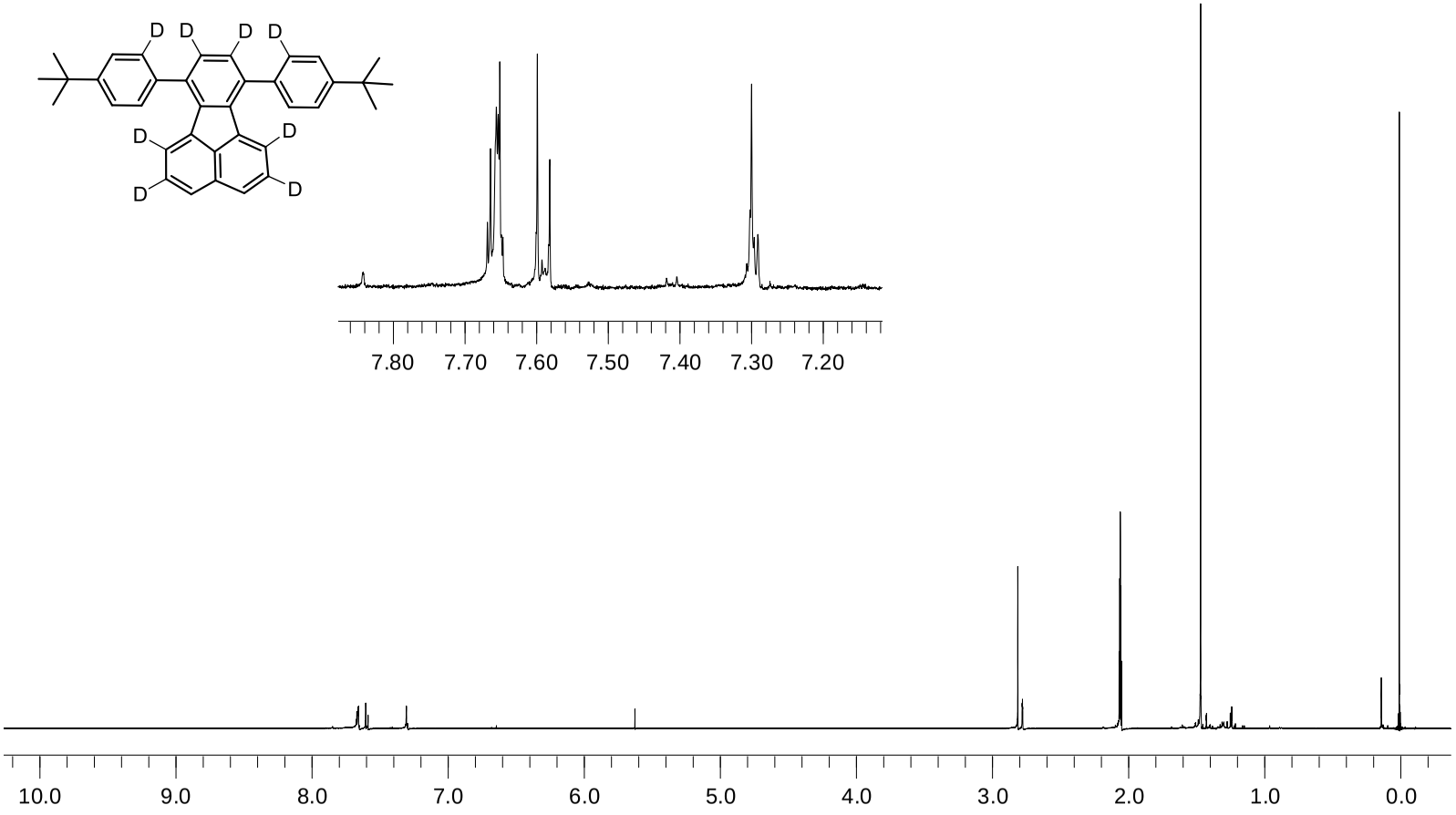

^{1}H NMR (500 MHz, Acetone-d_6)

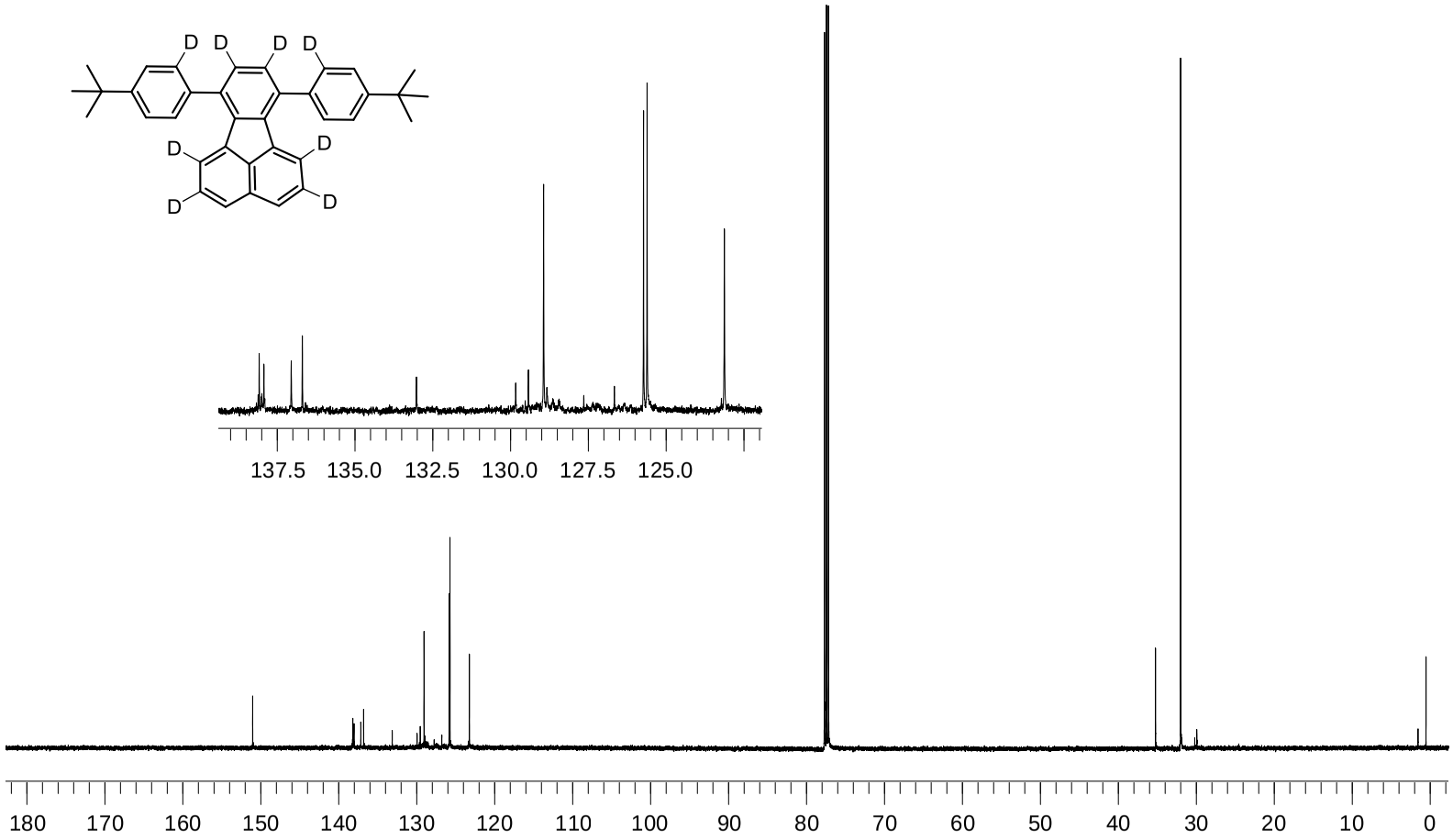

^{13}C NMR (125 MHz, $CDCl_3$)

3.12.12. 7,10-*Bis*(4-*tert*-butylphenyl)fluoranthene-d_1

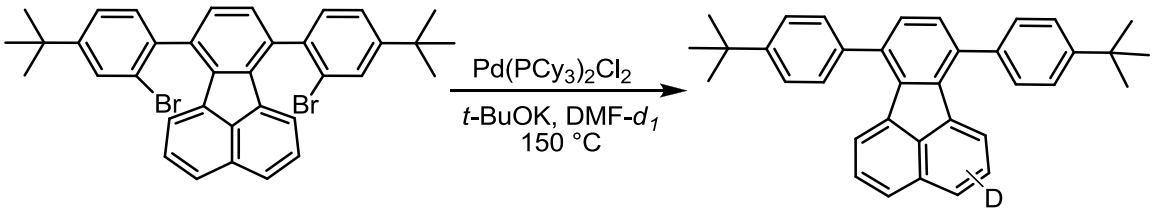

To a flame-dried, nitrogen purged pressure vessel, equipped with a magnetic stir bar, was added 20.0 mg (0.0321 mmol) (7,10-*bis*(2-bromo-4-*tert*-butylphenyl)fluoranthene and 3.20 mg (0.00321 mmol) $Pd(PCy_3)_2Cl_2$. Dimethylformamide-d_1 (0.30 mL) was added via syringe, and the mixture was stirred. Potassium *tert*-butoxide (144 mg, 1.28 mmol) was added, and the vessel was sealed. The mixture was placed in a pre-heated oil bath (150 ˚C) for 16 h. The reaction mixture was then cooled to room temperature, and flushed through a short pad of alumina with dichloromethane as the eluent. Solvent was removed under reduced pressure to provide 9.50 mg (84%) of a tan solid. **^{1}H NMR** (500 MHz, Acetone-d_6) δ(ppm): 7.86-7.84 (m, 2H), 7.68-7.65 (m, 2H), 7.61-7.58 (m, 2H), 7.44-7.41 (m, 2H), 7.31-7.29 (m, 3H), 1.48 (s, 18H). **HRMS** (DART-TOF): Calc'd for $C_{36}H_{34}D$ $(M+1)^+$ 468.2801, found 468.2776. **EI-MS** *m/z* (rel. abundance, %): 470 (5), 469 (25), 468 (70), 467 (100), 466 (65).

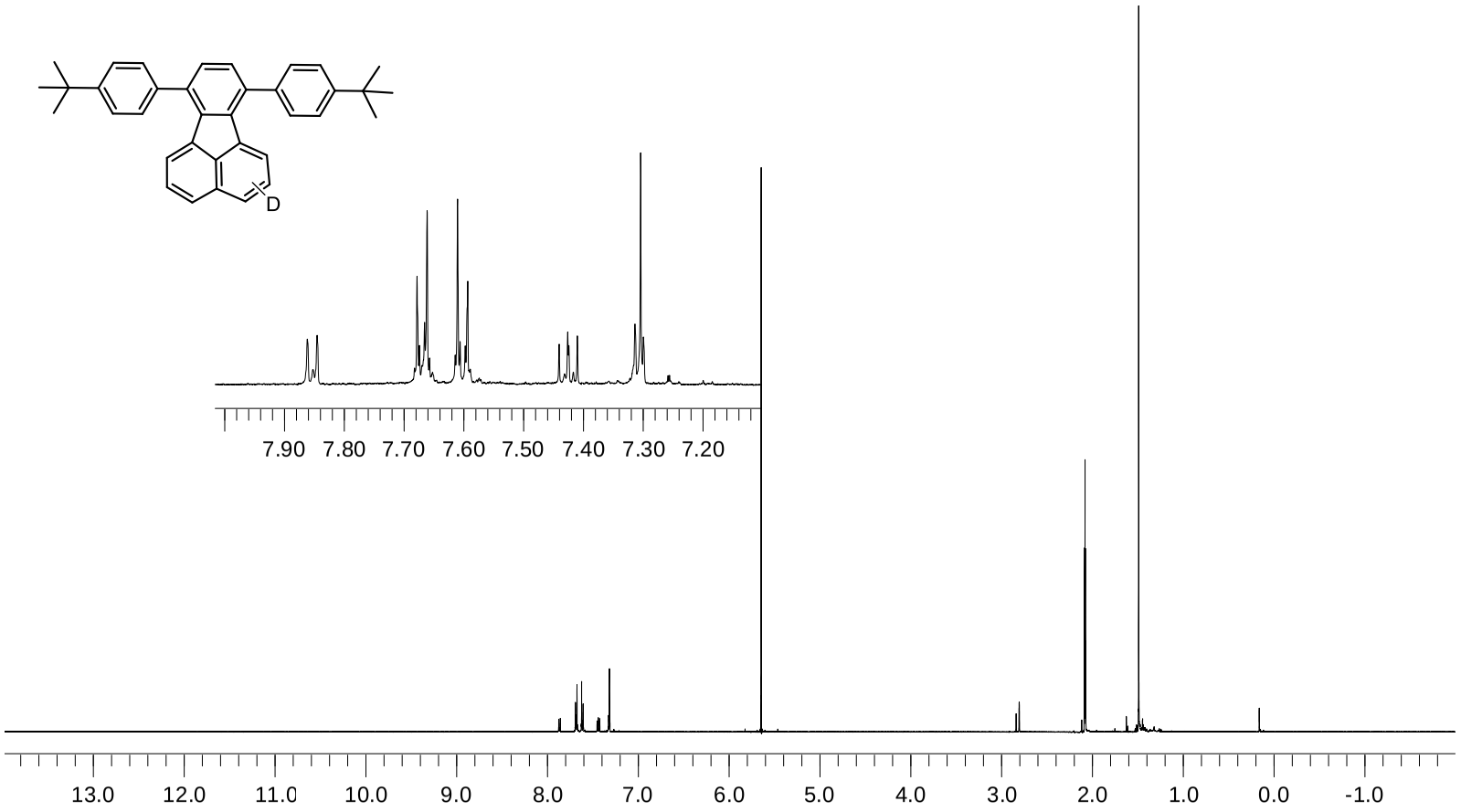

^{1}H NMR (500 MHz, Acetone-d_6)

3.12.13. 7,10-*Bis*(4-*tert*-butylphenyl)fluoranthene

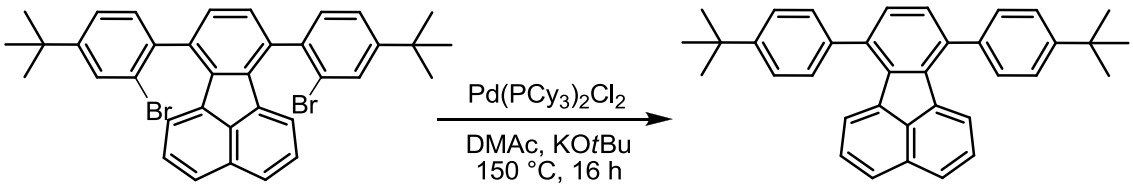

To a flame-dried, nitrogen purged pressure vessel, equipped with a magnetic stir bar, was added 20.0 mg (0.0321 mmol) 7,10-*bis*(2-bromo-4-*tert*-butylphenyl)fluoranthene and 3.20 mg (0.00321 mmol) $Pd(PCy_3)_2Cl_2$. DMAc (0.30 mL) was added via syringe, and the mixture was stirred. Potassium *tert*-butoxide (144 mg, 1.28 mmol) was added, and the vessel was sealed. The mixture was placed in a pre-heated oil bath (150 ˚C) for 16 h. The reaction mixture was then cooled to room temperature, and flushed through a short pad of alumina with dichloromethane as the eluent. Solvent was removed under reduced pressure to provide 14.3 mg (96%) of a tan solid. **^{1}H NMR** (500 MHz, $CDCl_3$) δ(ppm): 7.74 (d, *J* = 8.0 Hz, 2H), 7.59-7.56 (m, 8H), 7.37 (t, *J* = 8.0 Hz, 2H), 7.28 (d, *J* = 8.0 Hz, 2H), 7.27 (s, 2H), 1.46 (s, 18H). **^{1}H NMR** (500 MHz, Acetone-d_6) δ(ppm): 7.78 (d, *J* = 8.5 Hz, 2H), 7.61 (dt, *J* = 8.0 Hz, *J* = 2.0 Hz, 4H), 7.56 (dt, *J* = 8.0 Hz, *J* = 2.0 Hz, 4H), 7.37 (t, *J* = 8.5 Hz, 2H), 7.29 (d, *J* = 8.0 Hz, 2H), 7.24 (s, 2H), 1.48 (s, 18H). **^{13}C NMR** (125 MHz, $CDCl_3$) δ(ppm): 150.7, 138.0, 137.8, 136.7, 136.4, 132.8, 129.8, 129.31, 129.29, 128.7, 127.5, 126.62, 126.60, 125.5, 123.0, 34.8, 31.5. **HRMS** (DART-TOF): Calc'd for $C_{36}H_{35}$ $(M+1)^+$ 467.2738, found 467.2713.

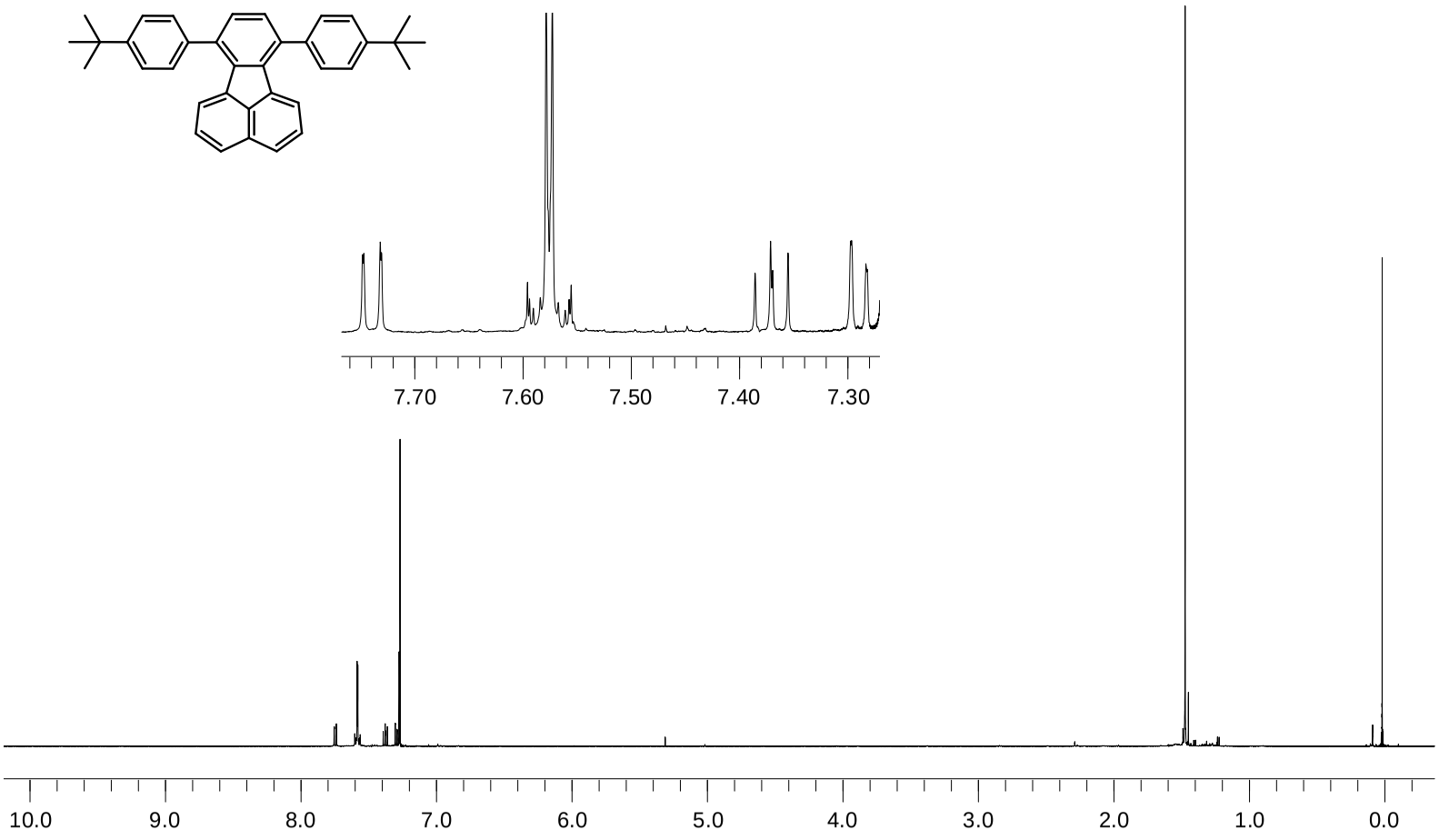

^{1}H NMR (500 MHz, $CDCl_3$)

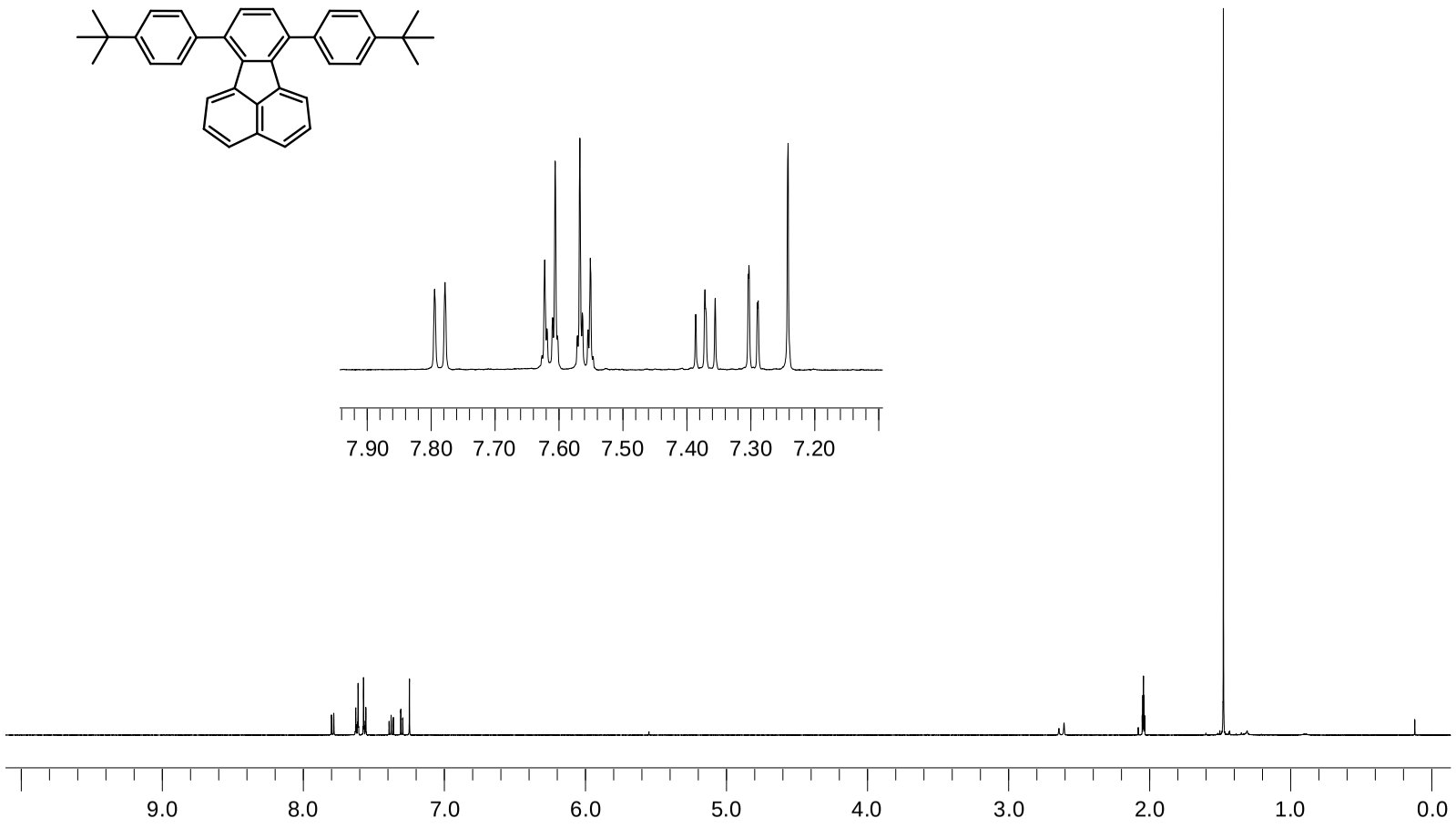

^{1}H NMR (500 MHz, Acetone-d_6)

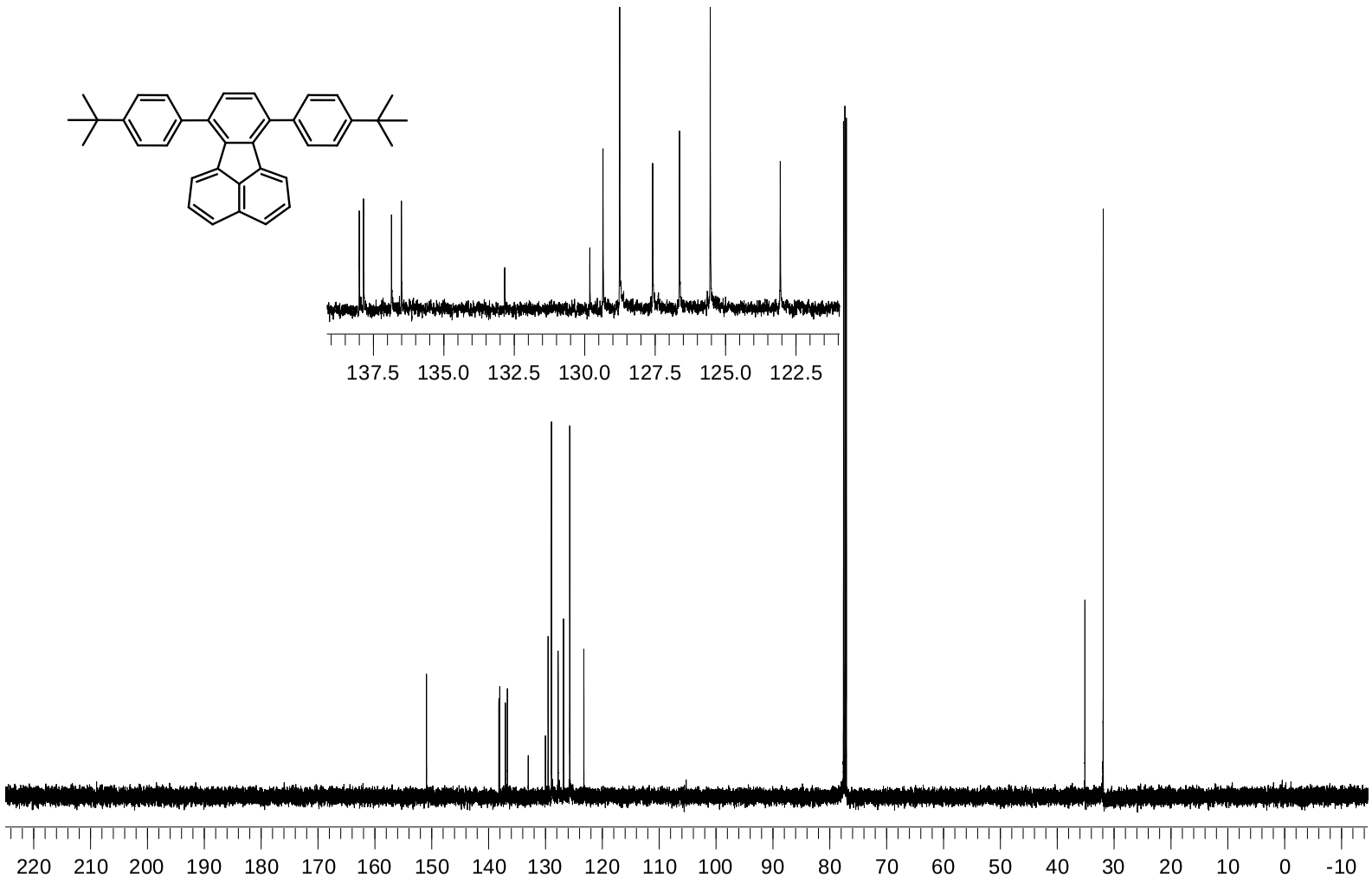

^{13}C NMR (125 MHz, $CDCl_3$)

7,10-*Bis*(4-*tert*-butylphenyl)fluoranthene

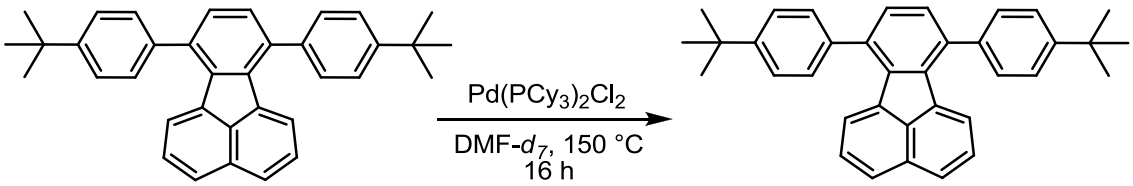

To a flame-dried, nitrogen purged pressure vessel, equipped with a magnetic stir bar, was added 12.5 mg (0.0268 mmol) 7,10-*bis*(4-*tert*-butylphenyl)fluoranthene and 2.0 mg (0.00268 mmol) of $Pd(PCy_3)_2Cl_2$. Dimethylformamide-d_7 (0.19 mL) was added via syringe, and the mixture was stirred. The vessel was sealed, and the mixture was placed in a pre-heated oil bath (150 ˚C) for 16 h. The reaction mixture was then cooled to room temperature and flushed through a short pad of alumina with dichloromethane as the eluent. The solvent was removed under reduced pressure to afford 11.6 mg (93%) as a tan solid.

3.12.14. 7,10-*Bis*(4-*tert*-butylphenyl-d_2)fluoranthene-d_4

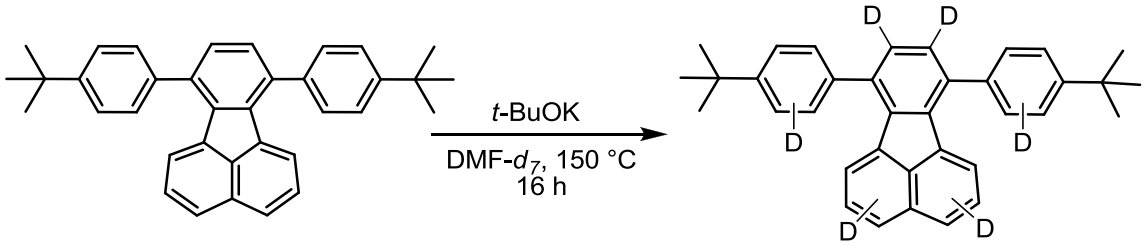

To a flame-dried, nitrogen purged pressure vessel, equipped with a magnetic stir bar, was added 12.5 mg (0.0268 mmol) 7,10-*bis*(4-*tert*-butylphenyl)fluoranthene. Dimethylformamide-d_7 (0.19 mL) was added via syringe, and the mixture was stirred. Potassium *tert*-butoxide (89.0 mg, 1.07 mmol) was added, and the vessel was sealed. The mixture was placed in a pre-heated oil bath (150 ˚C) for 16 h. The reaction mixture was then cooled to room temperature and flushed through a short pad of alumina with dichloromethane as the eluent. Solvent was removed under reduced pressure to provide 11.0 mg (88%) of a tan solid. **^{1}H NMR** (500 MHz, $CDCl_3$) δ(ppm): 7.81-7.78 (m), 7.63-7.58 (m), 7.32 (s), 1.47 (s). **HRMS** (DART-TOF): Calc'd for $C_{36}H_{29}D_6$ $(M+1)^+$ 473.3115, found 473.3124. **EI-MS** *m/z* (rel. abundance, %): 476 (30), 475 (80), 474 (100), 473 (70), 472 (30).

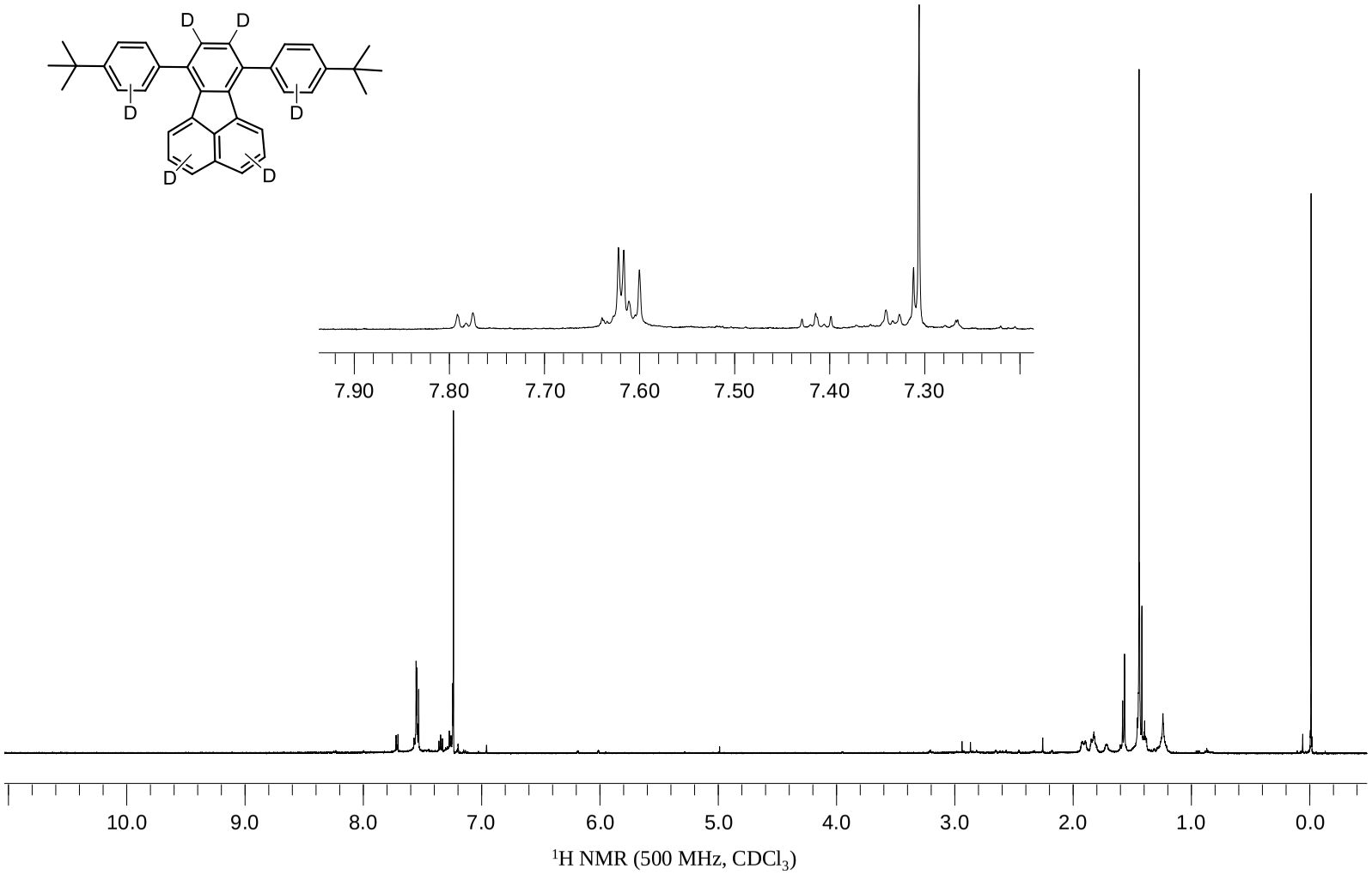

^{1}H NMR (500 MHz, $CDCl_3$)

3.12.15. 2-Bromo-4-*tert*-butyl-1-chlorobenzene

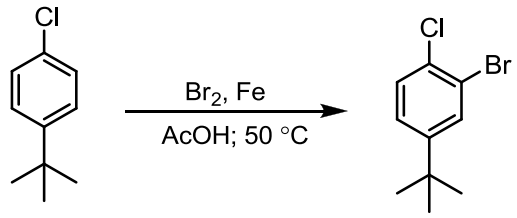

At room temperature, elemental bromine (47.4 g, 0.296 mol) was added dropwise to a stirred solution of 4-*tert*-butylchlorobenzene (10.0 g, 0.0595 mol), 1.31 g (0.0238 mol) iron powder and 30.0 mL glacial acetic acid. The reaction mixture was then stirred and heated to 50 ˚C for 24 h. The mixture was cooled to room temperature and quenched with 10% sodium bisulfate and extracted with hexanes. The organic extracts were washed with water, dried over magnesium sulfate and concentrated to dryness under reduced pressure to give 13.9 g (95%) of the desired product as a clear oil. **^{1}H NMR** (500 MHz, $CDCl_3$) δ(ppm): 7.60 (d, *J* =2.5 Hz, 1H), 7.35 (d, *J* =8.5 Hz, 1H), 7.25 (dd, *J* =8.5, 2.0 Hz, 1H), 1.29 (s, 9H). **^{13}C NMR** (125 MHz, $CDCl_3$) δ(ppm): 151.6, 131.3, 130.9, 129.8, 125.7, 122.1, 34.4, 30.9. **HRMS** (DART-TOF): Calc'd for $C_{10}H_{12}BrCl$ (M^+) 245.9811, found 245.9809.

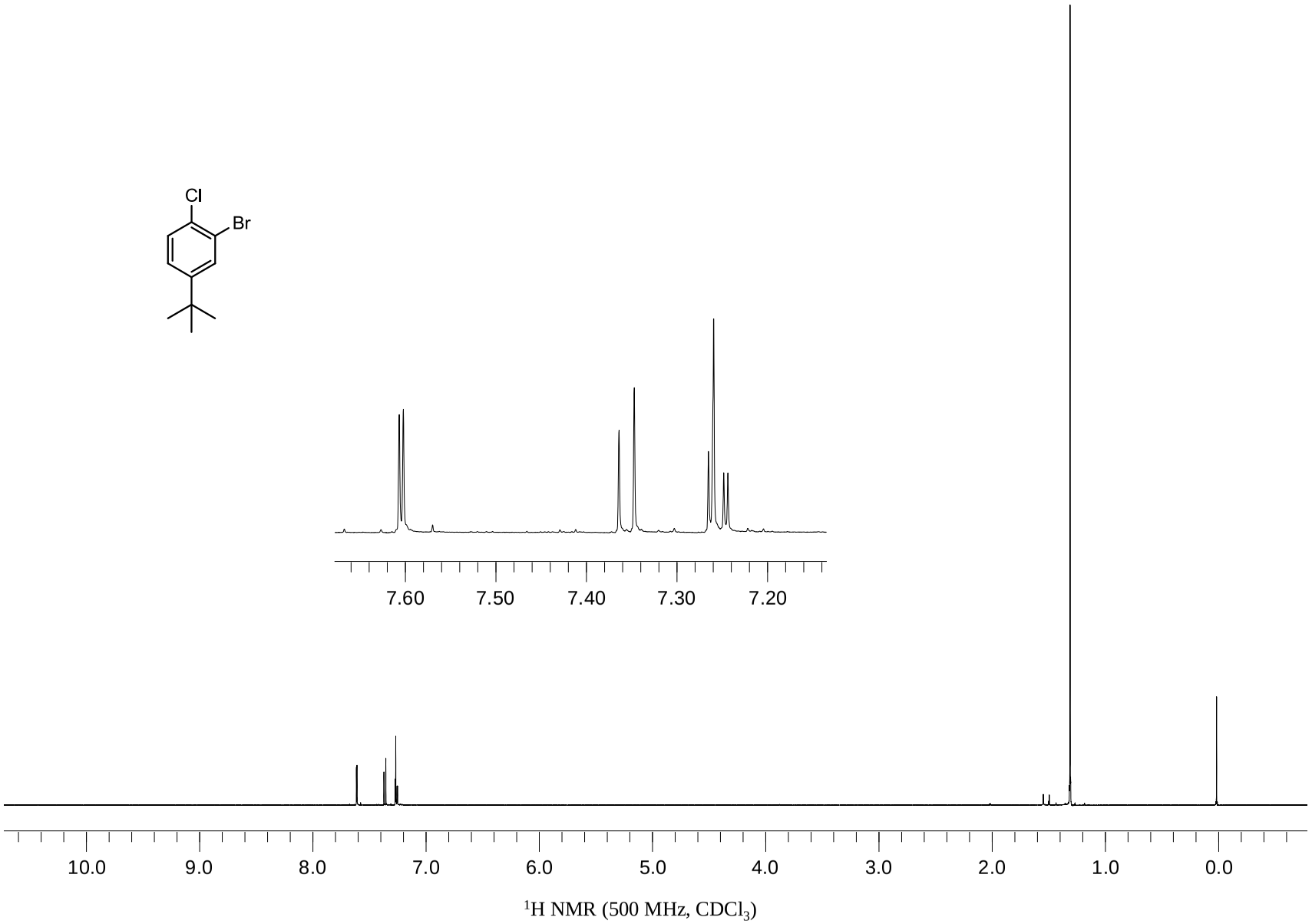

^{1}H NMR (500 MHz, $CDCl_3$)

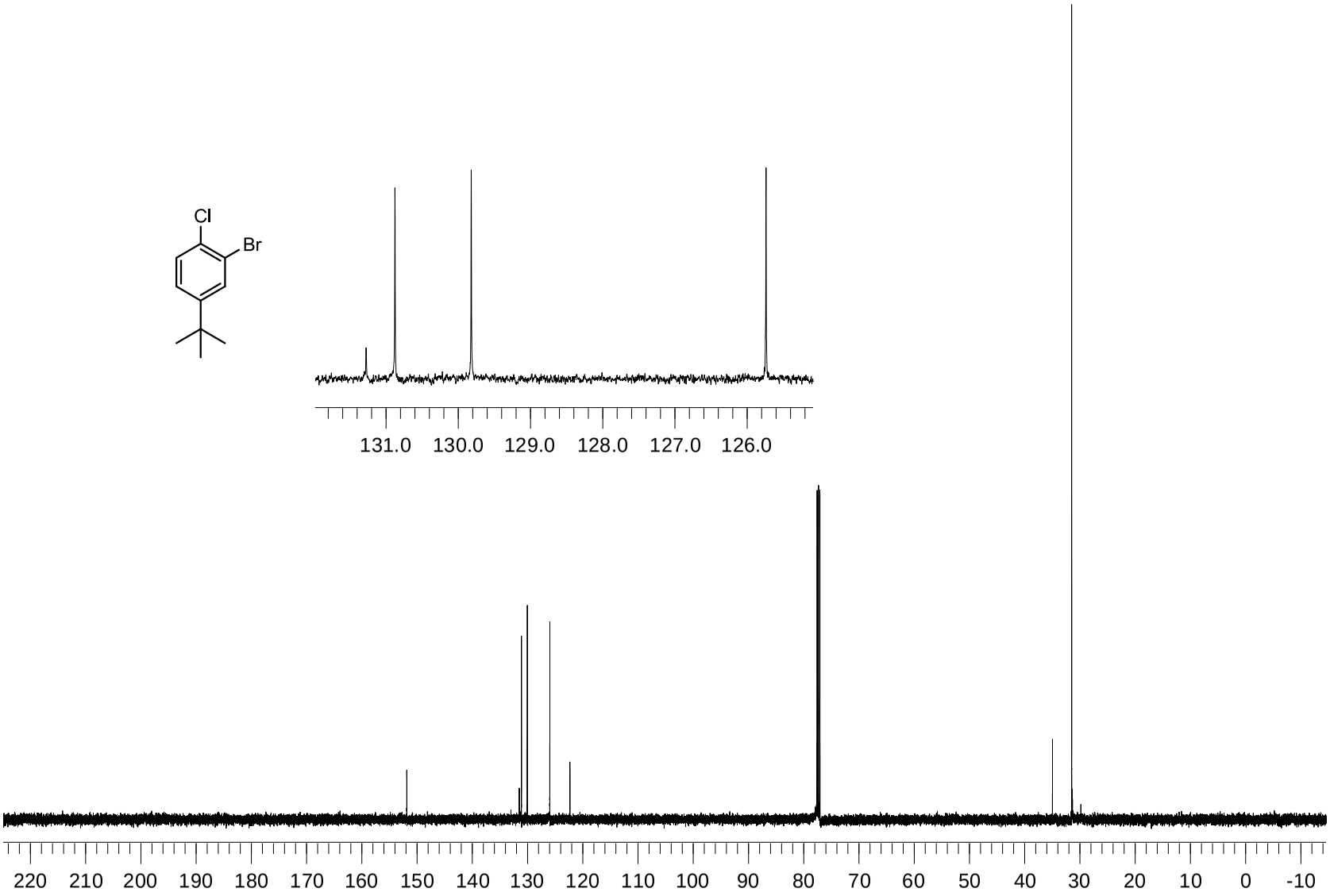

^{13}C NMR (125 MHz, $CDCl_3$)

3.12.16. 4-*Tert*-butyl-1-chloro-2-methylbenzene

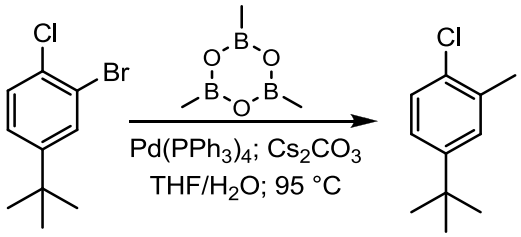

A solution of anhydrous tetrahydrofuran (135 mL) with 13.5 mL of water was degassed for 15 min. To a large pressure vessel, flame-dried and purged with nitrogen, was added 3.51 g (3.05 mmol) *tetrakis*(triphenylphosphine) palladium(0), cesium carbonate (59.3 g, 0.182 mol) and 15.0 g (0.0607 mol) of 2-bromo-4-*tert*-butyl-1-chlorobenzene. The degassed solvents were added to the reaction mixture and stirred. Trimethylboroxine (7.62 g, 0.0607 mol) was added to the reaction mixture; the vessel was sealed and placed in a pre-heated oil bath (95 ˚C) overnight. The mixture was cooled to room temperature and flushed through a short pad of silica gel with hexanes as the eluent. The solution was extracted with water, dried over magnesium sulfate and concentrated to dryness under reduced pressure to give 9.78 g (89%) of the desired product as a clear oil. **^{1}H NMR** (500 MHz, $CDCl_3$) δ(ppm): 7.21 (d, *J* = 8.5 Hz , 1H), 7.19 (d, *J* = 2.5 Hz, 1H), 7.10 (dd, *J* = 8.5 Hz, 2.5 Hz, 1H), 2.33 (s, 3H), 1.26 (s, 9H). **^{13}C NMR** (125 MHz, $CDCl_3$) δ(ppm): 149.7, 135.2, 131.3, 128.5, 128.0, 124.2, 34.4, 31.3, 20.3. **HRMS** (DART-TOF): Calc'd for $C_{11}H_{15}Cl$ $(M+1)^+$ 182.0862 , found 182.0858.

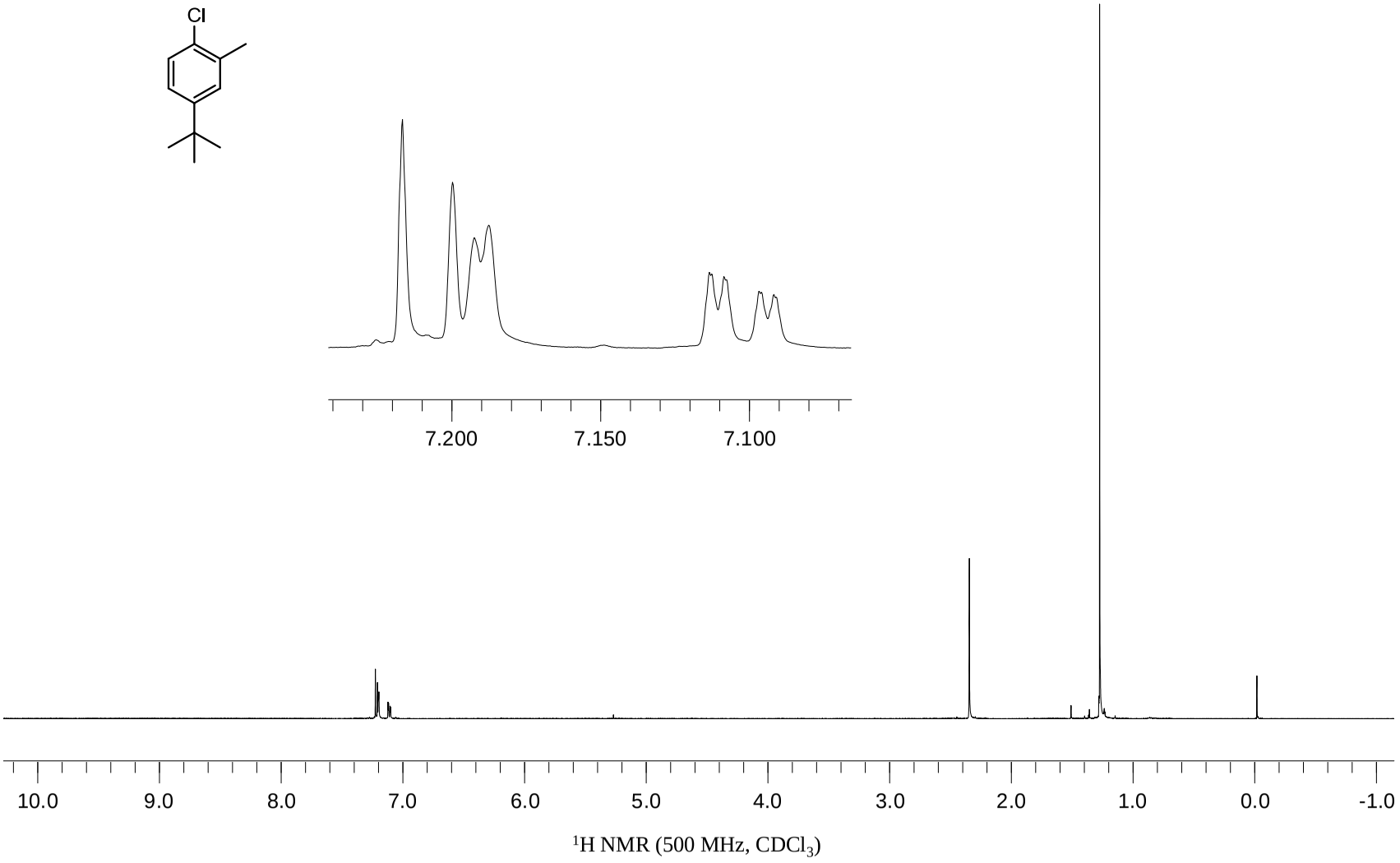
Cl
7.200
7.150
7.100
10.0
9.0
8.0
7.0
6.0
5.0
4.0
3.0
2.0
1.0
0.0
-1.0
^{1}H NMR (500 MHz, $CDCl_3$)

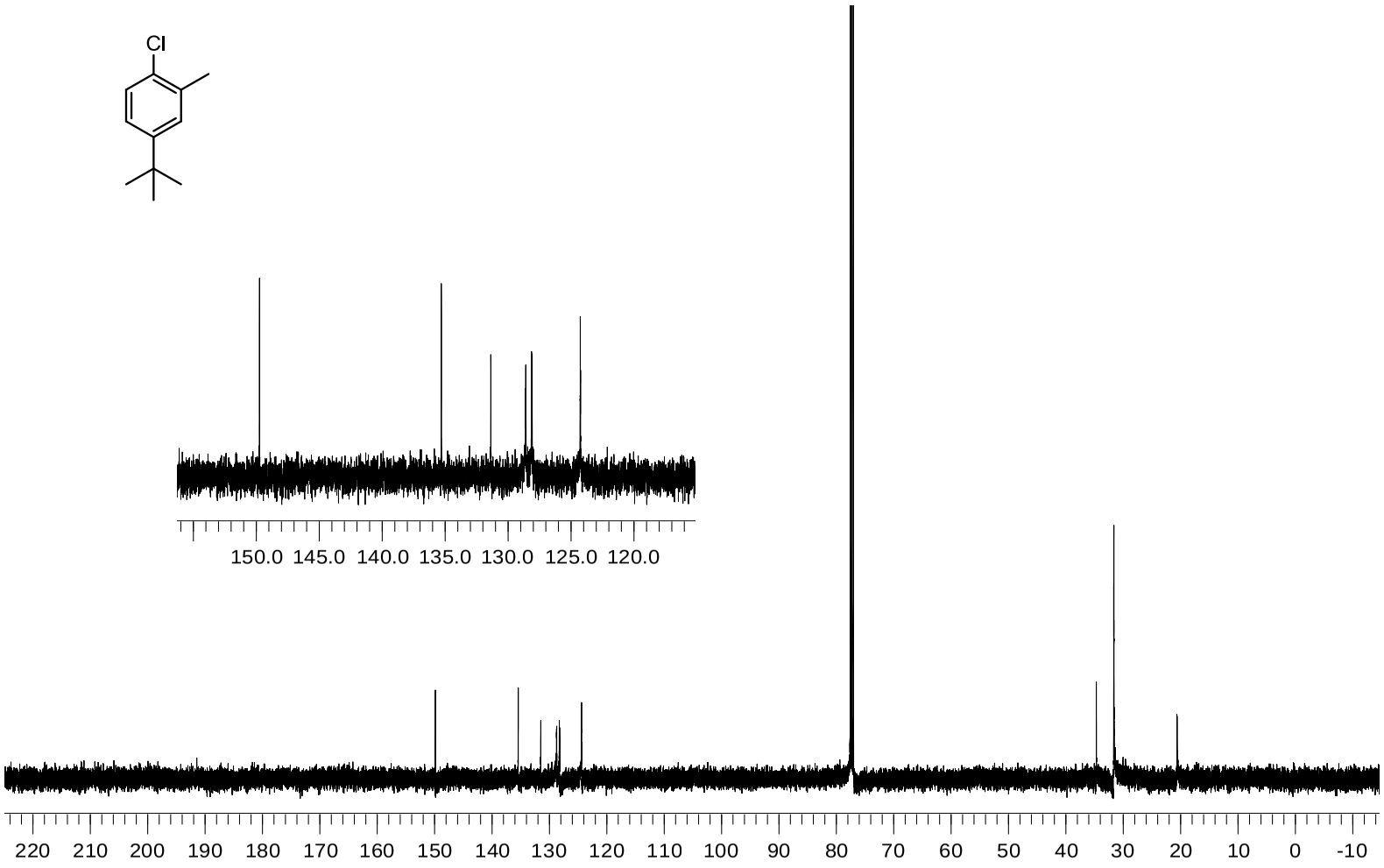

^{13}C NMR (125 MHz, $CDCl_3$)

3.12.17. 2-(Bromomethyl)-4-*tert*-butyl-1-chlorobenzene

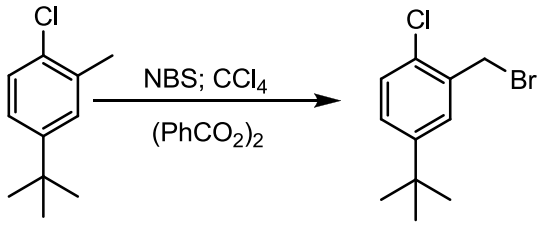

To a solution of 4-*tert*-butyl-1-chloro-2-methylbenzene (9.78 g, 0.0537 mol) in 78.0 mL carbon tetrachloride, was added *N*-bromosuccinimide (10.5 g, 0.0591 mol) and benzoyl peroxide (~10 mg). The reaction mixture was stirred and heated to reflux for 4 h. The mixture was cooled to room temperature, and the succinimide was removed by filtration. The filtrate was washed with 10% KOH(aq), and the organic layer was dried over magnesium sulfate and concentrated to dryness under reduced pressure to afford 13.5 g (96%) of the desired product as a clear oil. **^{1}H NMR** (500 MHz, $CDCl_3$) δ(ppm): 7.43 (d, *J* = 2.5 Hz, 1H), 7.30 (s, 1H), 7.28 (d, *J* = 2.5 Hz, 1H), 4.60 (s, 2H), 1.31 (s, 9H). **^{13}C NMR** (125 MHz, $CDCl_3$) δ(ppm): 150.6, 134.6, 131.2, 129.5, 128.2, 127.3, 34.6, 31.22, 31.18. **HRMS** (DART-TOF): Calc'd for $C_{11}H_{13}BrCl$ $(M-1)^+$ 258.9889, found 258.9897.

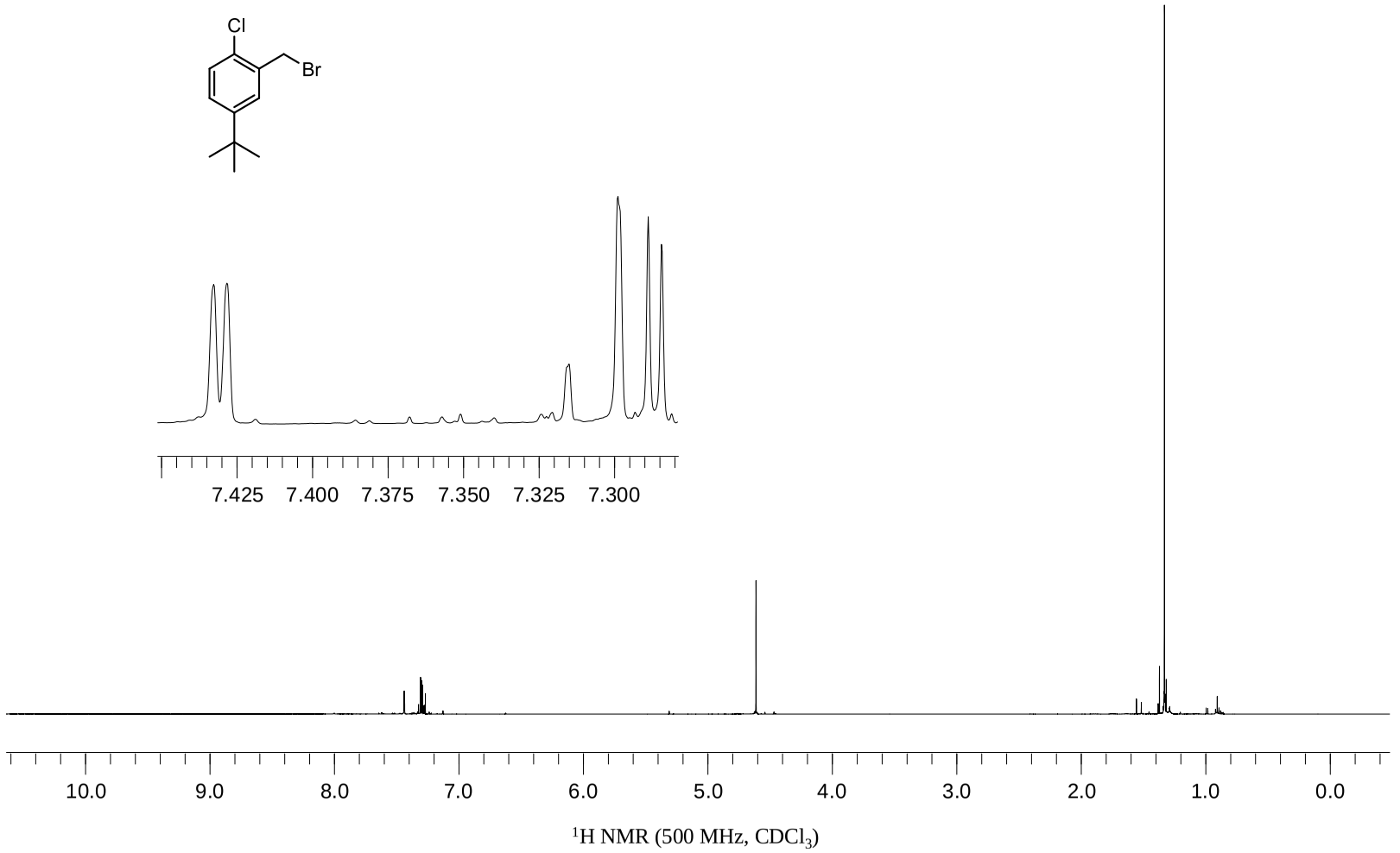

^{1}H NMR (500 MHz, $CDCl_3$)

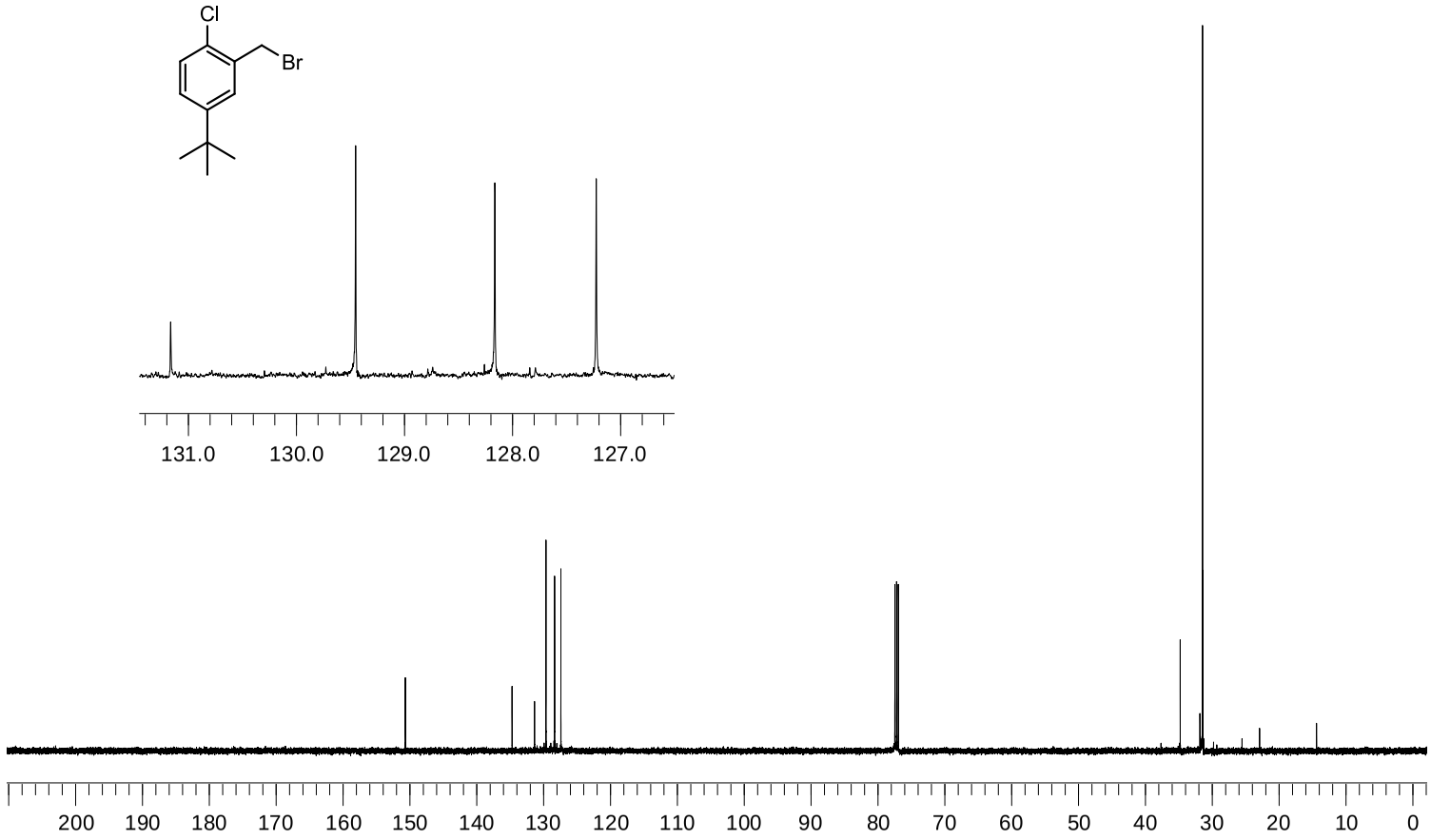

^{13}C NMR (125 MHz, $CDCl_3$)

3.12.18. 1,3-*Bis*(5-*tert*-butyl-2-chlorophenyl)propan-2-one

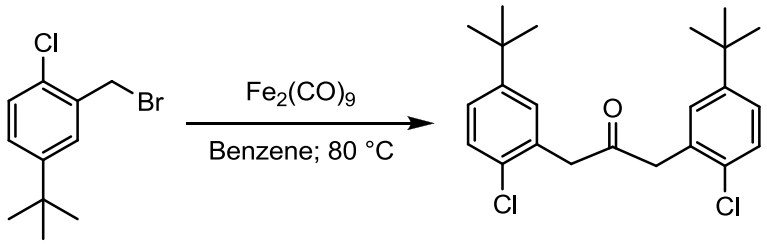

To a flame-dried, nitrogen purged round bottom flask was added 25.0 g (0.0689 mol) $Fe_2(CO)_9$.[§] Anhydrous benzene (400 mL) was added via cannula immediately, and the reaction was stirred. 2-(Bromomethyl)-4-*tert*-butyl-1-chlorobenzene (18.0 g, 0.0689 mol) was added, and the reaction was heated at reflux for 24 h. The reaction mixture was cooled to room temperature and flushed through a short pad of silica gel with dichloromethane as the eluent. The solvent was concentrated to dryness under reduced pressure. Chromatography of the crude product on silica gel with 1:1 hexanes: dichloromethane provided 8.65 g (64%) of a pale yellow oil. **^{1}H NMR** (500 MHz, $CDCl_3$) δ(ppm): 7.30 (d, *J* = 8.5 Hz, 2H), 7.24 (dd, *J* = 8.5 Hz, *J* = 2.5 Hz, 2 H), 7.20 (d, *J* = 2.5 Hz, 2H), 3.91 (s, 4H), 1.29 (s, 18 H). **^{13}C NMR** (125 MHz, $CDCl_3$) δ(ppm): 203.7, 150.2, 131.9, 131.4, 129.0, 128.3, 125.9, 47.4, 34.5, 31.3. **IR** (NaCl, cm^{-1}): 1725 (C=O). **HRMS** (DART-TOF): Calc'd for $C_{23}H_{29}Cl_2O$ $(M+1)^+$ 391.1595, found 391.1589.

[§] $Fe_2(CO)_9$ is pyrophoric and must be handled with care. After addition under nitrogen, the solvent must be added quickly. Once submerged in solvent, the reagent is stable.

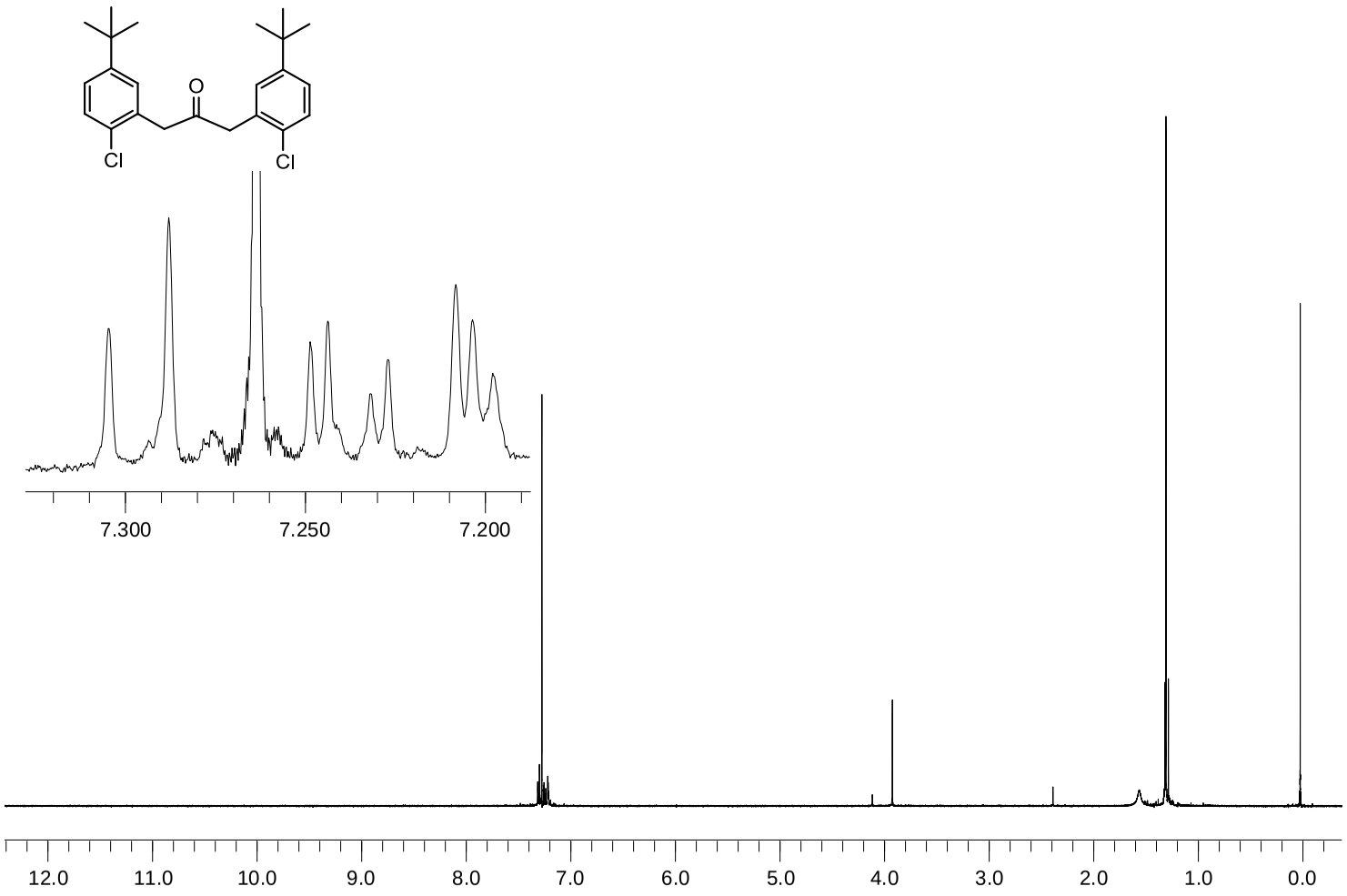

^{1}H NMR (500 MHz, $CDCl_3$)

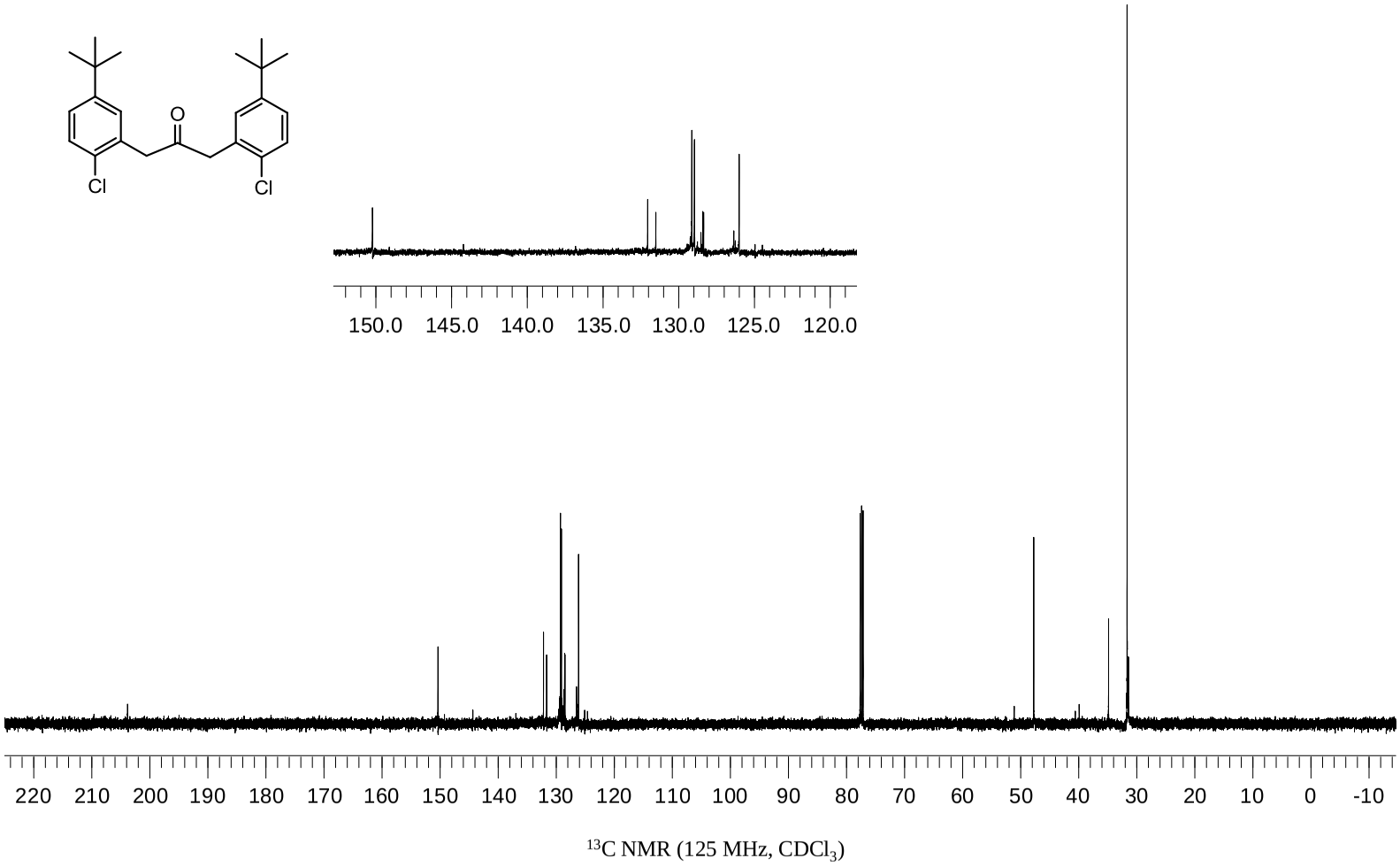

^{13}C NMR (125 MHz, $CDCl_3$)

3.12.19. 7,9-*Bis*(5-*tert*-butyl-2-chlorophenyl)-8*H*-cyclopenta[*a*]acenaphthylen-8-one

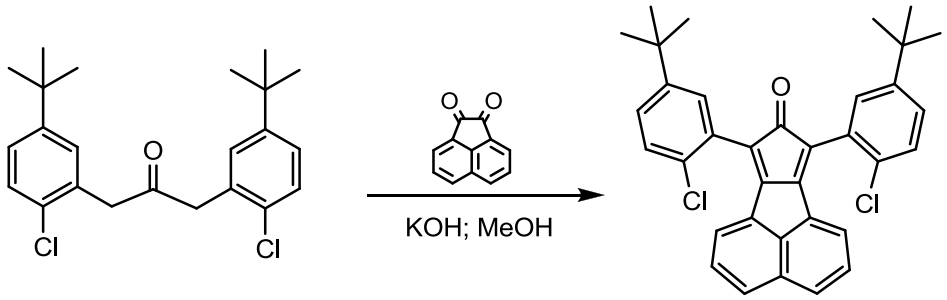

To a large Erlenmeyer flask was added 8.65 g (0.0221 mol) of 1,3-*bis*(5-*tert*-butyl-2-chlorophenyl)propan-2-one and 4.05 g (0.0221 mol) of acenaphthenequinone. A solution of potassium hydroxide (1.63 g, 0.0313 mol) in 208 mL of methanol was added, and the reaction mixture was stirred at room temperature for 2 h. The purple solution was allowed to sit overnight without stirring. The resulting purple precipitate was collected by filtration to provide 6.47 g (55%) of the desired product. **MP:** 152-158 ˚C. **^{1}H NMR** (500 MHz, $CDCl_3$, for a mixture of diastereomers) δ(ppm): 7.87 (d, *J* = 8.5 Hz, 2H), 7.60-7.57 (m, 5H), 7.51 (s, 1H of minor diastereomer), 7.47 (d, *J* = 8.5 Hz, 2H), 7.39 (d, *J* = 8.5 Hz, 2H), 1.36 (s, 18 H). **^{13}C NMR** (125 MHz, $CDCl_3$, for a mixture of diastereomers) δ(ppm): 200.6, 199.6, 156.2, 155.8, 149.6, 145.2, 131.9, 131.7, 131.5, 131.4, 131.2, 131.1, 130.0, 129.8, 129.7, 129.6, 129.4, 128.9, 128.45, 128.41, 127.7, 126.89, 126.85, 123.5, 122.8, 120.7, 119.9, 34.7, 31.3. **IR** (KBr, cm^{-1}): 1708 (C=O). **HRMS** (DART-TOF): Calc'd for $C_{35}H_{31}Cl_2O$ $(M+1)^+$ 537.1752, found 537.1753.

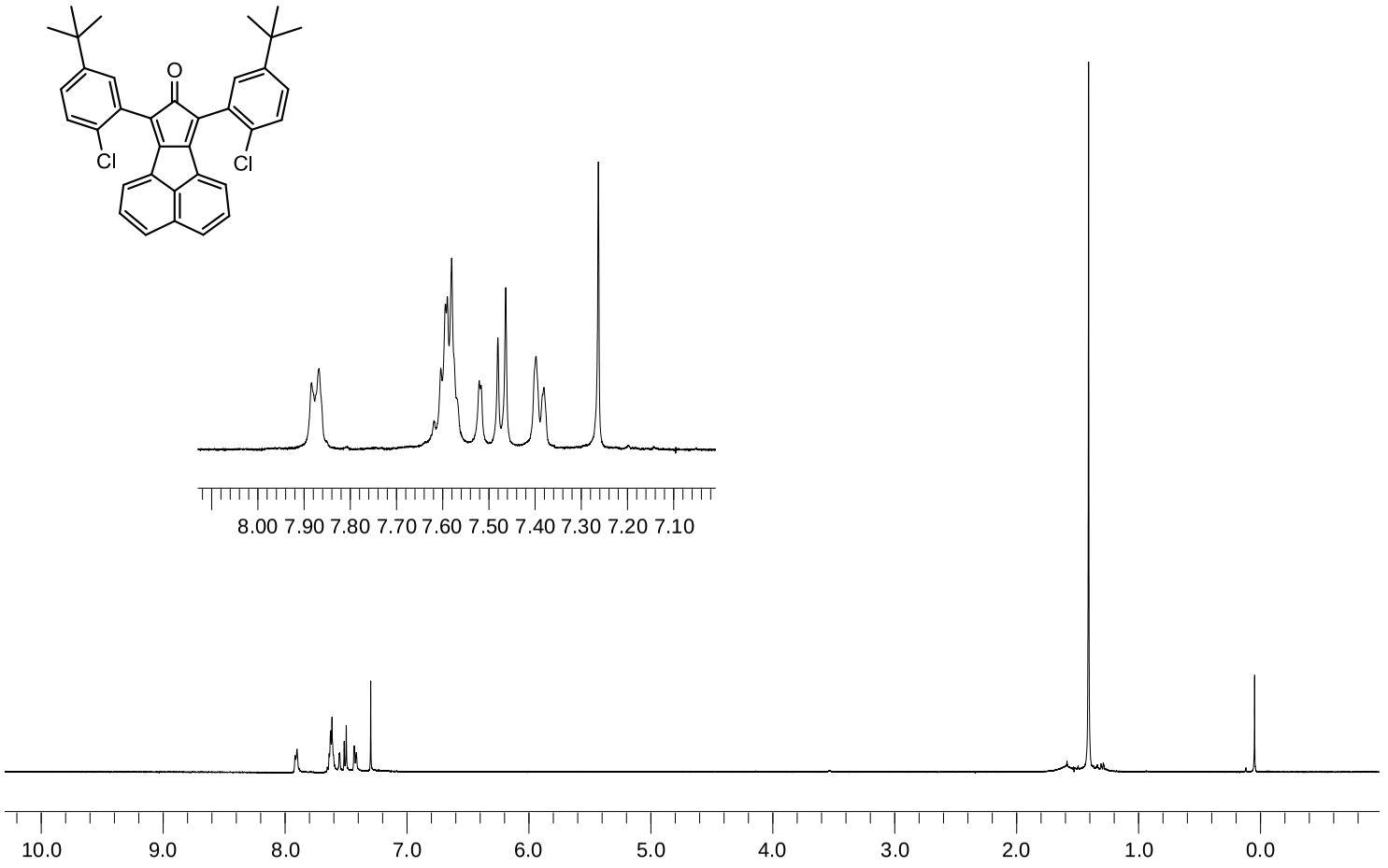

^{1}H NMR (500 MHz, $CDCl_3$)

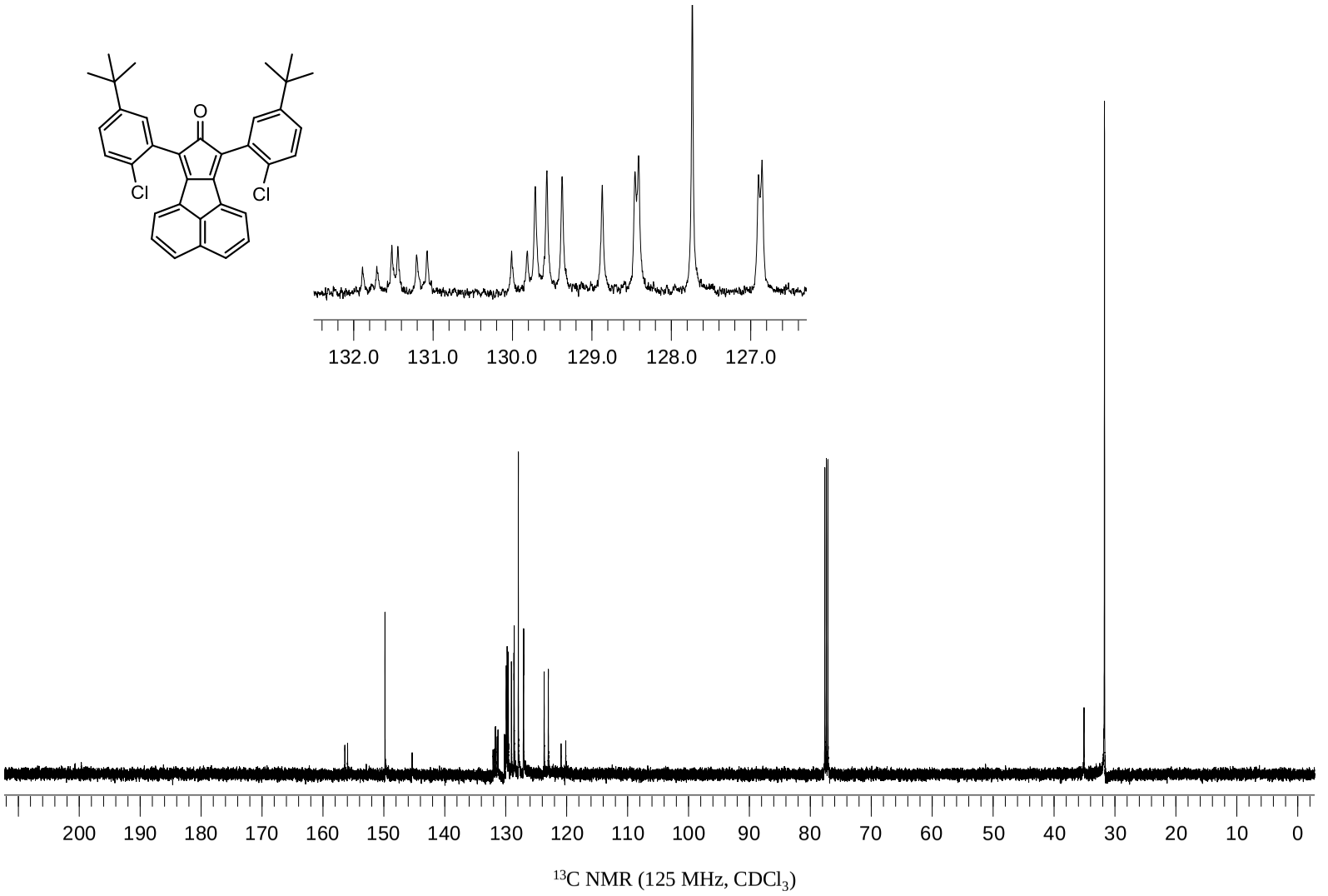

^{13}C NMR (125 MHz, $CDCl_3$)

3.12.20. 7,10-*Bis*(5-*tert*-butyl-2-chlorophenyl)fluoranthene

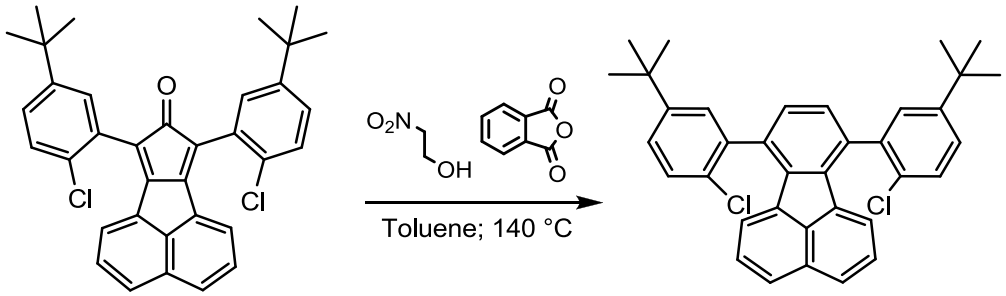

To a flame-dried round bottom flask with reflux condenser attached, 3.00 g (5.58 mmol) of 7,9-*bis*(5-*tert*-butyl-2-chlorophenyl)-8*H*-cyclopenta[*a*]acenaphthylen-8-one was added under nitrogen. To this, 12.6 g (0.139 mol) of nitroethanol and 20.6 g (0.139 mol) of phthalic anhydride were added. Anhydrous toluene (130 mL) was added, and the reaction mixture was stirred and heated to 140 ˚C for 24 h. The reaction was cooled to room temperature, and the toluene was decanted off. The remaining solids in the reaction flask were extracted with dichloromethane and washed with 10% NaOH(aq) twice. The toluene extracts were combined with the dichloromethane extracts and washed again with 10% NaOH. The organic extracts were dried over magnesium sulfate and concentrated to dryness under reduced pressure. A dark brown solid was collected and flushed through a long silica gel plug with 3:1 hexanes: dichloromethane to provide 2.53 g (85%) of a yellow solid. **MP:** 160-163 ˚C. **^{1}H NMR** (500 MHz, $CDCl_3$, for a mixture of diastereomers) δ(ppm): 7.76 (d, *J* = 8.5 Hz, 2H), 7.66 (d, *J* = 2.5 Hz, 2H of major diastereomer), 7.61 (d, *J* = 2.5 Hz, 2H of minor diastereomer), 7.58 (dd, *J* = 8.0 Hz, 2.5 Hz, 2H), 7.51 (dd, *J* = 8.0 Hz, 2.5 Hz, 2H), 7.39 (t, *J* = 8.0 Hz, 2H), 7.38 (s, 2H), 6.92 (d, *J* = 7.0 Hz, 2H), 1.39 (s, 18H). **^{13}C NMR** (125 MHz, $CDCl_3$, for a mixture of

diastereomers) δ(ppm): 150.3, 150.18, 138.6, 137.3, 136.26, 136.24, 135.39, 135.36, 132.71, 132.69, 130.48, 130.36, 129.78, 129.46, 129.35, 128.93, 128.9, 128.8, 128.6, 127.7, 126.7, 126.3, 122.61, 122.59, 34.79 34.76, 31.39, 31.37. **HRMS** (DART-TOF): Calc'd for $C_{36}H_{33}Cl_2$ $(M-1)^+$ 535.1959, found 535.1968.

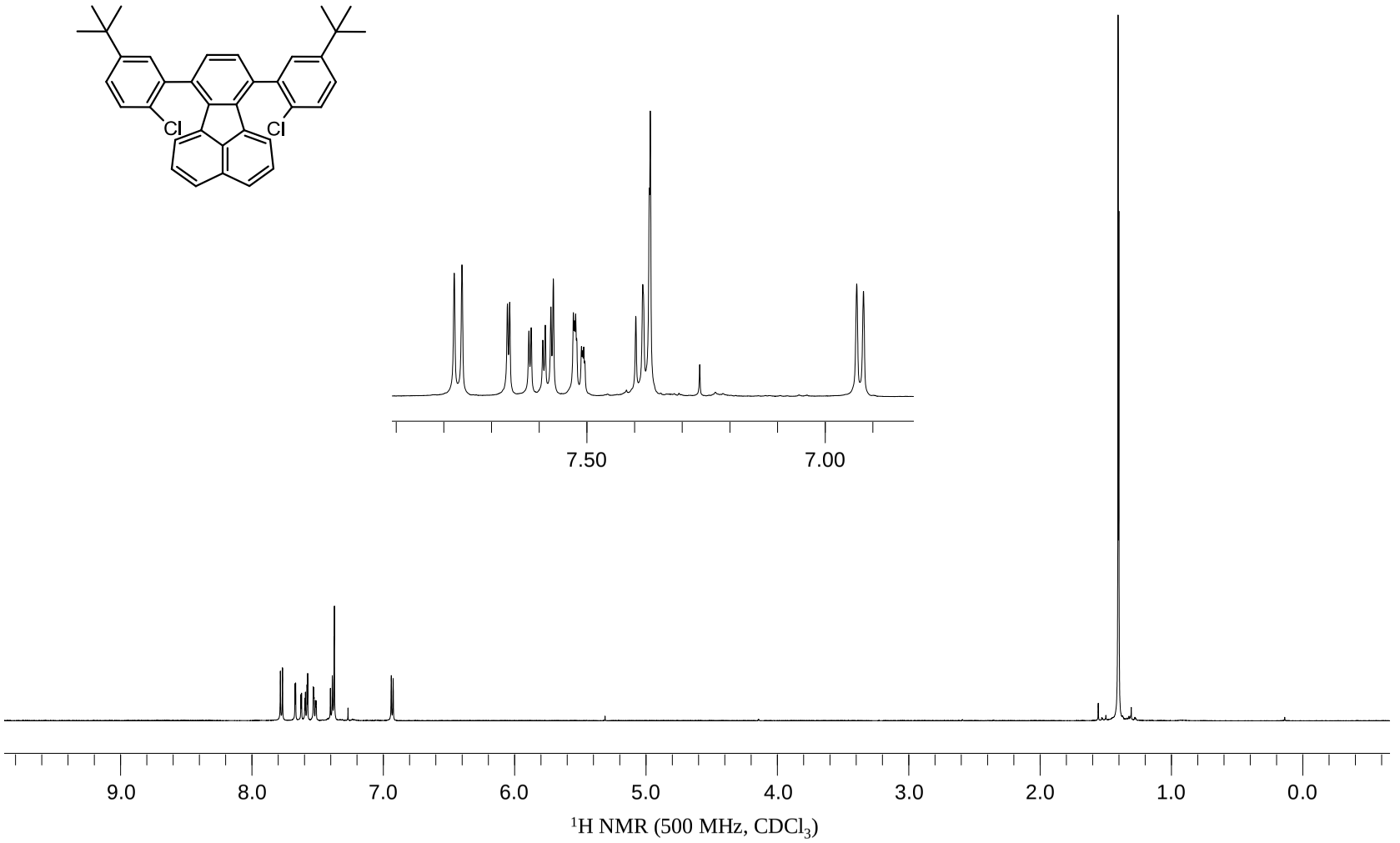
Cl
Cl
7.50
7.00
9.0
8.0
7.0
6.0
5.0
4.0
3.0
2.0
1.0
0.0
^{1}H NMR (500 MHz, $CDCl_3$)

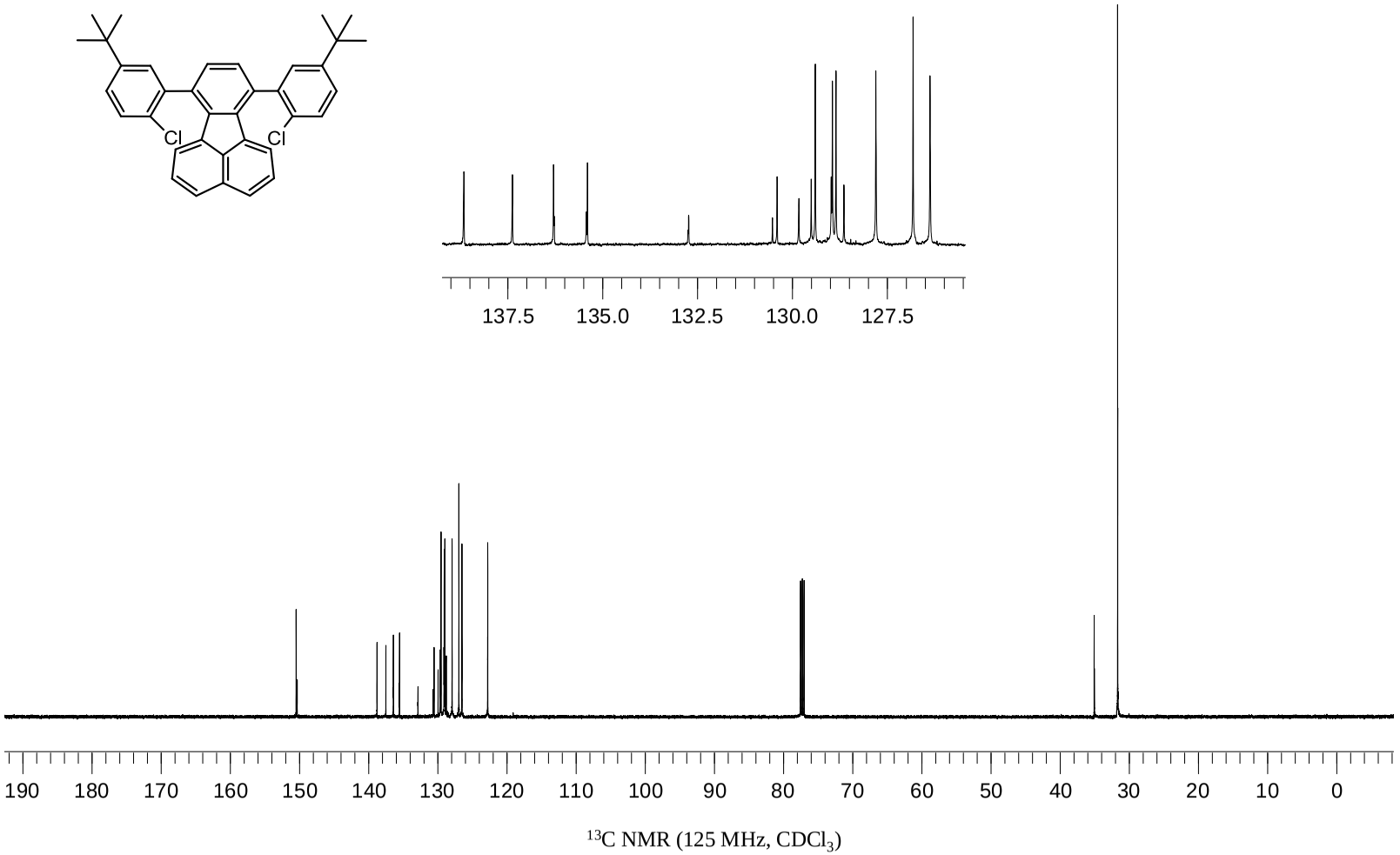

^{13}C NMR (125 MHz, $CDCl_3$)

3.12.21. 5,10-Di-*tert*-butyldibenzo[*a,g*]corannulene

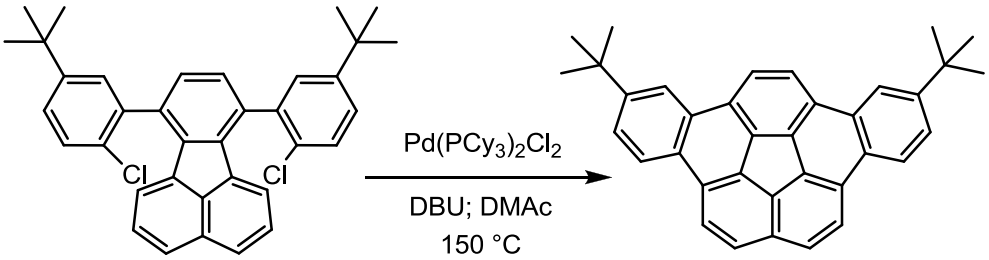

To a flame-dried, nitrogen purged pressure vessel equipped with a stir bar, 2.00 g (3.73 mmol) of 7,10-*bis*(5-*tert*-butyl-2-chlorophenyl)fluoranthene and 276 mg (0.373 mmol) of $Pd(PCy_3)_2Cl_2$ were added under a nitrogen atmosphere. Anhydrous DMAc (35.0 mL) and DBU (22.7 mL) were added via syringe and the reaction mixture was stirred. The vessel was sealed and heated in a pre-heated oil bath at 150 ˚C for 3 d. The mixture was cooled to room temperature and flushed through a short pad of neutral alumina with dichloromethane as the eluent. The filtrate was washed with 10% HCl(aq) twice and once with water. The organic layer was dried over magnesium sulfate and concentrated to dryness under reduced pressure. The product was washed with hexanes to provide 1.44 g (84%) of the desired product as a yellow solid. **MP:** >250 ˚C (dec). **^{1}H NMR** (500 MHz, $CDCl_3$) δ(ppm): 8.70 (d, *J* = 2.5 Hz, 2 H), 8.57 (d, *J* = 8.5 Hz, 2H), 8.36 (s, 2H), 8.22 (d, *J* = 8.5 Hz, 2H), 7.95 (d, *J* = 8.5 Hz, 2H), 7.80 (d, *J* = 8.5 Hz, *J* = 2.5 Hz, 2H), 1.53 (s, 18 H). **^{13}C NMR** (125 MHz, $CDCl_3$) δ(ppm): 150.7, 136.1, 135.3, 134.8, 133.4, 131.0, 130.3, 129.1, 129.0, 127.8, 125.3, 125.0, 124.7, 124.4, 121.6, 35.5, 31.9. **HRMS** (DART-TOF): Calc'd for $C_{36}H_{31}$ $(M-1)^+$ 463.2425, found 463.2456.

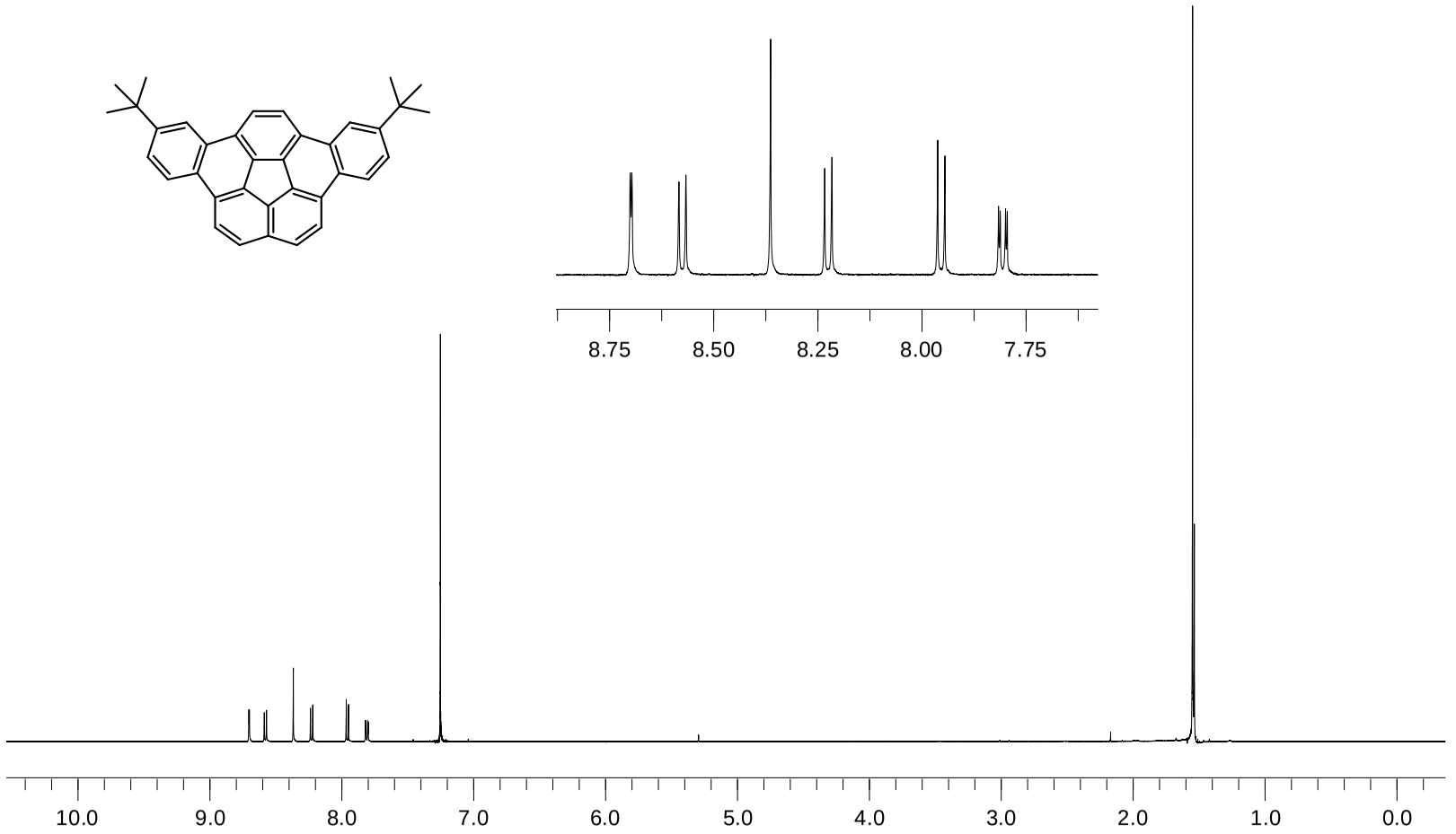

^{1}H NMR (500 MHz, $CDCl_3$)

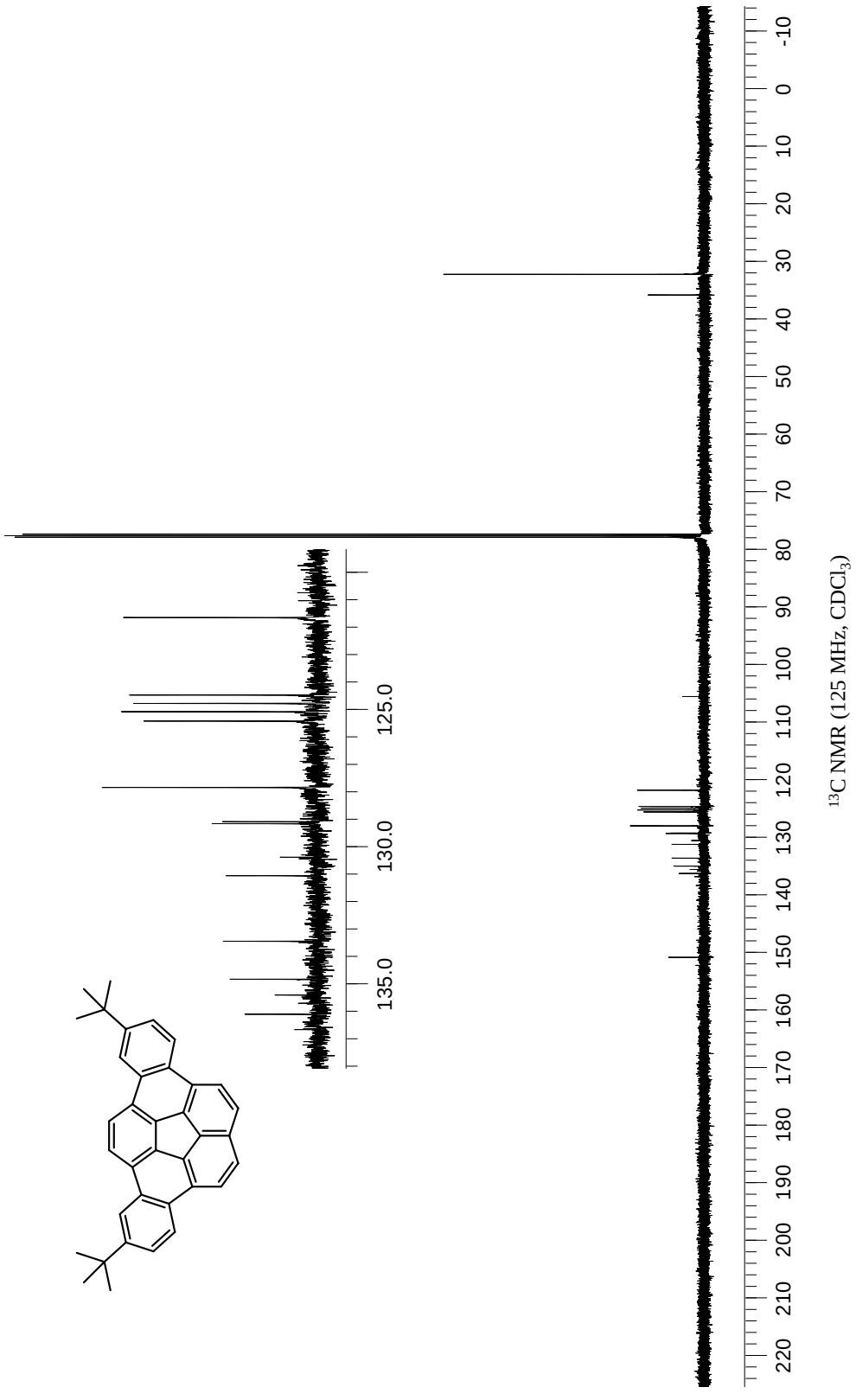

^{13}C NMR (125 MHz, $CDCl_3$)

3.12.22. 1-Bromo-5,10-di-*tert*-butyldibenzo[*a,g*]corannulene

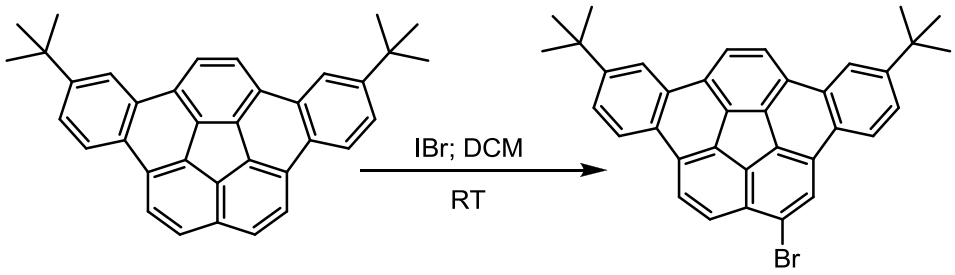

To a flame-dried, nitrogen purged round bottom flask equipped, with a magnetic stir bar, was added 100 mg (0.216 mmol) of 5,10-di-*tert*-butyldibenzo[*a*,*g*]corannulene and 89.0 mg (0.433 mmol) of iodine monobromide. Anhydrous dichloromethane (5.50 mL) was added, and the reaction mixture was stirred at room temperature for 4 h. The reaction was quenched with sodium bisulfate and extracted with dichloromethane and water. The organic layer was dried with magnesium sulfate and concentrated to dryness under reduced pressure. The crude product was washed with hot hexanes to provide 75.0 mg (64%) of the desired product as a tan solid.[**] **MP:** >260 ˚C (dec.). **^{1}H NMR** (500 MHz, $CDCl_3$) δ(ppm): 8.69 (d, *J* = 2 Hz, 1H), 8.67 (d, *J* = 2 Hz, 1H), 8.57 (d, *J* = 8.5 Hz, 1H), 8.48 (d, *J* = 8.5 Hz, 1H), 8.35 (d, *J* = 8.0 Hz, 1H), 8.32 (d, *J* = 8.0 Hz, 1H), 8.26 (d, *J* = 8.5 Hz, 1H), 8.04 (d, *J* = 9.0 Hz, 1H), 7.83 (dd, *J* = 8.0 Hz, *J* = 1.5 Hz, 1H), 7.82 (dd, *J* = 8.0 Hz, *J* = 1.5 Hz, 1H), 1.55 (s, 9H), 1.50 (s, 9H). **^{13}C NMR** (125 MHz, $CDCl_3$) δ(ppm): 150.3, 150.2, 134.2, 134.0, 133.8, 133.4, 133.1, 132.9, 132.8, 130.0, 129.3, 129.2, 128.8, 128.4, 128.2, 128.0, 127.6, 127.2, 126.3, 126.2, 124.8, 124.7, 124.49,

[**] Slight over bromination is often problematic in this reaction and purification was hampered due to contamination of over brominated material.

124.48, 124.1, 124.0, 121.4, 121.1, 35.2, 35.1, 31.7, 31.6. **HRMS** (DART-TOF): Calc'd for $C_{36}H_{30}Br$ $(M-1)^+$ 541.1531, found 541.1541.

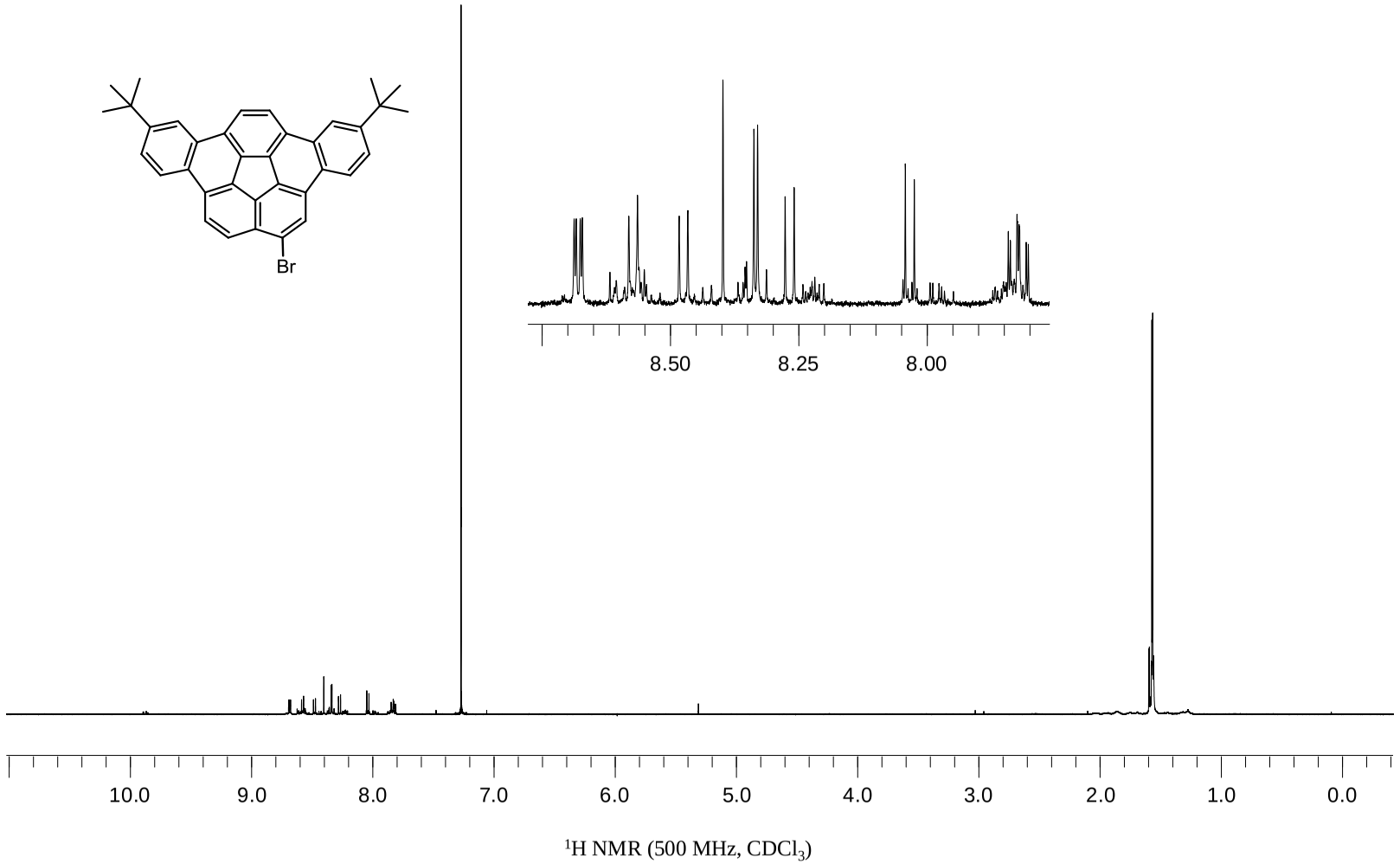

^{1}H NMR (500 MHz, $CDCl_3$)

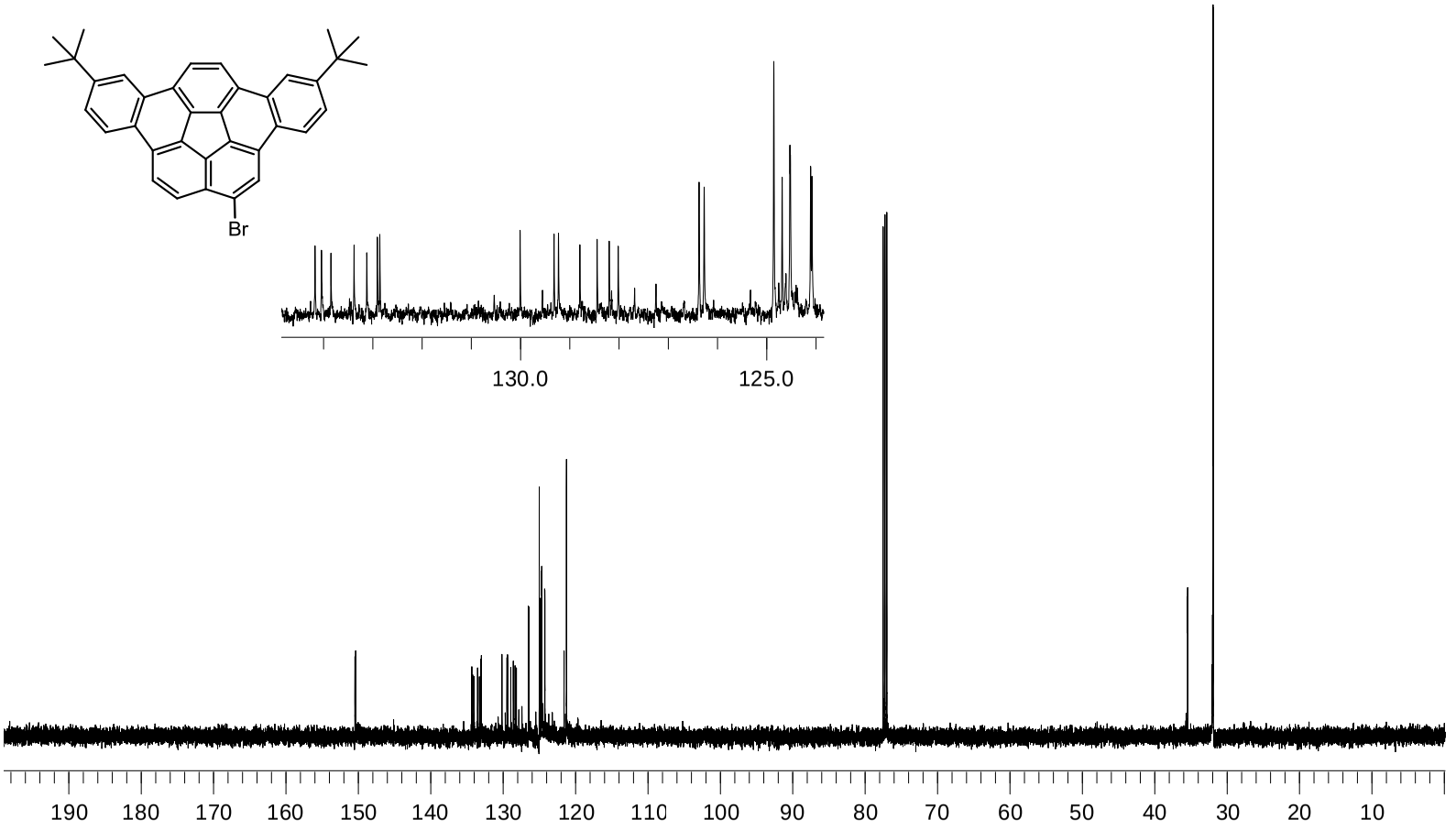

^{13}C NMR (125 MHz, $CDCl_3$)

3.12.23. 1,1′-Bi(5,10-di-*tert*-butyldibenzo[*a,g*]corannulenyl)

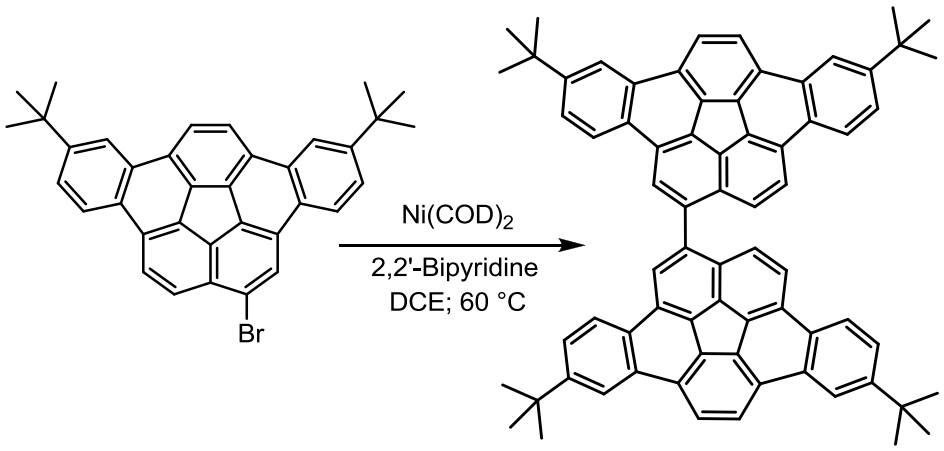

To a flame-dried, nitrogen purged Schlenk flask, equipped with a magnetic stir bar, was added 106 mg (0.196 mmol) of 1-bromo-5,10-di-*tert*-butyldibenzo[*a,g*]corannulene, 63.6 mg (0.236 mmol) of $Ni(COD)_2$, 37.6 mg (0.236 mmol) of 2,2′-bipyridine and 24.0 μL of 1,5-cyclooctadiene. Anhydrous dimethylformamide (0.80 mL) was added, and the reaction was placed in a pre-heated oil bath (60 ˚C) with stirring for 5 h. The reaction was cooled to room temperature and diluted with dichloromethane. The mixture was flushed through a short pad of silica gel with dichloromethane as the eluent and washed with water and 10% NaOH(aq). The organic extract was dried with magnesium sulfate and concentrated to dryness under reduced pressure. The crude product was washed with hot methanol to provide 67.0 mg (74%) of the desired product as a yellow solid. **MP:** >320 ˚C (dec.). **^{1}H NMR** (500 MHz, $CDCl_3$) δ(ppm): 8.78 (d, *J* = 2.0 Hz, 2H), 8.75 (d, *J* = 2.0 Hz, 2H), 8.65 (d, *J* = 8.5 Hz, 2H), 8.61 (s, 2H), 8.52 (d, *J* = 8.5 Hz, 2H), 8.48-8.44 (m, 6H), 8.08 (d, *J* = 8.5 Hz, 2H), 7.86-7.84 (m, 2H), 7.78 (dd, *J* = 8.5 Hz, 1.5 Hz, 2H), 1.59 (s, 18H), 1.57 (s, 18H). **^{13}C NMR** (125 MHz, $CDCl_3$) δ(ppm): 150.6, 150.4, 139.9,

135.7, 135.6, 135.5, 134.9, 134.4, 133.4, 133.2, 133.1, 130.7, 130.6, 130.1, 129.0, 128.9, 128.8, 127.9, 127.4, 125.8, 125.2, 125.1, 125.0, 124.9, 124.7, 124.5, 124.4, 124.0, 121.3.

HRMS (MALDI-TOF): Calc'd for $C_{72}H_{58}$ 922.4533, found 922.4553.

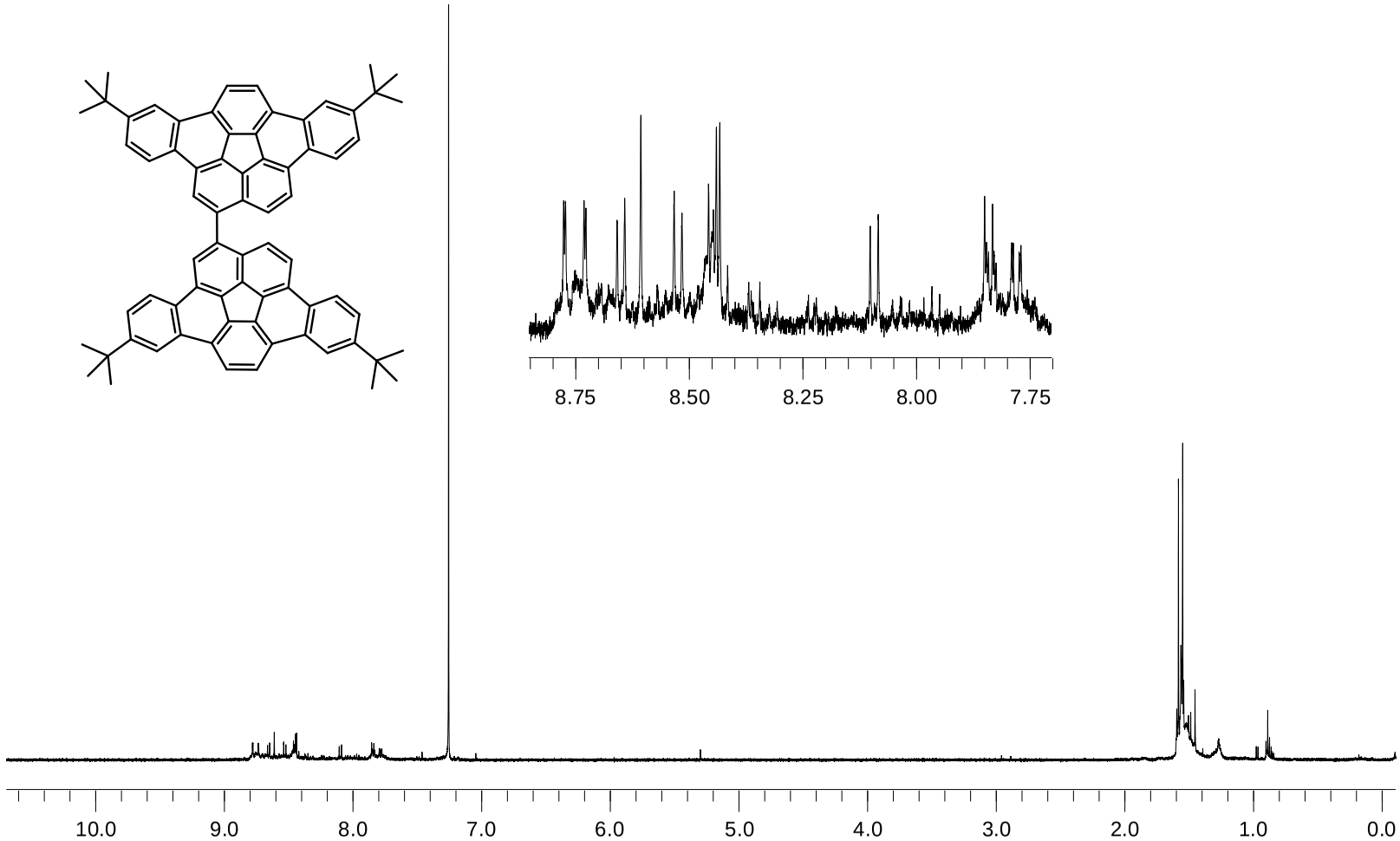

^{1}H NMR (500 MHz, $CDCl_3$)

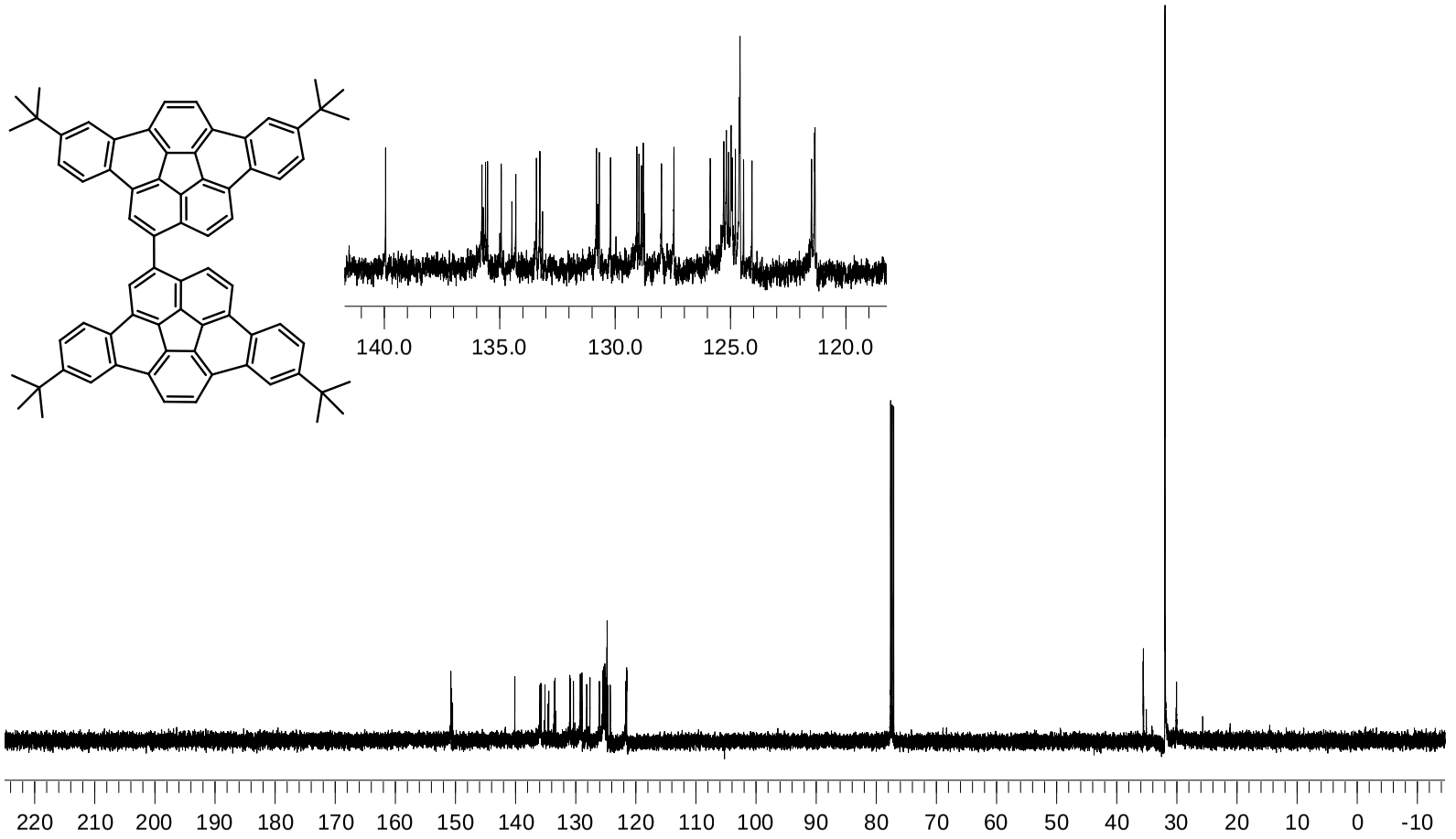

^{13}C NMR (125 MHz, $CDCl_3$)

3.12.24. Tetra-*tert*-butyl-*peri*-*bis*(dibenzo[*a,g*]corannulene)

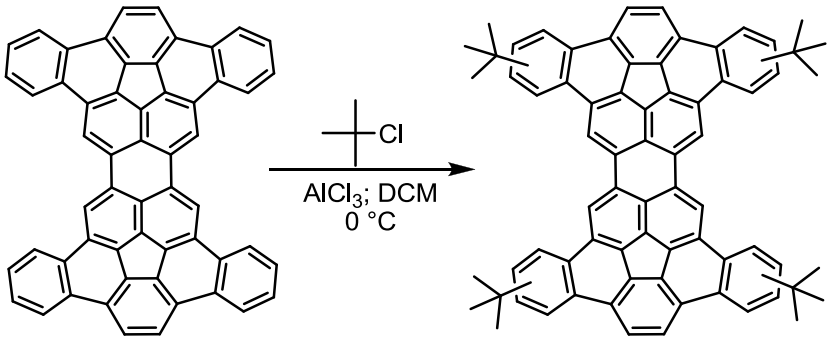

To a flame dried round bottom flask, equipped with a magnetic stir bar and purged with nitrogen, was added 3.65 g (17.9 mmol) aluminum chloride and 500 mg (0.718 mmol) *peri*-*bis*(dibenzo[*a,g*]corannulene). Anhydrous dichloromethane (50.0 mL) was added via syringe, and the mixture was stirred and cooled to 0 ˚C. To a separate flame dried, nitrogen purged round bottom flask was added 50 mL of *tert*-butyl chloride and 50.0 mL of anhydrous dichloromethane. The solution was transferred to the reaction mixture dropwise via syringe at 0 ˚C for 30 min. Upon complete addition of the *tert*-butyl chloride solution, the reaction mixture was gradually warmed to room temperature and stirred, with a nitrogen purge through a dichloromethane reservoir, for 24 h. The reaction mixture was quenched with ice cold water and extracted with dichloromethane. The organic layer was dried with magnesium sulfate, and the solvent was removed under reduced pressure. The resulting red oily material was flushed through a long alumina column with a solvent gradient of 100% hexanes to 2:1 hexanes: dichloromethane to 100% dichloromethane. Evaporation of solvent afforded 297 mg (45%) of the desired

product as a mixture of isomers as a red solid. **MP:** >250 ˚C (dec). **HRMS** (MALDI-TOF, DCTB): Calc'd for $C_{72}H_{56}$ (M^+) 920.4377, found 920.4382.

MALDI-TOF MS (DCTB Matrix)

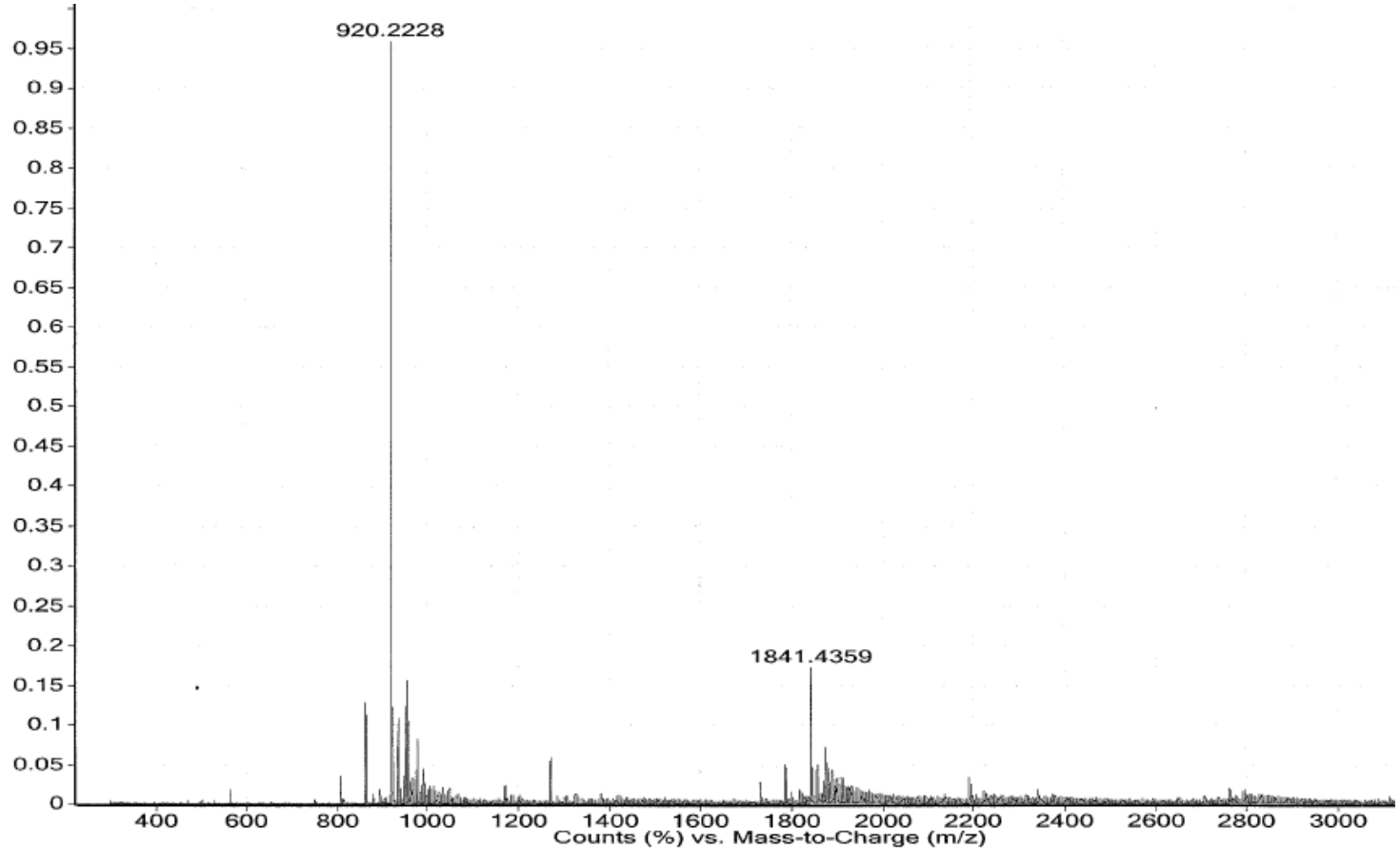

3.12.25. Tetra-*tert*-butyl-tetrabenzo[*a,g,o,u*]-7,8,15,16-tetrahydrocircum[5.6.5]quinarene-7,8,15,16-tetracarboxylic acid 7,8:15,16-*bis*(*N*-methylimide)

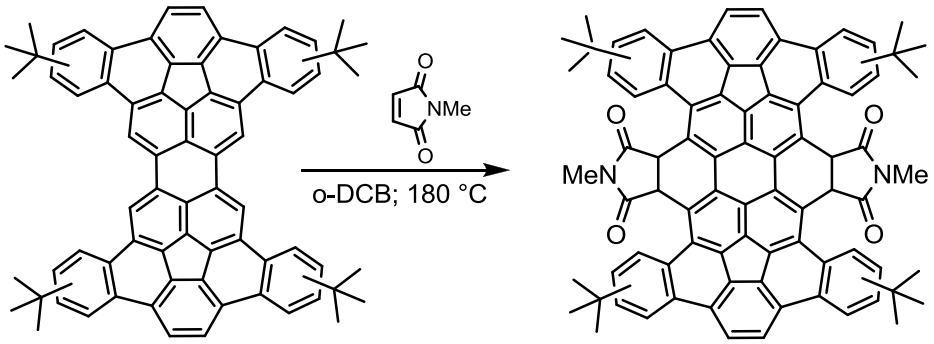

To a flame-dried, nitrogen purged pressure vessel, equipped with a magnetic stir bar, was added 242 mg (0.263 mmol) of tetra-*tert*-butyl-*peri*-*bis*(dibenzo[*a,g*]corannulene) and 361 mg (3.25 mmol) of *N*-methylmaleimide. Anhydrous *o*-dichlorobenzene (8.00 mL) was added to the reaction mixture, and the mixture was stirred. The vessel was capped and placed in a pre-heated oil bath (180 ˚C) for 5 d. The reaction mixture was cooled to room temperature, and the solvent was removed under reduced pressure. The resulting red solid was washed with hot hexanes and dried under vacuum to provide 205 mg (85%) of a bright red solid. **MP:** >280 ˚C (dec). **UV-Vis** (CH_2Cl_2) λ_{max} (ε, $cm^{-1}M^{-1}$): 284 (69131), 358 (sh, 22317), 498 (7240), 532 (6521). **HRMS** (MALDI-TOF, DCTB): Calc'd for $C_{82}H_{62}N_2O_4$ (M^+) 1138.4709, found 1138.4704.

MALDI-TOF MS (DCTB Matrix)

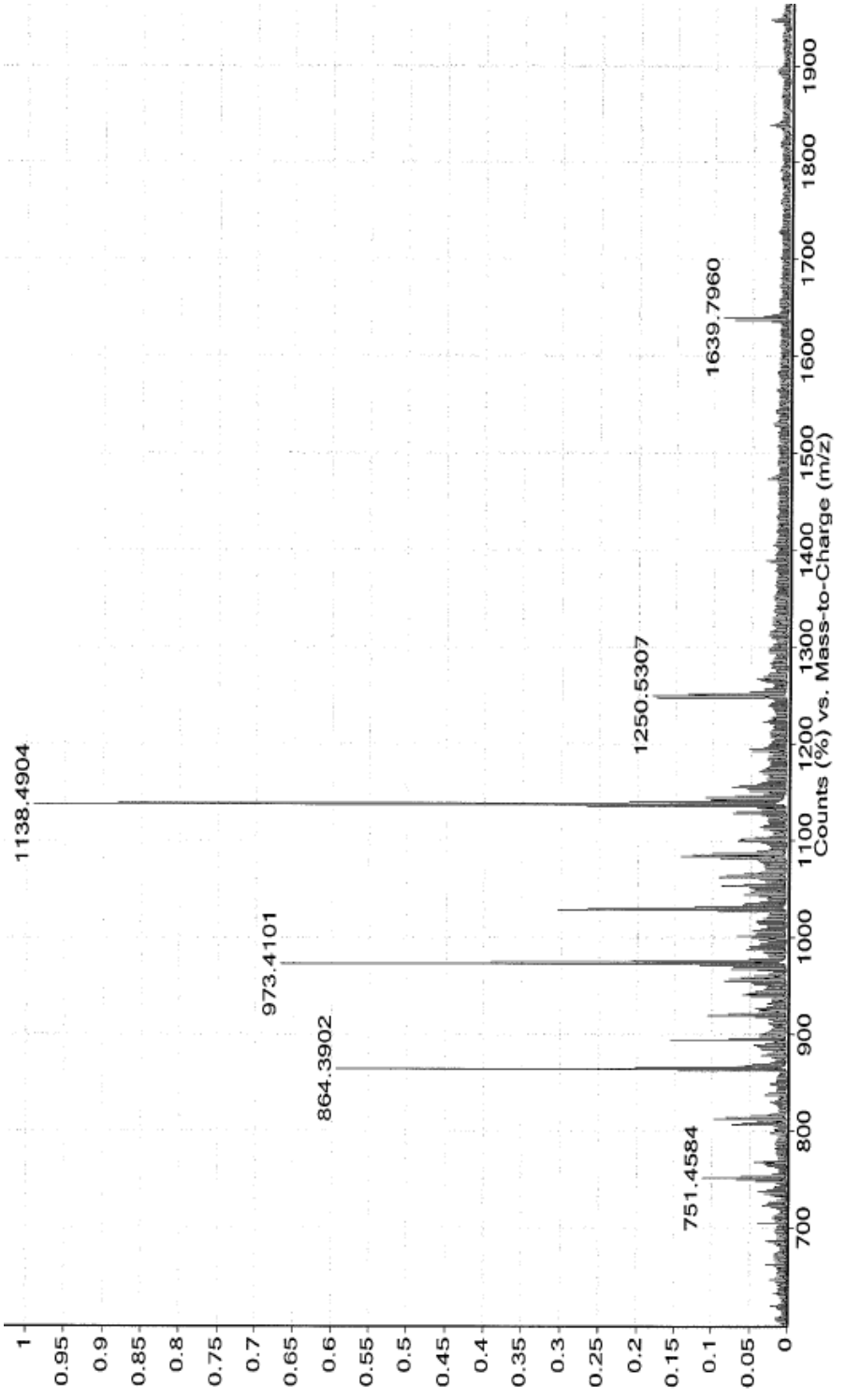

UV Spectrum of
Tetra-*tert*-butyl-tetrabenzo[*a,g,o,u*]-7,8,15,16-tetrahydrocircum[5.6.5]quinarene-7,8,15,16-tetracarboxylic acid 7,8:15,16-*bis*(*N*-methylimide)

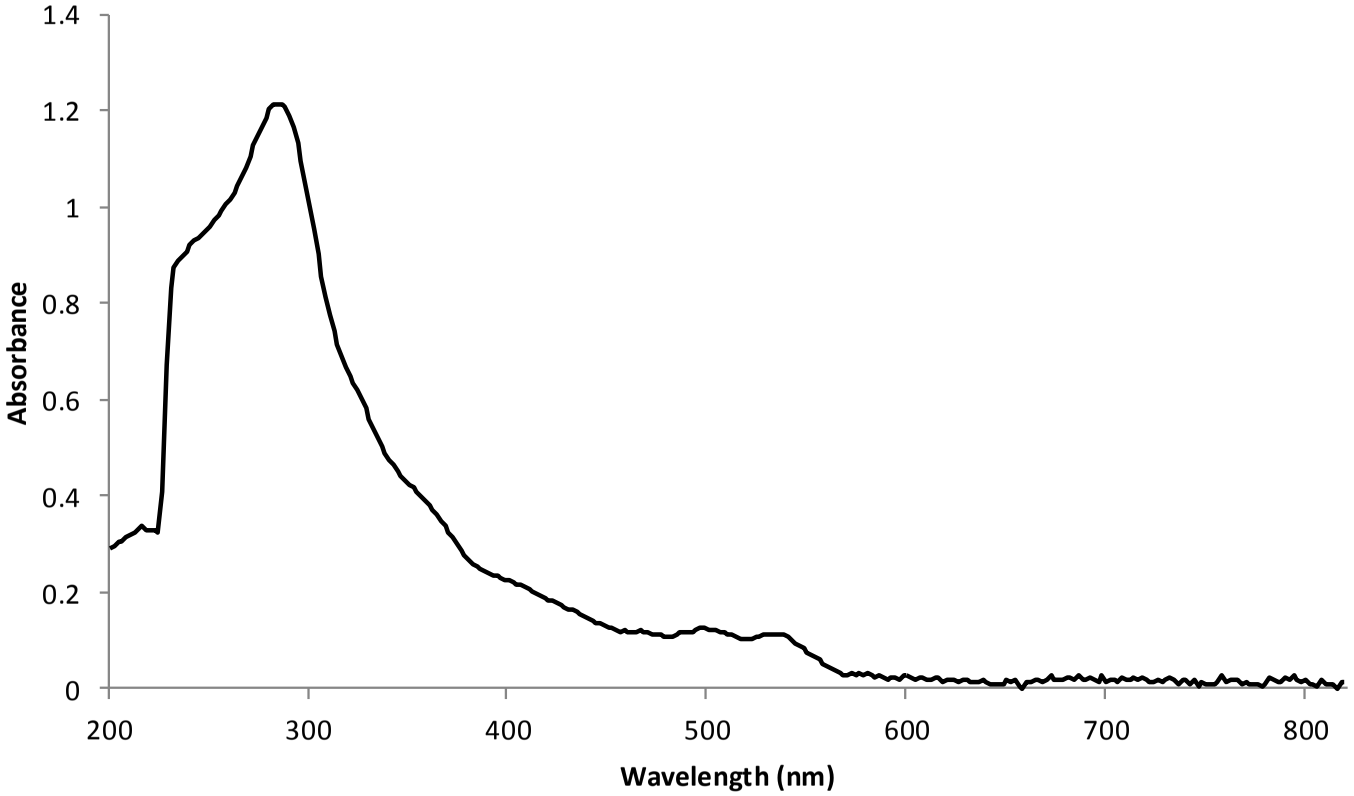

3.12.26. Tetra-*tert*-butyl-tetrabenzo[*a,g,o,u*]circum[5.6.5]quinarene-7,8,15,16-tetracarboxylic anhydride

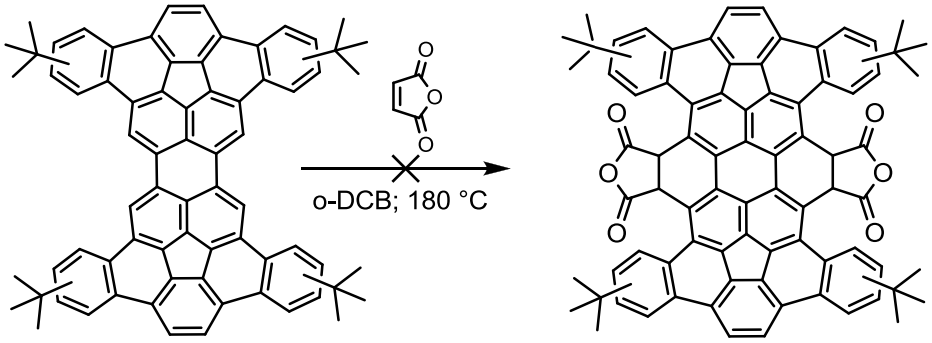

To a flame-dried, nitrogen purged pressure vessel, equipped with a magnetic stir bar, was added 50 mg (0.0718 mmol) of tetra-*tert*-butyl-*peri*-*bis*(dibenzo[*a,g*]corannulene) and 140 mg (1.44 mmol) of maleic anhydride. Anhydrous *o*-dichlorobenzene (1.00 mL) was added to the reaction mixture, and the mixture was stirred. The vessel was capped and placed in a pre-heated oil bath (180 ˚C) for 5 d. The reaction mixture was cooled to room temperature, and the solvent was removed under reduced pressure. The resulting red solid was washed with hot hexanes and dried under vacuum. Only starting material was recovered, which was confirmed by MALDI-TOF mass spectrometry.

3.12.27. Tetra-*tert*-butyl-tetrabenzo[*a,g,o,u*]circum[5.6.5]quinarene-7,8,15,16-tetracarboxylic acid 7,8:15,16-*bis*(*N*-methylimide)

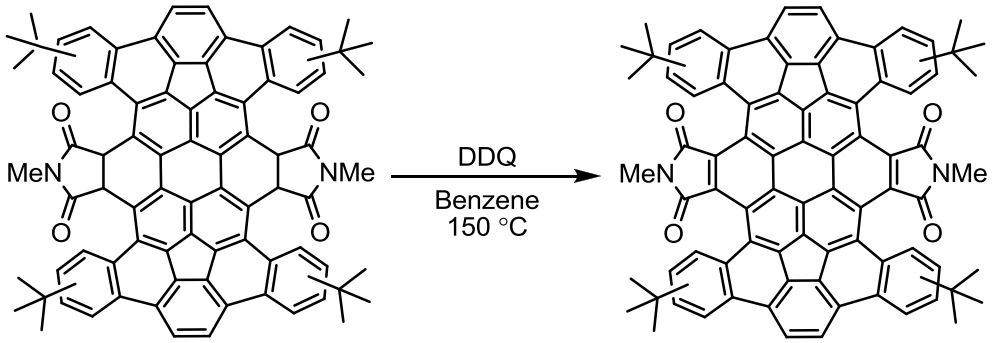

To a flame-dried, nitrogen purged pressure vessel, equipped with a magnetic stir bar, was added 222 mg (0.195 mmol) of tetra-*tert*-butyl-tetrabenzo[*a,g,o,u*]-7,8,15,16-tetrahydrocircum[5.6.5]quinarene-7,8,15,16-tetracarboxylic acid 7,8:15,16-*bis*(*N*-methylimide) and 1.11 g (4.87 mmol) of 2,3-dichloro-5,6-dicyano-1,4-benzoquinone. Anhydrous benzene (5.00 mL) was added, and the vessel was sealed. The vessel was placed in a pre-heated oil bath (150 ˚C) for 15 h. The reaction mixture was cooled to room temperature and quenched with saturated sodium bicarbonate (100 mL). The mixture was extracted with dichloromethane and water twice. The organic extracts were dried with magnesium sulfate, and solvent was removed under reduced pressure to provide 199 mg (90%) of a bright red solid. **MP:** >280 ˚C (dec). **UV-Vis** (CH_2Cl_2) λ_{max} (ε, $cm^{-1}M^{-1}$): 246 (17017), 284 (17050), 352 (8862), 430 (7024), 498 (1634), 540 (2377). **HRMS** (MALDI-TOF, DCTB): Calc'd for $C_{82}H_{58}N_2O_4$ (M^+) 1134.4331, found 1134.4339.

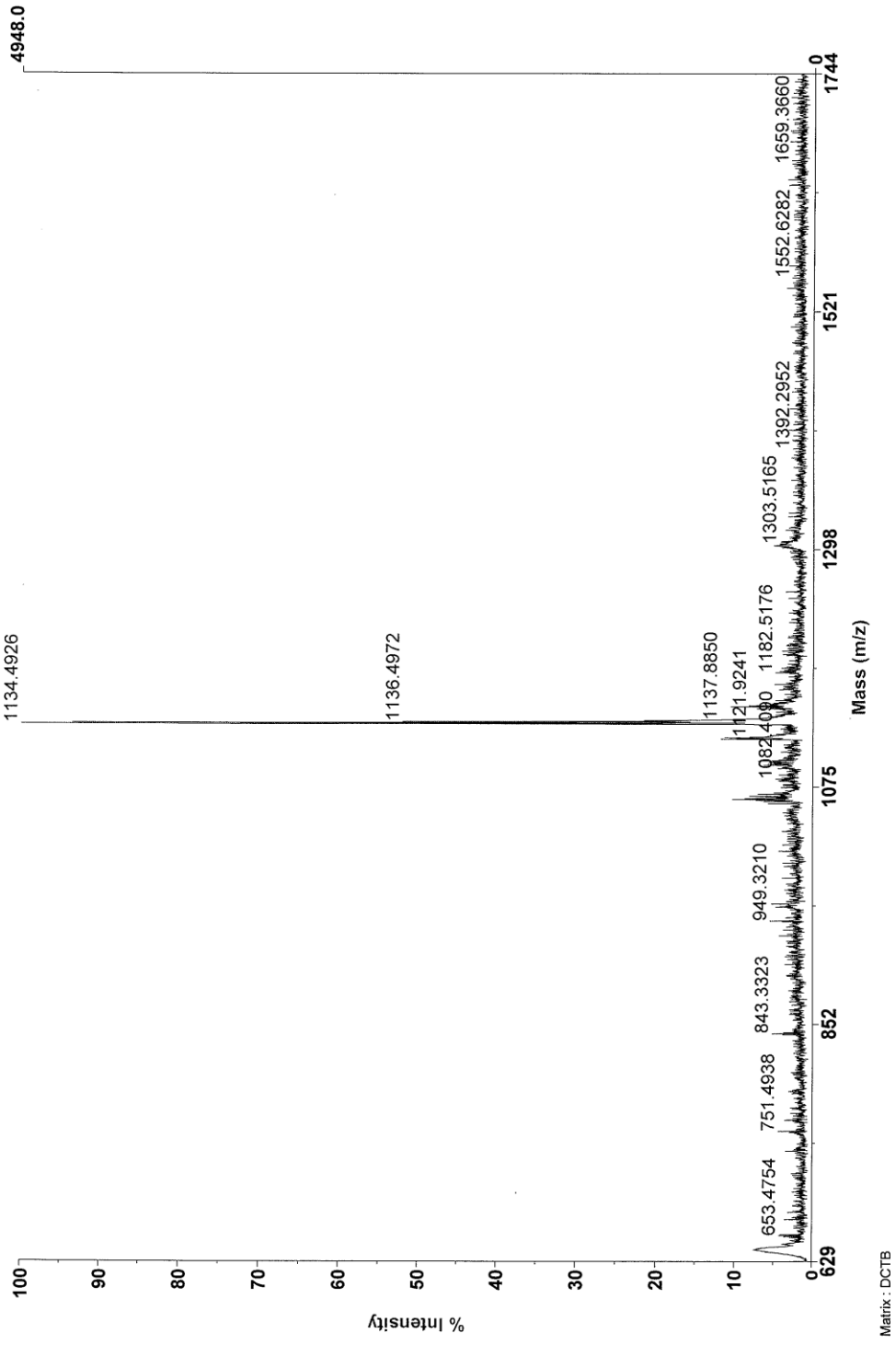
4948.0
1134.4926
1136.4972
1137.8850
1121.9241
1182.5176
1303.5165
1392.2952
1552.6282
1659.3660
1082.4080
949.3210
843.3323
751.4938
653.4754
100
90
80
70
60
50
40
30
20
10
0
629
852
1075
1298
1521
1744
Mass (m/z)
% Intensity
Matrix : DCTB

UV Spectrum of
Tetra-*tert*-butyl-tetrabenzo[*a*,*g*,*o*,*u*]circum[5.6.5]quinarene-7,8,15,16-tetracarboxylic acid 7,8:15,16-*bis*(*N*-methylimide)

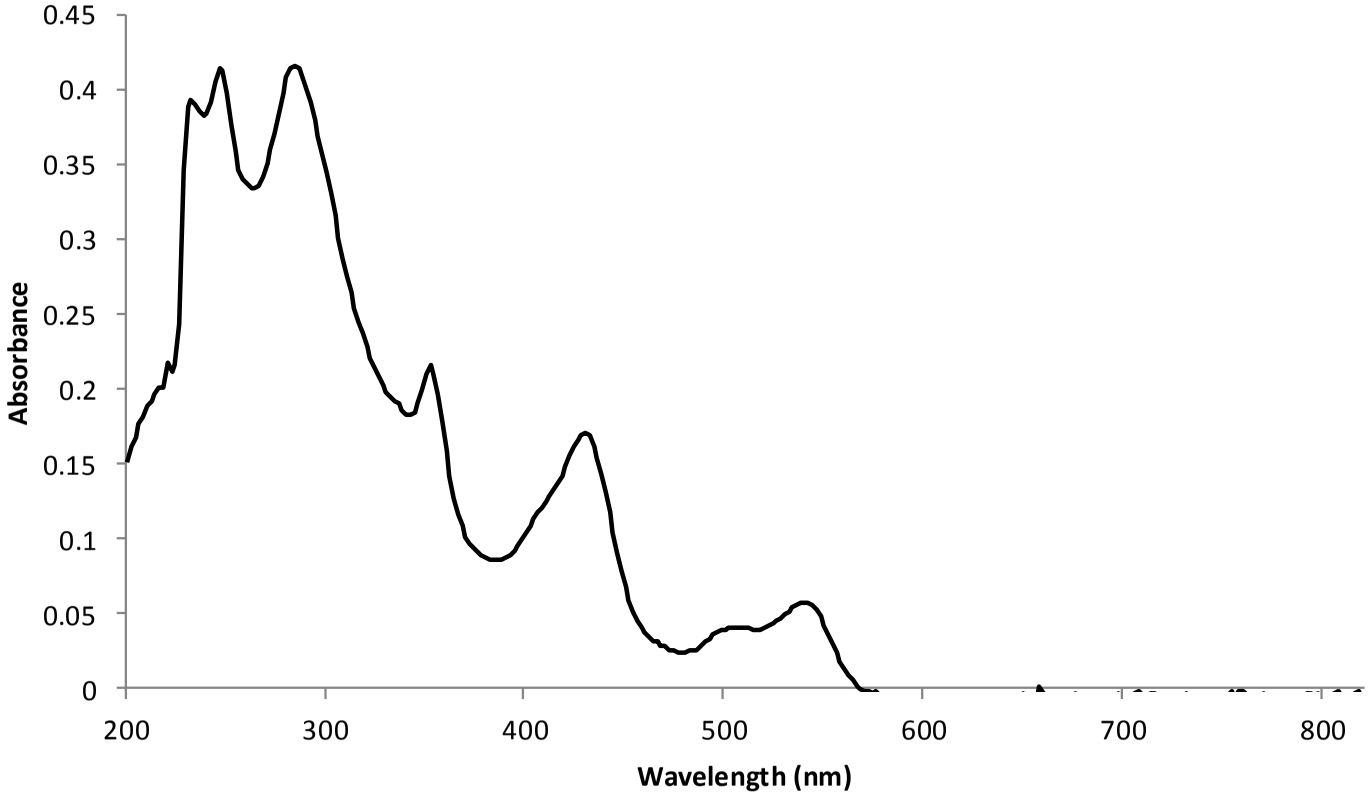

3.12.28. 2-(2,4,4-Trimethylpentan-2-yl)isoindoline-1,3-dione

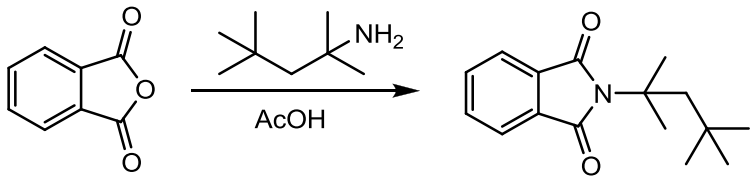

To a flame-dried round bottom flask purged with nitrogen, equipped with a magnetic stir bar, was added 5.00 g (33.8 mmol) of phthalic anhydride and 25.0 mL of glacial acetic acid. The mixture was stirred and 6.54 g (50.7 mmol) *tert*-octylamine was added dropwise. The reaction mixture was stirred and heated to reflux overnight. The reaction mixture was cooled to room temperature and poured into ice water. The mixture was extracted with dichloromethane, and the organic extracts were dried with magnesium sulfate. Solvent was evaporated under reduced pressure, and the crude oil was flushed through a short pad of alumina with 1:1 dichloromethane: hexanes as the eluent to afford 4.12 g (47%) as a white solid. **Mp**: 54-57 ˚C. **^{1}H NMR** (500 MHz, $CDCl_3$) δ(ppm): 7.74 (AA′ of AA′XX′, 2H), 7.65 (XX′ of AA′XX′, 2H), 1.99 (s, 2H), 1.75 (s, 6H), 0.910 (s, 9H). **^{13}C NMR** (125 MHz, DMSO) δ(ppm): 170.0, 134.9, 131.8, 123.1, 60.8, 50.7, 31.8, 31.2, 30.1. **IR** (KBr, cm^{-1}) 1708 (C=O). **HRMS** (DART-TOF): Calc'd for $C_{16}H_{22}NO_2$ $(M+1)^+$ 260.1650, found 260.1640.

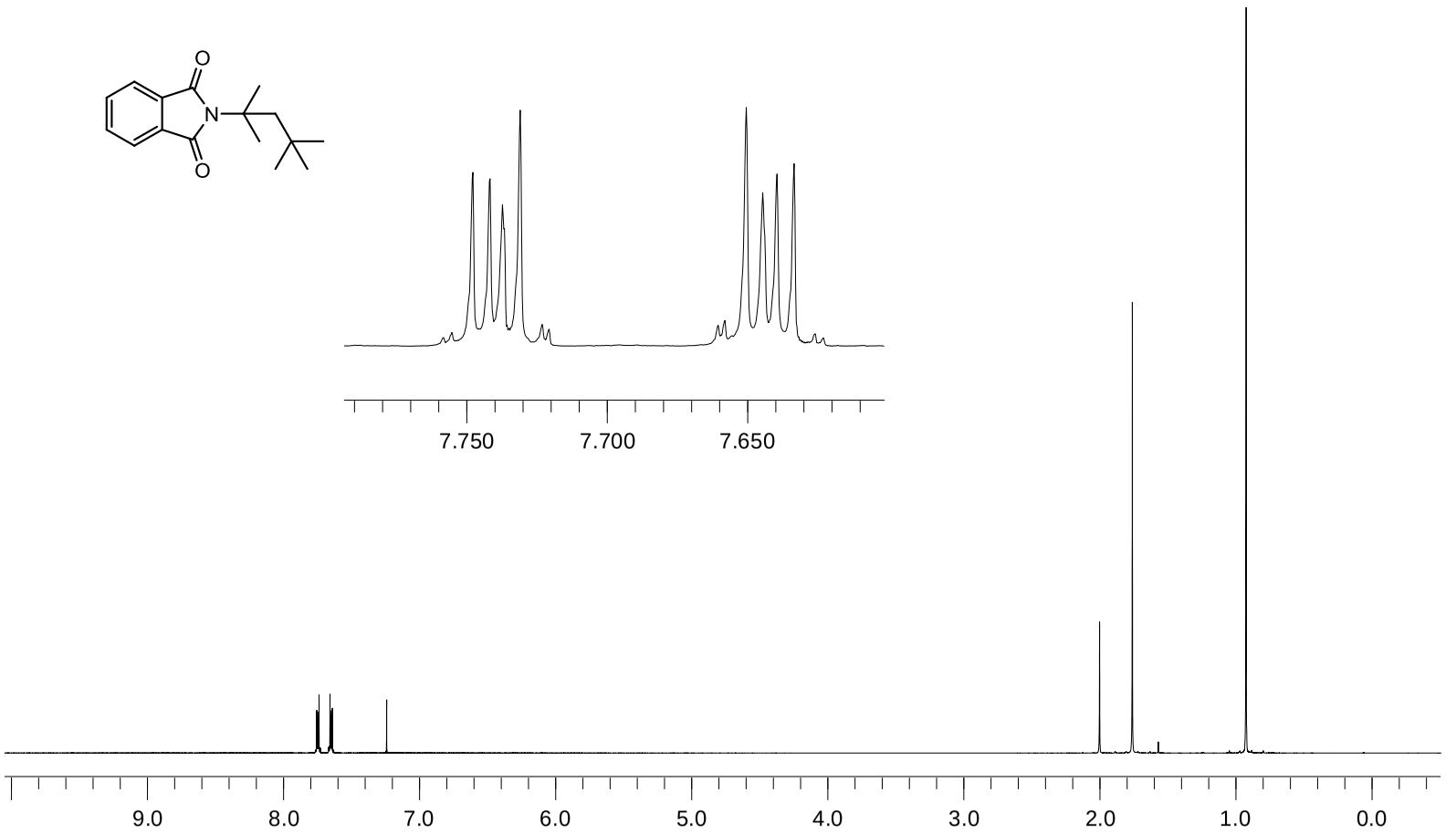

^{1}H NMR (500 MHz, $CDCl_3$)

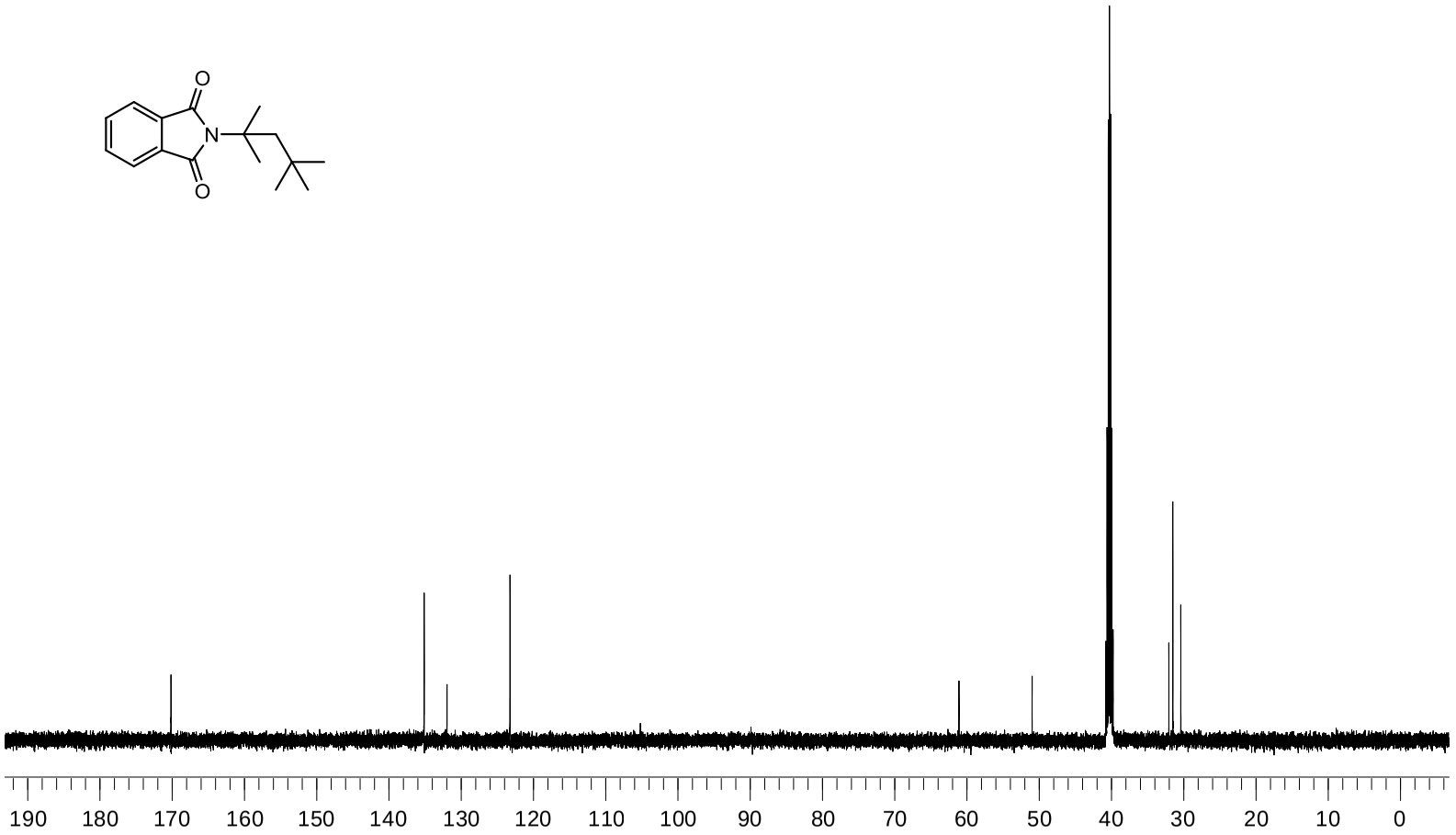

^{13}C NMR (125 MHz, DMSO)

3.12.29. Phthalic anhydride

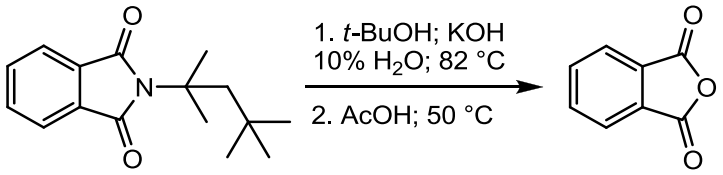

To a round bottom flask equipped with a reflux condenser and magnetic stir bar was added 100 mg (0.386 mmol) of 2-(2,4,4-trimethylpentan-2-yl)isoindoline-1,3-dione and 12.9 mL of *tert*-butanol. KOH (2.16 g, 0.0386 mol) and 1.29 mL of water were added to the mixture and stirred. The mixture was heated to reflux for 3 h. The mixture was then cooled to 50 ˚C, and 40 mL of glacial acetic acid was added. The solution was stirred at 50 ˚C for 30 min, then cooled to room temperature and diluted in water. The solution was extracted with dichloromethane and dried over magnesium sulfate. Solvent was removed under reduced pressure to provide 56 mg (98%) of the desired product as a white solid. Spectra matched those reported in the literature.[13]

3.12.30. Tetra-*tert*-butyl-tetrabenzo[*a,g,o,u*]circum[5.6.5]quinarene-7,8,15,16-tetracarboxylic anhydride

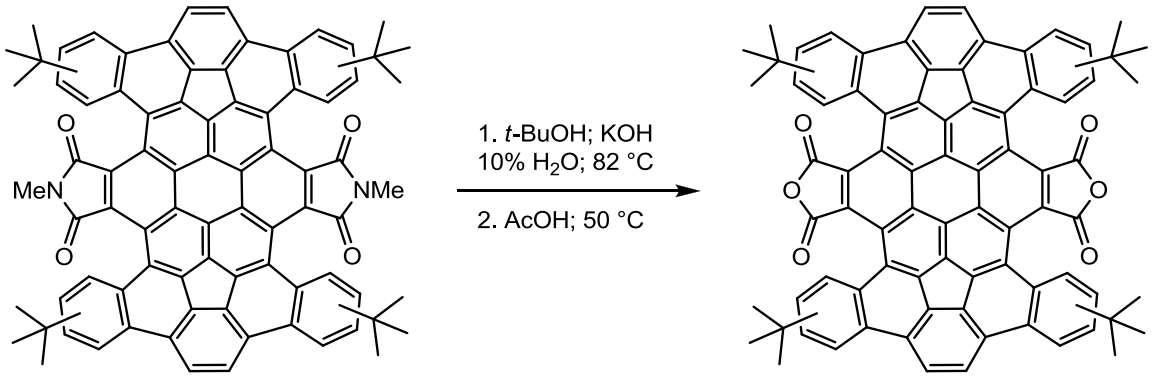

To a round bottom flask equipped with a reflux condenser and magnetic stir bar, was added 151 mg (0.133 mmol) tetra-*tert*-butyl-tetrabenzo[*a,g,o,u*]circum[5.6.5]quinarene-7,8,15,16-tetracarboxylic acid 7,8:15,16-*bis*(*N*-methylimide) and 4.50 mL of *tert*-butanol. Potassium hydroxide (1.48 g, 0.0266 mol) and 0.45 mL of water were added to the mixture and stirred. The mixture was heated to reflux for 2 d. The mixture was cooled to 50 ˚C, and 40 mL of acetic acid was added. The solution was stirred for 1 h, then cooled to room temperature and diluted in water. The solution was then extracted with dichloromethane and dried over magnesium sulfate. Solvent was removed under reduced pressure to provide 144 mg (98%) of the desired product as a red solid. **MP:** >300 ˚C (dec.). **UV-Vis** (CH_2Cl_2) λ_{max} (ε, $cm^{-1}M^{-1}$): 288 (16307), 354 (7279), 430 (5003), 498 (1742), 536 (2016). **HRMS** (MALDI-TOF, DCTB): Calc'd for $C_{80}H_{52}O_6$ M^+ 1108.3764, found 1108.3812.

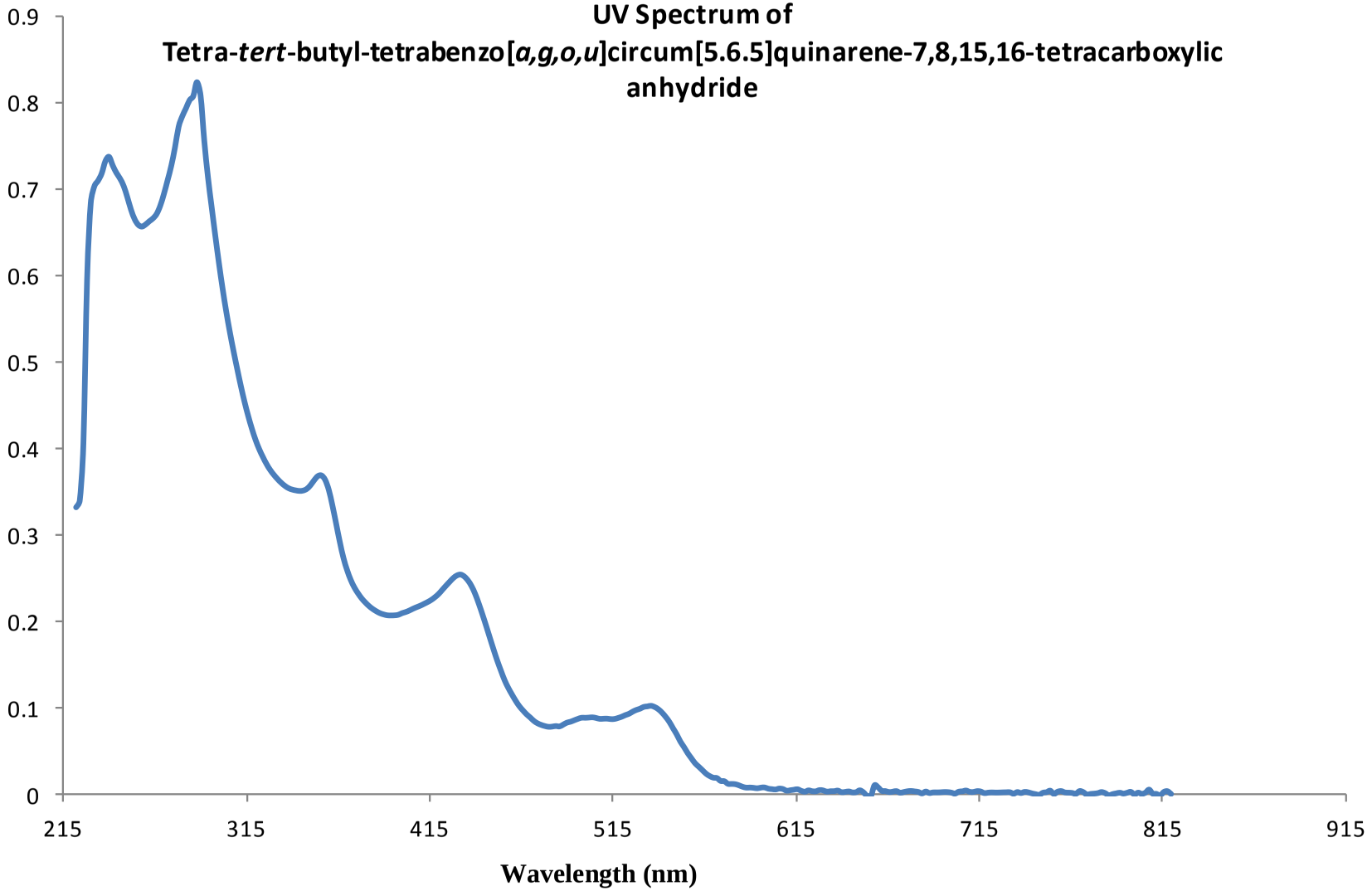
UV Spectrum of
Tetra-tert-butyl-tetrabenzo[a,g,o,u]circum[5.6.5]quinarene-7,8,15,16-tetracarboxylic anhydride
0.9
0.8
0.7
0.6
0.5
0.4
0.3
0.2
0.1
0
215
315
415
515
615
715
815
915
Wavelength (nm)

MALDI-TOF MS (DCTB Matrix)

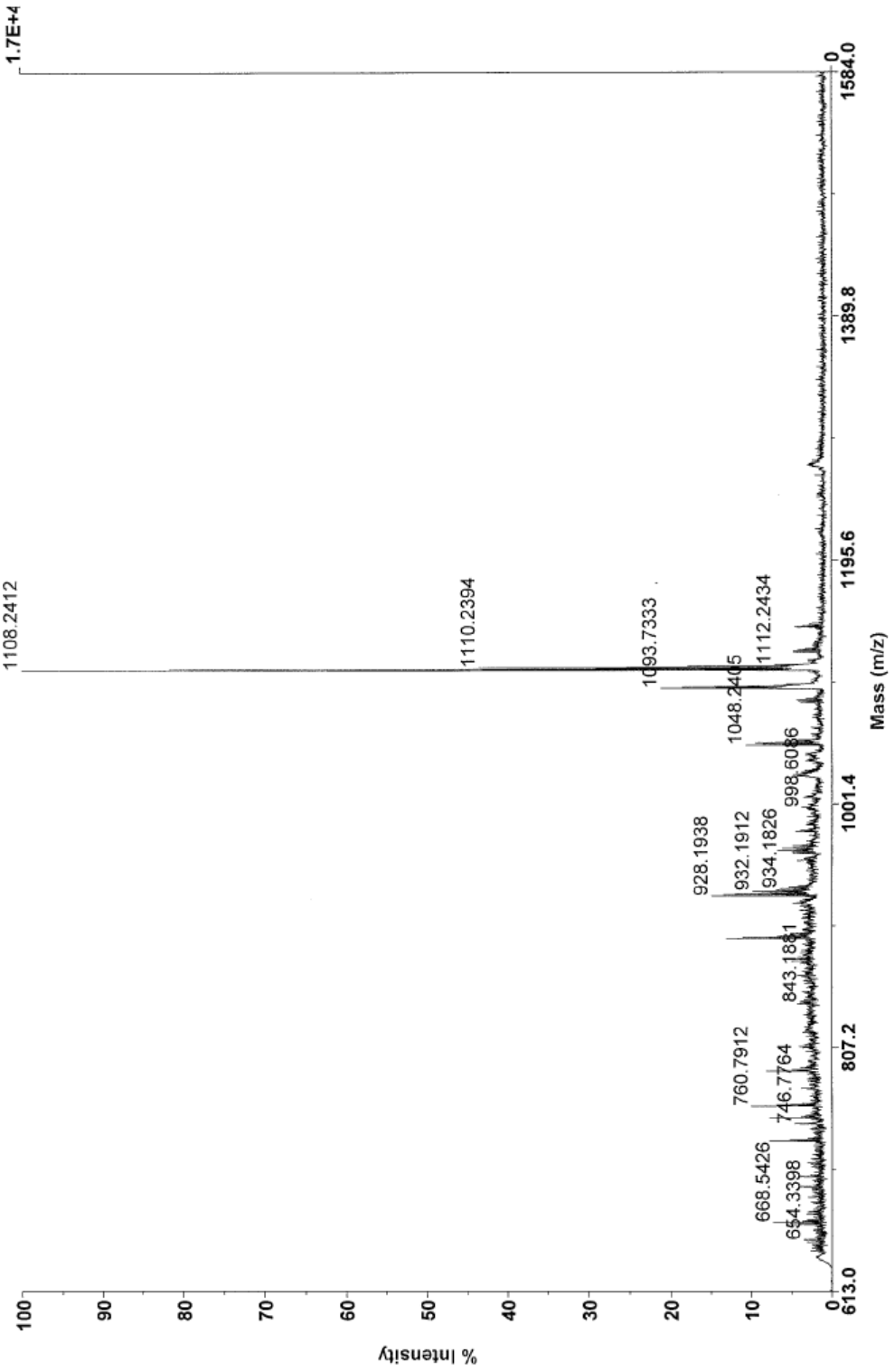

3.12.31. Dibenzo[*a,g*]corannulene

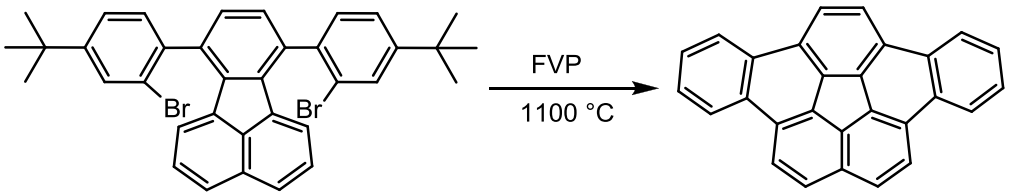

7,10-*Bis*(2-bromo-4-*tert*-butylphenyl)fluoranthene (50.0 mg, 0.0806 mmol) was suspended on quartz sand and placed in two oven-dried quartz boats. The boats were placed in a quartz tube with a steady stream of nitrogen carrier gas. The tube was placed in a pyrolysis set up as previously described. The material was sublimed and pyrolyzed at 1100 ˚C with a sublimation temperature ranging from 75-175 ˚C. The system pressure was maintained at 0.50 torr for the duration of the experiment. At the conclusion of the experiment, the system was cooled to room temperature, and the crude pyrolysates were extracted from the tube and trap with distilled dichloromethane. The solvent was removed under reduced pressure to provide a crude brown solid. The crude material was flushed through a short pad of neutral alumina with dichloromethane as the eluent, affording 8.4 mg (30%) of dibenzo[*a,g*]corannulene, with the *tert*-butyl groups gone, as a tan solid.

3.12.32. $C_{60}H_{12}$ (FVP of Tetra-*tert*-butyl-tetrabenzo[*a,g,o,u*]circum[5.6.5]quinarene-7,8,15,16-tetracarboxylic anhydride)

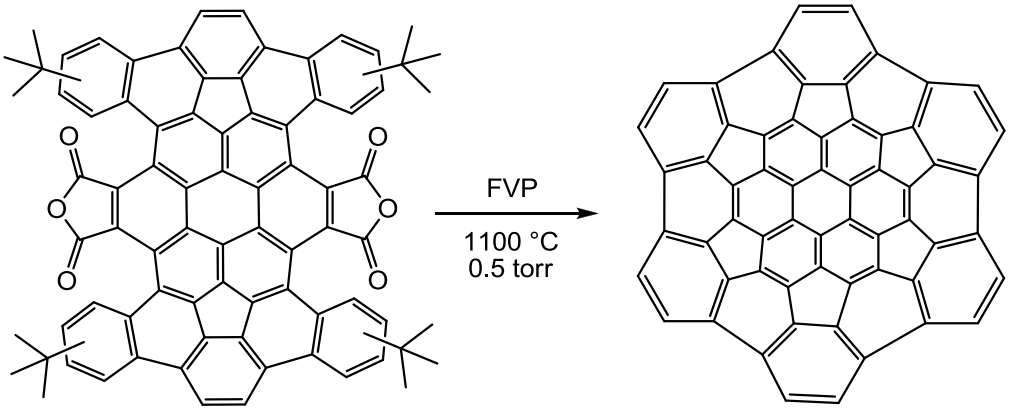

Flash vacuum pyrolysis was performed on 150 mg (0.0135 mmol) of tetra-*tert*-butyl-tetrabenzo[*a,g,o,u*]circum[5.6.5]quinarene-7,8,15,16-tetracarboxylic anhydride at 1100 ˚C and 0.50 torr.[††] The starting material was absorbed directly onto quartz sand and placed in two quartz boats. The boats were placed inside a quartz tube, and a strong magnetic bar was used to push the boats into the center of the sublimation oven. The hot zone was then heated to 1100 ˚C, and the sample was quickly pushed into the hot zone, with a slow flow of high purity nitrogen gas, to carry the material through the oven.[‡‡] An orange material was collected at the end of the tube and in the liquid nitrogen cooled trap over the course of a few minutes. Upon complete sublimation of the starting material, the apparatus was cooled, and the liquid nitrogen traps were removed. The system was closed off from the vacuum pump and allowed to equilibrate and warm prior to opening the entire system to the atmosphere. The crude product, 13 mg, was removed from the tube and trap with dichloromethane. A small amount of charred material was recovered and

[††] A detailed description of the FVP apparatus can be found in Chapter 3.
[‡‡] Sublimation of the starting material was not possible, even at elevated temperatures (600 ˚C). The material sublimed readily and cleanly when subjected directly to the hot zone at 1100 ˚C.

filtered away from the soluble materials, which were subsequently concentrated to dryness. The crude orange material was determined to contain a significant amount of the byproduct, *p*-terphenyl, which could not be removed from the crude mixture. This byproduct was identified by ^{1}H NMR and GCMS. **HRMS** (MALDI-TOF, DCTB): Calc'd for $C_{60}H_{12}$ 732.0934, found 732.0953. **UV-Vis** (CH_2Cl_2) λ_{max} (cm^{-1}, for crude mixture): 234, 280, 336, 426, 520. **UV-Vis** (CH_2Cl_2) λ_{max} (cm^{-1}, for crude mixture with *p*-terphenyl blank): 240, 320, 338, 426, 520. **UV-Vis** (CH_2Cl_2) λ_{max} (cm^{-1}, *p*-terphenyl): 280.

MALDI-TOF (DCTB)

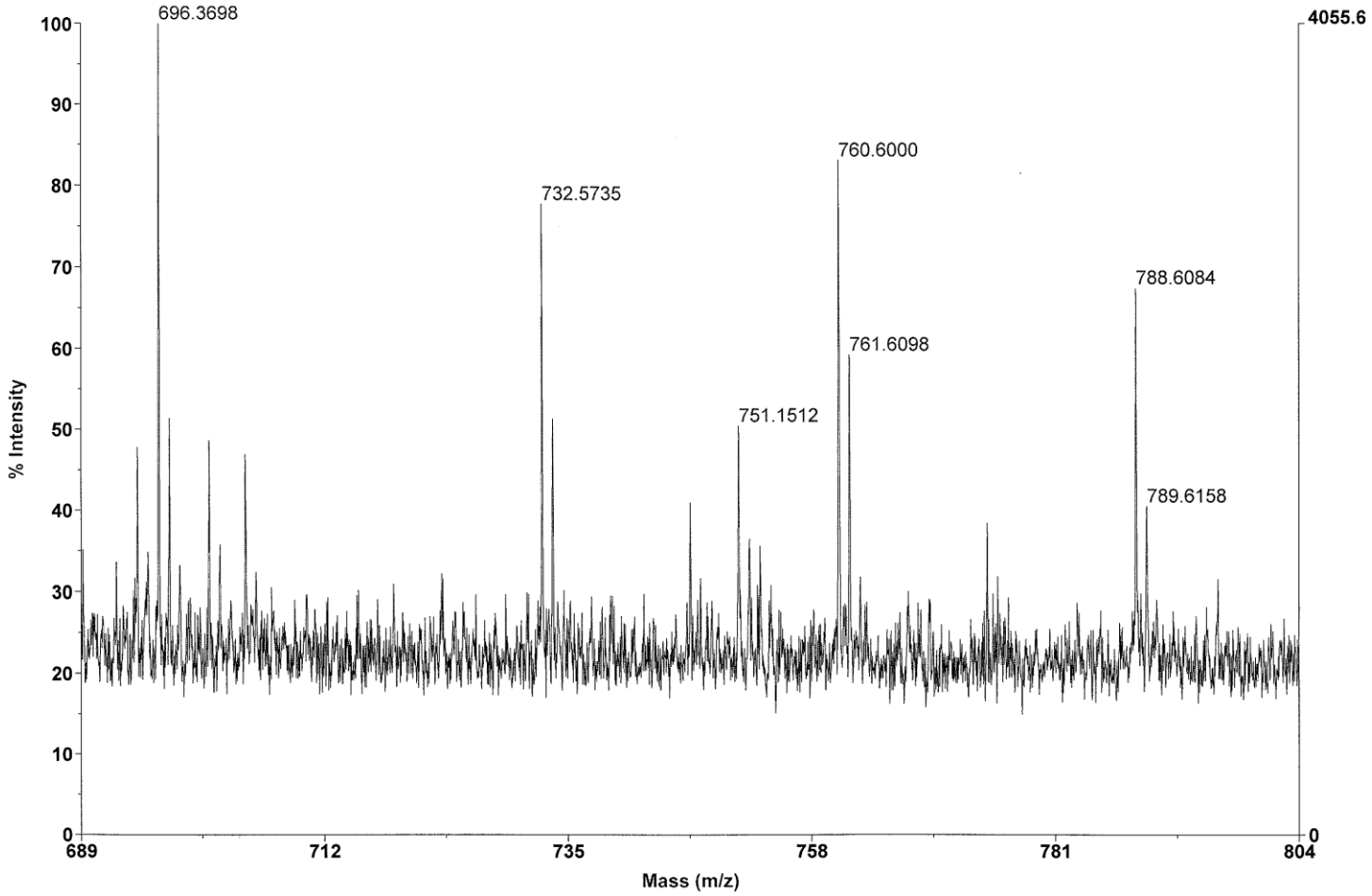

MALDI-TOF Mass Spectrum of CH_2Cl_2-soluble Products from FVP of Tetra-*tert*-butyl-tetrabenzo[*a,g,o,u*]circum[5.6.5]quinarene-7,8,15,16-tetracarboxylic anhydride

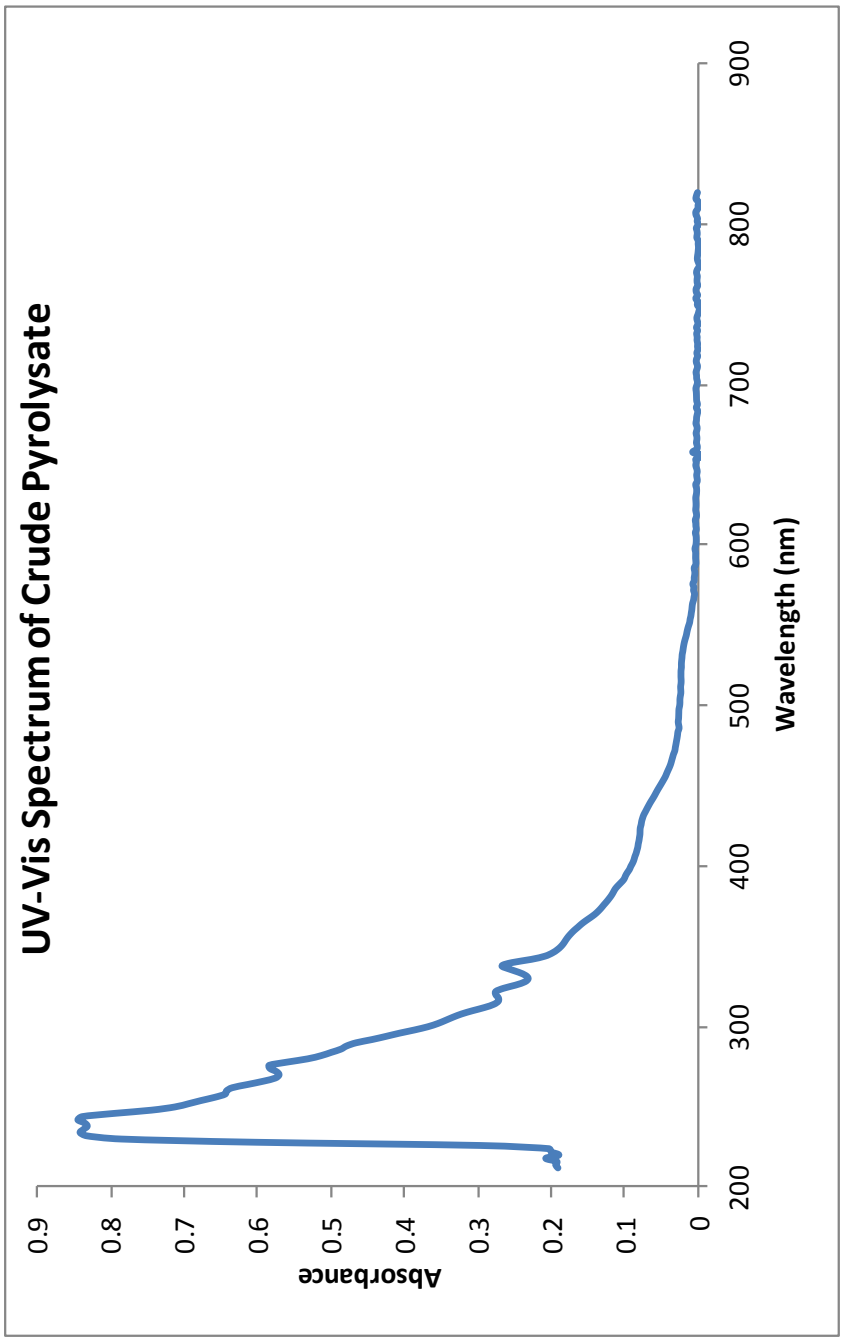
UV-Vis Spectrum of Crude Pyrolysate
Absorbance
0.9
0.8
0.7
0.6
0.5
0.4
0.3
0.2
0.1
0
200
300
400
500
600
700
800
900
Wavelength (nm)

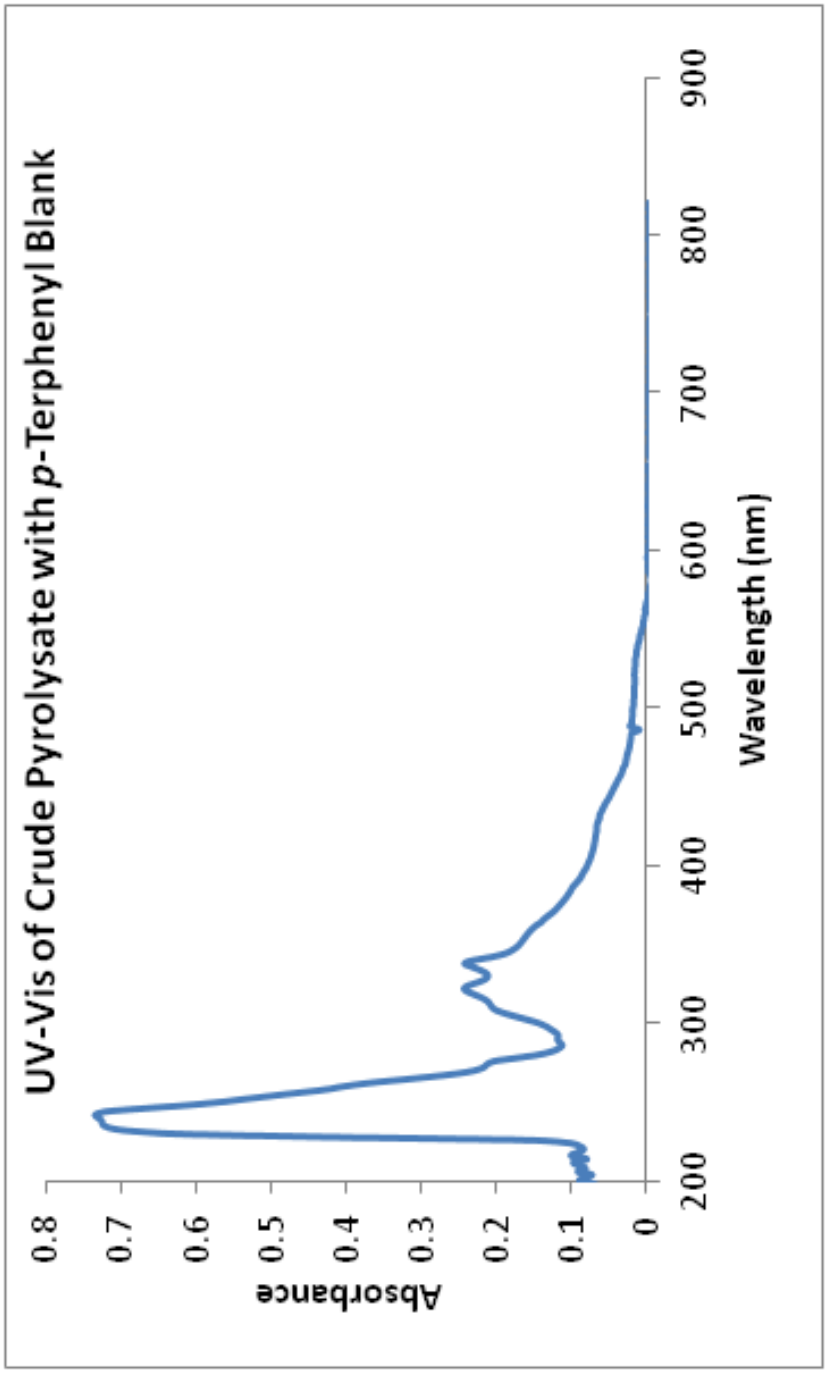
UV-Vis of Crude Pyrolysate with p-Terphenyl Blank
Absorbance
0.8
0.7
0.6
0.5
0.4
0.3
0.2
0.1
0
200
300
400
500
600
700
800
900
Wavelength (nm)

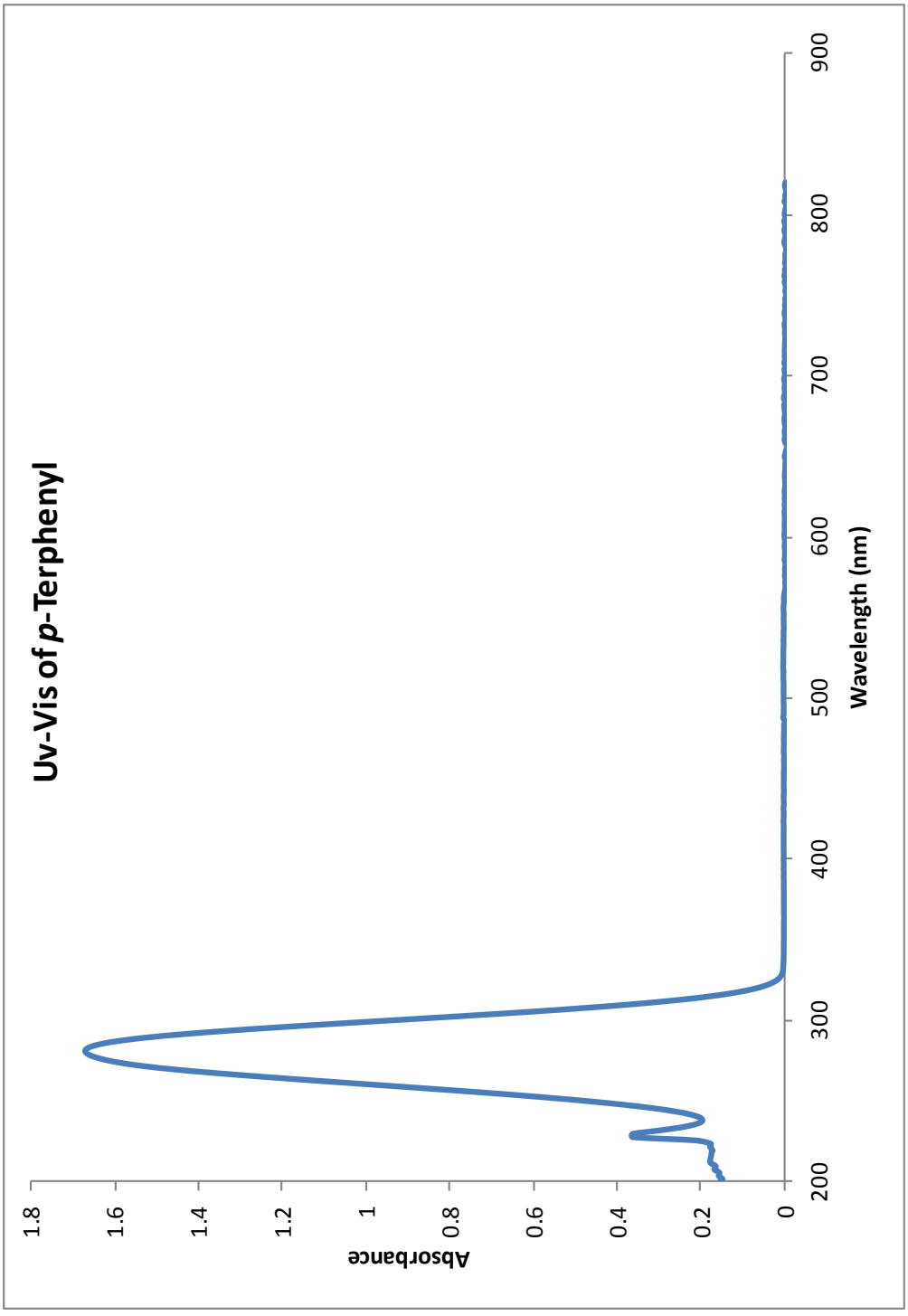
Uv-Vis of p-Terphenyl
Absorbance
1.8
1.6
1.4
1.2
1
0.8
0.6
0.4
0.2
0
200
300
400
500
600
700
800
900
Wavelength (nm)

3.13 References

[1] (a) Koch, K. H.; Fahnenstich, U.; Baumgarten, M.; Müllen, K. *Synthetic Metals* **1991**, *41-43*, 1619-1622. (b) Bohnen, V.; Koch, K.; Lüttke, W.; Müllen, K. *Angew. Chem.* **1990**, 102, 548-550. (c) Pradhan, A.; Dechambenoit, P.; Bock, H.; Durola, F. *Angew. Chem. Int. Ed*. **2011**, *50*, 12582 –12585.

[2] Reisch, H. A.; Bratcher, M. S.; Scott, L. T. *Org. Lett.* **2000**, *2*, 1427-1430

[3] (a) Sun, H.; Gorelsky, S. I.; Stuart, D. R.; Campeau,L.; Fagnou, K. *J. Org. Chem.* **2010**, *75*, 8180–8189. (b) Garca-Cuadrado, D.; Mendoza, P.; Braga, A. A. C.; Maseras, F.; Echavarren, A. M. *J. Am. Chem. Soc.* **2007**, *129*, 6880-6886.

[4] Larsen, C. H.; Anderson, K. W.; Tundel, R. E.; Buchwald, S. L. *Synlett* **2006**, *18*, 2941-2946.

[5] Liégault, B.; Lapointe, D.; Caron, L.; Vlassova, A.; Fagnou, K. *J. Org. Chem.* **2009**, *74*, 1826–1834.

[6] (a) Sharp, P. R. *J. Organomet. Chem.* **2003**, *683*, 288-294. (b) Begum, R.; James, A. J.; Sharp, P. R. *Organometallics* **2005**, *24*, 2670 – 2678. (c) Singh, A.; Sharp, P. R. *J. Am. Chem. Soc.* **2006**, *128*, 5998 – 5999.

[7] Chen, T.; Liu, R. *Org. Lett.* **2011**, *13*, 4644–4647.

[8] Tsefrikas, V. M. Ph.D. Dissertation, Boston College, Chestnut Hill, MA, 2007.

[9] Handa, N. V.; Mendoza, K. D.; Shirtcliff, L. D. *Org. Lett.* **2011**, *13*, 4724-4727.

[10] For more detail on the Pyrolysis apparatus, see; (a) Necula, A.; Scott, L. T. *J. Anal. Appl. Pyrolysis* **2000**, *54*, 65. (b) Scott, L. T.; Bratcher, M. S.; Hagen, S. *J. Amer. Chem. Soc.* **1996**, *118*, 8743-8745.

[11] (a) Scott, L. T.; Boorum, M. M.; McMahon, B. J.; Hagen, S.; Mack, J.; Blank, J.; Wegner, H.; de Meijere, A. *Science* **2002**, *295*, 1500. (b) Scott, L. T.; Jackson, E. A.; Zhang, Q.; Steinberg, B. D.; Bancu, M.; Li, B. *J. Am. Chem. Soc.* **2012**, *134*, 107−110.

[12] Brown, R. F. C. *Aust. J. Chem.* **2010**, *63*, 1002–1006.

[13] Schinkovitz, A.; Pro, S. M.; Main, M.; Chen, S.; Jaki, B. U.; Lankin, D. C.; Pauli, G. F. *J. Nat. Prod.* **2008,** *71*, 1604.

Chapter 4

A Convenient Method for the Perdeuteration of Polycyclic Aromatic Hydrocarbons

4.1 Introduction

Method development for the efficient H/D exchange of polycyclic aromatic hydrocarbons (PAHs) is a field that has been studied in recent years.[1] To date, a variety of metal,[2] acid[3] and base[4] catalyzed H/D exchange reactions of aromatic hydrocarbons have been reported. Furthermore, utilization of near-critical or supercritical D_2O has provided a 'green' route towards perdeuterated PAHs;[5] however, all mentioned methods typically involve a specialized set-up, high temperatures and/or long reaction times. Aiming to provide a method for the convenient and efficient deuterium exchange of aromatic hydrogen atoms, a general method utilizing low cost and readily accessible materials has been developed.

4.2 *N,N*-dimethylformamide-d_7 as a Deuterium Source

It has been well documented that *N,N*-dimethylformamide (DMF) undergoes rapid decomposition to carbon monoxide and dimethylamine in the presence of base.[6] The decomposition products of DMF have been utilized as synthetic building blocks in many syntheses. The sodium hydride decomposition of DMF is well known, providing a route to sodium dimethylamide, which has been used as a base for a variety of reactions.[7] It should be noted that this method not only produces sodium dimethylamide but also evolves hydrogen and carbon monoxide gas, which on scale, is a serious concern. Furthermore, the rate of DMF decomposition is fast, but only after an unpredictable incubation period, causing uncontrollable exothermic reactions, even at room temperature.

Owing to these concerns, another base was considered for the decomposition of DMF. It had been shown that potassium *tert*-butoxide reacts in a controllable manner with DMF and can even be heated at elevated temperatures.[6] It was proposed that utilizing DMF-d_7 (**4-1**) as the deuterium source for the H/D exchange of PAHs would be facilitated by the decomposition of the **4-1** with potassium *tert*-butoxide (**4-2**). The decomposition was expected to generate an equivalent of carbon monoxide, *tert*-butanol-d_1 (**4-4**) and potassium dimethylamide-d_6 (**4-3**), which is in equilibrium with dimethylamine-d_7 (**4-5**) and **4-2**, as shown in Scheme 4-1. It should also be possible to use DMF-d_1, which in the presence of **4-2** would decompose to form dimethylamine-d_1, providing a comparable price and deuterium source as DMF-d_7.

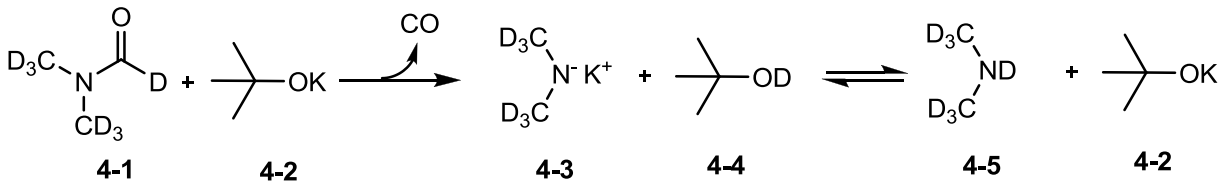

Scheme 4-1. Decomposition of DMF-d_7 by Potassium t*ert*-Butoxide

In the presence of a PAH, it is expected that these reagents, when heated, should promote H/D exchange. Reagents **4-1** and **4-2** were combined, and a planar or curved polycyclic aromatic hydrocarbon was added to the mixture and heated under microwave irradiation for 1 h at 170 ˚C to provide the perdeuterated PAH, as shown in Table 4-1. Initial conditions were optimized with pyrene (**4-6**), a commercially available PAH, as shown in Scheme 4-2.

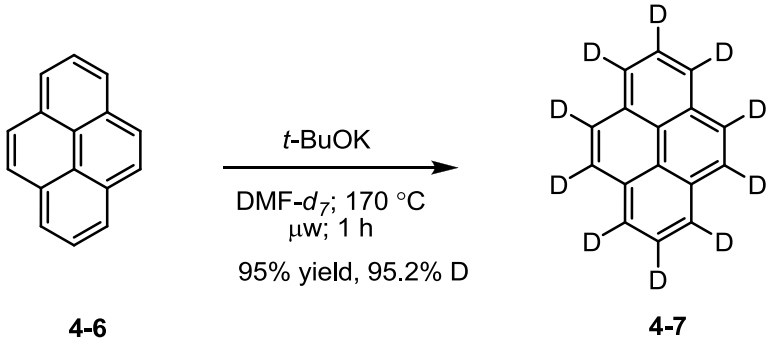

4-6 **4-7**

Scheme 4-2. Perdeuteration of Pyrene

Table 4-1. H/D Exchange of Polycyclic Aromatic Hydrocarbons[a]

Entry	PAH	Time (h)	Temp. (° C)	Product	Yield (%)	% D [b]
1	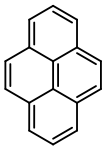	1	170[c]	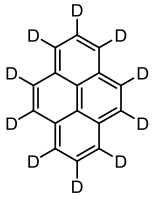	95	95.2
2		24	150[d]		95	95.0
3	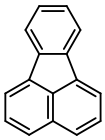	1	170[c]	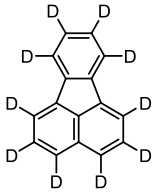	75	94.4
4		1	170[c]	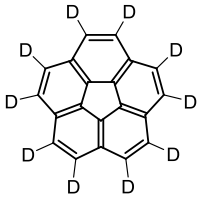	80	>98
5	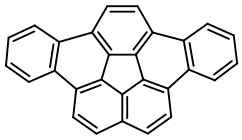	1	170[c]	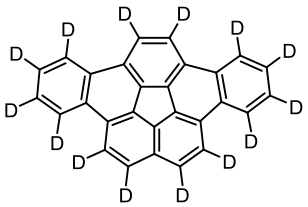	71	95.5

[a] Reaction condition: 20 equivalents *t*-BuOK (sublimed) and [0.20 M] DMF-d_7. [b] Deuterium incorporation was determined by ^{1}H NMR integration with 1,3,5-trimethoxybenzene as an internal standard. [c] Reaction was run in a microwave reactor. [d] Reaction was run in a pressure vessel.

It was found that twenty equivalents of potassium *tert*-butoxide in a 0.20 M solution of **4-6** in DMF-d_7 under microwave irradiation provided **4-7** in a 95% yield with a 95.2% deuterium incorporation (Table 4-1, entry 1). This reaction was also run on the bench top, in a sealed glass pressure vessel, at 150 ˚C, for 24 h (entry 2) which provided identical results as those found using microwave irradiation for 1 h.

Analysis of **4-7** by mass spectrometry revealed that the reaction had incorporated 10 deuterium atoms onto **4-6**. As shown in Figure 4-1, the EI-MS shows the most abundant species is **4-7**; however, there are lesser amounts of pyrene-d_9 (*m/z* 211), pyrene-d_8 (*m/z* 210), and pyrene-d_7 present in the product mixture. In order to determine the efficiency of this process, quantitative deuterium incorporation was determined using ^{1}H NMR integration with an internal standard, which allowed for quantification of any residual hydrogen atoms present in the mixture. This analysis indicated a 95.2% deuterium incorporation for **4-7**.

Optimization of this method aiming to exchange the remaining hydrogen atoms in the product mixture with deuterium was explored. It was found that a decrease in the reaction time under microwave irradiation lead to diminished deuterium incorporation. Conversely, increasing the reaction time did not result in an increase in deuterium incorporation. Pyrene-d_{10}, **4-7**, was resubjected to the same reaction conditions as in Scheme 2; however, the H/D ratio was not significantly improved. Increasing the amount of solvent, **4-1**, and/or increasing the equivalents of the base, **4-2**, did not improve the deuterium incorporation. It was further determined that the purity and moisture content of

the base, **4-2**, play a significant role in the percent of deuterium incorporation; best results were obtained with freshly sublimed **4-2** or from commercially available sublimed **4-2**.

The mixture was analyzed by two mass spectrometry methods; EI-MS and high resolution DART-TOF. Both methods show almost identical ratios of peak heights, which indicates that these analysis methods likely do not significantly diminish the D/H ratio. To confirm this, commercially available **4-7** (98% D) was analyzed, and it was found to have a comparable mass spectrum to **4-7** prepared under the present method (Figure 4-1). The commercially available **4-7** was also analyzed by ^{1}H NMR, with an internal standard, and was confirmed to have a deuterium incorporation of 98.6%. Further analysis of **4-7**, prepared under present conditions, by ^{13}C NMR confirmed the formation of **4-7** and incorporation of 10 deuterium atoms, as shown in Figure 4-2.

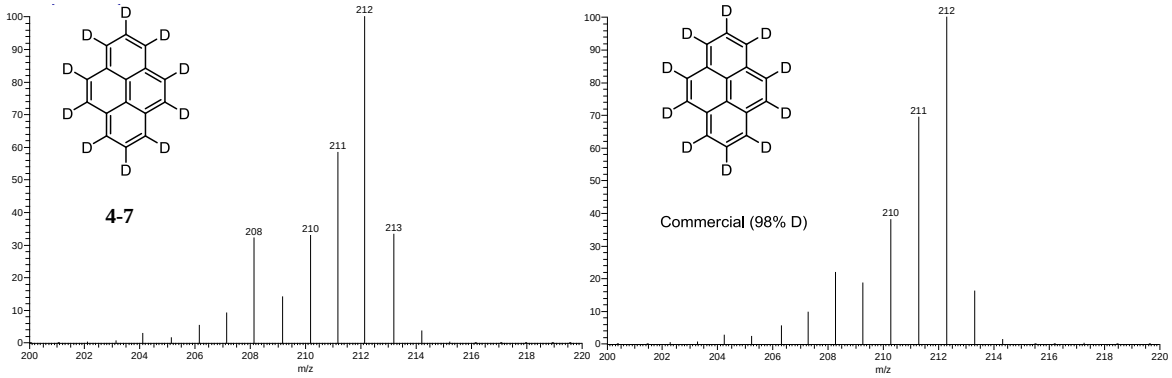

Figure 4-1. EI-MS of Pyrene-*d_{10}*

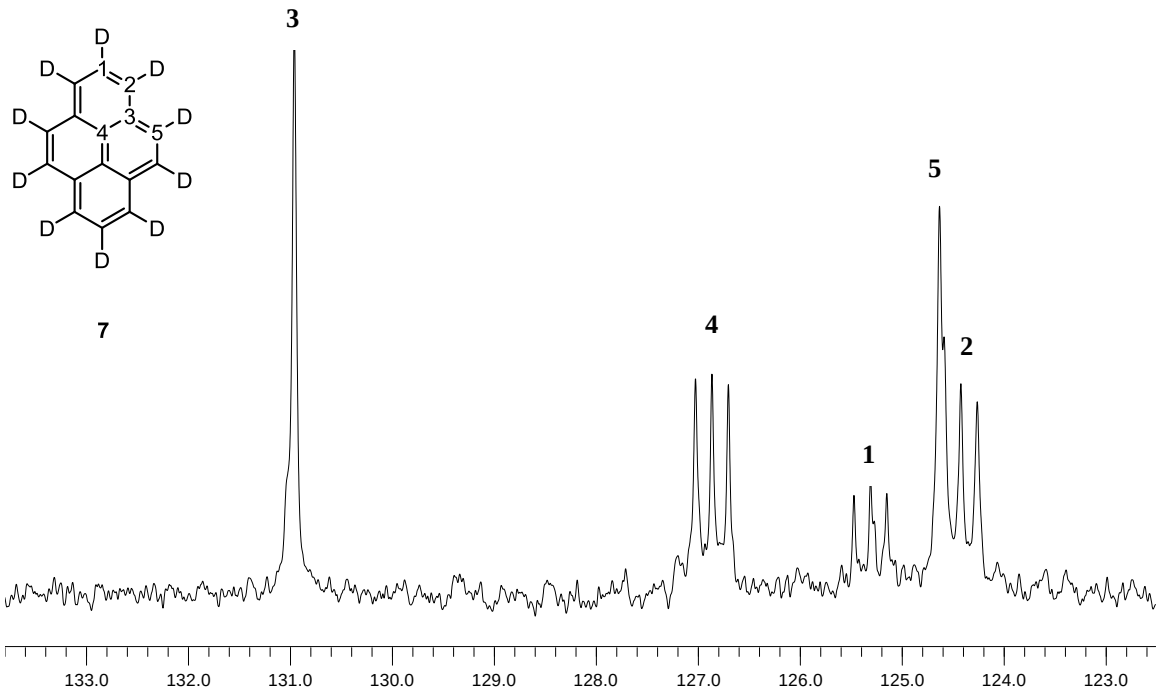

Figure 4-2. ^{13}C NMR (150 MHz, $CDCl_3$, no proton decoupling, 300 pulses, 60 s pulse delay) of Pyrene-d_{10}

This method is not limited to pyrene and was applied to another commercially available PAH, fluoranthene. Fluroanthene-d_{10} was prepared with the same conditions as **4**-**7** in a 75% yield and 94.4% deuterium incorporation (Table 4-1, entry 3). The method was further applied to less generic PAHs, specifically geodesic polyarenes, which have been utilized as building blocks for organic electronic materials. Applying this general and convenient method to these larger, curved polycyclic aromatic hydrocarbons allowed for the synthesis of perdeuterated compounds that were not previously easily accessible by other methods. The perdeuteration of two geodesic polyarenes was explored. Corannulene[8] and dibenzo[*a*,*g*]corannulene[9] are both curved polycyclic aromatic hydrocarbons which have been of interest for a variety of synthetic and materials applications. Accessing these molecules in their perdeuterated form would allow for

further studies of these molecules as synthetic intermediates. Applying the potassium *tert*-butoxide and DMF-d_7 conditions, under microwave irradiation, to both corannulene (Table 4-1, entry 4) and dibenzo[*a*,*g*]corannulene (Table 4-1, entry 5) afforded the perdeuterated geodesic polyarenes in good yields and high deuterium incorporation. All compounds were again analyzed by EI-MS, as shown in Figure 4-3, and the deuterium incorporation was determined by ^{1}H NMR.

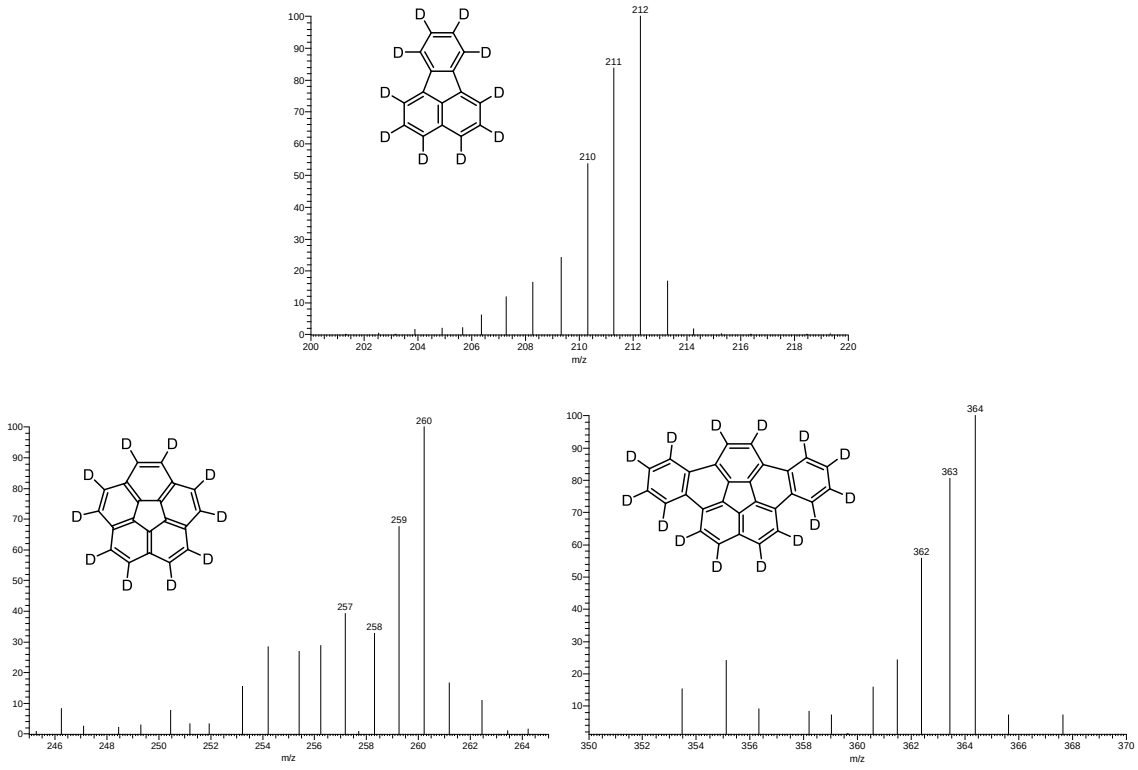

Figure 4-3. EI-MS of Perdeutero Polycyclic Aromatic Hydrocarbons

4.3 Conclusion

The development of a convenient and relatively inexpensive method for the preparation of perdeuterated polycyclic aromatic hydrocarbons has been developed. Utilizing readily accessible reagents and short reaction times, the synthesis of common and exotic PAH's

has provided a new route towards these perdeuterated synthetic intermediates. More importantly, this method affords efficient H/D exchange, comparable to the levels found in commercially available perdeuterated standards. The ease and convenience of the short reaction times and accessibility of the reagents should allow for a wide variety of applications of this method in the future.

4.4. Experimental Section

4.4.1. General Experimental

All chemicals were purchased and used without further purification unless otherwise noted. Deuterated materials, *N*,*N*-dimethylformamide-d_7 (99.5% D) and Pyrene-d_{10} (98% D), were purchased from Cambridge Isotope Laboratories; independent analysis of these materials by ^{1}H NMR integration with an internal standard and EI-MS confirmed the percent deuterium incorporation. Potassium *tert*-butoxide (sublimed grade, 99.99% trace metals basis) was purchased from Aldrich and stored sealed under nitrogen in a dessicator. Microwave irradiation was performed with a CEM Discover LabMate reactor with the IntelliVent™ Pressure Control System. EI-MS were obtained with a Thermo Finnigan Trace DSQ. High resolultion mass spectrometry was performed at the Boston College Mass Spectrometry facilities. NMR spectra were recorded at the Boston College Nuclear Magnetic Resonance Center on 500 and 600 MHz Varian instruments. NMR shifts are referenced in ppm downfield from TMS, using chloroform-d_1 (δ_H = 7.26 ppm, δ_C= 77.23 ppm). ^{13}C NMR spectra were recorded at 125 MHz with no proton decoupling and a 60 second pulse delay. Deuterium incorporation was determined by ^{1}H NMR integration (500 MHz) with 1,3,5-trimethoxybenzene as an internal standard. For example, pyrene-d_{10} (0.0573 mmol) and 1,3,5-trimethoxybenzene (0.00238 mmol) were mixed in 0.70 mL of $CDCl_3$. The residual hydrogen signals from pyrene-d_{10} were integrated (8.5 per 1H) versus the internal standard (7.34 per H). From the integration, the number of moles of residual hydrogen present in the pyrene-d_{10} sample was calculated

based on the known moles of the internal standard and found to be 0.00276 mmol. The moles of residual hydrogen present in the pyrene-d_{10} sample (0.00276 mmol) was divided by the total number of moles of pyrene-d_{10} (0.0573 mmol), providing the percent residual hydrogen (4.8 % H). Chromatography was performed with Sorbent Technologies silica gel (porosity = 60 Å, particle size = 32-63 μm).

4.4.2. Pyrene-1,2,3,4,5,6,7,8,9,10-d_{10}

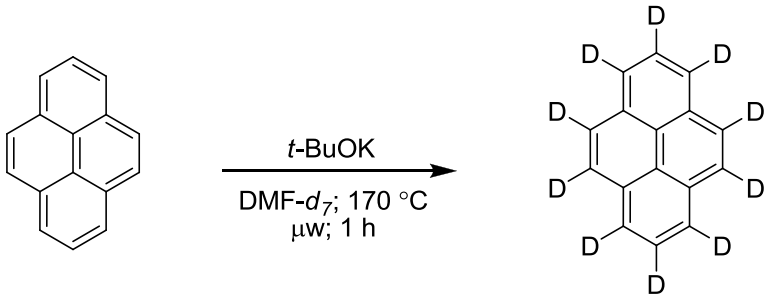

To a flame-dried, nitrogen purged 10 mL microwave vessel equipped with a magnetic stir bar was added 50.0 mg (0.248 mmol) pyrene and 1.00 mL dimethylformamide-d_7. The mixture was stirred, and sublimed* potassium *tert*-butoxide was added (0.555 g, 4.95 mmol). The microwave vessel was capped and placed in a microwave reactor for 1 hour at 170 ˚C. The mixture was cooled to room temperature and immediately flushed through a short pad of silica gel with dichloromethane as the eluent. Evaporation of solvent provided 49.9 mg (95%) of deuterated pyrene as a tan solid. ^{1}H NMR analysis (500 MHz, $CDCl_3$) with 1,3,5-trimethoxybenzene as an internal standard showed 95.2% D incorporation. **^{1}H NMR** (500 MHz, $CDCl_3$) δ(ppm): 8.21 (s, 4H), 8.10 (s, 4H), 8.03 (s, 2H). **^{13}C NMR** (125 MHz, $CDCl_3$, no proton decoupling, 300 pulses, 60 s pulse delay) δ(ppm): 130.9 (s), 126.8 (t, J = 24.0 Hz), 125.3 (t, J = 24.5 Hz), 124.6 (s), 124.4 (t, J = 24.0 Hz). **HRMS** (DART-TOF): Calc'd for $C_{16}HD_{10}$ $(M+1)^+$ 213.1488, found 213.1490. **DART-TOF** %D incorporation: 45% d_{10} : 38% d_9 : 8.5% d_8.[10] See Figure 4-1 for EI-MS data.

* The potassium *tert*-butoxide was either freshly sublimed or commercially available sublimed potassium *tert*-butoxide was used. Any additional moisture resulted in diminished deuterium incorporation.

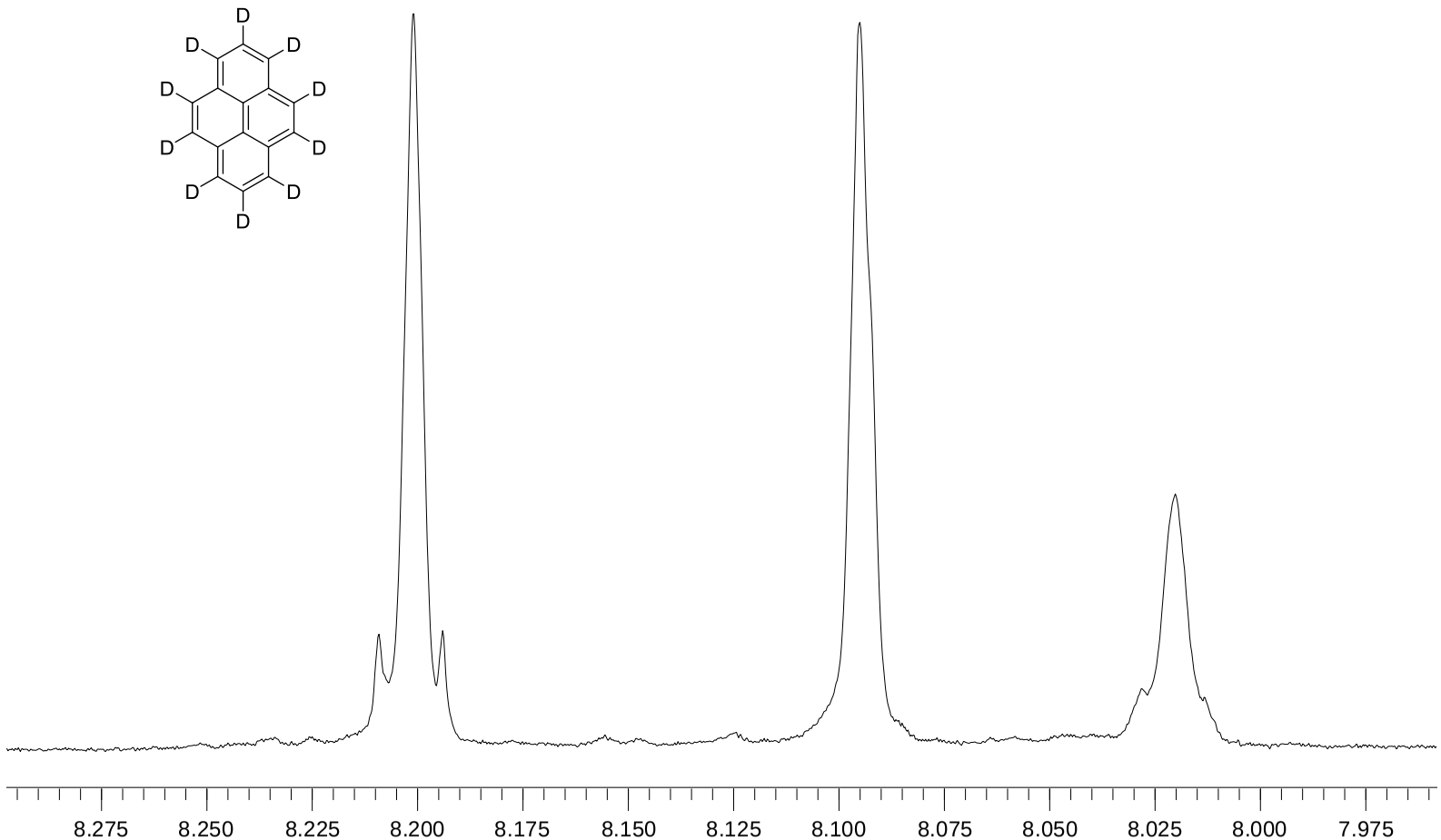

^{1}H NMR (500 MHz, $CDCl_3$)

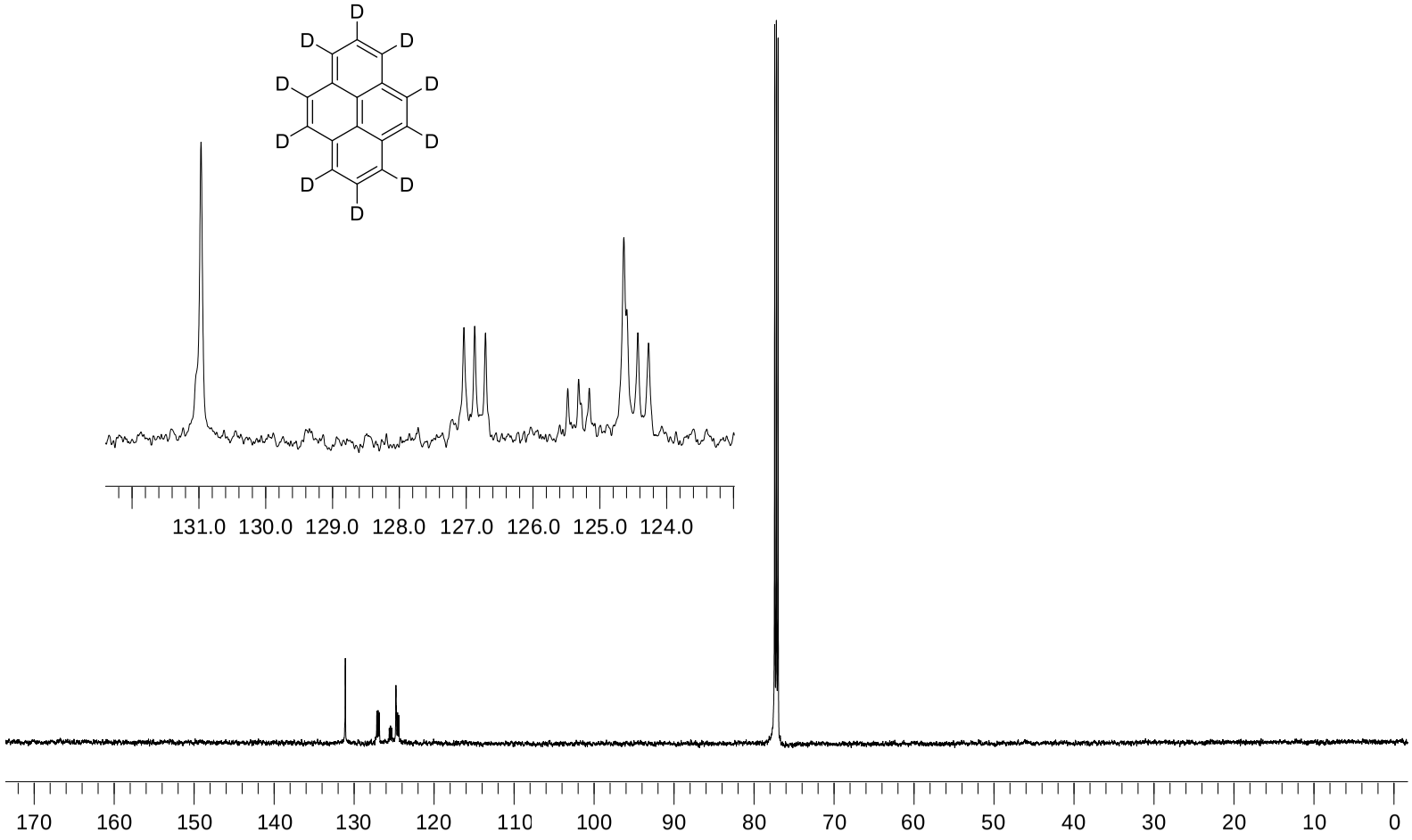

^{13}C NMR (150 MHz, $CDCl_3$, no proton decoupling, 300 pulses, 60 s pulse delay)

4.4.3. Fluoranthene-1,2,3,4,5,6,7,8,9,10-d_{10}

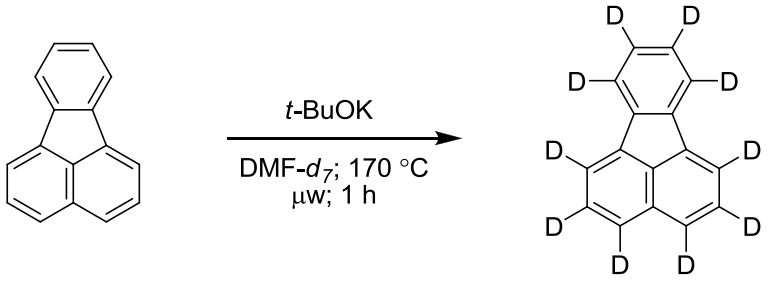

To a flame-dried, nitrogen purged 10 mL microwave vessel, equipped with a magnetic stir bar was added 50 mg (0.248 mmol) fluoranthene and 1.0 mL dimethylformamide-d_7. The mixture was stirred, and sublimed* potassium *tert*-butoxide was added (0.555 g, 4.95 mmol). The vessel was capped and placed in a microwave reactor for 1 hour at 170 ˚C. The mixture was cooled to room temperature and immediately flushed through a short pad of silica gel with dichloromethane as the eluent. Evaporation of solvent provided 39.0 mg (75%) of deuterated fluoranthene as a tan solid. ^{1}H NMR analysis (500 MHz, $CDCl_3$) with 1,3,5-trimethoxybenzene as an internal standard showed 94.4% D incorporation. **^{1}H NMR** (500 MHz, $CDCl_3$) δ(ppm): 7.99-7.97 (m), 7.95 (s), 7.93-7.92 (m), 7.85 (s), 7.64 (s), 7.39 (s). **^{13}C NMR** (125 MHz, $CDCl_3$, no proton decoupling, 376 pulses, 60 s pulse delay) δ(ppm): 139.1 (s), 136.6 (s), 132.2 (s), 129.6 (s), 127.2 (t, J = 23.9 Hz), 126.9-126.6 (m), 125.9 (t, J = 24.0 Hz), 121.2-120.8 (m), 119.2 (t, 24.0 Hz). **HRMS** (DART-TOF): Calc'd for $C_{16}D_{10}$ (M^+) 212.1410, found 212.1418. See Figure 4-3 for EI-MS data.

* The potassium *tert*-butoxide was either freshly sublimed, or commercially available sublimed potassium *tert*-butoxide was used. Any additional moisture resulted in diminished deuterium incorporation.

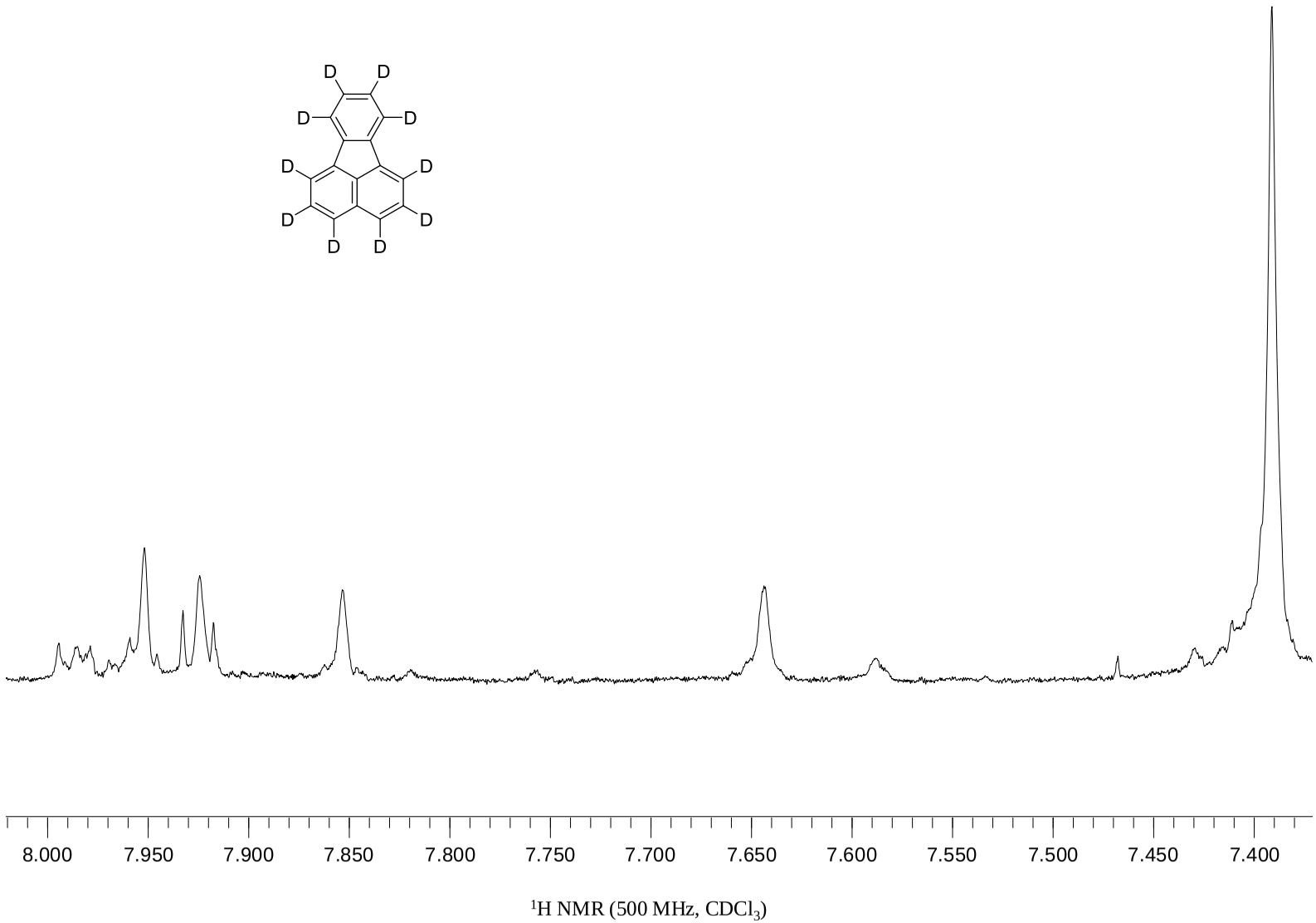

^{1}H NMR (500 MHz, $CDCl_3$)

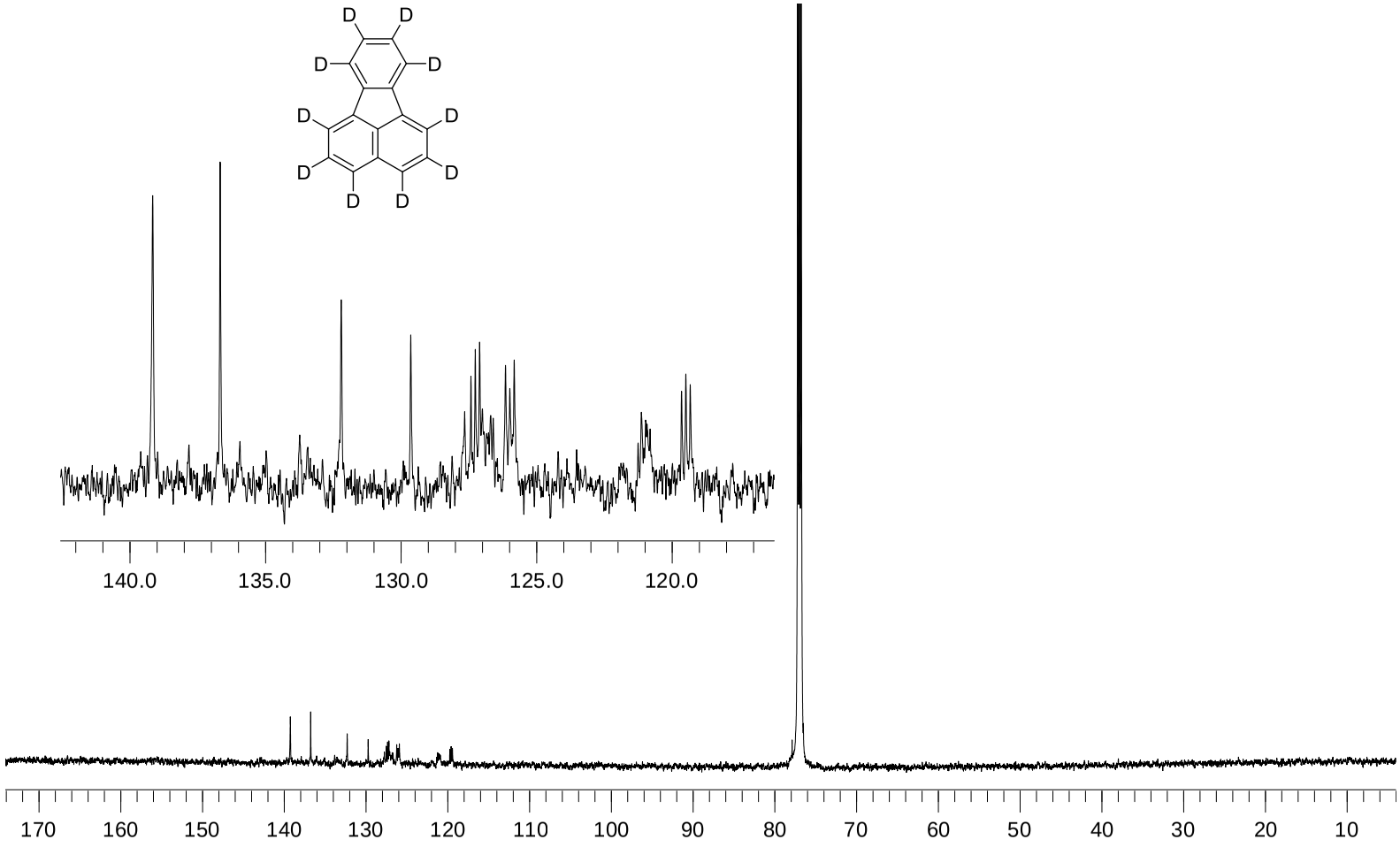

^{13}C NMR (150 MHz, $CDCl_3$, no proton decoupling, 376 pulses, 60 s pulse delay)

4.4.4. Corannulene-1,2,3,4,5,6,7,8,9,10-d_{10}

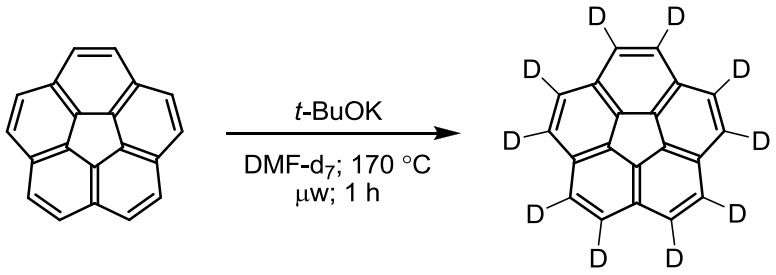

To a flame-dried, nitrogen purged 10 mL microwave vessel, equipped with a magnetic stir bar was added 20.0 mg (0.0800 mmol) corannulene and 0.40 mL dimethylformamide-d_7. The mixture was stirred, and sublimed* potassium *tert*-butoxide was added (0.179 g, 1.60 mmol). The vessel was capped and placed in a microwave reactor for 1 hour at 170 ˚C. The mixture was cooled to room temperature and immediately flushed through a short pad of silica gel with dichloromethane as the eluent. Evaporation of solvent provided 16.7 mg (80%) of deuterated corannulene as a tan solid. ^{1}H NMR analysis (500 MHz, $CDCl_3$) with 1,3,5-trimethoxybenzene as an internal standard showed >98% D incorporation. **^{1}H NMR** (500 MHz, $CDCl_3$) δ(ppm): 7.77 (s, 10H). **^{13}C NMR** (125 MHz, $CDCl_3$, no proton decoupling, 3184 pulses, 60 s pulse delay) δ(ppm): 134.9 (s), 129.7 (s), 125.6 (t, J = 22.0Hz). **HRMS** (DART-TOF): Cacl'd for $C_{20}D_{10}$ (M^+) 260.1410, found 260.1411. See Figure 4-3 for EI-MS data.

* The potassium *tert*-butoxide was either freshly sublimed, or commercially available sublimed potassium *tert*-butoxide was used. Any additional moisture resulted in diminished deuterium incorporation

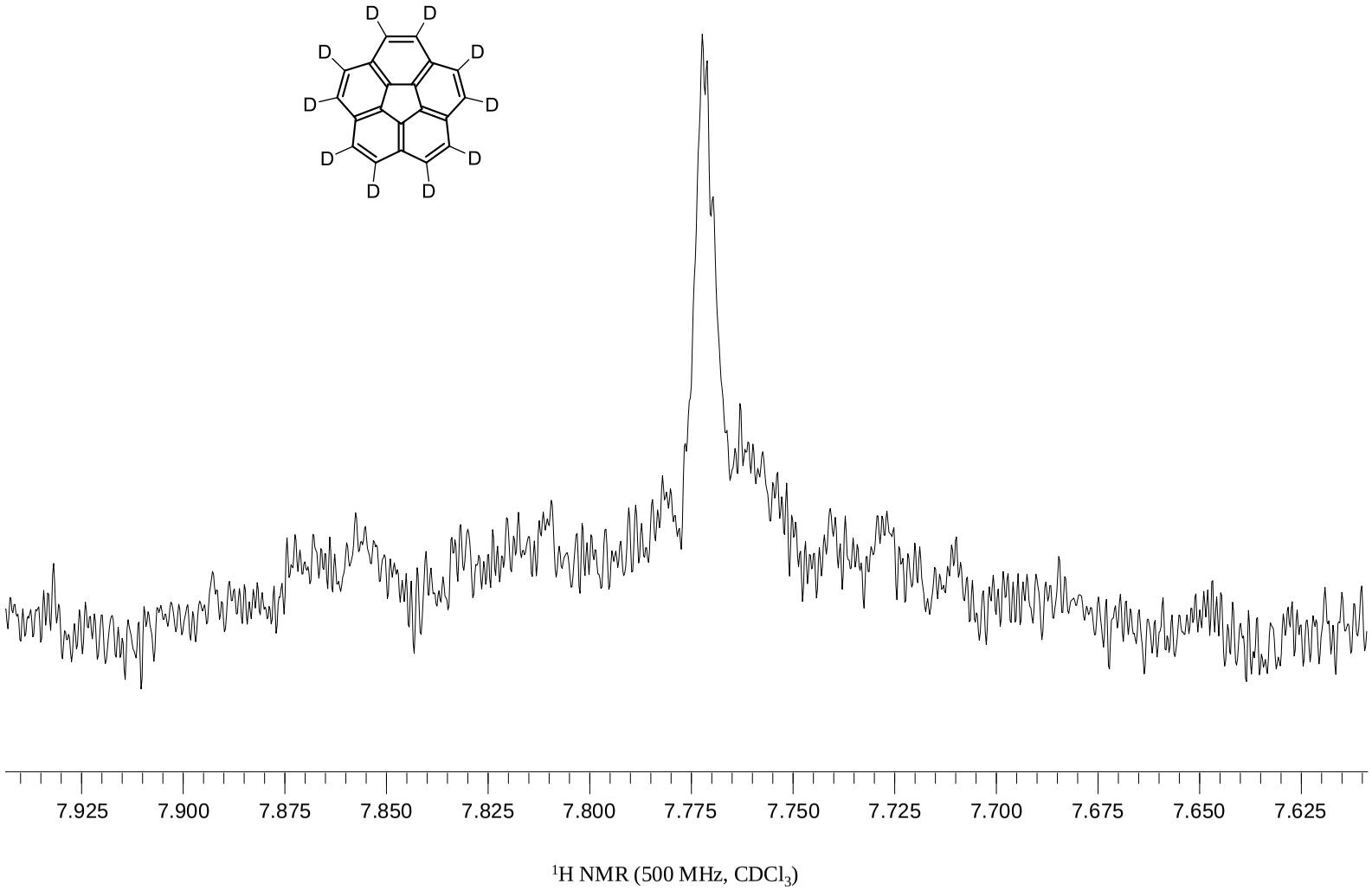

^{1}H NMR (500 MHz, $CDCl_3$)

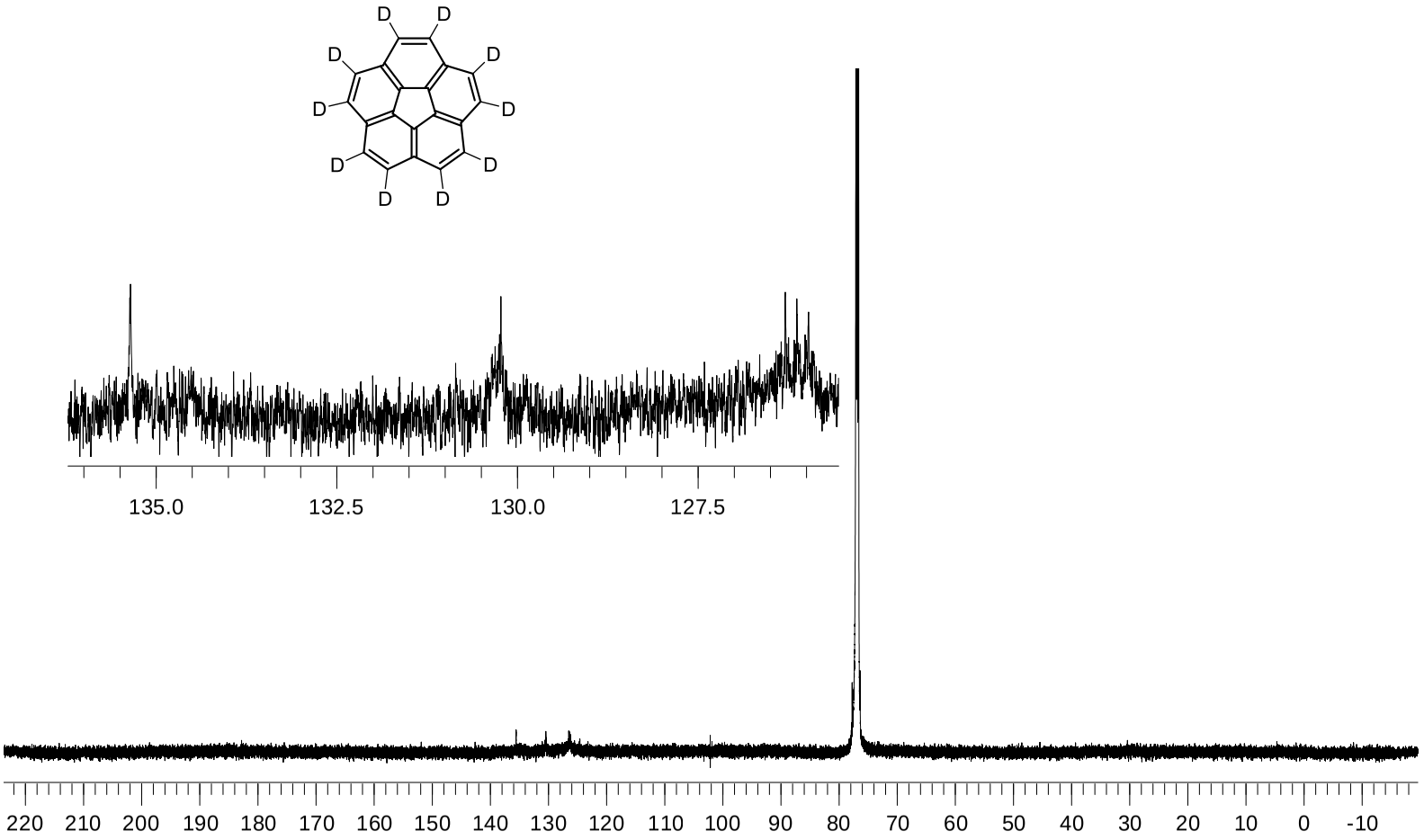

^{13}C NMR (150 MHz, $CDCl_3$, no proton decoupling, 3184 pulses, 60 s pulse delay)

4.4.5. Dibenzo[*a,g*]corannulene-1,2,3,4,5,6,7,8,9,10,11,12,13,14-d_{14}

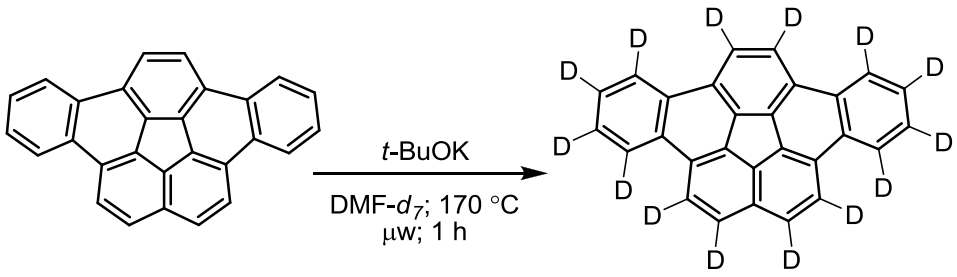

To a flame-dried, nitrogen purged 10 mL microwave vessel, equipped with a magnetic stir bar was added 20.0 mg (0.0571 mmol) dibenzo[*a,g*]corannulene and 0.30 mL dimethylformamide-d_7. The mixture was stirred, and sublimed* potassium *tert*-butoxide was added (0.128 g, 1.14 mmol). The vessel was capped and placed in a microwave reactor for 1 hour at 170 ˚C. The mixture was cooled to room temperature and immediately flushed through a short pad of silica gel with dichloromethane as the eluent. Evaporation of solvent provided a light brown solid in 14.7 mg (71%) as a tan solid. ^{1}H NMR analysis (500 MHz, $CDCl_3$) with 1,3,5-trimethoxybenzene as an internal standard showed 95.5% D incorporation. **^{1}H NMR** (500 MHz, $CDCl_3$) δ(ppm): 8.73-8.66 (m), 8.34 (s), 8.26 (m), 7.98 (m), 7.78 (s). **^{13}C NMR** (125 MHz, $CDCl_3$, no proton decoupling, 2696 pulses, 60 s pulse delay) δ(ppm): 135.8 (s), 134.8 (s), 134.1 (s), 133.0 (s), 132.9 (s), 130.0 (s), 128.5 (s), 128.3 (s), 126.8-126.2 (m), 125.6-125.3 (m), 124.7-123.9 (m). **HRMS** (APPI): Cacl'd for $C_{28}D_{14}$ (M^+) 364.1968, found 364.1959. See Figure 4-3 for EI-MS data.

* The potassium *tert*-butoxide was either freshly sublimed, or commercially available sublimed potassium *tert*-butoxide was used. Any additional moisture resulted in diminished deuterium incorporation

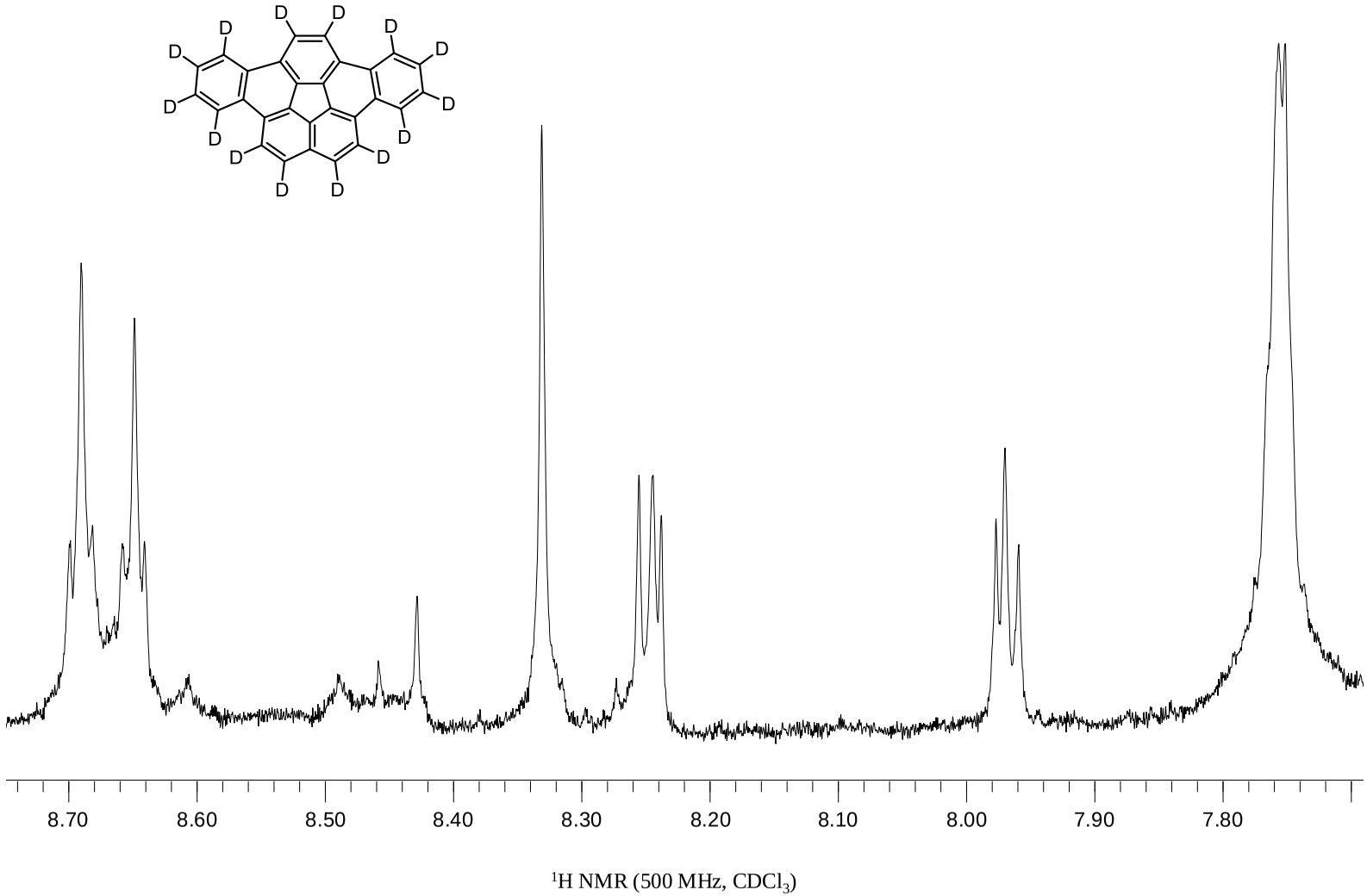

^{1}H NMR (500 MHz, $CDCl_3$)

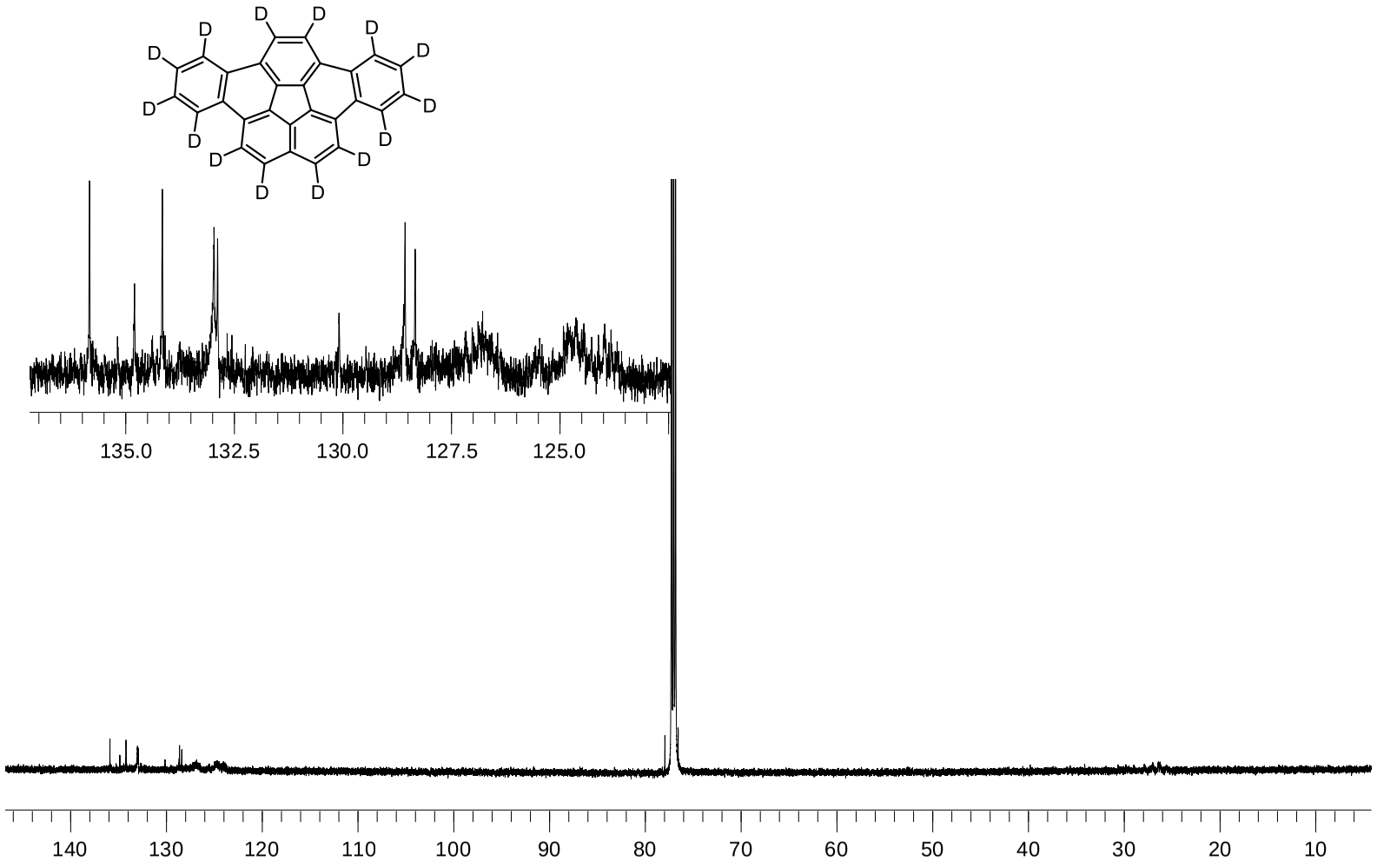

^{13}C NMR (150 MHz, $CDCl_3$, no proton decoupling, 2696 pulses, 60 s pulse delay)

4.5 References

[1] Junk T.; Catallo, W. J. *Chem. Soc. Rev*., **1997**, *26*, 401.

[2] For metal catalyzed H/D exchange, see: a) Garnett, J. L.; Hodges, R. J. *J. Am. Chem. Soc*. **1967**, *89*, 4546. b) Garnett, J. L.; Long, M. A.; McLaren, A. B.; Peterson, K. B. *J. Chem. Soc., Chem. Commun*. **1973**, 749. c) Castellani, C. B.; Perotti, A.; Scrivanti, M.; Vidari, G. *Tetrahedron* **2000**, *56*, 8161. d) Ellames, G. J.; Gibson, J. S.; Herbert, J. M.; Kerr, W. J.; McNeill, A. H. *Tetrahedron Lett*. **2001**, *42*, 6413. e) Klei, S. R.; Golden, J. T.; Tilley, T. D.; Bergman, R. G. *J. Am. Chem. Soc*. **2002**, *124*, 2092. f) Branch, C. S.; Barron, A. R. *J. Am. Chem. Soc*. **2002**, *124*, 14156. g) Qiao-Xia, G.; Bao-Jian, S.; Hai-Qing, G.;Tamotsu, T. *Chin. J. Chem.* **2005**, *23*, 341.

[3] For acid catalyzed H/D exchange, see: Shabanova, E.; Schaumburg, K.; Kamounah, F. S. *J. Chem. Res., Synop*. **1999**, 364.

[4] For base catalyzed H/D exchange, see: Yao, J.; Evilia, R. F. *J. Am. Chem. Soc*. **1994**, *116*, 11229.

[5] For supercritical D_2O, see: a) Junk T.; Catallo, W. J. *Tetrahedron Lett.*, **1996**, *37*, 3445. b) Boix, C.; Poliakoff, M. *Tetrahedron Lett*. **1999**, *40*, 4433. b) Kalpala, J.; Hartonen, K.; Huhdanpää, M.; Riekkola, M. *Green Chem.* **2003**, *5*, 670.

[6] Muzart, J. *Tetrahedron*, **2009**, *65*, 8313‑8323.

[7] Nasipuri, D.; Bhattacharyya, A.; Hazra, B. G. *J. Chem. Soc*., **1971**, 660.

[8] Scott, L. T.; Cheng, P.-C.; Hashemi, M. M.; Bratcher, M. S.; Meyer, D. T.; Warren, H. B. *J. Am. Chem. Soc.* **1997**, *119*, 10963.

[9] Reisch, H. A.; Bratcher, M. S.; Scott, L. T. *Org. Lett.* **2000**, *2*, 1427.

[10] Analysis by high resolution DART-TOF mass spectrometry coupled with MassWorks sCLIPS analysis (Cerno Bioscience) allowed for the accurate calculation of the percent deuterium incorporation.

Chapter 5

A Novel Heteroatom Containing Geodesic Polyarene: Synthesis of Dibenzo[*g,m*]azacorannulene

5.1 Introduction

Advancements in the synthesis of a wide variety of geodesic polyarenes has led to extensive studies of these materials.[1] A natural expansion in the field of geodesic polyarenes would be, and has been, to explore ways to manipulate the properties of these materials. Most studies have involved expanding the aromatic core by synthesizing larger delocalized systems or by creating significant curvature of the hydrocarbon framework. In recent years, focus has turned towards incorporating heteroatoms into the geodesic polyarene, which would provide an opportunity to tune the electronic properties of these materials.[2]

The first curved, or bowl-shaped, heteroatom containing polyarene was prepared in 1999 by Imamura *et al.*, in which sulfur was successfully incorporated into a sumanene core, as shown in Scheme 5-1.[3] Flash vacuum pyrolysis, at 1000 ˚C, of precursors **5-1** and **5-2** afforded trithiasumanene (**5-3**) in 35% yield. The X-ray crystal structure of **5-3** has a shallower bowl depth than the hydrocarbon sumanene, which is representative of the longer C-S bonds, compared to the C-C bonds of sumanene, flattening the molecule.

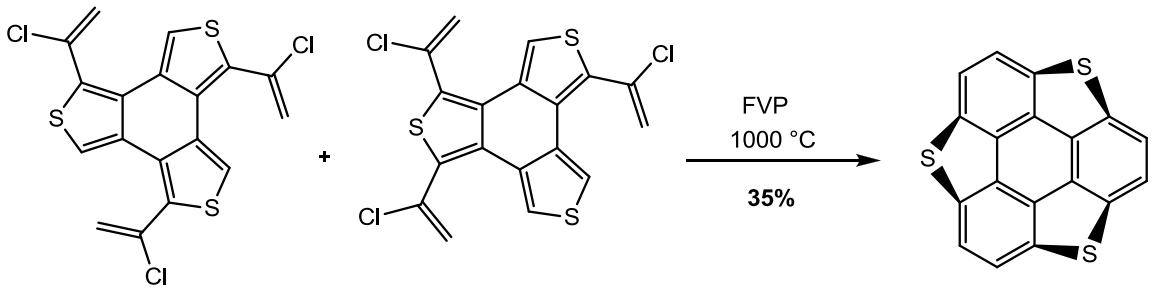

5-1 **5-2** **5-3**

Scheme 5-1. Synthesis of Trithiasumanene

Ten years later, the synthesis of a more diverse group of heterasumanenes has been achieved by Furukawa *et al.*[4] and Saito *et al.*[5] As shown in Scheme 3-2, a trisilasumanene, **5-5**, was synthesized under mild conditions via a novel sila-Friedel-Crafts reaction with disila compound **5-4**.[4]

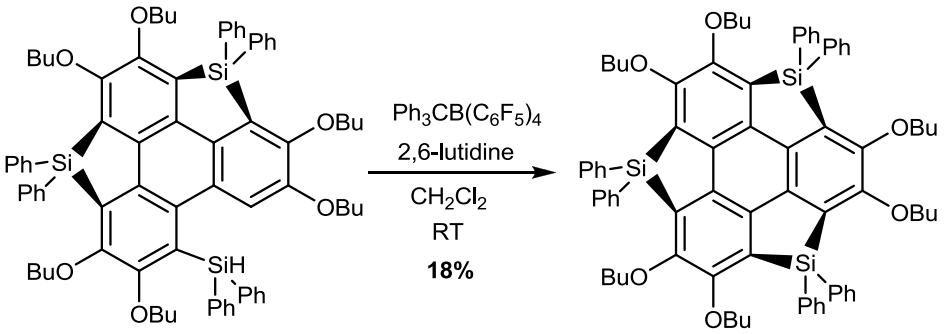

5-4 **5-5**

Scheme 5-2. Furukawa's Synthesis of Trisilasumanene

Shown in Scheme 5-3, the synthesis of sumanene with three different heteroatoms was achieved by Saito.[5] Beginning with the sila-sulfursumanene derivative, **5-6**, a sila-sulfur and either sila or tin heteroatom was successfully incorporated to form **5-7**. With all three of these syntheses, the heteroatom containing geodesic polyarenes are almost flat, due to the larger heteroatoms.

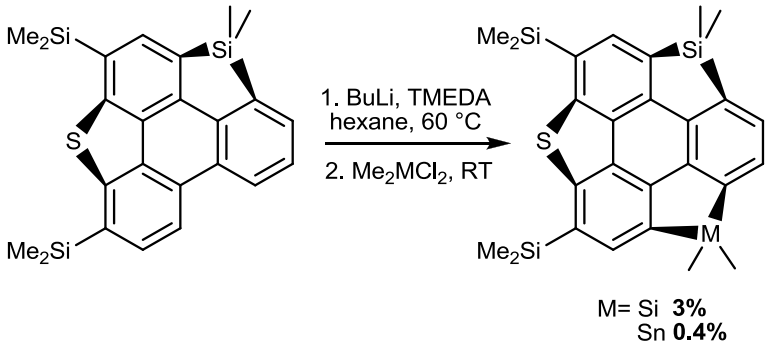

5-6 **5-7**

Scheme 5-3. Saito's Synthesis of a Multiple Heteroatom Containing Sumanene

5.2 Synthesis of Dibenzo[*g,m*]azacorannulene

The incorporation of nitrogen into a geodesic polyarene had yet to be accomplished until 2007 in the Scott laboratory.[6] Incorporation of a nitrogen atom into the framework of dibenzo[*a*,g]corannulene was explored extensively. As shown in Scheme 5-4, a retrosynthetic analysis of the desired dibenzo[*g,m*]azacorannulene (**5-8**) is comparable to that of the synthesis of dibenzo[*a,g*]corannulene. It was proposed to synthesize **5-8** from intermediate **5-9**, which incorporated the nitrogen atom on the isoquinoline moiety of the molecule. Compound **5-9** can be envisioned from an azaacenapthenequinone, **5-10**, and the known symmetrical ketone, **5-11**.

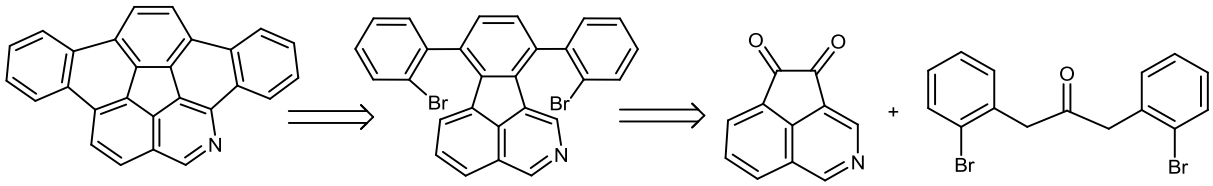

5-8 **5-9** **5-10** **5-11**

Scheme 5-4. Retrosynthetic Analysis of Dibenzo[*g,m*]azacorannulene

Unlike the synthesis of dibenzo[*a,g*]corannulene, the necessary quinone, **5-10**, was not commercially available. Fortunately, a synthesis of this molecule has been previously accomplished by Rabideau *et al.*, which can be achieved beginning from 9-bromo-isoquinoline (**5-12**), as shown in Scheme 5-5.[7] A Sonogashira coupling of **5-12** with TMS-acetylene afforded 4-((trimethylsilyl)ethynyl)isoquinoline (**5-13**) in 96% yield. This material was deprotected with potassium hydroxide in methanol to form **5-14** in 70% yield.

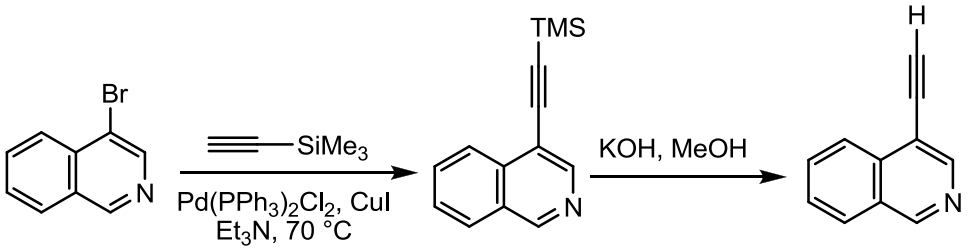

5-12 **5-13** **5-14**

Scheme 5-5. Synthesis of 4-Ethynylisoquinoline

The free acetylene, **5-14**, was subjected to pyrolysis conditions, as reported by Rabideau, at 950 ˚C to afford the cyclopenta[*de*]isoquinoline (**5-15**) in 39% yield, as shown in Scheme 5-6. Oxidation with benzeneseleninic anhydride afforded the quinone, **5-10**, in 65%.

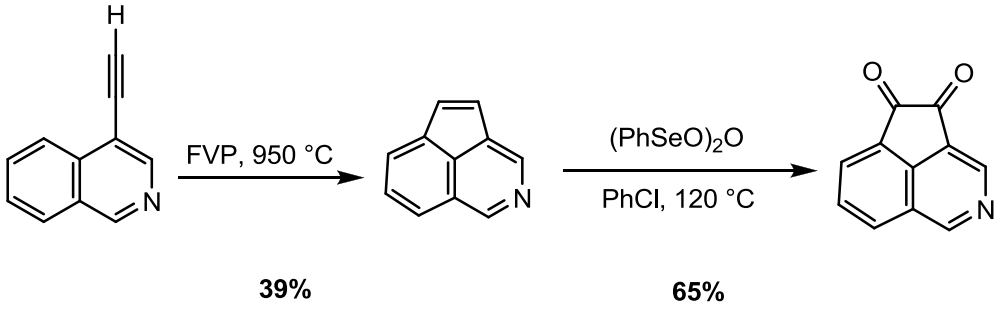

5-14 **5-15** **5-10**

Scheme 5-6. Synthesis of Cyclopenta[*de*]isoquinoline-4,5-dione

With the synthesis of **5-10** complete, the molecular framework was built up towards the target, **5-8**. A double Aldol condensation of **5-10** and **5-11** with potassium hydroxide in methanol afforded **5-16** in 75% yield as a purple precipitate, as shown in Scheme 5-7.

The convenient Diels-Alder/ retro Diels-Alder with norbornadiene afforded **5-9** in 78% yield. With the successful synthesis of **5-9**, flash vacuum pyrolysis was explored.

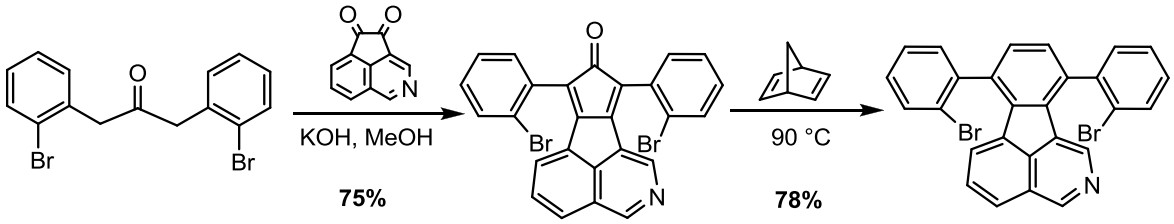

5-11 **5-16** **5-9**

Scheme 5-7. Synthesis of 7,10-*Bis*(2-bromophenyl)indeno[1,2,3-*de*]isoquinoline

Subjecting **5-9** to pyrolysis conditions afforded the desired product, **5-8**, in varying yields, dependent on the temperature of the hot zone and the flow rate of nitrogen. The FVP apparatus was set up as previously described in Chapter 3. The starting material, **5-8**, was absorbed onto quartz sand, to maximize surface area, and placed in a quartz boat. The sample was placed in the sublimation oven, which was heated to 75 ˚C, with the hot zone temperature set at 1000 ˚C. The sublimation temperature was slowly increased by 5 ˚C, every 5 minutes until the final temperature, 175 ˚C, was reached. A steady, but slow flow of nitrogen was applied during the entirety of the experiment. Over the course of sublimation, a yellow color was collected at the end of the quartz tube and in the liquid nitrogen cooled trap. Once the apparatus was cooled, the tube and traps were washed with dichloromethane, affording a yellow crude solid. Immediate purification on reverse phase C18 preparative layer chromatography afforded 10.3 mg (28% yield) of the desired dibenzo[*g*,*m*]azacorannulene (**5-8**), which was confirmed by ^{1}H NMR, shown in Figure 5-1.

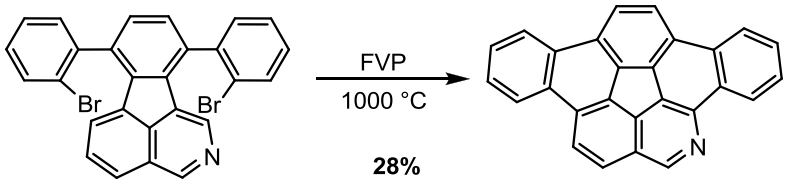

5-9 **5-8**

Scheme 5-8. Pyrolysis to form Dibenzo[*g,m*]azacorannulene

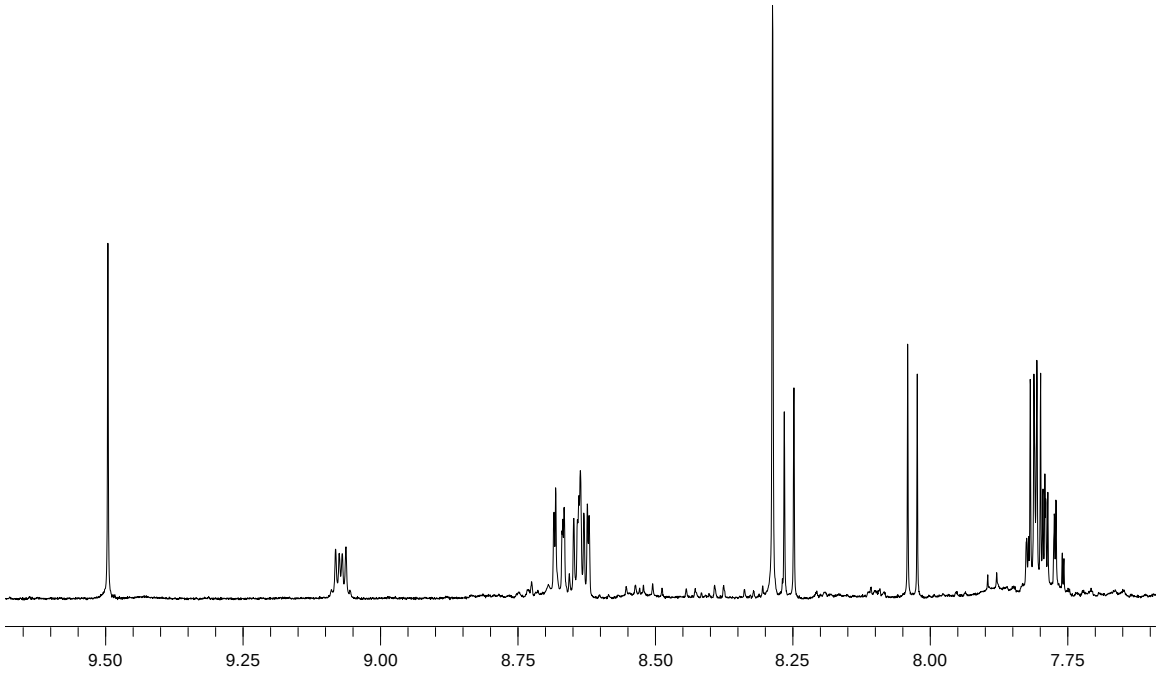

Figure 5-1. ^{1}H NMR of Dibenzo[*g,m*]azacorannulene

It was found that higher pyrolysis temperatures, upwards of 1100 ˚C, diminished the mass recovery. Also, the scale was limited, and no more than 60 mg could be pyrolyzed at a time; a larger scale lead to diminished yields. Furthermore, the flow rate of nitrogen greatly affected the outcome of the reaction. Due to the limitations of our FVP apparatus, there was no definitive way to quantitate the exact flow rate of nitrogen; however, the nitrogen inlet was only opened enough to allow for a moderate amount of nitrogen to be introduced into the system, while still allowing for the system to maintain an internal

pressure of 0.65-0.75 torr. It was discovered that the moderate flow rate of nitrogen gas forced the reactive intermediates through the hot zone rapidly, allowing for complete cyclization and providing the desired product **5-8**. If the flow rate was low, allowing for an internal pressure of approximately 0.35 torr, a byproduct was observed and suspected to be a nitrile, as shown in Scheme 5-9. This byproduct was presumably formed through the formation of the desired product **5-8**, which then underwent direct C-N bond fragmentation to form **5-18**, or C-C bond fragmentation (**5-17**), followed by rearrangement to form **5-20**. From **5-18** and **5-20**, a precedented 5/6-ring swap may form nitriles **5-19** and **5-21**.[8]

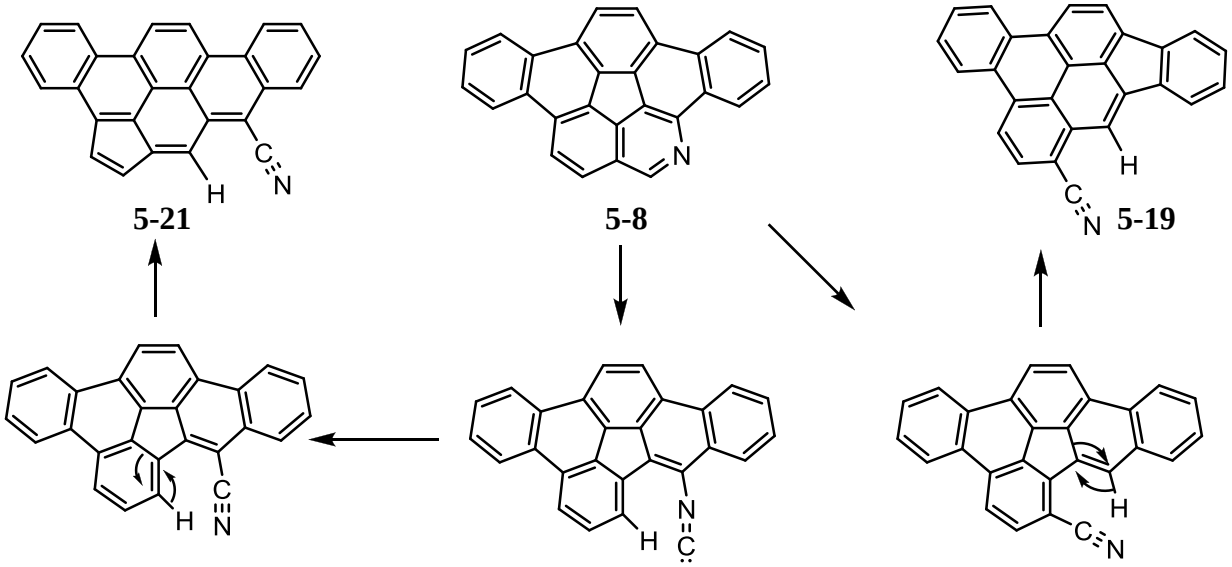

Scheme 5-9. Proposed Formation of a Nitrile Byproduct

Analysis of the byproduct by HRMS confirmed that the molecular formula was $C_{27}H_{14}N$ (*m/z* 351) and IR confirmed the presence of a nitrile, with a C≡N stretching frequency at 2363 cm^{-1}. NMR analysis, as shown in Figure 5-2, coupled with NMR calculations

(B3LYP/6-311++G(d,p))[9] provided insight into which isomer of the nitrile was formed, as shown in Table 5-1.

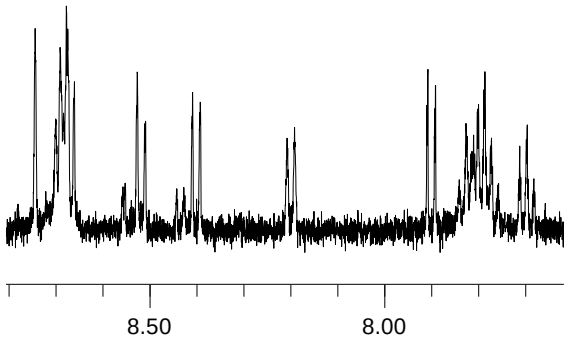

Figure 5-2. 1 H NMR of the Nitrile Byproduct

Table 5-1. Calculated NMR Results

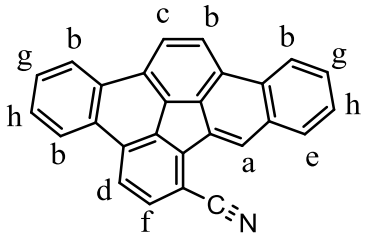

5-18

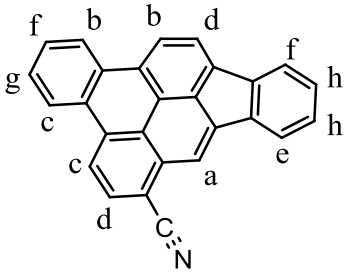

5-19

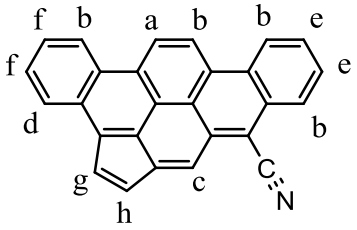

5-21

	Chemical Shifts (ppm)						
	Experimental	Calculated for 5-18*	Δ	Calculated for 5-19*	Δ	Calculated for 5-21*	Δ
a	**8.74**	**8.87**	**0.13**	**8.92**	**0.18**	**9.12**	**0.38**
b	8.70-8.66	8.75-8.68	~0.04	8.87	~0.19	8.98-8.84	~0.22
c	8.51	8.57	0.06	8.77	0.26	8.84	0.33
d	8.40	8.39	0.01	8.23	0.17	8.62	0.22
e	8.20	8.16	0.04	7.98	0.22	8.31	0.11
f	7.89	7.83	0.06	7.75	0.14	7.90	0.01
g	7.82-7.77	7.69-7.63	~0.13	7.60	~0.19	7.79-7.72	~0.05
h	7.71-7.68	7.61-7.54	~0.10	7.28	~0.41	6.97	~0.71
Δ Ave.			0.04		0.14		0.25

*****NMR calculations performed using Gaussian '09 GIAO B3LYP/6-311++G(d,p)

Although the calculated chemical shifts did not match the experimental spectra exactly, the calculated chemical shifts of **5-18** corresponded more closely with the experimental spectra (Figure 5-2), where the singlet furthest downfield, at 8.74 ppm, corresponds well to **5-18** versus **5-19** and **5-21**, where that singlet would be anticipated to be even further downfield, at 8.92 ppm and 8.84 ppm, respectively. Calculations were not performed on **5-20** since there would not be a singlet in the spectrum. Unfortunately, this material decomposed readily to an unknown byproduct and complete characterization by ^{13}C NMR was hampered.

Focus was turned towards growing an X-ray quality crystal of **5-8**, which would provide significant information about the bowl depth and C=N bond distances. Unfortunately, as previously reported,[5] **5-8** is extremely sensitive to water and acid, rendering the bench-top synthesis of this molecule unrealistic. It had been shown that exposure of **5-8** to silica gel was enough to hydrolyze the spring-loaded C=N bond, which is easily susceptible to nucleophilic attack due to the added strain in this curved molecule. Again, this issue was confirmed, and formation of the amino aldehyde, **5-22** was observed upon the compound standing on the bench top, Scheme 5-10.

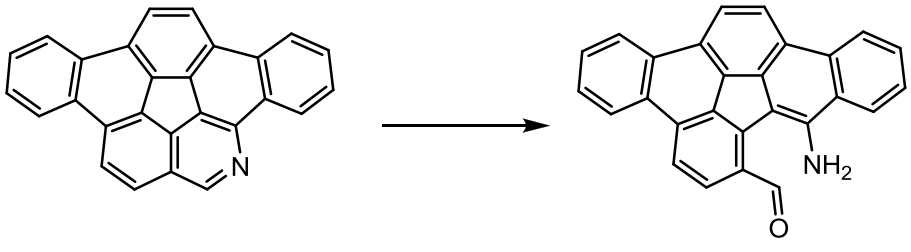

5-8 **5-22**

Scheme 5-10. Hydrolysis of Dibenzo[*g,m*]azacorannulene

It was clear that this compound needed to be handled under an inert atmosphere in order to insure its stability. Despite all efforts to maintain the integrity of this material, hydrolysis of **5-8** to form **5-22** occurred in solution (in dry solvents), even under nitrogen. This complicated matters greatly when attempting to grow an X-ray quality crystal, since the material was continuously undergoing a chemical reaction. Slow evaporation in carbon disulfide, chloroform, dichloromethane, dichloromethane/hexanes and ethanol/dichloromethane were unsuccessful, typically recovering degraded powdered-out material. Diffusion chambers were attempted, but the same unsuccessful results were obtained. Sublimation of the pure material, **5-8**, under vacuum over the course of many days lead to decomposition.

5.3 Conclusion

The successful synthesis of **5-8** was completed in 28% yield, and the pyrolysis results were significantly improved from the first report of this nitrogen containing geodesic polyarene. With access to the first nitrogen atom containing geodesic polyarene, significant efforts were focused towards obtaining the crystal structure of **5-8**; however, the instability of this molecule rendered it incompatible with crystal growing techniques. A few byproducts were observed (**5-18** and **5-22**), which arose due to the significant strain associated with the C-N bond in this curved molecule.

5.4 Experimentals

5.4.1. 4-((Trimethylsilyl)ethynyl)isoquinoline

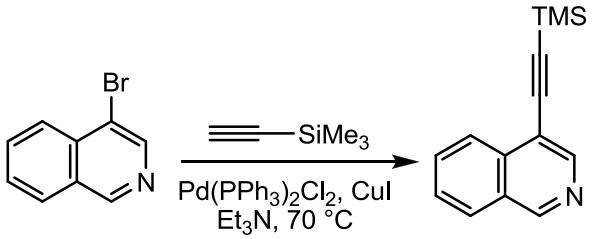

To a flame-dried, nitrogen purged pressure vessel equipped with a stir bar was added 2.50 g (12.0 mmol) of 4-bromoisoquinoline, 0.250 g (0.720 mmol) of $Pd(PPh_3)_2Cl_2$ and 0.160 g (0.840 mmol) of CuI. To this mixture, 1.41 g (14.5 mmol) of trimethylsilylacetylene and 10.0 mL of Et_3N was added via syringe. The vessel was sealed and placed in a pre-heated oil bath at 70 ˚C for 5 h. The mixture was cooled to room temperature, diluted with water and extracted with Et_2O. The organic layer was concentrated to dryness under reduced pressure to provide 2.65 g (97%) of the desired product as a brown oil. **^{1}H NMR** (500 MHz, $CDCl_3$) δ(ppm): 9.21 (bs, 1H), 8.72 (bs, 1H), 8.23 (d, *J* = 8.5 Hz, 1H), 7.99 (d, *J* = 8.0 Hz, 1H), 7.80 (ddd, *J* = 8.5 Hz, *J* = 7.0 Hz, 1.0 Hz, 1H), 7.67 (ddd, *J* = 8.0 Hz, 7.0 Hz, 1.0 Hz, 1H), 0.29 (s, 9H). (Lit.[6])

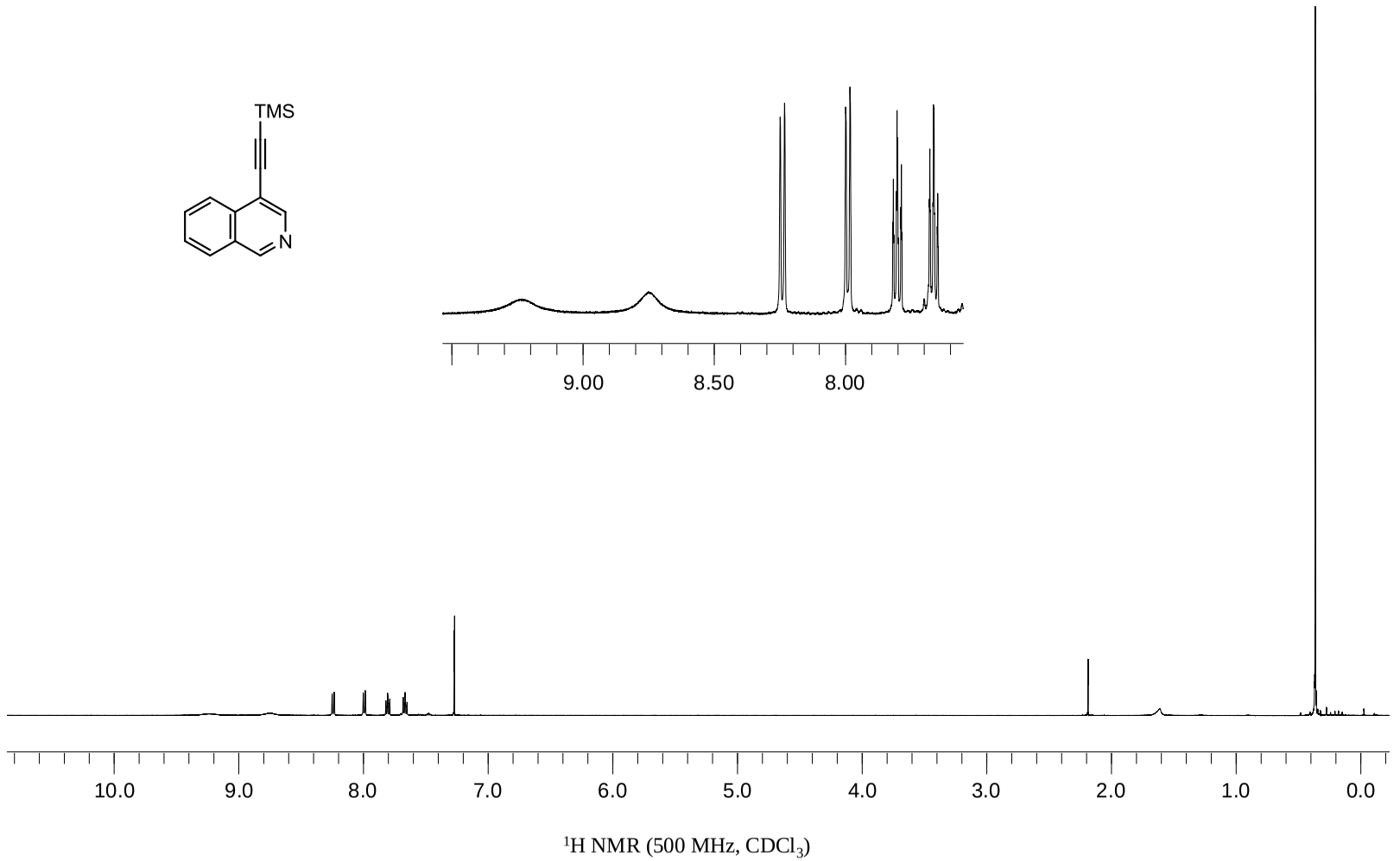

^{1}H NMR (500 MHz, $CDCl_3$)

5.4.2. 4-Ethynylisoquinoline

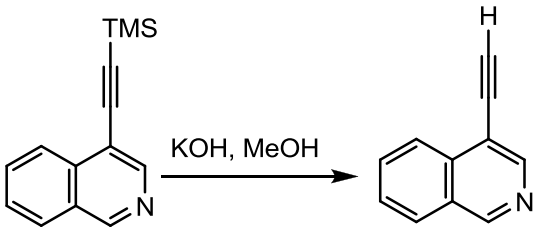

To a 10.0 mL solution of 1N KOH(aq) was added 2.50 g (11.4 mmol) of 4-((trimethylsilyl)ethynyl)isoquinoline in 5.00 mL of methanol dropwise. The mixture was stirred at room temperature for 1 h. The resulting suspension was acidified with 3N HCl, and methanol was removed by evaporation. The resulting residue was dissolved in water, neutralized with K_2CO_3, extracted with diethyl ether and concentrated to dryness under vacuum. Alumina chromatography with ether as the eluent afforded 1.22 g (70%) of the desired product as a tan solid. **^{1}H NMR** (500 MHz, $CDCl_3$) δ(ppm): 9.22 (s, 1H), 8.74 (s, 1H), 8.26 (d, *J* = 8.0 Hz, 1H), 8.00 (d, *J* = 8.0 Hz, 1H), 7.80 (t, *J* = 8.5 Hz, 1H), 7.68 (t, *J* = 8.5, 1H), 3.55 (s, 1H). (Lit.[6])

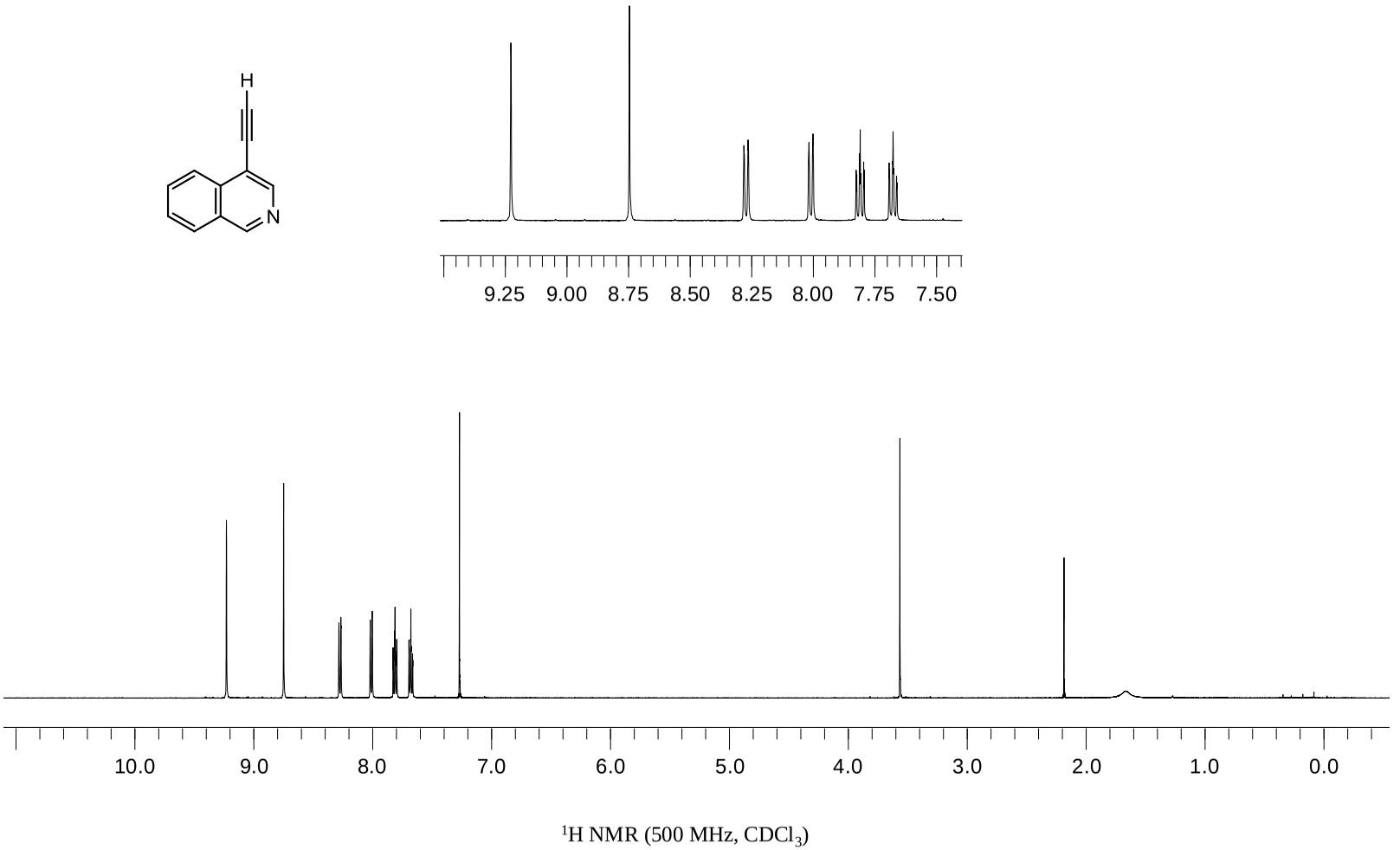

^{1}H NMR (500 MHz, $CDCl_3$)

5.4.3. Cyclopenta[*de*]isoquinoline

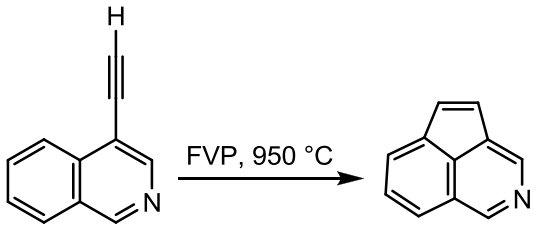

4-Ethynylisoquinoline (1.70 g, 0.0111 mol) was suspended on quartz sand and placed in three quartz boats. The boats were place in a quartz tube with a steady stream of nitrogen carrier gas. The tube was placed in a pyrolysis set up as previously described. The material sublimed and pyrolyzed at 950 ˚C with a sublimation temperature ranging from 50-100 ˚C, and the system pressure was maintained at 0.5-0.6 mm Hg throughout the experiment. At the conclusion of the reaction, the crude pyrolysates were extracted from the tube and traps using dichloromethane. Chromatography on silica gel using 5:1 dichloromethane: ethyl acetate as the eluent afforded 0.945 g (55%) of the desired product as a brown solid. Spectra matched those reported in the literature.[10]

5.4.4. Cyclopenta[*de*]isoquinoline-4,5-dione

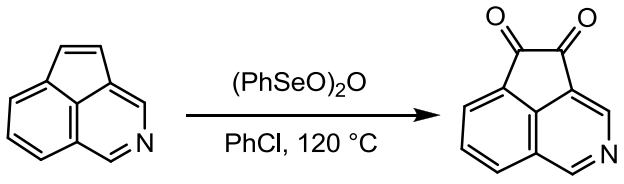

To a round bottom flask equipped with a magnetic stir bar and reflux condenser was added 0.945 g (0.00617 mol) of cyclopenta[*de*]isoquinoline in 100 mL of chlorobenzene. Benzeneseleninic anhydride (4.43 g, 0.0124 mol) was added, and the reaction mixture was stirred at reflux for 24 h. The reaction mixture was cooled to room temperature and flushed through a short pad of silica gel with dichloromethane as the eluent to provide 1.01 g (83%) of the desired product as an orange solid. **^{1}H NMR** (500 MHz, $CDCl_3$) δ(ppm): 9.70 (s, 1H), 9.19 (s, 1H), 8.44 (d, *J* = 8.5 Hz, 1H), 8.33 (d, *J* = 8.0 Hz, 1H), 7.99 (t, *J* = 8.5 Hz, 1H). (Lit.[10])

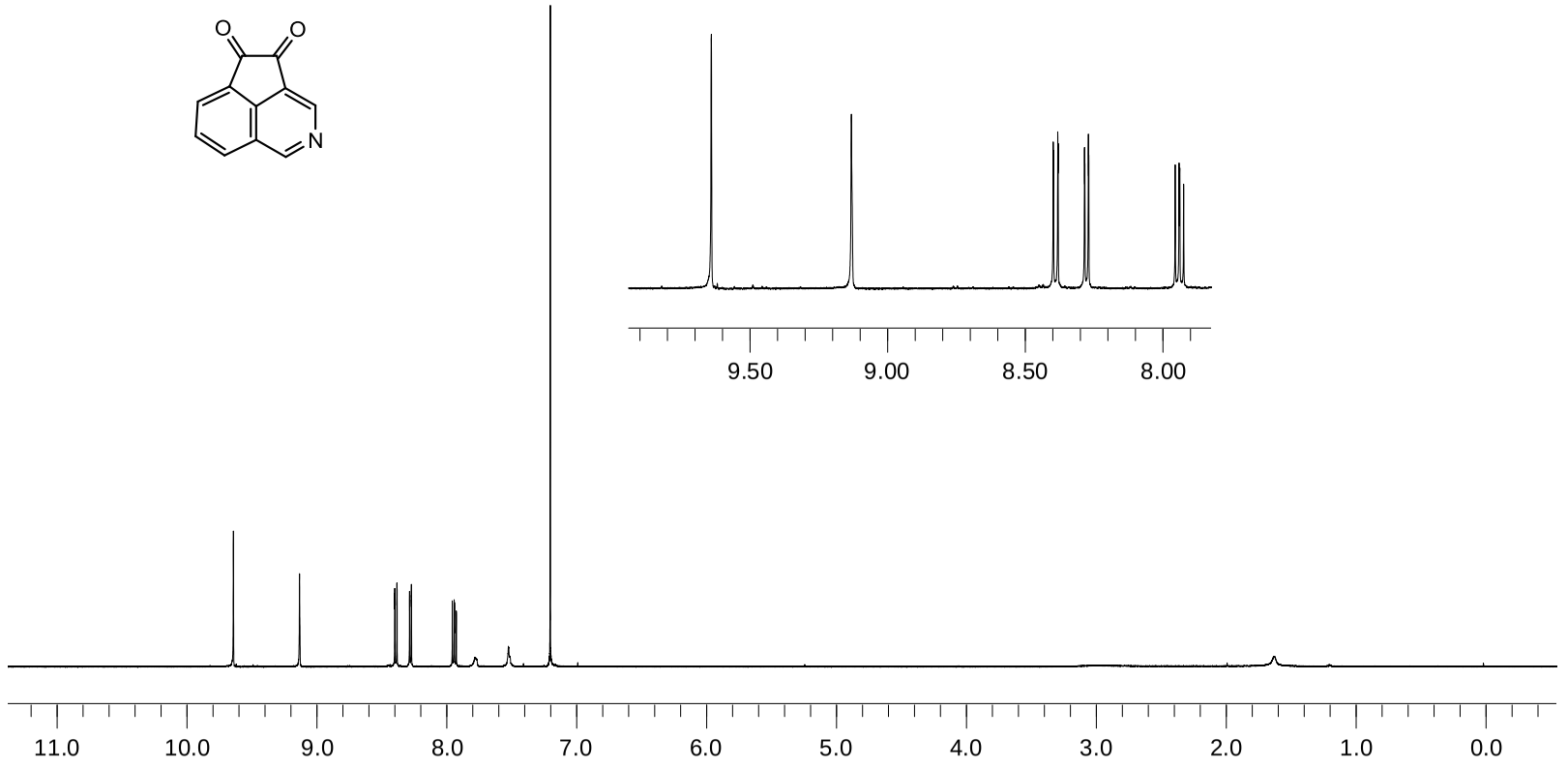

^{1}H NMR (500 MHz, $CDCl_3$)

5.4.5. 7,9-*Bis*(2-bromophenyl)-8*H*-pentaleno[1,2,3-*de*]isoquinolin-8-one

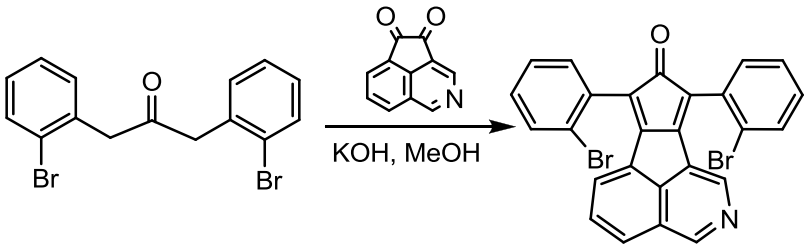

To a 500 mL Erlenmeyer flask, 2.01 g (5.46 mmol) of 1,3-*bis*(2-bromophenyl)propan-2-one and 1.00 g (5.46 mmol) of cyclopenta[*de*]isoquinoline-4,5-dione were added. KOH (0.261 g, 7.09 mmol) was dissolved in methanol (50.0 mL), and the basic solution was added to the reaction mixture. The mixture was stirred at room temperature for 2 h. A color change from yellow to purple was observed instantly upon addition of the basic solution. The resulting suspension was allowed to sit overnight without stirring. The purple precipitate was removed by vacuum filtration and washed with methanol to give 2.10 g (75%) of the desired product. **^{1}H NMR** (500 MHz, $CDCl_3$, for a mixture of diastereomers) δ(ppm): 9.34 (s, 1H), 8.710 (s, 1H, of major diastereomer), 8.702 (s, 1H of minor diastereomer), 8.04 (d, *J* = 7.5 Hz, 1H), 7.82-7.78 (m, 4H), 7.59-7.48 (m, 4H), 7.39-7.34 (m, 2H). (Lit.[6])

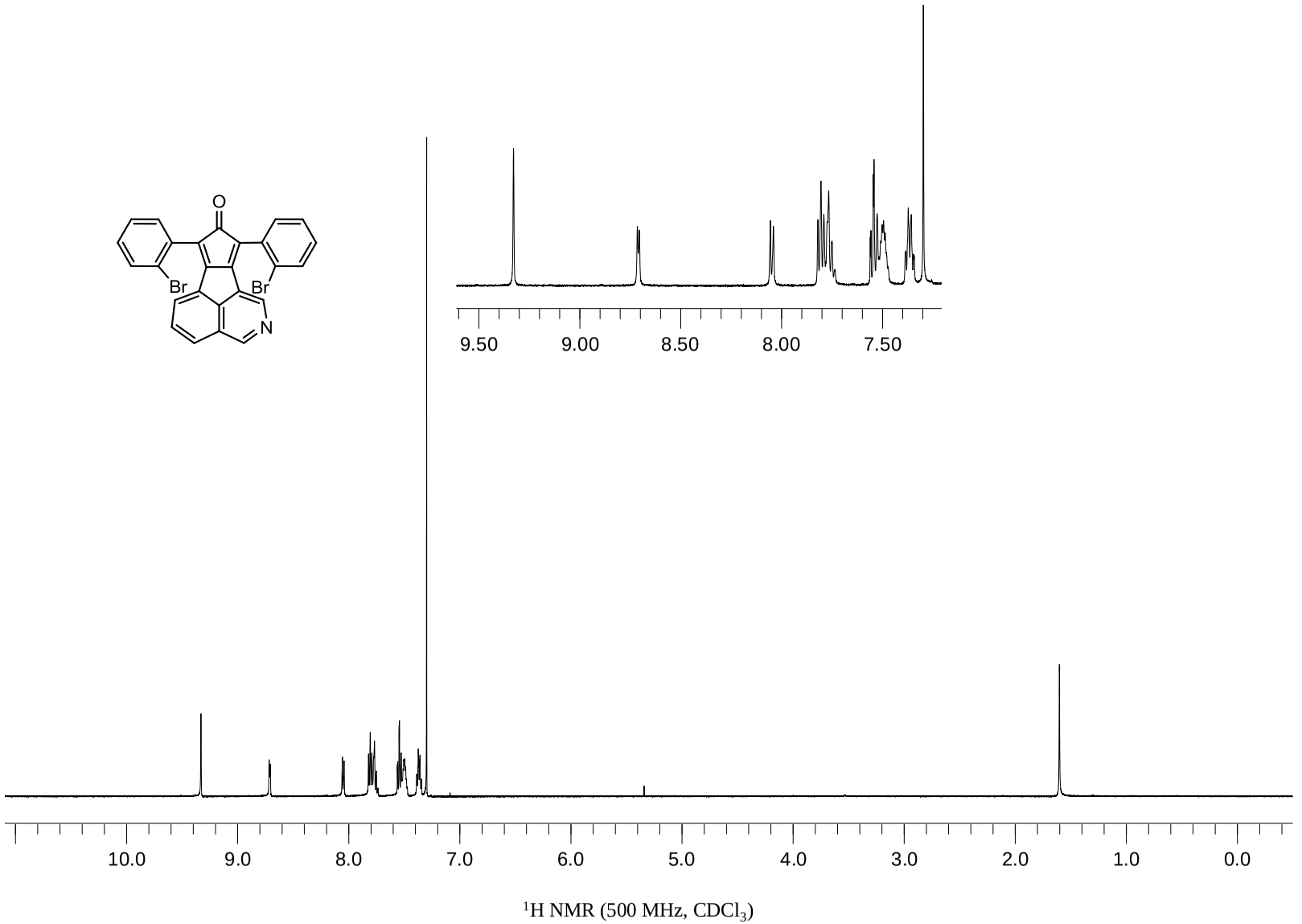

^{1}H NMR (500 MHz, $CDCl_3$)

5.4.6. 7,10-*Bis*(2-bromophenyl)indeno[1,2,3-*de*]isoquinoline

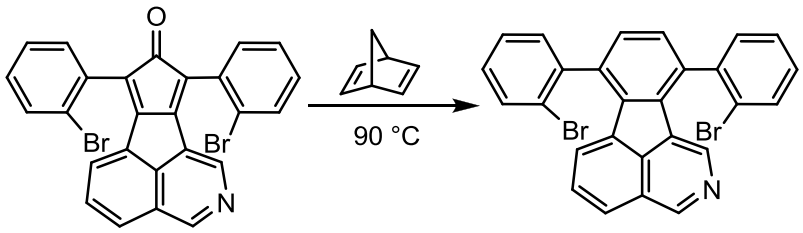

To a round bottom flask, 1.20 g (2.33 mmol) of 7,10-*bis*(2-bromophenyl)indeno[1,2,3-*de*]isoquinoline and 50.0 mL norbornadiene were added. The reaction mixture was stirred at reflux for 3 d. The mixture was cooled to room temperature, and the solvent was removed under reduced pressure. The resulting oily residue was purified by silica gel chromatography with 3:1 hexanes: dichloromethane as the eluent to afford 0.930 g (78 %) of the desired product as a yellow solid. **^{1}H NMR** (500 MHz, $CDCl_3$) δ(ppm): 9.21 (s, 1H), 7.95 (s, 1H), 7.87 (t, *J* = 8.5 Hz, 3H), 7.61 (t, *J* = 7.5 Hz, 2H of minor diastereomer), 7.56 (t, *J* = 7.5 Hz, 2H of major diastereomer), 7.49-7.44 (m, 3H), 7.38-7.34 (m, 2H), 7.00 (d, *J* = 7 Hz, 1H). (Lit.[6])

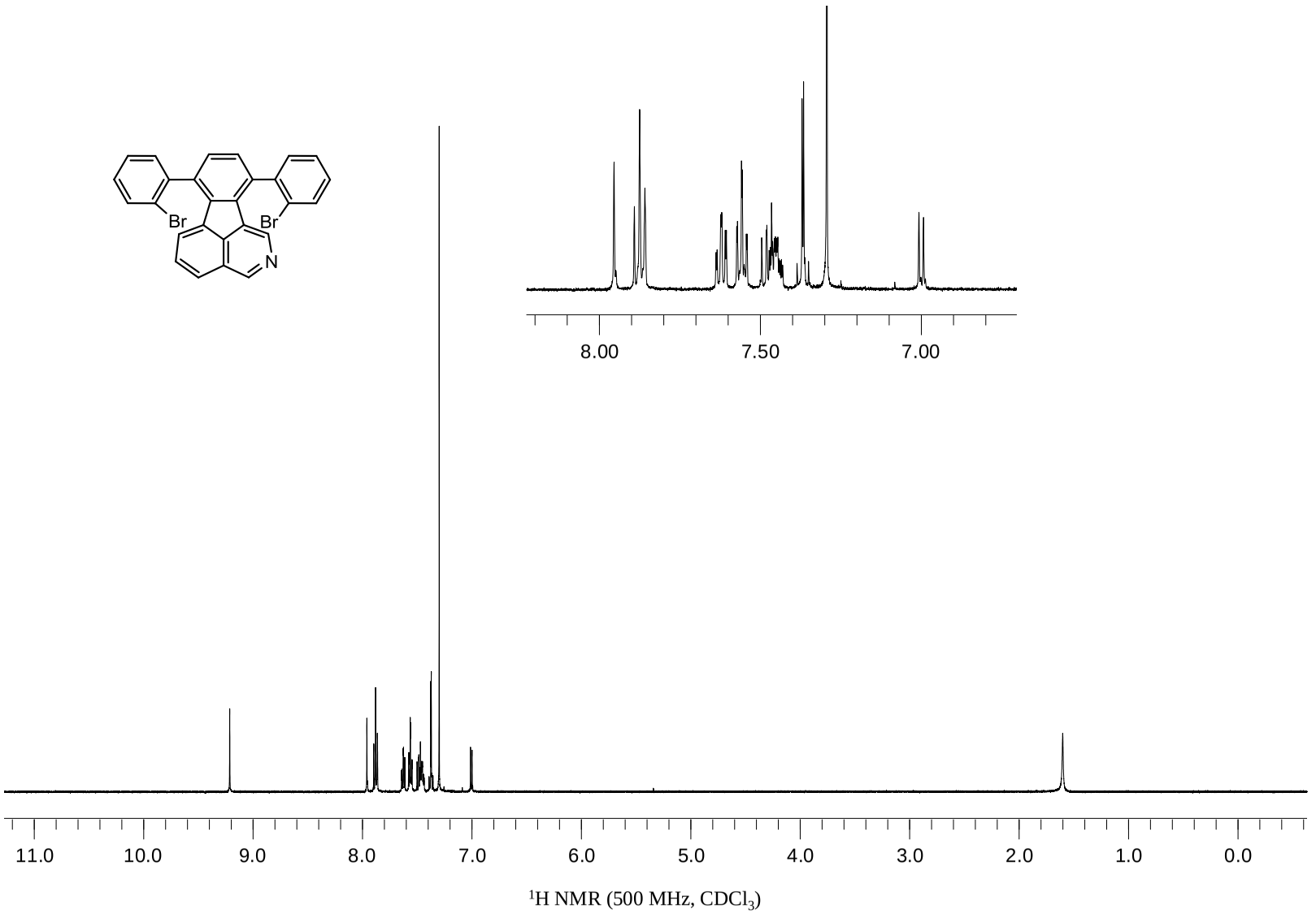

^{1}H NMR (500 MHz, $CDCl_3$)

5.4.7. Dibenzo[*g,m*]azacorannulene (5-8) and Indeno[4,3,2,1-*fghi*]picene-1-carbonitrile (5-18)

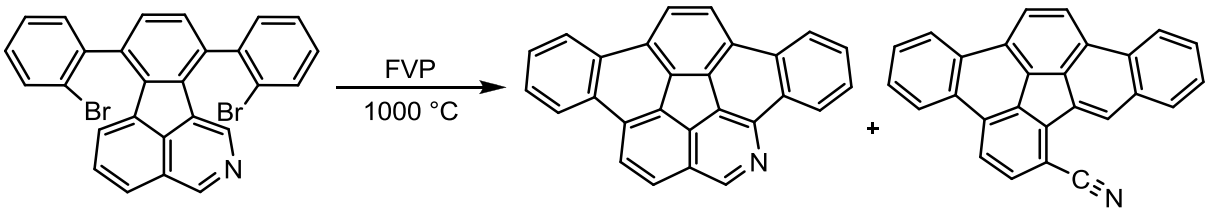

5-8 **5-18**

7,10-*Bis*(2-bromophenyl)indeno[1,2,3-*de*]isoquinoline (54.7 mg, 0.107 mmol) was suspended on quartz sand and placed in two oven-dried quartz boats. The boats were placed in a quartz tube with a steady stream of nitrogen carrier gas. The tube was placed in a pyrolysis set up as previously described. The material was sublimed and pyrolyzed at 1000 ˚C with a sublimation temperature ranging from 75-175 ˚C. The system pressure was maintained at 0.572-0.531 torr for the duration of the experiment. At the conclusion of the experiment, the system was cooled to room temperature, and the crude pyrolysates were extracted from the tube and trap with distilled dichloromethane immediately. The solvent was removed under reduced pressure to provide a crude brown solid. The crude material was purified on reverse phase C18 preparative layer chromatography using a 2:1 acetonitrile: dichloromethane as the eluent, affording 10.7 mg (28%) of the desired product (**5-8**) as a yellow solid.[*] **HRMS** (DART-TOF): Calc'd for $C_{27}H_{14}N$ $(M+1)^+$ 352.1126, found 352.1136. **^{1}H NMR** (500 MHz, $CDCl_3$): 9.50 (s, 1H), 9.08-9.06 (m, 1H), 8.68-8.62 (m, 3H), 8.29 (s, 2H), 8.25 (d, *J* = 8.5 Hz, 1H), 8.03 (d, *J* = 8.5 Hz, 1H), 7.82-7.79 (m, 4H). (Lit.[6])

[*] Exposure to air and moisture will result in decomposition, hydrolysis of the C-N bond, over a short period of time.

Indeno[4,3,2,1-*fghi*]picene-1-carbonitrile: Byproduct, **5-18**, was collected over the course of multiple reactions. Decomposition over time of the byproduct inhibited ^{13}C NMR analysis. **MP**: >300 ˚C (dec.). **HRMS** (DART-TOF): Calc'd for $C_{27}H_{14}N$ $(M+1)^+$ 352.1126, found 352.1111. **^{1}H NMR** (500 MHz, $CDCl_3$): 8.74 (s, 1H), 8.70-8.66 (m, 4H), 8.51 (d, *J* = 8.0 Hz, 1H), 8.40 (d, *J* = 8.5 Hz, 1H), 8.20 (d, *J* = 8.0 Hz), 7.89 (d, *J* = 8.0 Hz, 1H), 7.82-7.77 (m, 3H), 7.71-7.68 (m, 1H). **IR** (NaCl, cm^{-1}): 2363 (C≡N).

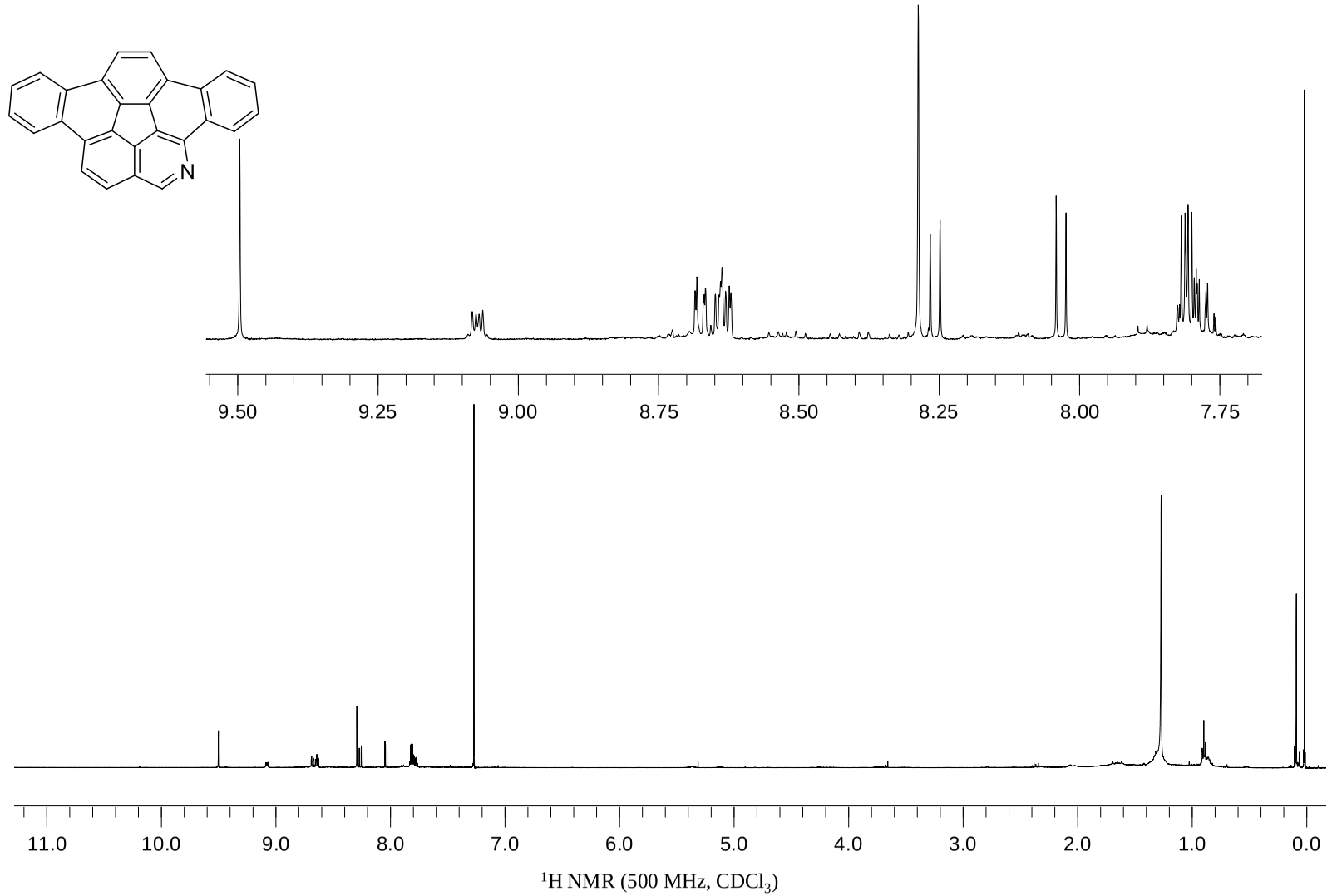

^{1}H NMR (500 MHz, $CDCl_3$)

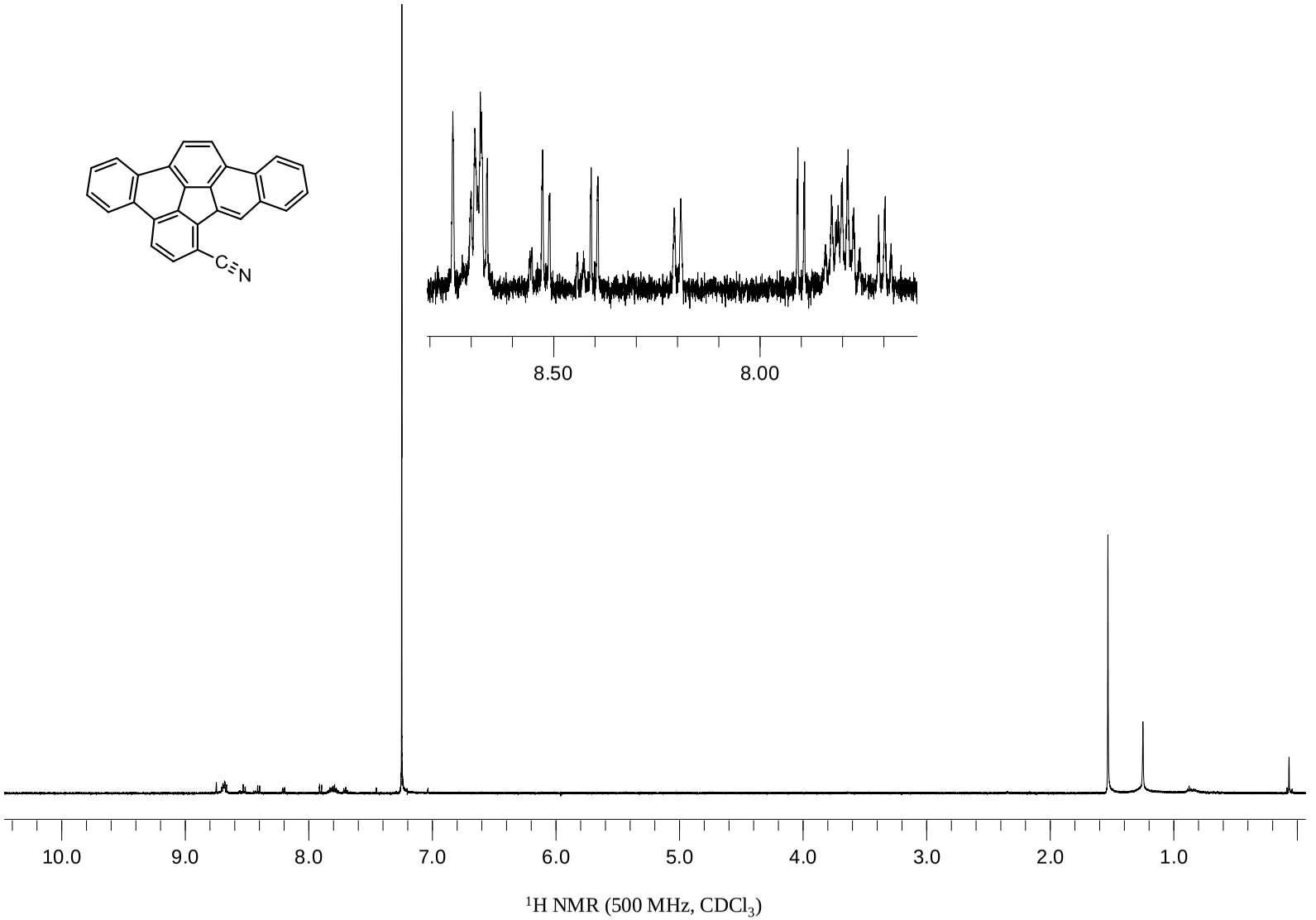

^{1}H NMR (500 MHz, $CDCl_3$)

5.5 References

[1] Tsefrikas, V. M.; Scott, L. T. *Chem. Rev*. **2006**, *106*, 4868.

[2] For theoretical studies of heterasumanenes: (a) Priyakumar, U. D.; Sastry, G. N. *J. Org. Chem.* **2001**, *66*, 6523. (b) Sastry, G. N.; Priyakumar, U. D. J. *Chem. Soc., Perkin Trans*. *2* **2001**, 30.

[3] Imamura, K.; Takimiya, K.; Otsubo, T.; Aso, Y. *Chem. Commun*. **1999**, 1859.

[4] (a) Furukawa, S.; Kobayashi, J.; Kawashima, T. *J. Am. Chem. Soc*. **2009**, *131*, 14192. (b) Furukawa, S.; Kobayashi, J.; Kawashima, T. *Dalton Trans*. **2010**, *39*, 9329.

[5] Saito, M.; Tanikawa, T.; Tajima, T.; Guo, J. D.; Nagase, S. *Tetrahedron Lett.* **2010**, *51*, 672.

[6] Tsefrikas, V. M. Ph.D. Dissertation, Boston College, Chestnut Hill, MA, 2007.

[7] Clayton, M. D.; Marcinow, Z.; Rabideau, P. W. *Tetrahedron Lett.* **1998,** *39*, 9127.

[8] Bratcher, M. S. Ph. D. Dissertation, Boston College, Chestnut Hill, MA, 1996.

[9] Gaussian 09, Gaussian, Inc., Wallingford, CT.

[10] Clayton, M. D.; Marcinow, Z.; Rabideau, P. W. *Tetrahedron Lett*.**1998,** *39*, 9127.

Appendix A

XYZ Coordinates for Structures in Chapter 1

Calculated DFT (B3LYP/6-31G*//AM1)XYZ Coordinates for 1-11

Cartesian Coordinates (Angstroms)

	Atom		X	Y	Z
1	H	H1	-1.0507113	-3.3669506	-0.5550253
2	C	C1	-1.5446859	-2.4249266	-0.7724667
3	C	C6	-0.7395955	-1.3000734	-1.0202194
4	C	C3	-3.5226096	-1.1378824	-1.0139149
5	C	C5	-1.3577271	0.0029335	-1.1865498
6	C	C2	-2.9767343	-2.3563339	-0.6729048
7	C	C4	-2.7345440	0.0062133	-1.2631165
8	C	C10	-0.7339452	1.3029386	-1.0173310
9	C	C9	-1.5337592	2.4297749	-0.7620188
10	H	H9	-1.0352233	3.3684215	-0.5402956
11	C	C8	-2.9660256	2.3666267	-0.6600450
12	C	C7	-3.5175052	1.1525473	-1.0075608
13	C	C11	1.5446918	2.4249319	-0.7725513
14	C	C12	0.7395996	1.3000764	-1.0202761
15	C	C13	3.5226153	1.1378795	-1.0139575
16	C	C14	1.3577266	-0.0029383	-1.1865608
17	C	C15	2.9767408	2.3563410	-0.6729797
18	C	C16	2.7345454	-0.0062208	-1.2631347
19	C	C17	0.7339485	-1.3029331	-1.0172997
20	C	C18	1.5337620	-2.4297671	-0.7619737
21	C	C19	2.9660272	-2.3666223	-0.6600106
22	C	C20	3.5175035	-1.1525469	-1.0075442
23	H	H21	1.0352209	-3.3684035	-0.5402212
24	H	H23	1.0507153	3.3669654	-0.5551585
25	C	C58	3.9161045	-3.3180334	-0.0503875
26	C	C22	4.8097560	-0.7148053	-0.5897662
27	C	C23	5.6495682	-1.4720523	0.2001267
28	C	C24	5.2358179	-2.8771468	0.3699968
29	C	C25	4.8130349	0.6969261	-0.5941120
30	C	C26	3.9318440	3.3077196	-0.0711907
31	C	C27	5.2499515	2.8636677	0.3507019
32	C	C28	5.6566417	1.4553089	0.1905915
33	C	C29	6.6481406	-0.7069808	0.8937043
34	H	H11	7.3765736	-1.2097344	1.5245101
35	C	C30	6.6515798	0.6899875	0.8890973
36	H	H13	7.3824726	1.1933720	1.5165461
37	C	C31	3.5567915	-4.6571809	0.1869094
38	H	H6	2.5753473	-5.0001085	-0.1296440
39	C	C32	4.4226256	-5.5526325	0.7987262
40	H	H12	4.1128355	-6.5816174	0.9593162
41	C	C33	6.0834870	-3.8134242	0.9900241

42	H	H15	7.0748119	-3.4941834	1.3000984
43	C	C34	5.6946408	-5.1281578	1.2023305
44	H	H14	6.3786402	-5.8257234	1.6778014
45	C	C35	3.5792374	4.6503697	0.1561587
46	H	H10	2.5989317	4.9953748	-0.1616626
47	C	C36	4.4504297	5.5465233	0.7592820
48	H	H5	4.1460209	6.5783210	0.9118704
49	H	H4	7.0935663	3.4792868	1.2725820
50	C	C37	6.1031373	3.8007298	0.9618592
51	H	H17	6.4094246	5.8171617	1.6324424
52	C	C38	5.7210377	5.1190770	1.1641144
53	C	C39	-4.8130334	-0.6969236	-0.5940844
54	C	C40	-4.8097514	0.7148058	-0.5897547
55	C	C41	-3.9160978	3.3180428	-0.0504203
56	C	C59	-5.2358009	2.8771509	0.3699909
57	C	C43	-5.6495634	1.4720621	0.2001311
58	C	C44	-3.9318532	-3.3077124	-0.0711387
59	C	C45	-5.2499769	-2.8636669	0.3507092
60	C	C46	-5.6566580	-1.4553041	0.1906064
61	C	C47	-6.6515824	-0.6899717	0.8891125
62	H	H16	-7.3824802	-1.1933379	1.5165709
63	C	C49	-6.6481318	0.7069955	0.8937157
64	H	H22	-7.3765515	1.2097518	1.5245356
65	C	C48	-6.0834400	3.8134172	0.9900714
66	H	H8	-7.0747468	3.4941775	1.3002027
67	C	C50	-3.5567741	4.6571929	0.1868596
68	H	H19	-2.5753496	5.0001173	-0.1297549
69	C	C51	-4.4225844	5.5526385	0.7987108
70	H	H7	-4.1127996	6.5816261	0.9592885
71	C	C52	-5.6945773	5.1281465	1.2023760
72	H	H3	-6.3785474	5.8256986	1.6779118
73	C	C53	-6.1031947	-3.8007578	0.9617849
74	H	H20	-7.0936450	-3.4793421	1.2724682
75	C	C54	-3.5792498	-4.6503645	0.1561949
76	H	H24	-2.5989200	-4.9953423	-0.1615809
77	C	C55	-4.4504736	-5.5465441	0.7592388
78	H	H18	-4.1460753	-6.5783492	0.9118039
79	C	C56	-5.7211082	-5.1191142	1.1640040
80	H	H2	-6.4095348	-5.8172216	1.6322406

Calculated DFT (B3LYP/6-31G*//AM1)XYZ Coordinates for 1-43

Cartesian Coordinates (Angstroms)

	Atom		X	Y	Z
1	C	C	1.4093063	2.0527141	-0.0386185
2	C	C1	0.6791783	0.7929142	0.3705845
3	C	C2	3.4535265	0.8075755	0.4919636
4	C	C3	1.3302331	-0.4466744	0.7331173
5	C	C4	2.9156132	1.9317886	-0.0562519

6	C	C5	2.6883054	-0.3643672	0.9051747
7	C	C6	0.7290548	-1.7518544	0.7301638
8	C	C7	1.5555876	-2.8863560	0.6579627
9	C	C8	2.9736919	-2.7869103	0.6057333
10	C	C9	3.5016448	-1.5199966	0.8262383
11	C	C10	-1.5562563	-2.8863001	0.6585841
12	C	C11	-0.7293446	-1.7517607	0.7302743
13	C	C12	-3.5019863	-1.5195105	0.8269164
14	C	C13	-1.3303017	-0.4464333	0.7332668
15	C	C14	-2.9743007	-2.7865487	0.6068005
16	C	C15	-2.6883725	-0.3639810	0.9054970
17	C	C16	-0.6789955	0.7930478	0.3706800
18	C	C17	-1.4088705	2.0529079	-0.0386807
19	C	C18	-2.9152674	1.9321947	-0.0562245
20	C	C19	-3.4533448	0.8080443	0.4919637
21	C	C20	-3.8403653	2.7423059	-0.8381911
22	C	C21	-4.7705767	0.3134704	0.1487672
23	C	C22	-5.5942443	0.9400404	-0.7665300
24	C	C23	-5.1571289	2.2687941	-1.1635758
25	C	C24	-4.8049454	-1.1028433	0.3578665
26	C	C25	-3.9629549	-3.7655400	0.1543212
27	C	C26	-5.2591190	-3.3549547	-0.3086847
28	C	C27	-5.6437295	-1.9449727	-0.3412378
29	C	C28	-6.6047632	0.0989113	-1.3345047
30	H	H	-7.3528370	0.5533032	-2.0019547
31	C	C29	-6.6271991	-1.2741433	-1.1357274
32	H	H1	-7.3903617	-1.8769210	-1.6509099
33	C	C30	-3.4472062	4.0016287	-1.3354112
34	H	H2	-2.4330956	4.3690765	-1.1207578
35	C	C31	-4.3059911	4.7874161	-2.0823849
36	H	H3	-3.9784109	5.7717676	-2.4484032
37	C	C32	-6.0110913	3.0919134	-1.9237832
38	H	H4	-7.0266289	2.7332075	-2.1535051
39	C	C33	-5.6005046	4.3339482	-2.3725852
40	H	H5	-6.2840031	4.9679681	-2.9563708
41	C	C34	-3.6440828	-5.1330075	0.1424736
42	H	H6	-2.6549348	-5.4540383	0.5041515
43	C	C35	-4.5538937	-6.0809214	-0.3039912
44	H	H7	-4.2856706	-7.1477328	-0.2989776
45	H	H8	-7.1542547	-4.0272016	-1.1090477
46	C	C36	-6.1572586	-4.3366005	-0.7584547
47	H	H9	-6.5359997	-6.4343315	-1.1071002
48	C	C37	-5.8147440	-5.6812819	-0.7566474
49	C	C38	4.7707449	0.3129319	0.1489827
50	C	C39	4.8047110	-1.1033978	0.3575721
51	C	C40	3.9622204	-3.7660149	0.1532279
52	C	C41	5.2587026	-3.3554666	-0.3088980
53	C	C42	5.6433872	-1.9455644	-0.3415033
54	C	C43	3.8410736	2.7419544	-0.8377136
55	C	C44	5.1581527	2.2686871	-1.1623337
56	C	C45	5.5948204	0.9396139	-0.7658281

57	C	C46	6.6050346	0.0983898	-1.3342888
58	H	H10	7.3532573	0.5528667	-2.0015168
59	C	C47	6.6268478	-1.2747699	-1.1361084
60	H	H11	7.3897577	-1.8776180	-1.6515597
61	C	C48	6.1572643	-4.3369384	-0.7580314
62	H	H12	7.1543614	-4.0274273	-1.1082524
63	C	C49	3.6431190	-5.1334667	0.1402821
64	H	H13	2.6537043	-5.4545990	0.5012973
65	C	C50	4.5531538	-6.0812514	-0.3059892
66	H	H14	4.2846114	-7.1480298	-0.3019827
67	C	C51	5.8146228	-5.6815603	-0.7571159
68	H	H15	6.5358561	-6.4344964	-1.1078540
69	C	C52	6.0126927	3.0923961	-1.9212312
70	H	H16	7.0283683	2.7338285	-2.1505991
71	C	C53	3.4480235	4.0014041	-1.3346634
72	H	H17	2.4337751	4.3686955	-1.1202513
73	C	C54	4.3073406	4.7877561	-2.0803802
74	H	H18	3.9799541	5.7723496	-2.4459097
75	C	C55	5.6022313	4.3346599	-2.3696060
76	H	H19	6.2860596	4.9690885	-2.9525542
77	C	C56	0.7826300	3.2059176	0.7569962
78	C	C57	-0.7820889	3.2063025	0.7564914
79	C	C58	1.1669674	3.1964573	2.2424426
80	C	C59	-1.1674970	3.1979415	2.2415977
81	N	N	-0.0005546	3.1736233	3.0295622
82	O	O	2.3066953	3.2669851	2.7085360
83	O	O1	-2.3073905	3.2705348	2.7070005
84	H	H20	1.1463927	4.1806231	0.3348338
85	H	H21	-1.1450395	4.1808691	0.3333730
86	C	C64	-0.0016135	3.1020887	4.4580995
87	H	H24	-0.9137150	3.6229885	4.8545775
88	H	H25	0.9266874	3.5936975	4.8542971
89	H	H26	-0.0190857	2.0301469	4.7938342
90	H	H30	-1.1230046	2.2448667	-1.1231287
91	H	H31	1.1235164	2.2449967	-1.1229900
92	H	H44	-1.0908864	-3.8798996	0.5767471
93	H	H47	1.0900024	-3.8799345	0.5760928

Calculated DFT (B3LYP/6-31G*//AM1)XYZ Coordinates for 1-45

Cartesian Coordinates (Angstroms)

	Atom		X	Y	Z
1	C	C	-0.1143280	2.1072253	1.4098728
2	C	C1	-0.4815918	0.8352096	0.6790387
3	C	C2	-0.6103816	0.8482077	3.4530749
4	C	C3	-0.8051029	-0.4148403	1.3303337
5	C	C4	-0.0986870	1.9899899	2.9161407
6	C	C5	-0.9831831	-0.3372773	2.6876989
7	C	C6	-0.7596036	-1.7192988	0.7292240
8	C	C7	-0.6522083	-2.8502548	1.5566310

9	C	C8	-0.6049325	-2.7481825	2.9750284
10	C	C9	-0.8680481	-1.4891646	3.5020585
11	C	C10	-0.6522083	-2.8502548	-1.5566310
12	C	C11	-0.7596036	-1.7192988	-0.7292240
13	C	C12	-0.8680481	-1.4891646	-3.5020585
14	C	C13	-0.8051029	-0.4148403	-1.3303337
15	C	C14	-0.6049325	-2.7481825	-2.9750284
16	C	C15	-0.9831831	-0.3372773	-2.6876989
17	C	C16	-0.4815918	0.8352096	-0.6790387
18	C	C17	-0.1143280	2.1072253	-1.4098728
19	C	C18	-0.0986870	1.9899899	-2.9161407
20	C	C19	-0.6103816	0.8482077	-3.4530749
21	C	C20	0.6545347	2.8259982	-3.8415068
22	C	C21	-0.2541746	0.3658243	-4.7715139
23	C	C22	0.6384192	1.0229206	-5.5960789
24	C	C23	0.9919675	2.3639503	-5.1593083
25	C	C24	-0.4156842	-1.0567290	-4.8058034
26	C	C25	-0.1207033	-3.7112448	-3.9642366
27	C	C26	0.3268236	-3.2850742	-5.2607732
28	C	C27	0.3104400	-1.8748218	-5.6453418
29	C	C28	1.2330762	0.2014338	-6.6077495
30	H	H	1.8836604	0.6782839	-7.3567391
31	C	C29	1.0806122	-1.1773970	-6.6299830
32	H	H1	1.6147408	-1.7625046	-7.3939838
33	C	C30	1.1125181	4.1001553	-3.4483385
34	H	H2	0.8904931	4.4598328	-2.4331167
35	C	C31	1.8320123	4.9099786	-4.3082469
36	H	H3	2.1677589	5.9050893	-3.9804631
37	C	C32	1.7229757	3.2117882	-6.0145921
38	H	H4	1.9619984	2.8612377	-7.0308863
39	C	C33	2.1329839	4.4671520	-5.6040818
40	H	H5	2.6949431	5.1200373	-6.2882132
41	C	C34	-0.0617867	-5.0774601	-3.6452336
42	H	H6	-0.4122968	-5.4108641	-2.6561494
43	C	C35	0.4167942	-6.0094833	-4.5551196
44	H	H7	0.4487676	-7.0758672	-4.2868464
45	H	H8	1.1488970	-3.9295343	-7.1564258
46	C	C36	0.8099081	-4.2506395	-6.1590557
47	H	H9	1.2312537	-6.3350341	-6.5375063
48	C	C37	0.8549727	-5.5945155	-5.8161998
49	C	C38	-0.2541746	0.3658243	4.7715139
50	C	C39	-0.4156842	-1.0567290	4.8058034
51	C	C40	-0.1207033	-3.7112448	3.9642366
52	C	C41	0.3268236	-3.2850742	5.2607732
53	C	C42	0.3104400	-1.8748218	5.6453418
54	C	C43	0.6545347	2.8259982	3.8415068
55	C	C44	0.9919675	2.3639503	5.1593083
56	C	C45	0.6384192	1.0229206	5.5960789
57	C	C46	1.2330762	0.2014338	6.6077495
58	H	H10	1.8836604	0.6782839	7.3567391
59	C	C47	1.0806122	-1.1773970	6.6299830

60	H	H11	1.6147408	-1.7625046	7.3939838
61	C	C48	0.8099081	-4.2506395	6.1590557
62	H	H12	1.1488970	-3.9295343	7.1564258
63	C	C49	-0.0617867	-5.0774601	3.6452336
64	H	H13	-0.4122968	-5.4108641	2.6561494
65	C	C50	0.4167942	-6.0094833	4.5551196
66	H	H14	0.4487676	-7.0758672	4.2868464
67	C	C51	0.8549727	-5.5945155	5.8161998
68	H	H15	1.2312537	-6.3350341	6.5375063
69	C	C52	1.7229757	3.2117882	6.0145921
70	H	H16	1.9619984	2.8612377	7.0308863
71	C	C53	1.1125181	4.1001553	3.4483385
72	H	H17	0.8904931	4.4598328	2.4331167
73	C	C54	1.8320123	4.9099786	4.3082469
74	H	H18	2.1677589	5.9050893	3.9804631
75	C	C55	2.1329839	4.4671520	5.6040818
76	H	H19	2.6949431	5.1200373	6.2882132
77	C	C56	-0.9477913	3.2334257	0.7813761
78	C	C57	-0.9477913	3.2334257	-0.7813761
79	C	C58	-2.4187108	3.1829012	1.1426026
80	C	C59	-2.4187108	3.1829012	-1.1426026
81	O	O2	-3.2194387	3.1581848	0.0000000
82	O	O	-3.0186030	3.2151839	2.2028638
83	O	O1	-3.0186030	3.2151839	-2.2028638
84	H	H20	-0.5547260	4.2216449	1.1449061
85	H	H21	-0.5547260	4.2216449	-1.1449061
86	H	H30	0.9632379	2.3360658	-1.1259355
87	H	H31	0.9632379	2.3360658	1.1259355
88	H	H44	-0.5388720	-3.8412606	-1.0920132
89	H	H47	-0.5388720	-3.8412606	1.0920132

Calculated DFT (B3LYP/6-31G*//AM1)XYZ Coordinates for 1-47

Cartesian Coordinates (Angstroms)

	Atom		X	Y	Z
1	C	C	1.4821681	1.9147500	0.4167448
2	C	C1	0.7287772	0.8044541	0.8112616
3	C	C2	3.4816297	0.6536908	0.6313891
4	C	C3	1.3436708	-0.4676539	1.1090816
5	C	C4	2.9107333	1.8173789	0.1565844
6	C	C5	2.7222455	-0.4539179	1.1392701
7	C	C6	0.7284069	-1.7765296	1.1481179
8	C	C7	1.4968259	-2.9326160	1.0473693
9	C	C8	2.9190221	-2.8967122	0.8707733
10	C	C9	3.4959243	-1.6539929	1.0147425
11	C	C10	-1.4979273	-2.9319155	1.0479526
12	C	C11	-0.7289246	-1.7761493	1.1482239
13	C	C12	-3.4963442	-1.6523451	1.0152651
14	C	C13	-1.3436088	-0.4669789	1.1088975

15	C	C14	-2.9200998	-2.8954137	0.8718608
16	C	C15	-2.7221591	-0.4525696	1.1391363
17	C	C16	-0.7281142	0.8047575	0.8108412
18	C	C17	-1.4809291	1.9152311	0.4157593
19	C	C18	-2.9096529	1.8182233	0.1550836
20	C	C19	-3.4810591	0.6551134	0.6306086
21	C	C20	-3.8294673	2.6203996	-0.6684572
22	C	C21	-4.7366390	0.1137379	0.1538098
23	C	C22	-5.4519957	0.6892738	-0.8746333
24	C	C23	-5.0332409	2.0437756	-1.2098445
25	C	C24	-4.7524138	-1.2951679	0.3970259
26	C	C25	-3.8096684	-3.9244204	0.3420483
27	C	C26	-5.0604425	-3.5733790	-0.2682349
28	C	C27	-5.4789118	-2.1798707	-0.3757212
29	C	C28	-6.3556263	-0.1937118	-1.5457183
30	H	H	-7.0211881	0.2181310	-2.3195191
31	C	C29	-6.3704751	-1.5609406	-1.3070025
32	H	H1	-7.0454926	-2.1999199	-1.8964303
33	C	C30	-3.5910745	3.9759629	-0.9579962
34	H	H2	-2.7765782	4.5131927	-0.4511577
35	C	C31	-4.4062675	4.7084411	-1.8083482
36	H	H3	-4.1770621	5.7655283	-2.0103104
37	C	C32	-5.8394904	2.8022585	-2.0767056
38	H	H4	-6.7479323	2.3426615	-2.4964508
39	C	C33	-5.5281560	4.1145009	-2.3918190
40	H	H5	-6.1686417	4.6909980	-3.0749471
41	C	C34	-3.4393840	-5.2791341	0.3950664
42	H	H6	-2.4852244	-5.5540588	0.8705518
43	C	C35	-4.2584970	-6.2683138	-0.1272053
44	H	H7	-3.9541535	-7.3239455	-0.0706258
45	H	H8	-6.8300207	-4.3325041	-1.2578905
46	C	C36	-5.8675608	-4.5975171	-0.7930811
47	H	H9	-6.1253320	-6.7138797	-1.1357324
48	C	C37	-5.4770627	-5.9260440	-0.7242266
49	C	C38	4.7369676	0.1120129	0.1543566
50	C	C39	4.7521053	-1.2970333	0.3967115
51	C	C40	3.8080673	-3.9258171	0.3401537
52	C	C41	5.0589428	-3.5750693	-0.2700866
53	C	C42	5.4781027	-2.1816701	-0.3766963
54	C	C43	3.8310771	2.6198265	-0.6661607
55	C	C44	5.0345112	2.0428347	-1.2080789
56	C	C45	5.4525158	0.6878126	-0.8738221
57	C	C46	6.3556216	-0.1952777	-1.5456564
58	H	H10	7.0212441	0.2166386	-2.3193705
59	C	C47	6.3699136	-1.5626513	-1.3076719
60	H	H11	7.0446558	-2.2016335	-1.8973479
61	C	C48	5.8655028	-4.5993008	-0.7955402
62	H	H12	6.8281230	-4.3345319	-1.2600848
63	C	C49	3.4370777	-5.2803337	0.3926001
64	H	H13	2.4828710	-5.5549927	0.8681913
65	C	C50	4.2556657	-6.2696241	-0.1302210

66	H	H14	3.9508181	-7.3251196	-0.0740631
67	C	C51	5.4743659	-5.9276566	-0.7272746
68	H	H15	6.1222468	-6.7156278	-1.1391444
69	C	C52	5.8411932	2.8015166	-2.0743832
70	H	H16	6.7491290	2.3415038	-2.4949032
71	C	C53	3.5936840	3.9758754	-0.9544599
72	H	H17	2.7795336	4.5131977	-0.4472012
73	C	C54	4.4094553	4.7084524	-1.8042054
74	H	H18	4.1811463	5.7657376	-2.0052272
75	C	C55	5.5308196	4.1143284	-2.3882149
76	H	H19	6.1715968	4.6909190	-3.0710148
77	C	C56	0.7758254	3.2139488	0.2638170
78	C	C57	-0.7742682	3.2141926	0.2629495
79	C	C58	1.1628365	4.1501770	1.4326574
80	C	C59	-1.1624903	4.1509472	1.4310450
81	N	N	-0.0001722	4.6347915	2.0534053
82	O	O	2.3013110	4.4797859	1.7755606
83	O	O1	-2.3012687	4.4812938	1.7722125
84	H	H20	1.1052407	3.6948183	-0.7010140
85	H	H21	-1.1025207	3.6946874	-0.7024718
86	C	C64	-0.0010452	5.4677350	3.2174102
87	H	H24	-0.9179641	6.1154287	3.2077899
88	H	H25	0.9231023	6.1051836	3.2165283
89	H	H26	-0.0091269	4.8366882	4.1466162
90	H	H44	-1.0061351	-3.9160518	1.0284884
91	H	H47	1.0045824	-3.9165167	1.0278253

Calculated DFT (B3LYP/6-31G*//AM1)XYZ Coordinates for 1-49

Cartesian Coordinates (Angstroms)

	Atom		X	Y	Z
1	C	C	-0.5470414	1.9935291	1.4827189
2	C	C1	-0.8990129	0.8699421	0.7282353
3	C	C2	-0.7303782	0.7300925	3.4827872
4	C	C3	-1.1512553	-0.4118348	1.3432587
5	C	C4	-0.2981130	1.9108982	2.9135451
6	C	C5	-1.1884083	-0.3977854	2.7215128
7	C	C6	-1.1368243	-1.7217201	0.7287080
8	C	C7	-0.9920420	-2.8718038	1.4990926
9	C	C8	-0.8229441	-2.8273520	2.9222812
10	C	C9	-1.0199777	-1.5910571	3.4972460
11	C	C10	-0.9920420	-2.8718038	-1.4990926
12	C	C11	-1.1368243	-1.7217201	-0.7287080
13	C	C12	-1.0199777	-1.5910571	-3.4972460
14	C	C13	-1.1512553	-0.4118348	-1.3432587
15	C	C14	-0.8229441	-2.8273520	-2.9222812
16	C	C15	-1.1884083	-0.3977854	-2.7215128
17	C	C16	-0.8990129	0.8699421	-0.7282353
18	C	C17	-0.5470414	1.9935291	-1.4827189
19	C	C18	-0.2981130	1.9108982	-2.9135451

20	C	C19	-0.7303782	0.7300925	-3.4827872
21	C	C20	0.4821451	2.7487089	-3.8387190
22	C	C21	-0.2397418	0.2096633	-4.7418982
23	C	C22	0.7594572	0.8280844	-5.4629971
24	C	C23	1.0386311	2.1961762	-5.0468132
25	C	C24	-0.4243054	-1.2080325	-4.7566189
26	C	C25	-0.2563360	-3.8333154	-3.8158146
27	C	C26	0.3321872	-3.4567971	-5.0697277
28	C	C27	0.3803955	-2.0597587	-5.4878322
29	C	C28	1.4618714	-0.0262423	-6.3705464
30	H	H	2.2140585	0.4176405	-7.0403008
31	C	C29	1.2801155	-1.4022842	-6.3843770
32	H	H1	1.8916303	-2.0160376	-7.0631956
33	C	C30	0.7120069	4.1158206	-3.6024627
34	H	H2	0.1913831	4.6304254	-2.7823883
35	C	C31	1.5199161	4.8863040	-4.4258389
36	H	H3	1.6737344	5.9522462	-4.1999178
37	C	C32	1.8636094	2.9927668	-5.8601859
38	H	H4	2.2970859	2.5518189	-6.7715698
39	C	C33	2.1202002	4.3186315	-5.5522982
40	H	H5	2.7704371	4.9256593	-6.1989807
41	C	C34	-0.2532363	-5.1894413	-3.4471248
42	H	H6	-0.7124504	-5.4844557	-2.4909823
43	C	C35	0.3029856	-6.1561044	-4.2708136
44	H	H7	0.2895795	-7.2136587	-3.9680208
45	H	H8	1.3406133	-4.1737941	-6.8462384
46	C	C36	0.8927590	-4.4581884	-5.8812603
47	H	H9	1.3170440	-6.5590347	-6.1444268
48	C	C37	0.8788442	-5.7889173	-5.4922943
49	C	C38	-0.2397418	0.2096633	4.7418982
50	C	C39	-0.4243054	-1.2080325	4.7566189
51	C	C40	-0.2563360	-3.8333154	3.8158146
52	C	C41	0.3321872	-3.4567971	5.0697277
53	C	C42	0.3803955	-2.0597587	5.4878322
54	C	C43	0.4821451	2.7487089	3.8387190
55	C	C44	1.0386311	2.1961762	5.0468132
56	C	C45	0.7594572	0.8280844	5.4629971
57	C	C46	1.4618714	-0.0262423	6.3705464
58	H	H10	2.2140585	0.4176405	7.0403008
59	C	C47	1.2801155	-1.4022842	6.3843770
60	H	H11	1.8916303	-2.0160376	7.0631956
61	C	C48	0.8927590	-4.4581884	5.8812603
62	H	H12	1.3406133	-4.1737941	6.8462384
63	C	C49	-0.2532363	-5.1894413	3.4471248
64	H	H13	-0.7124504	-5.4844557	2.4909823
65	C	C50	0.3029856	-6.1561044	4.2708136
66	H	H14	0.2895795	-7.2136587	3.9680208
67	C	C51	0.8788442	-5.7889173	5.4922943
68	H	H15	1.3170440	-6.5590347	6.1444268
69	C	C52	1.8636094	2.9927668	5.8601859
70	H	H16	2.2970859	2.5518189	6.7715698

71	C	C53	0.7120069	4.1158206	3.6024627
72	H	H17	0.1913831	4.6304254	2.7823883
73	C	C54	1.5199161	4.8863040	4.4258389
74	H	H18	1.6737344	5.9522462	4.1999178
75	C	C55	2.1202002	4.3186315	5.5522982
76	H	H19	2.7704371	4.9256593	6.1989807
77	C	C56	-0.4189805	3.2944175	0.7741064
78	C	C57	-0.4189805	3.2944175	-0.7741064
79	C	C58	-1.5873787	4.2080384	1.1380264
80	C	C59	-1.5873787	4.2080384	-1.1380264
81	O	O2	-2.2160693	4.7045661	0.0000000
82	O	O	-2.0464796	4.6001377	2.1973077
83	O	O1	-2.0464796	4.6001377	-2.1973077
84	H	H20	0.5398630	3.7899192	1.1058989
85	H	H21	0.5398630	3.7899192	-1.1058989
86	H	H44	-0.9317560	-3.8547272	-1.0080256
87	H	H47	-0.9317560	-3.8547272	1.0080256

Calculated DFT (B3LYP/6-31G*//AM1)XYZ Coordinates for 1-51

Cartesian Coordinates (Angstroms)

	Atom		X	Y	Z
1	C	C1	1.5276957	2.3524101	0.1765483
2	C	C6	0.7303585	1.1921922	0.3807808
3	C	C3	3.4796237	0.9790966	0.2297748
4	C	C5	1.3412032	-0.1037587	0.4693250
5	C	C2	2.9589530	2.2520843	-0.0252090
6	C	C4	2.7061755	-0.1455945	0.5108032
7	C	C65	0.6799939	-1.3720633	0.3096657
8	C	C72	1.4143976	-2.7051320	0.0991812
9	C	C8	2.9468870	-2.5758858	-0.0089708
10	C	C7	3.4656759	-1.3476025	0.2619104
11	C	C71	-1.4104536	-2.7061915	0.0971662
12	C	C12	-0.6774748	-1.3725640	0.3083218
13	C	C62	-3.4631211	-1.3507715	0.2583192
14	C	C14	-1.3400753	-0.1049249	0.4669524
15	C	C15	-2.9429285	-2.5784457	-0.0120926
16	C	C16	-2.7048998	-0.1480504	0.5069650
17	C	C17	-0.7304247	1.1916032	0.3792740
18	C	C9	-1.5286699	2.3509925	0.1734903
19	C	C19	-2.9596139	2.2491076	-0.0299808
20	C	C20	-3.4792403	0.9758552	0.2253472
21	C	C21	-3.9753538	3.1689374	-0.6339049
22	C	C22	-4.7502701	0.4936903	-0.2196879
23	C	C23	-5.6087736	1.2284117	-1.0006176
24	C	C24	-5.2463766	2.6496646	-1.1313015
25	C	C25	-4.7432184	-0.9179264	-0.1922552
26	C	C26	-3.8593089	-3.5145725	-0.6587917
27	C	C27	-5.1834922	-3.0910770	-1.0973121
28	C	C28	-5.5978020	-1.6943542	-0.9493438

29	C	C29	-6.6077008	0.4475235	-1.6762986
30	H	H11	-7.3518590	0.9362504	-2.2990641
31	C	C30	-6.6044537	-0.9466475	-1.6501647
32	H	H13	-7.3425743	-1.4643814	-2.2566444
33	C	C31	-3.7654701	4.5544900	-0.7923064
34	H	H6	-2.8926768	5.0111289	-0.3550158
35	C	C32	-4.6754041	5.3910662	-1.4251091
36	H	H12	-4.4547162	6.4518385	-1.5085568
37	C	C33	-6.1440670	3.5278324	-1.7642418
38	H	H15	-7.0891859	3.1304894	-2.1228133
39	C	C34	-5.8733963	4.8772076	-1.9254867
40	H	H14	-6.5948257	5.5257365	-2.4147979
41	C	C35	-3.4712792	-4.8433981	-0.9407775
42	H	H10	-2.4825467	-5.1761734	-0.6406111
43	C	C36	-4.3116047	-5.7381627	-1.5817074
44	H	H5	-3.9759591	-6.7537495	-1.7727836
45	C	C63	-6.0102198	-4.0335673	-1.7394188
46	C	C61	-5.5955733	-5.3337643	-1.9760142
47	C	C39	4.7512114	0.4983289	-0.2155198
48	C	C40	4.7454979	-0.9133975	-0.1885090
49	C	C41	3.8642113	-3.5107967	-0.6557807
50	C	C42	5.1879904	-3.0857896	-1.0940537
51	C	C43	5.6010518	-1.6889203	-0.9452928
52	C	C44	3.9733592	3.1730011	-0.6293660
53	C	C45	5.2441099	2.6546983	-1.1286593
54	C	C46	5.6087787	1.2340090	-0.9966882
55	C	C47	6.6088219	0.4540046	-1.6722278
56	H	H16	7.3530618	0.9433943	-2.2944414
57	C	C49	6.6073218	-0.9400096	-1.6456663
58	H	H22	7.3468436	-1.4568831	-2.2510794
59	C	C48	6.0152899	-4.0267742	-1.7376704
60	H	H8	7.0080009	-3.7168983	-2.0525508
61	C	C50	3.4775235	-4.8398172	-0.9387344
62	H	H19	2.4893706	-5.1740871	-0.6384269
63	C	C51	4.3183617	-5.7330298	-1.5810917
64	H	H7	3.9835616	-6.7487372	-1.7730295
65	C	C52	5.6017317	-5.3269870	-1.9757383
66	H	H3	6.2680387	-6.0269950	-2.4716406
67	C	C53	6.1383877	3.5330043	-1.7664220
68	H	H20	7.0824289	3.1359724	-2.1286694
69	C	C54	3.7619196	4.5583874	-0.7879087
70	H	H24	2.8911183	5.0146087	-0.3469092
71	C	C55	4.6686072	5.3950767	-1.4253081
72	H	H18	4.4462677	6.4554924	-1.5099784
73	C	C56	5.8650145	4.8816605	-1.9298853
74	H	H2	6.5831645	5.5299785	-2.4241644
75	C	C57	0.7826780	3.6759211	0.2118969
76	C	C58	-0.7847459	3.6753594	0.2107479
77	C	C69	1.1598746	4.4230665	1.5140453
78	C	C70	-1.1647456	4.4220741	1.5122014
79	N	N1	-0.0030081	4.7952003	2.1672666

80	O	O1	2.2745973	4.6637050	1.9270028
81	O	O2	-2.2803881	4.6618985	1.9229304
82	C	C13	0.7849171	-3.7034887	1.1419543
83	C	C18	-0.7818094	-3.7025547	1.1417877
84	C	C60	1.1705018	-3.3363823	2.5768971
85	C	C59	-1.1645781	-3.3298723	2.5759269
86	N	N2	0.0023284	-3.1379208	3.3096622
87	O	O3	-2.2845711	-3.2218023	3.0293310
88	O	O4	2.2930062	-3.2392706	3.0262461
89	H	H30	1.1248447	4.3021369	-0.6186344
90	H	H32	-1.1258682	4.3018765	-0.6199333
91	H	H29	1.0850156	-3.1003717	-0.8768745
92	H	H33	-1.0798352	-3.1014611	-0.8784660
93	C	C10	-0.0039884	5.4993790	3.4421341
94	H	H23	-0.9085286	6.1064534	3.5001189
95	H	H34	0.8913077	6.1203384	3.4949061
96	H	H35	0.0043532	4.7874617	4.2738841
97	C	C11	-0.0044235	-2.7606245	4.7147629
98	H	H9	0.9819972	-2.9793095	5.1249922
99	H	H36	-0.7791351	-3.3279403	5.2344279
100	H	H41	-0.2176029	-1.6924154	4.8222112
101	H	H1	-1.1669608	-4.7100674	0.9574266
102	H	H25	1.1693540	-4.7107797	0.9549247
103	H	H17	-6.2616374	-6.0350701	-2.4705047
104	H	H21	-7.0034737	-3.7251519	-2.0540749

Calculated DFT (B3LYP/6-31G*//AM1)XYZ Coordinates for 1-53

Cartesian Coordinates (Angstroms)

	Atom		X	Y	Z
1	C	C1	-0.3478238	2.4013420	1.5299213
2	C	C6	-0.5418007	1.2414971	0.7300725
3	C	C3	-0.3892706	1.0287522	3.4800703
4	C	C5	-0.6171881	-0.0551255	1.3405687
5	C	C2	-0.1469155	2.3043884	2.9609418
6	C	C4	-0.6562695	-0.0979575	2.7049344
7	C	C65	-0.4443212	-1.3213011	0.6788142
8	C	C72	-0.2146368	-2.6508511	1.4142293
9	C	C8	-0.1130700	-2.5234172	2.9469808
10	C	C7	-0.3968480	-1.2976078	3.4644335
11	C	C71	-0.2146368	-2.6508511	-1.4142293
12	C	C12	-0.4443212	-1.3213011	-0.6788142
13	C	C62	-0.3968480	-1.2976078	-3.4644335
14	C	C14	-0.6171881	-0.0551255	-1.3405687
15	C	C15	-0.1130700	-2.5234172	-2.9469808
16	C	C16	-0.6562695	-0.0979575	-2.7049344
17	C	C17	-0.5418007	1.2414971	-0.7300725
18	C	C9	-0.3478238	2.4013420	-1.5299213
19	C	C19	-0.1469155	2.3043884	-2.9609418

20	C	C20	-0.3892706	1.0287522	-3.4800703
21	C	C21	0.4437411	3.2317408	-3.9768058
22	C	C22	0.0581304	0.5522111	-4.7520334
23	C	C23	0.8294939	1.2958295	-5.6114634
24	C	C24	0.9456084	2.7183632	-5.2484779
25	C	C25	0.0452078	-0.8594406	-4.7457021
26	C	C26	0.5379855	-3.4536426	-3.8664007
27	C	C27	0.9675705	-3.0242107	-5.1916672
28	C	C28	0.8071591	-1.6279337	-5.6029402
29	C	C29	1.5101058	0.5221517	-6.6131311
30	H	H11	2.1248409	1.0173846	-7.3595770
31	C	C30	1.4978565	-0.8721740	-6.6110212
32	H	H13	2.1060517	-1.3830511	-7.3525602
33	C	C31	0.5837516	4.6190193	-3.7670623
34	H	H6	0.1410682	5.0719220	-2.8950947
35	C	C32	1.2037073	5.4641998	-4.6779832
36	H	H12	1.2710082	6.5261609	-4.4588297
37	C	C33	1.5682660	3.6044456	-6.1452927
38	H	H15	1.9324826	3.2122442	-7.0903435
39	C	C34	1.7115511	4.9560673	-5.8747400
40	H	H14	2.1919496	5.6108869	-6.5962927
41	C	C35	0.8294885	-4.7817326	-3.4830734
42	H	H10	0.5374291	-5.1195509	-2.4934841
43	C	C36	1.4702001	-5.6712873	-4.3292338
44	H	H5	1.6667619	-6.6872478	-3.9980442
45	C	C63	1.6113655	-3.9608572	-6.0235142
46	C	C61	1.8564710	-5.2610530	-5.6136675
47	C	C39	0.0581304	0.5522111	4.7520334
48	C	C40	0.0452078	-0.8594406	4.7457021
49	C	C41	0.5379855	-3.4536426	3.8664007
50	C	C42	0.9675705	-3.0242107	5.1916672
51	C	C43	0.8071591	-1.6279337	5.6029402
52	C	C44	0.4437411	3.2317408	3.9768058
53	C	C45	0.9456084	2.7183632	5.2484779
54	C	C46	0.8294939	1.2958295	5.6114634
55	C	C47	1.5101058	0.5221517	6.6131311
56	H	H16	2.1248409	1.0173846	7.3595770
57	C	C49	1.4978565	-0.8721740	6.6110212
58	H	H22	2.1060517	-1.3830511	7.3525602
59	C	C48	1.6113655	-3.9608572	6.0235142
60	H	H8	1.9195507	-3.6481713	7.0172778
61	C	C50	0.8294885	-4.7817326	3.4830734
62	H	H19	0.5374291	-5.1195509	2.4934841
63	C	C51	1.4702001	-5.6712873	4.3292338
64	H	H7	1.6667619	-6.6872478	3.9980442
65	C	C52	1.8564710	-5.2610530	5.6136675
66	H	H3	2.3499339	-5.9583777	6.2847713
67	C	C53	1.5682660	3.6044456	6.1452927
68	H	H20	1.9324826	3.2122442	7.0903435
69	C	C54	0.5837516	4.6190193	3.7670623
70	H	H24	0.1410682	5.0719220	2.8950947

71	C	C55	1.2037073	5.4641998	4.6779832
72	H	H18	1.2710082	6.5261609	4.4588297
73	C	C56	1.7115511	4.9560673	5.8747400
74	H	H2	2.1919496	5.6108869	6.5962927
75	C	C57	-0.3793345	3.7237579	0.7805936
76	C	C58	-0.3793345	3.7237579	-0.7805936
77	C	C69	-1.6744376	4.4773439	1.1440557
78	C	C70	-1.6744376	4.4773439	-1.1440557
79	O	O5	-2.3330459	4.8806098	0.0000000
80	O	O1	-2.1179945	4.7219032	2.2274587
81	O	O2	-2.1179945	4.7219032	-2.2274587
82	C	C13	-1.2414341	-3.6631469	0.7798936
83	C	C18	-1.2414341	-3.6631469	-0.7798936
84	C	C60	-2.6789350	-3.3085790	1.1493778
85	C	C59	-2.6789350	-3.3085790	-1.1493778
86	O	O6	-3.4350955	-3.1250783	0.0000000
87	O	O3	-3.1573875	-3.1941779	-2.2395145
88	O	O4	-3.1573875	-3.1941779	2.2395145
89	H	H30	0.4478781	4.3520588	1.1280708
90	H	H32	0.4478781	4.3520588	-1.1280708
91	H	H29	0.7661178	-3.0343159	1.0856198
92	H	H33	0.7661178	-3.0343159	-1.0856198
93	H	H1	-1.0513740	-4.6670646	-1.1710002
94	H	H25	-1.0513740	-4.6670646	1.1710002
95	H	H17	2.3499339	-5.9583777	-6.2847713
96	H	H21	1.9195507	-3.6481713	-7.0172778

Calculated DFT (B3LYP/6-31G*//AM1)XYZ Coordinates for 1-55

Cartesian Coordinates (Angstroms)

	Atom		X	Y	Z
1	C	C1	1.4687609	2.4632681	0.5349041
2	C	C6	0.7266780	1.3020291	0.7815693
3	C	C3	3.4568543	1.1763599	0.4093805
4	C	C5	1.3466771	0.0013788	0.8616842
5	C	C2	2.8768308	2.4086537	0.1860105
6	C	C4	2.7229135	0.0028769	0.7861904
7	C	C65	0.7295909	-1.3006388	0.7827223
8	C	C72	1.4743117	-2.4606171	0.5378664
9	C	C8	2.8822922	-2.4033223	0.1894212
10	C	C7	3.4595083	-1.1694235	0.4109466
11	C	C71	-1.4684006	-2.4637069	0.5359226
12	C	C12	-0.7264724	-1.3023101	0.7821532
13	C	C62	-3.4564596	-1.1768675	0.4094644
14	C	C14	-1.3464642	-0.0016484	0.8616427
15	C	C15	-2.8763257	-2.4091650	0.1864915
16	C	C16	-2.7226826	-0.0032378	0.7861403
17	C	C17	-0.7293711	1.3004077	0.7820530
18	C	C9	-1.4740817	2.4602197	0.5364910
19	C	C19	-2.8822250	2.4028552	0.1885185

20	C	C20	-3.4593786	1.1689438	0.4107371
21	C	C21	-3.7630398	3.3348885	-0.5335860
22	C	C22	-4.6543411	0.7090017	-0.2618836
23	C	C23	-5.2930666	1.4494907	-1.2345148
24	C	C24	-4.8962736	2.8505619	-1.2774328
25	C	C25	-4.6523701	-0.7190598	-0.2630093
26	C	C26	-3.7541208	-3.3421967	-0.5378311
27	C	C27	-4.8874772	-2.8594452	-1.2826286
28	C	C28	-5.2886421	-1.4596412	-1.2370924
29	C	C29	-6.1031627	0.6885548	-2.1336753
30	H	H11	-6.7044128	1.2214919	-2.8860491
31	C	C30	-6.1010043	-0.6994666	-2.1348777
32	H	H13	-6.7005762	-1.2327823	-2.8881748
33	C	C31	-3.5595514	4.7258877	-0.5174161
34	H	H6	-2.8156989	5.1649138	0.1641858
35	C	C32	-4.3323451	5.5953538	-1.2737585
36	H	H12	-4.1353120	6.6771959	-1.2356652
37	C	C33	-5.6563428	3.7477050	-2.0476115
38	H	H15	-6.5069984	3.3608447	-2.6303007
39	C	C34	-5.3729721	5.1038361	-2.0656669
40	H	H14	-5.9764601	5.7908620	-2.6767338
41	C	C35	-3.5471652	-4.7326794	-0.5235408
42	H	H10	-2.8042200	-5.1709650	0.1594830
43	C	C36	-4.3159256	-5.6027672	-1.2831503
44	H	H5	-4.1163308	-6.6842054	-1.2465279
45	C	C63	-5.6430101	-3.7570225	-2.0567319
46	C	C61	-5.3557090	-5.1123263	-2.0769350
47	C	C39	4.6528608	0.7183085	-0.2629237
48	C	C40	4.6543510	-0.7097408	-0.2621714
49	C	C41	3.7626443	-3.3353574	-0.5330608
50	C	C42	4.8946783	-2.8509427	-1.2787040
51	C	C43	5.2923439	-1.4501178	-1.2352332
52	C	C44	3.7552150	3.3417758	-0.5376320
53	C	C45	4.8894567	2.8590725	-1.2813230
54	C	C46	5.2897112	1.4589953	-1.2366225
55	C	C47	6.1015886	0.6988111	-2.1347018
56	H	H16	6.7016035	1.2321739	-2.8875835
57	C	C49	6.1027965	-0.6891995	-2.1340228
58	H	H22	6.7036880	-1.2220826	-2.8864885
59	C	C48	5.6523491	-3.7479430	-2.0513087
60	H	H8	6.5012429	-3.3610958	-2.6362605
61	C	C50	3.5595662	-4.7263877	-0.5158079
62	H	H19	2.8181022	-5.1652375	0.1685579
63	C	C51	4.3304907	-5.5958466	-1.2739640
64	H	H7	4.1339210	-6.6777642	-1.2352610
65	C	C52	5.3685818	-5.1040446	-2.0689986
66	H	H3	5.9699628	-5.7909805	-2.6820846
67	C	C53	5.6470937	3.7569581	-2.0530125
68	H	H20	6.4985383	3.3713382	-2.6353656
69	C	C54	3.5483319	4.7323836	-0.5234453
70	H	H24	2.8035310	5.1706374	0.1575654

71	C	C55	4.3188459	5.6025938	-1.2812022
72	H	H18	4.1192374	6.6840207	-1.2445350
73	C	C56	5.3604446	5.1123958	-2.0727246
74	H	H2	5.9621780	5.7999880	-2.6847397
75	C	C57	0.7698511	3.7720239	0.6148519
76	C	C58	-0.7777876	3.7703740	0.6162605
77	C	C69	1.1591162	4.4846086	1.9313634
78	C	C70	-1.1662568	4.4813779	1.9338950
79	N	N1	-0.0033074	4.8469723	2.6315323
80	O	O1	2.2989608	4.7500788	2.3218882
81	O	O2	-2.3060129	4.7434424	2.3270444
82	C	C13	0.7781615	-3.7706471	0.6188948
83	C	C18	-0.7695011	-3.7725085	0.6165914
84	C	C60	1.1662056	-4.4800159	1.9373729
85	C	C59	-1.1592967	-4.4850569	1.9328773
86	N	N2	0.0029187	-4.8463909	2.6341265
87	O	O3	-2.2990781	-4.7515173	2.3227730
88	O	O4	2.3060827	-4.7401838	2.3314635
89	H	H30	1.1014789	4.4175574	-0.2479213
90	H	H32	-1.1122888	4.4158553	-0.2454805
91	C	C10	-0.0027445	5.4608119	3.9245612
92	H	H23	-0.9240429	6.0928928	4.0341300
93	H	H34	0.9170228	6.0954696	4.0320883
94	H	H35	-0.0007488	4.6751263	4.7274767
95	C	C11	-0.0020597	-5.4552719	3.9296964
96	H	H9	0.9666099	-6.0011237	4.0855907
97	H	H36	-0.8645850	-6.1706310	3.9987437
98	H	H41	-0.1147932	-4.6714242	4.7263740
99	H	H1	-1.1005393	-4.4178582	-0.2466975
100	H	H25	1.1131395	-4.4167336	-0.2420601
101	H	H17	-5.9555353	-5.7997045	-2.6910909
102	H	H21	-6.4930627	-3.3712555	-2.6409786

Calculated DFT (B3LYP/6-31G*//AM1)XYZ Coordinates for 1-57

Cartesian Coordinates (Angstroms)

	Atom		X	Y	Z
1	C	C1	-0.5893602	2.4593595	1.4785344
2	C	C6	-0.8160313	1.3009557	0.7274511
3	C	C3	-0.5613301	1.1743165	3.4698798
4	C	C5	-0.9096492	-0.0019406	1.3410577
5	C	C2	-0.3042308	2.4060136	2.9021727
6	C	C4	-0.8943919	-0.0007392	2.7173476
7	C	C65	-0.8077681	-1.3043744	0.7277248
8	C	C72	-0.5748110	-2.4606247	1.4804742
9	C	C8	-0.2939052	-2.4044019	2.9051583
10	C	C7	-0.5572420	-1.1731796	3.4714173
11	C	C71	-0.5748110	-2.4606247	-1.4804742
12	C	C12	-0.8077681	-1.3043744	-0.7277248
13	C	C62	-0.5572420	-1.1731796	-3.4714173

14	C	C14	-0.9096492	-0.0019406	-1.3410577
15	C	C15	-0.2939052	-2.4044019	-2.9051583
16	C	C16	-0.8943919	-0.0007392	-2.7173476
17	C	C17	-0.8160313	1.3009557	-0.7274511
18	C	C9	-0.5893602	2.4593595	-1.4785344
19	C	C19	-0.3042308	2.4060136	-2.9021727
20	C	C20	-0.5613301	1.1743165	-3.4698798
21	C	C21	0.3740376	3.3375596	-3.8184302
22	C	C22	0.0315896	0.7166089	-4.7064434
23	C	C23	0.9564143	1.4584954	-5.4098737
24	C	C24	1.0313932	2.8567235	-5.0064341
25	C	C25	0.0317752	-0.7115245	-4.7084266
26	C	C26	0.3786304	-3.3337100	-3.8282996
27	C	C27	1.0208217	-2.8529943	-5.0245663
28	C	C28	0.9515105	-1.4521149	-5.4191356
29	C	C29	1.7900023	0.6985371	-6.2896526
30	H	H11	2.4974507	1.2323687	-6.9430101
31	C	C30	1.7855400	-0.6896214	-6.2959275
32	H	H13	2.4837192	-1.2225211	-6.9593162
33	C	C31	0.3991283	4.7260607	-3.5971934
34	H	H6	-0.2080445	5.1699735	-2.7952956
35	C	C32	1.1045833	5.5957008	-4.4163419
36	H	H12	1.0976811	6.6754819	-4.2041729
37	C	C33	1.7506249	3.7543755	-5.8144416
38	H	H15	2.2610730	3.3709593	-6.7117040
39	C	C34	1.8055434	5.1071220	-5.5212914
40	H	H14	2.3748318	5.7945780	-6.1633445
41	C	C35	0.4082559	-4.7220278	-3.6083710
42	H	H10	-0.1767026	-5.1664296	-2.7906469
43	C	C36	1.0901534	-5.5928750	-4.4463199
44	H	H5	1.0818028	-6.6732566	-4.2355922
45	C	C63	1.7154964	-3.7515052	-5.8528217
46	C	C61	1.7649567	-5.1066100	-5.5687077
47	C	C39	0.0315896	0.7166089	4.7064434
48	C	C40	0.0317752	-0.7115245	4.7084266
49	C	C41	0.3786304	-3.3337100	3.8282996
50	C	C42	1.0208217	-2.8529943	5.0245663
51	C	C43	0.9515105	-1.4521149	5.4191356
52	C	C44	0.3740376	3.3375596	3.8184302
53	C	C45	1.0313932	2.8567235	5.0064341
54	C	C46	0.9564143	1.4584954	5.4098737
55	C	C47	1.7900023	0.6985371	6.2896526
56	H	H16	2.4974507	1.2323687	6.9430101
57	C	C49	1.7855400	-0.6896214	6.2959275
58	H	H22	2.4837192	-1.2225211	6.9593162
59	C	C48	1.7154964	-3.7515052	5.8528217
60	H	H8	2.2093497	-3.3642629	6.7580733
61	C	C50	0.4082559	-4.7220278	3.6083710
62	H	H19	-0.1767026	-5.1664296	2.7906469
63	C	C51	1.0901534	-5.5928750	4.4463199
64	H	H7	1.0818028	-6.6732566	4.2355922

65	C	C52	1.7649567	-5.1066100	5.5687077
66	H	H3	2.3094039	-5.7965461	6.2305374
67	C	C53	1.7506249	3.7543755	5.8144416
68	H	H20	2.2610730	3.3709593	6.7117040
69	C	C54	0.3991283	4.7260607	3.5971934
70	H	H24	-0.2080445	5.1699735	2.7952956
71	C	C55	1.1045833	5.5957008	4.4163419
72	H	H18	1.0976811	6.6754819	4.2041729
73	C	C56	1.8055434	5.1071220	5.5212914
74	H	H2	2.3748318	5.7945780	6.1633445
75	C	C57	-0.6279804	3.7674060	0.7734399
76	C	C58	-0.6279804	3.7674060	-0.7734399
77	C	C69	-1.9048369	4.5220121	1.1377952
78	C	C70	-1.9048369	4.5220121	-1.1377952
79	O	O5	-2.5958061	4.9274493	0.0000000
80	O	O1	-2.4060892	4.8546860	2.1980339
81	O	O2	-2.4060892	4.8546860	-2.1980339
82	C	C13	-0.6038803	-3.7684273	0.7738354
83	C	C18	-0.6038803	-3.7684273	-0.7738354
84	C	C60	-1.8748541	-4.5334497	1.1377615
85	C	C59	-1.8748541	-4.5334497	-1.1377615
86	O	O6	-2.5573876	-4.9530462	0.0000000
87	O	O3	-2.3794593	-4.8609712	-2.1980855
88	O	O4	-2.3794593	-4.8609712	2.1980855
89	H	H30	0.2582639	4.3821755	1.1074451
90	H	H32	0.2582639	4.3821755	-1.1074451
91	H	H1	0.2872209	-4.3766110	-1.1077987
92	H	H25	0.2872209	-4.3766110	1.1077987
93	H	H17	2.3094039	-5.7965461	-6.2305374
94	H	H21	2.2093497	-3.3642629	-6.7580733